

**A STUDY OF GROWTH AND  
DEVELOPMENT IN THE DISTAL RADIUS  
USING THE  
METAPHYSEAL INDEX**

A thesis submitted to the University of Manchester for the degree of

Doctor of Philosophy

in the Faculty of Medical and Human Sciences

**2011**

**LIANNE CATHERINE ROSE REDDIE**

**SCHOOL OF MEDICINE**

## **Table of Contents**

<b>Table of Contents</b>	2
<b>List of Figures and Tables</b>	6
<b>Abstract</b>	10
<b>Declaration</b>	11
<b>Copyright Statement</b>	11
<b>Dedication</b>	12
<b>Acknowledgements</b>	12
<b>The Author</b>	12
<b>List of Abbreviations</b>	13
<b>1. Overview</b>	15
1.1 Introduction	15
1.2 Motivations	15
1.3 Approach	17
1.4 Aims, Objectives and Hypotheses	18
1.5 Structure of Thesis	20
<b>2. Bone Structure, Growth and Development</b>	22
2.1 Introduction	22
2.2 The Anatomy of Bone	22
2.3 Bone Types and Organisation	24
2.4 Relevant Cells and Functions	24
2.5 The Origins of Bone Cells and Tissues	29
2.6 Ossification	29
2.7 Mineralisation	31
2.8 Bone Modelling and Remodelling	33
2.8.1 The Remodelling Cycle	35
2.9 The Utah Paradigm of Skeletal Physiology and the Mechanostat	36
2.10 The Functional Muscle-Bone Unit	37
2.11 Biomechanics of the Human Skeletal System	38
2.12 Distal Radial Fractures	40
2.13 Summary	41

<b>3. Quantitative Assessment of the Skeleton</b>	<b>42</b>
3.1 Introduction	42
3.2 X-Rays and Radiographs	42
3.2.1 Introduction to X-Rays and the Production of Radiographs	42
3.2.2 How X-Rays Produce an Image	43
3.2.3 Resolution, Dose and Contrast	44
3.3 Radiogrammetry & Digital X-Ray Radiogrammetry (DXR)	44
3.4 Bone-Age Assessment	46
3.5 Peripheral Quantitative Computed Tomography (pQCT)	48
3.6 Dual Energy X-Ray Absorptiometry (DXA)	51
3.7 The Metaphyseal Index (MI)	54
3.8 Puberty and Tanner Pubertal Stages	56
3.9 Summary	58
<b>4. Factors Affecting the Growth Plate</b>	<b>59</b>
4.1 Introduction	59
4.2 Genetic and Hormonal Actions in a Normal Growth Plate	59
4.3 Genetic and Hormonal Disorders	62
4.3.1 Constitutional Delay of Growth and Puberty	62
4.3.2 Neurofibromatosis Type I	64
4.3.3 Other Disorders	65
4.3.4 Hormonal Disorders	70
4.4 Nutrition	71
4.4.1 Minerals – Calcium and Phosphorus/Phosphate	72
4.4.2 Other Minerals	74
4.4.3 Vitamins	77
4.5 Exercise	86
4.6 Bisphosphonates	87
4.7 Summary	89
<b>5. Methods – Original Study Groups</b>	<b>91</b>
5.1 Introduction	91
5.2 The B16N2 Normal Children Study	91
5.3 The Gymnast Study	93
5.4 The NF1 Study	94
5.5 The CDGP Study	95
<b>6. Methods – Study Groups, Subjects and Quantitative Assessment</b>	<b>96</b>
6.1 Introduction	96
6.2 Normal Group Data	96

6.3	Gymnast Group Data .....	97
6.4	NF1 Group Data .....	97
6.5	CDGP Group Data .....	98
6.6	DXA Bone-Age Data .....	98
6.7	Data and Methods Summary .....	99
6.8	Quantitative Assessment .....	99
6.8.1	Image Acquisition – Radiographs .....	101
6.8.2	Digitising Radiographs .....	102
6.8.3	Image/Data Acquisition – pQCT .....	104
6.8.4	Image Acquisition – DXA .....	106
6.9	Anthropometric Data .....	107
6.10	Calculating the Metaphyseal Index .....	107
6.10.1	Assessing the Metaphyseal Index .....	111
6.11	TW3 Bone-Age Assessment Using Hand Radiographs .....	112
6.12	GP Bone-Age Assessment Using Radiographs and DXA Hand Images .....	114
6.13	DXR Measures .....	115
<b>7.</b>	<b>Methods – Analysis .....</b>	<b>116</b>
7.1	Statistical Analyses and Data Handling .....	116
7.2	Precision .....	116
7.3	Normal Group .....	116
7.3.1	TW3 Bone-Age Assessment .....	118
7.3.2	40% and 60% MI .....	118
7.3.3	Longitudinal Analysis .....	118
7.4	Gymnast Group .....	119
7.4.1	Longitudinal Analysis .....	119
7.5	NF1 Group .....	119
7.6	CDGP Group .....	120
7.6.1	Longitudinal Analysis .....	121
7.7	Comparison of All Groups .....	121
7.8	DXA Bone-Age Study .....	122
<b>8.</b>	<b>Results .....</b>	<b>123</b>
8.1	Introduction .....	123
8.2	Precision .....	123
8.3	Normal Group .....	125
8.3.1	TW3 Bone-Age Assessment .....	137
8.3.2	40% and 60% MI .....	138
8.3.3	Longitudinal Analysis .....	140
8.4	Gymnast Group .....	142
8.4.1	Longitudinal Analysis .....	148
8.5	NF1 Group .....	150
8.6	CDGP Group .....	156

8.6.1	Longitudinal Analysis .....	162
8.7	Comparison of All Groups .....	164
8.8	DXA Bone-Age Study .....	170
<b>9.</b>	<b>Discussion .....</b>	<b>172</b>
9.1	Introduction .....	172
9.2	Precision .....	172
9.3	Normal Group .....	173
9.3.1	TW3 Bone-Age Assessment .....	180
9.3.2	40% and 60% MI .....	180
9.3.3	Longitudinal Analysis .....	181
9.4	Gymnast Group .....	183
9.4.1	Longitudinal Analysis .....	189
9.5	NF1 Group .....	190
9.6	CDGP Group .....	196
9.6.1	Longitudinal Analysis .....	201
9.7	Comparison of All Groups .....	202
9.8	DXA Bone-Age Study .....	204
9.9	Challenges .....	206
9.10	Limitations .....	208
9.11	Comparisons with the Literature .....	209
9.12	Future Work .....	211
<b>10.</b>	<b>Conclusion .....</b>	<b>213</b>
10.1	Summary .....	219
<b>11.</b>	<b>References .....</b>	<b>220</b>
<b>12.</b>	<b>Appendices .....</b>	<b>244</b>
12.1	Appendix 1 – Abstracts and Posters .....	244
	Abstract 12.1A .....	244
	Abstract 12.1B .....	246
	Abstract 12.1C .....	248
12.2	Appendix 2 – Further Information regarding X-rays .....	250
	12.2.1 – X-Rays and How They are Generated .....	250
	12.2.2 – X-Rays and Their Interaction with Tissue .....	251
12.3	Appendix 3 – Tanner Pubertal Stage Self-Assessment Sheets ...	253
12.4	Appendix 4 - Figures from Chapter 8 Results .....	257

Word Count: 61,689

## List of Figures

(Figures with asterisks \* denote figures that have been placed in Section 12.4 - Appendix 4).

Figure 1.1	16
Figure 2.1	23
Figure 2.2	24
Figure 2.3	26
Figure 2.4	26
Figure 2.5	31
Figure 2.6	35
Figure 2.7	38
Figure 2.8	40
Figure 3.1	47
Figure 3.2	49
Figure 3.3	49
Figure 3.4	52
Figure 3.5	54
Figure 4.1	66
Figure 4.2	69
Figure 4.3	74
Figure 4.4	79
Figure 4.5	89
Figure 6.1	104
Figure 6.2	105
Figure 6.3	106
Figure 6.4	108
Figure 6.5	110
Figure 6.6	111
Figure 6.7	113
Figure 6.8	115
Figure 8.3A	126
Figure 8.3B	126
Figure 8.3C	127
Figure 8.3D	127
Figure 8.3E	129
Figure 8.3F	129
Figure 8.3G	130
Figure 8.3H	130
Figure 8.3I*	256

Figure 8.3J*	256
Figure 8.3K*	257
Figure 8.3L	135
Figure 8.3M	136
Figure 8.3.1A	137
Figure 8.3.2A	138
Figure 8.3.2B	139
Figure 8.3.2C*	257
Figure 8.3.2D*	258
Figure 8.3.2E*	258
Figure 8.3.2F*	259
Figure 8.3.2G*	259
Figure 8.3.3A	140
Figure 8.3.3B	141
Figure 8.4A	142
Figure 8.4B	143
Figure 8.4C*	260
Figure 8.4D*	260
Figure 8.4E*	261
Figure 8.4F*	261
Figure 8.4G*	262
Figure 8.4H*	262
Figure 8.4I	147
Figure 8.4.1A	148
Figure 8.4.1B	149
Figure 8.4.1C	149
Figure 8.5A	151
Figure 8.5B	151
Figure 8.5C*	264
Figure 8.5D*	264
Figure 8.5E*	265
Figure 8.5F*	265
Figure 8.5G*	266
Figure 8.5H*	266
Figure 8.5I	155
Figure 8.6A	156
Figure 8.6B	157
Figure 8.6C*	267

Figure 8.6D*	267
Figure 8.6E*	268
Figure 8.6F*	268
Figure 8.6G*	269
Figure 8.6H*	269
Figure 8.6I	160
Figure 8.6J	161
Figure 8.6K	162
Figure 8.6.1A	163
Figure 8.6.1B	163
Figure 8.7A*	270
Figure 8.7B*	270
Figure 8.7C*	271
Figure 8.7D	165
Figure 8.7E	167
Figure 8.7F	168
Figure 8.7G	169
Figure 8.8A	170
Figure 8.8B	171
Figure 9.3A	175
Figure 9.3B	177
Figure 9.3.2A	181
Figure 9.4A	184
Figure 9.4B	184
Figure 9.4C	187
Figure 9.12A & B	210
Figure 12.1A	245
Figure 12.1B	247
Figure 12.1C	249
Figure 12.2A	250
Figure 12.3A	253
Figure 12.3B	254
Figure 12.3C	255
Figure 12.3D	256



## List of Tables

Table 3.1	57
Table 3.2	57
Table 4.1	80
Table 4.2	90
Table 6.1	100
Table 6.2	101
Table 6.3	110
Table 8.2A	123
Table 8.2B	124
Table 8.3A	131
Table 8.3B	132
Table 8.3C	132
Table 8.3D	133
Table 8.3E	133
Table 8.3F	134
Table 8.4A	144
Table 8.4B	145
Table 8.4C	146
Table 8.5A	153
Table 8.5B	154
Table 8.5C	154
Table 8.6A	158
Table 8.6B	159
Table 8.6C	159
Table 8.7A	164
Table 8.7B	166
Table 8.7C	166
Table 8.7D	168
Table 8.8A	170
Table 12.2.2A	252

## Abstract

**Introduction:** Metaphyseal inwaisting is a process that occurs during long bone growth and remodelling of epiphyses and results in a proportional increase in growth plate width (GPW) and a decrease in metaphyseal width (MW). The Metaphyseal Index (MI) compares GPW to MW, usually in the distal femur. However, due to bone-age assessments, the most commonly performed radiograph in children is that of the hand/forearm. Previous work showed that gymnasts have a more widened growth plate at the distal radius than normal children, but these studies did not quantify the morphological changes using the MI and pQCT measures. Previous studies have shown that the use of DXA hand/forearm images for the purposes of bone-age assessment were unreliable for children aged 11 and under.

**Aims:** Examine distal radius morphology of 378 Normal subjects (155 male), 36 Gymnast subjects (15 male), 17 NF1 subjects (7 male) and 108 CDGP subjects (83 male) to calculate the precision of MI, MW and GPW measurements, to determine a normal reference range for the MI in Normal subjects and use this to compare to the other 3 groups, and to compare longitudinal measurements. Also, to investigate whether DXA software upgrades have improved the ability to make TW3 bone-age assessments, to investigate how closely DXA compares with standard radiographs using 98 (38 male) DXA hand images and radiographs, and calculate the precision (CV%) of the GP and TW3 bone-age assessment methods.

**Methods:** Anthropometric data, Tanner stage, posterior-anterior hand radiographs and pQCT scans of the non-dominant hand/forearm were obtained. MI was measured using a semi-automated computer-assisted method. Statistical analyses were used to compare males and females, and compare the Normal group to other groups. Also, DXA images and radiographs were assessed by the same assessor and the TW3 and GP bone-ageing methods were compared. A CV% was calculated for both comparisons.

**Results:** The CV% of MI, MW and GPW = 1.05%, 0.92% and 1.28% respectively. MI of males and females was not statistically different in any group. The MI of Gymnasts was significantly lower than the Normal group ( $p = 0.008$ ). The NF1 and CDGP groups were not significantly different from the Normal group. Longitudinal measurements indicated those with a low/high MI at the first visit were likely to have a low/high MI at the second visit, though occasionally the MI would decrease between visits. DXA bone-age assessments proved to be reliable in subjects of all ages assessed in this study and showed a CV% only slightly higher than standard radiographs (CV = 2.95% DXA vs 2.68% radiograph). The CV% of GP and TW3 methods = 2.68% & 1.61% respectively.

**Discussion:** The CV% of MI, MW and GPW shows these methods to be very precise. The mean MI of gymnasts is significantly lower than in normal children due to a widening of the growth plate and not due to a reduction in metaphyseal width. Insufficient subject numbers and smaller age ranges, particularly in the Gymnast and NF1 groups may play a part in the non-significant differences between them and the Normal group. DXA CV% shows that DXA is almost interchangeable with standard radiographs. The TW3 and GP CVs% show that TW3 bone-age assessment is more precise than the GP method. This confirms the tight control that the MW and GPW have in proportion to each other. This is the first study to quantify changes in distal radius morphology in normal, athlete and disease groups, and create a range of normal reference values, which could be useful for future work in this area.

## Declaration

No portion of the work referred to in the thesis has been submitted in support of an application for another degree or qualification of this or any other university or other institute of learning.

## Copyright Statement

i. The author of this thesis (including any appendices and/or schedules to this thesis) owns certain copyright or related rights in it (the “Copyright”) and s/he has given The University of Manchester certain rights to use such Copyright, including for administrative purposes.

ii. Copies of this thesis, either in full or in extracts and whether in hard or electronic copy, may be made **only** in accordance with the Copyright, Designs and Patents Act 1988 (as amended) and regulations issued under it or, where appropriate, in accordance with licensing agreements which the University has from time to time. This page must form part of any such copies made.

iii. The ownership of certain Copyright, patents, designs, trade marks and other intellectual property (the “Intellectual Property”) and any reproductions of copyright works in the thesis, for example graphs and tables (“Reproductions”), which may be described in this thesis, may not be owned by the author and may be owned by third parties. Such Intellectual Property and Reproductions cannot and must not be made available for use without the prior written permission of the owner(s) of the relevant Intellectual Property and/or Reproductions.

iv. Further information on the conditions under which disclosure, publication and commercialisation of this thesis, the Copyright and any Intellectual Property and/or Reproductions described in it may take place is available in the University IP Policy (see <http://www.campus.manchester.ac.uk/medialibrary/policies/intellectual-property.pdf>), in any relevant Thesis restriction declarations deposited in the University Library, The University Library’s regulations (see <http://www.manchester.ac.uk/library/aboutus/regulations>) and in The University’s policy on presentation of Theses.

## **Dedication**

This thesis is dedicated to my Dad, James Thomas Reddie (1931 – 2006).

## **Acknowledgements**

I would like to acknowledge all the help given to me by my supervisors and advisor, Professor Judith Adams, Dr Sue Astley, Dr Kate Ward and Dr Caroline Boggis. I would also like to thank my unofficial advisors, Mr John Denton, Dr Zulf Mughal, Professor Tim Cootes and Professor Catherine West for their valued input. I would like to acknowledge all the staff in Clinical Radiology for their help, Dr Steven Roberts, Dr Isla Gemmell, Dr Chris Rose and Dr Chris Roberts for their statistical expertise, Mr Mike Machin for data retrieval, my fellow PhD students and postdocs for their help and support, and everyone else who aided me in completing this thesis.

Finally I would like to thank my family, especially my mother Sonia and sister Adele, and my friends for their unending support throughout this endeavour.

## **The Author**

My background includes an Honours BSc in Anthropological Science from the University of Toronto and an MSc in Biomedical and Forensic Egyptology from the University of Manchester.

My work on the current thesis included assisting the radiographers on the mobile bone densitometry units during the B16N2 Normal Children's Study on several occasions. The rest of my work was all retrospective in nature and included using previously gathered plain film radiographs, pQCT scans, DXA scans and anthropometric data to perform all GP and TW3 bone-ages, devise the digitisation methods and digitise all radiographs, perform all MI measurements and calculations, and undertake all statistical calculations.

## List of Abbreviations

**Arm Length:** refers to forearm length, measured by a radiographer from the ulnar styloid process to the olecranon.

**BMC** (Bone mineral content): the amount of mineral present in a bone (g).

**BMD** (Bone mineral density): the amount of mineral present per unit of volume ( $\text{g}/\text{cm}^3$ ).

**BMDa** (Areal bone mineral density): a 2-dimensional estimate of BMD measured by DXA ( $\text{g}/\text{cm}^2$ ), calculated by dividing bone mineral content over bone area (BMC/BA).

**BMDaDXR** (Areal bone mineral density measured by DXR): same as BMDa but measured in the 2<sup>nd</sup>, 3<sup>rd</sup> and 4<sup>th</sup> metacarpals by DXR. The volume per projected area is calculated using the metacarpal cortical thickness and bone width, then the volume is multiplied by a density constant, which produces an estimate of BMDa in  $\text{g}/\text{cm}^2$  (Barnett and Nordin, 1960).

**BMAD** (Bone mineral apparent density): an attempt to compensate for the 2-dimensional nature of the BMDa measurement by using a 3-dimensional shape, such as a cube to represent a vertebral body, to improve the accuracy of the measurement.

**CrtThickDXR** (Cortical Bone Thickness Measured by DXR): this is a DXR measure calculated by the Sectra Pronosco system (Linköping, Sweden). A plain film radiograph is placed on a flatbed scanner and using specialised software, it calculates the average cortical thickness of the 2<sup>nd</sup>, 3<sup>rd</sup> and 4<sup>th</sup> metacarpals. Metacarpal cortical bone thickness can also be calculated manually by using callipers and a light-box to measure a plain film radiograph directly.

**CDGP** (Constitutional Delay of Growth and Puberty): one of the groups assessed in the current study.

**CSMA** (Cross-Sectional Muscle Area): this is a QCT measure calculated by removing voxels of certain thresholds (bone and fat) so that only muscle area is left.

**CV** (Co-efficient of Variation): this is the repeatability of a technique. It is calculated by taking repeat measurements of the same subjects using the same technique, all performed by the same researcher. The results of the two analyses are compared and the results are expressed as a percentage. Also known as intra-observer error or precision.

**DXR** (Digital X-ray Radiogrammetry): radiogrammetry measures, such as MCI, BMDaDXR and CrtThickDXR, calculated by a computer program such as the Sectra Pronosco system (Linköping, Sweden).

**GPW** (Growth plate width): a term used in calculating the metaphyseal index (MI) whereby the widest part of the distal radial growth plate is measured.

**MCI** (Metacarpal Index): this is a DXR measure calculated by the Sectra Pronosco system (Linköping, Sweden). A plain film radiograph is placed on a flatbed scanner and using specialised software, it calculates the average cortical thicknesses and bone widths of the 2<sup>nd</sup>, 3<sup>rd</sup> and 4<sup>th</sup> metacarpals. MCI is the sum of the cortical thicknesses divided by the bone width. MCI can also be calculated manually by using callipers and a light-box to measure a plain film radiograph directly.

**MI** (Metaphyseal index): a ratio of half of the metaphyseal width divided by the growth plate width,  $0.5MW/GPW$ .

**Moment of Inertia**: measure of distribution of material around the central axis of a bone.

**MW** (Metaphyseal width): a term used in calculating the metaphyseal index (MI) whereby half of the metaphyseal width is measured,  $0.5MW$ , and divided by the distal radial growth plate width (GPW).

**NF1** (Neurofibromatosis Type 1): one of the groups assessed in the current study.

**OI** (Osteogenesis imperfecta): a genetic disorder manifesting at birth. OI types I, II, III and IV are the result of a dominant mutation in the genes controlling type I collagen manufacture. There is either too little collagen produced or the collagen quality is poor causing an increased risk of fracture from minor trauma throughout life. OI types VII and VIII are the result of recessive mutations in collagen associated genes, specifically the genes controlling cartilage-associated-protein (CRTAP) and prolyl 3-hydroxylase 1 (P3H1) respectively. The specific causes of OI types V and VI have not as yet been identified.

**pSSI** (Polar Strength-strain index): an estimate of torsional and bending strength measured by pQCT and calculated using the section modulus and cortical BMD.

**Section Modulus**: the ratio of the moment of inertia of a bone cross-section undergoing stress, to the greatest distance of a bone element from the neutral axis. This is an estimate of bone strength ( $\text{mm}^3$ ).

**toBMD** (total BMD): pQCT is able to separate BMD into cortical and trabecular BMD. Total refers to cortical and trabecular BMD combined.

## **1. Overview**

### **1.1 Introduction**

Bone geometry can provide important information about the health of an individual, and in the case of children, bone geometry can provide information about development. Bone geometry can be measured in a number of different ways. The current study sets out to create a database of normal reference values for children aged 5-20 (155 male) years using a bone geometry measurement technique called the Metaphyseal Index (MI), and use these reference values to compare with values obtained from other disease and exercise groups. The only two papers published using the MI technique have dealt with the distal femur (Land et al., 2006, Ward et al., 2005a), however the most common radiograph taken clinically is that of the hand/forearm for fracture assessment (Cooper et al., 2004, Landin, 1983) and bone-ageing. Therefore the current study aims to use the MI to examine the distal radius. An additional study was performed to determine whether bone-age could be assessed successfully using an image obtained by a DXA scanner as opposed to the gold-standard of Radiographs. Having obtained reference data, its utility in a number of different groups/conditions can be determined.

### **1.2 Motivations**

The current study was inspired by a paper entitled Quantification of Metaphyseal Modeling in Children Treated with Bisphosphonates (Ward et al., 2005a). The paper outlines a novel method for quantifying the metaphyseal growth and morphology of the distal femur called the MI. The MI is a ratio of two measurements: growth plate width (GPW) and metaphyseal width (MW), specifically  $0.5MW/GPW$  (Fig 1.1). The MI was developed to examine metaphyseal modelling of the distal femur by creating a normal reference database and comparing these values to values obtained from children that had been treated with bisphosphonates for localised conditions.

The distal femur, which was examined in the previous two studies (Land et al., 2006, Ward et al., 2005a) is a weight bearing bone. Therefore the distal radius may be a more appropriate site to study in terms of morphology changes. Also, the most common fracture site in children is at the distal radius (Khosla et al., 2003) and radiographs are often taken of the hand and forearm for fracture assessment. Once a database of

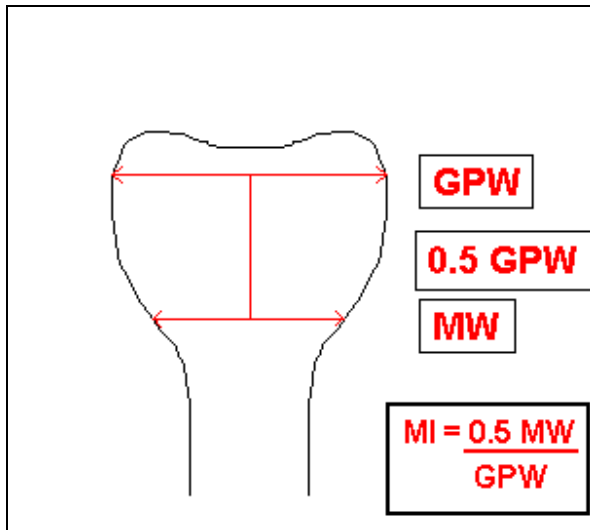


**Figure 1.1: How to calculate the MI: Measure GPW at its widest point. Take half that measurement and measure in a proximal direction towards the metaphysis. Measure the MW at that point.  $MI = 0.5MW / GPW$ .**

normal reference values for the distal radius was created, the MI was used to compare the morphology of the distal radius in other groups of children with diseases, nutrient deficiencies or taking medications that could alter the shape of the metaphysis. Given a baseline measurement, further follow-up measurements could be taken at appropriate intervals to monitor growth and treatment. In the case of bisphosphonate treatment, monitoring the morphology of the metaphysis can be used to avoid accidental overdose. It could also serve to further our understanding of growth and adaptation of long bones in various conditions.

The motivation behind the DXA bone-age study was a previous study that showed DXA could be used as an alternative to Radiographs when imaging the hand for bone-ageing, but only for children aged 12 and over (Ashby et al., 2002b). Since this original study was performed, the DXA software in our institution was upgraded. It was hypothesised that an increase in spatial resolution would allow a more accurate determination of bone-age in children, including those aged below 12 years.



### 1.3 Approach

The work began with the examination of a large group of normal children. The first step was determining inclusion and exclusion criteria and retrospectively taking images and information that met these criteria from an ongoing larger study. This was also done for the subsequent groups obtained: gymnast children, children with Neurofibromatosis type 1 (NF1) and Constitutional Delay of Growth and Puberty (CDGP). A precision study was undertaken that showed the computerised MI measurement technique was more repeatable than the manual one. Bone-age was assessed in all normal and CDGP cases and was used instead of chronological age to compare those 2 specific groups because of the delay in growth compared to chronological age experienced in CDGP. MI was assessed in all groups and in all longitudinal images and compared to age. An assessment was also used to determine if there were any correlations between MI and pQCT measures. Also, because the MI is an arbitrary ratio that was designed as a method of measuring the same site of the metaphysis regardless of the subject age or size of bone, there is a question as to whether or not this is necessarily the best site to measure the metaphysis. The formula for calculating the MI is  $0.5MW/GPW$ . The site of the metaphysis at which the MW is measured is the result of taking 50% of the GPW. However, using 50% of the GPW is an arbitrary measure and it is possible that taking 40% or 60% of the GPW would result in a statistically more useful area of the metaphysis being measured. This was investigated, although the choice to measure at 40% and 60% were also arbitrary.

The approach for the DXA bone-age study also involved taking images retrospectively from a larger study of normal children that met certain criteria: the children must have had a viable Radiograph and DXA hand scan taken on the same day. The bone-age assessment was performed on all Radiographs first and subsequently all DXA scans using the GP method (Greulich and Pyle, 1959) and was blinded to the subject's age. Repeat MI measurements were performed approximately three months after the original assessment to assess repeatability.

## 1.4 Aims, Objectives and Hypotheses

The aims and objectives of this PhD are as follows:

1. To describe normal bone growth and development, and how diseases, deficiencies, and lifestyle choices may disturb these, with an emphasis on the metaphysis of long bones – specifically the distal radius.
2. To measure the MI, MW and GPW of the distal radius in normal children, young gymnasts, children with neurofibromatosis type I (NF1), and children with congenital delay of growth and puberty (CDGP).
3. To analyse and compare MI, MW and GPW measurements in the various groups of children to determine a normal range of MI, and investigate how the MI in disease groups may differ from normal.
4. To perform bone-age assessments in the normal children and CDGP children using the TW3 method. (Chronological age is an inappropriate method by which to compare CDGP to normal children due to the nature of CDGP).
5. To investigate whether there is any correlation between pQCT measurements of the radius [e.g. total bone mineral density (toBMD), cross-sectional muscle area (CSMA), polar strength-strain index (pSSI), radius cortical area at the 50% site and cortical bone density at the 50% site], with the MI, MW and GPW values using both parametric and non-parametric statistical methods.
6. To assess the MI by altering the original ratio ( $0.5MW/GPW$ ) to determine whether 40% of the MW or 60% of the MW would result in a statistically more useful MW site being measured.
7. To compare bone-age assessments performed on DXA images of the hand (Hologic DXA scanner software version 12.4) to that performed conventionally from hand radiographs.

The hypotheses investigated are as follows:

1. MI should not be influenced by weight because the distal radius is not a weight bearing bone. The possible exception to this is in the gymnasts, in whom loading of the distal radius may present.
2. MI should be dependent on age: MI is lower in the younger age range (5-6 years), until it comes to a plateau in mid and late teenage years.
  - i) The children with pubertal delay should have a very similar MI development pattern to normal children, except that the increase and plateau will occur later.
3. MI should not be dependent on sex. Although the GPW and MW of males may be larger than in females, they should be in proportion, giving a similar ratio.
4. MI should not be dependent on height: bones of different lengths should still be in proportion.
5. MI should always be dependent on cross-sectional bone area at the metaphysis because the metaphyseal width is part of the MI ratio.
6. Increases in BMD and pSSI should not alter the MI because BMD and pSSI are not geometric measurements (i.e. will not influence the shape of the bone).
7. MI should be altered in the case of NF1 due to metaphyseal dysplasia being one of the possible features of this disease in relation to the distal radius. However the literature concentrates on this dysplasia presenting in the femur and tibia, which are weight-bearing bones. Therefore although a change in the MI is possible due to the distal radius not being a weight bearing bone, the change may be small.
8. MI should be related to cross-sectional muscle area (CSMA) as muscle causes the most stress placed on bone.
9. MI should not be altered in the case of CDGP as the main feature of this condition is a delay in growth (smaller bones) rather than a change in the morphology, which should not affect a measurement.

## 1.5 Structure of Thesis

Chapter 2 – Bone Structure, Growth and Development: background information on how bone grows, important cell types and actions, modelling, remodelling, biomechanics and fractures.

Chapter 3 – Factors Affecting the Growth Plate: Genetic, hormonal, nutritional, lifestyle and medication factors that could affect the growth plate area and the MI are discussed.

Chapter 4 – Quantitative Assessment of the Skeleton: X-rays, radiogrammetry, bone-age, pQCT, DXA, MI and Tanner Pubertal Stages are discussed.

Chapter 5 – Methods, Original Study Groups: Outlines the original studies from which parts of the data for the current study were obtained, including original inclusion and exclusion criteria.

Chapter 6 – Methods, Current Study Groups, Subjects and Quantitative Assessment: Outlines the MI, how it is calculated and image acquisition. There is a separate section outlining the methodology of bone-ageing using DXA images.

Chapter 7 – Methods, Statistical Analyses: Outlines the statistical analyses conducted in each group for the current study.

Chapter 8 - Results: Outlines the MI and pQCT results of each group, the TW3 bone-age results for the Normal and CDGP group, and the DXA GP bone-age results for the Normal group.

Chapter 9 – Discussion: Interpretation of results, challenges, study limitations and future work.

Chapter 10 – Conclusions: Summarises the results and discussion, and relates them back to the aims, objectives and hypotheses.

Chapter 11 – References

Chapter 12 – Appendices: Outlines published abstracts and posters, further information regarding X-rays and Tanner Pubertal stage self-assessment sheets.

Published Abstracts:

1. Reddie, L., Ashby, R., Adams, J. & Ward, K. (2007) Assessment of the Metaphyseal Index to Study Bone Development of the Distal Radius in Healthy Children. *Osteoporosis International*, 18, S324.

2. Reddie, L., Ward, K., Mughal, M., Astley, S. & Adams, J. (2009) The Metaphyseal Index for Assessing Development of the Distal Radius. *Calcified Tissue International*, 85, 181-182.
3. Reddie, L., Ward, K., Mughal, M., Astley, S. & Adams, J. (2010) The Metaphyseal Index of the Distal Radius: a comparison between gymnasts and normal children. *Bone*, 47, S103.

## **2. Bone Structure, Growth and Development**

### **2.1 Introduction**

Bone is an extremely resilient tissue that undergoes a variety of biochemical processes during growth and development. Bone provides the structural support for the human body in the form of an endoskeleton, i.e. an internal skeleton with other surrounding tissues. The skeleton has three main functions:

1. to provide structural support and a base for muscle and ligament attachment (allowing locomotion to occur).
2. to protect vital organs i.e. the ribs protecting the lungs.
3. to serve as a store for ions, which help regulate homeostasis.

This chapter will discuss bone anatomy, bone types and organisation, relevant cells and their functions as well as growth and adaptation.

### **2.2 The Anatomy of Bone**

Bone composition includes collagen, other non-collagenous proteins, and minerals such as calcium and phosphorus in the form of hydroxyapatite -  $\text{Ca}_5(\text{PO}_4)_3\text{OH}$ . The growth and development of bone allows it to maintain strength whilst being adequately functional to resist damage from everyday stresses.

A long bone e.g. humerus or radius, has epiphyses located at each end, the diaphysis or shaft comprising the middle section and the metaphyses, which are located in between the epiphyses and diaphysis at each end. The metaphysis of a long bone is the area where most of the trabecular bone is located. During growth, the epiphyses and diaphyses are separate, but at skeletal maturity they fuse together. A diagram of an adult human femur is illustrated in Figure 2.1 and typical stages of radial growth are illustrated in Figure 2.2. The periosteum is a two-layered fibrous connective tissue located on the outer surfaces of bone, except at the joints and ligament attachments. The endosteum is a vascular connective tissue that lines the inner bone surface adjacent to the marrow cavity. The undifferentiated cells present in these structures are important as following an injury, they can differentiate into specific cells to repair the bone (Slomianka, 2006).

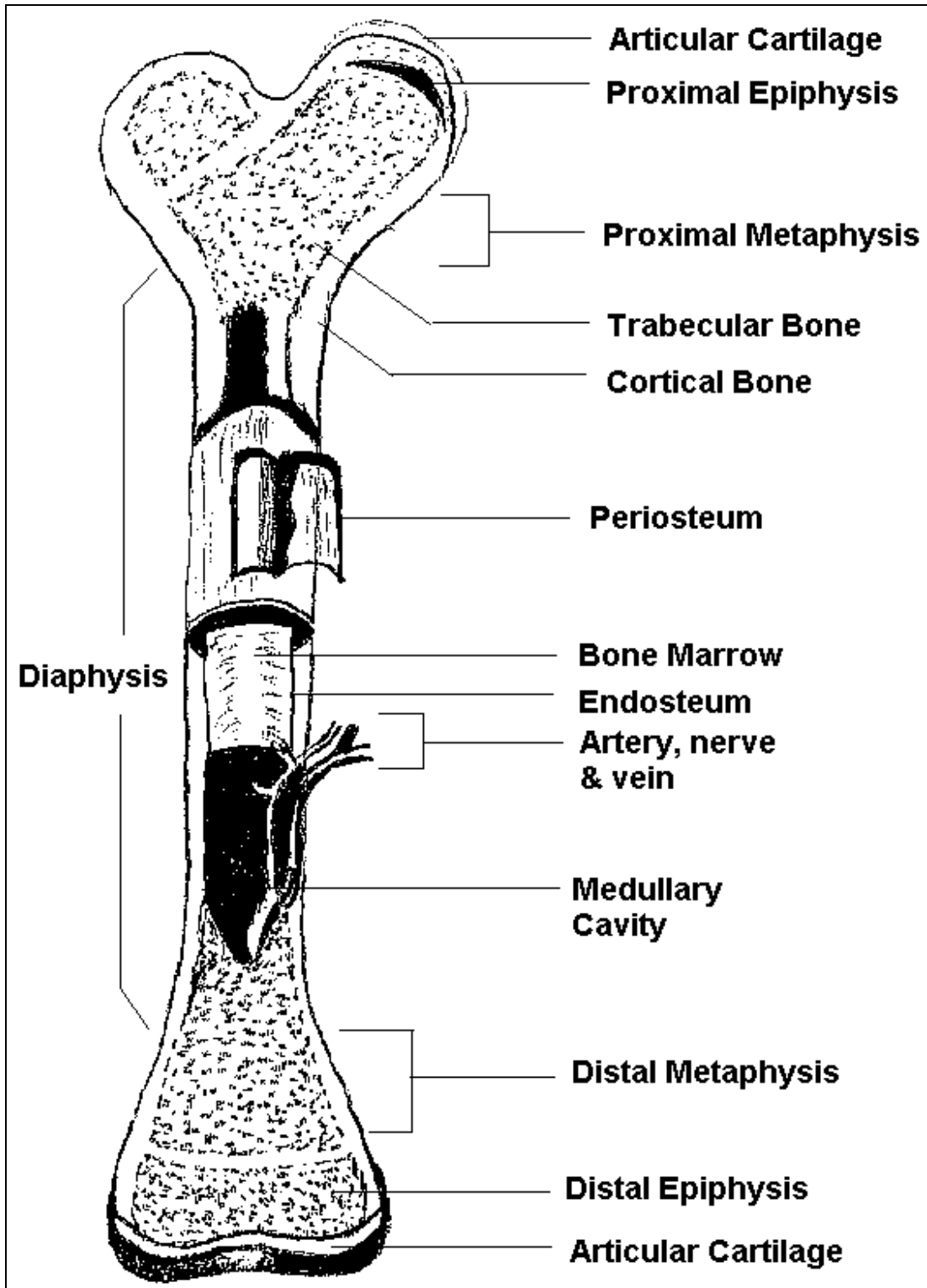
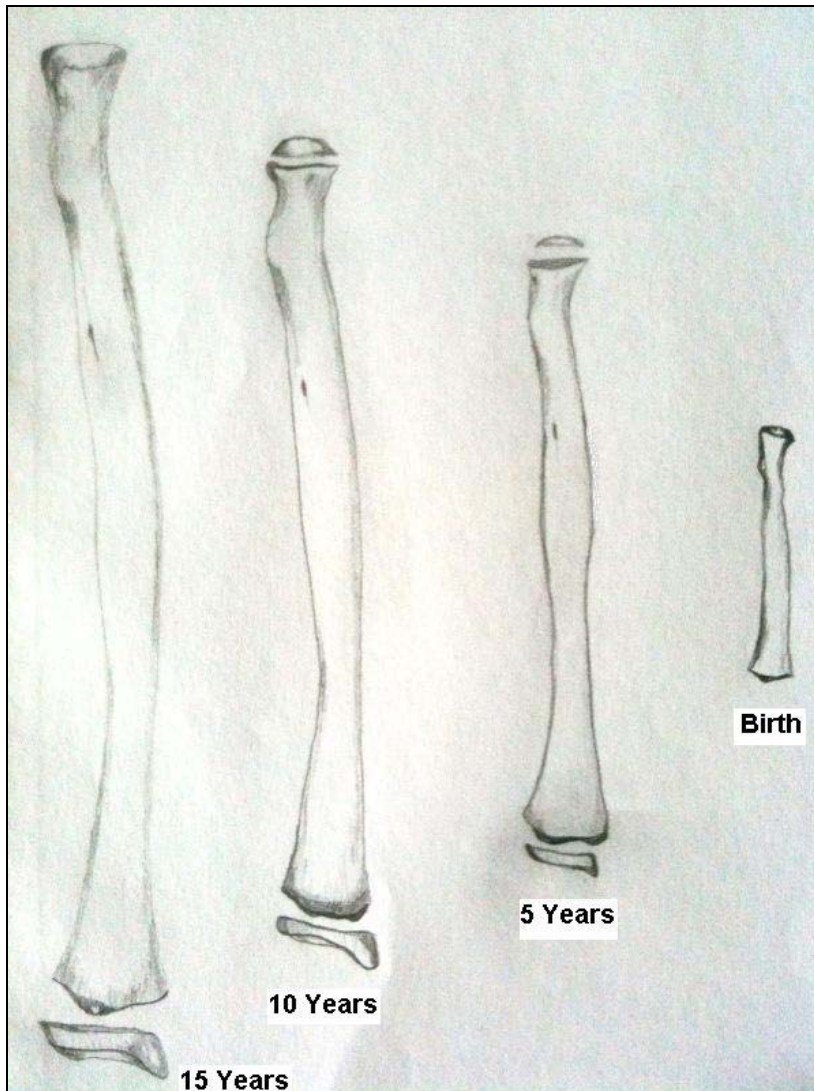


Figure 2.1: Diagram of an adult human femur, adapted from (Mature Long Bone - Femur, 2002).



**Figure 2.2: Developmental stages of a human radius from birth to 15 years, adapted from (Bass, 1995).**

### **2.3 Bone Types and Organisation**

There are two types of bone tissue; lamellar and woven bone. Woven bone is formed quickly during ossification and contains irregularly arranged collagen fibres, therefore making it relatively weak. Woven bone is typically found in foetal bones, recent fracture sites that have started to heal (fracture calluses), and in some diseases such as osteogenesis imperfecta, Paget's disease and certain bone tumours (Einhorn, 1996). Woven bone resembles the weave of a fabric when viewed using polarised-light microscopy, from which the name is derived. Lamellar bone is a more mature bone that



results from the remodelling of woven bone or pre-existing bone tissue. In a typical adult bone, the lamellar bone is organised in two different ways; cortical or compact bone, which forms the outer shell and is more dense, and cancellous, spongy or trabecular bone, which is found in the interior of bones.

Cortical bone has a complex structure based on osteons, which are formed when the vascular spaces in woven bone are filled in by osteoblasts depositing concentric rings of lamellar bone along the inner surface of the space in a tree-ring like structure until only the Haversian canal remains. The Haversian canal consists of a small tunnel with a blood vessel. Another type of canal called a Volkmann's canal is responsible for connecting Haversian canals at right angles so that the blood vessels can connect with each other. The lacunae are oblong-shaped spaces where osteocytes reside and are connected to one another by small canals called canaliculi. The main components of an osteon are illustrated in Figure 2.3. Primary osteons are formed during the modelling process. They are eventually replaced by secondary osteons when bone remodelling occurs. Trabecular bone forms an interconnecting mesh structure known as trabeculae. Flat bones (e.g. ilium) and small bones (e.g. phalanges) have interiors filled with trabecular bone, whereas long bones have their greatest concentrations of trabecular bone at the metaphyses and epiphyses. The trabecular structure in the metaphysis of an adult human femur is illustrated in Figure 2.4. Trabecular bone is organised into parallel lamellae, and concentric lamellae are found in the Haversian systems of cortical bone (Baron, 1999). Interstitial lamellae remnants remain after bone remodelling occurs.

## **2.4 Relevant Cells and Functions**

There are four main types of bone cells involved in the modelling and remodelling of bone; osteoblasts, osteocytes, osteoclasts and bone lining cells.

**Osteoblasts:** are the bone forming cells and are approximately cube-shaped. They secrete the elements of an extracellular bone matrix, which are mainly collagen and non-collagenous proteins including osteopontin, osteocalcin, osteonectin and bone sialoprotein (Aguila and Rowe, 2005, Rosen, 2004, Young et al., 1992), all of which have important functions in bone formation. Osteoblasts also aid in the bone mineralisation process by producing matrix vesicles. Here, the enzyme alkaline phosph-

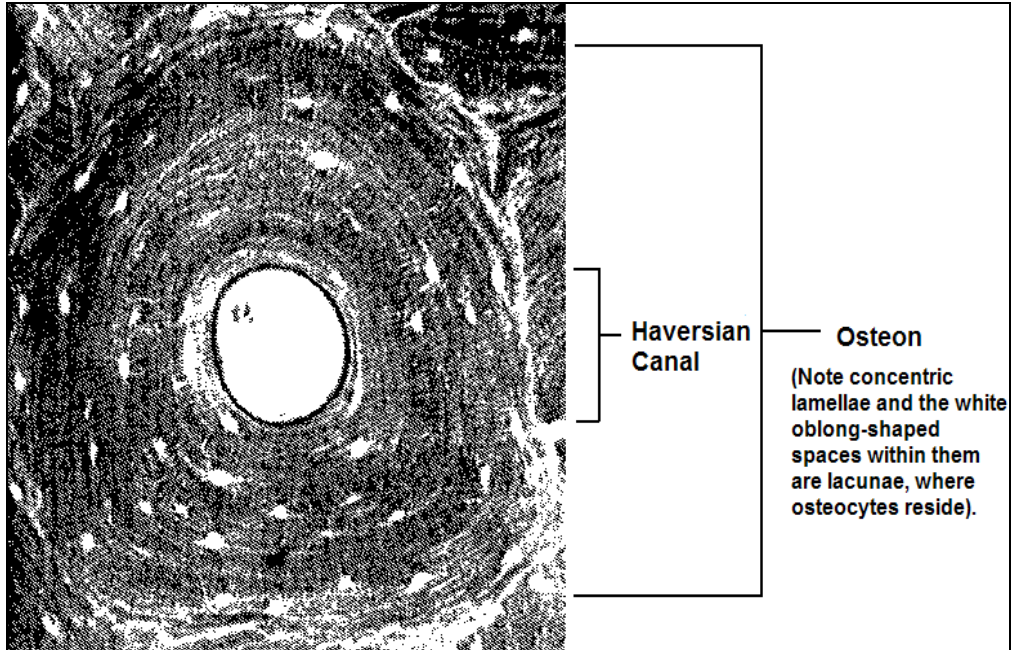


Figure 2.3: Photomicrograph of a human osteon. Reproduced and adapted with permission and copyright © of the British Editorial Society of Bone and Joint Surgery (Smith, 1960).

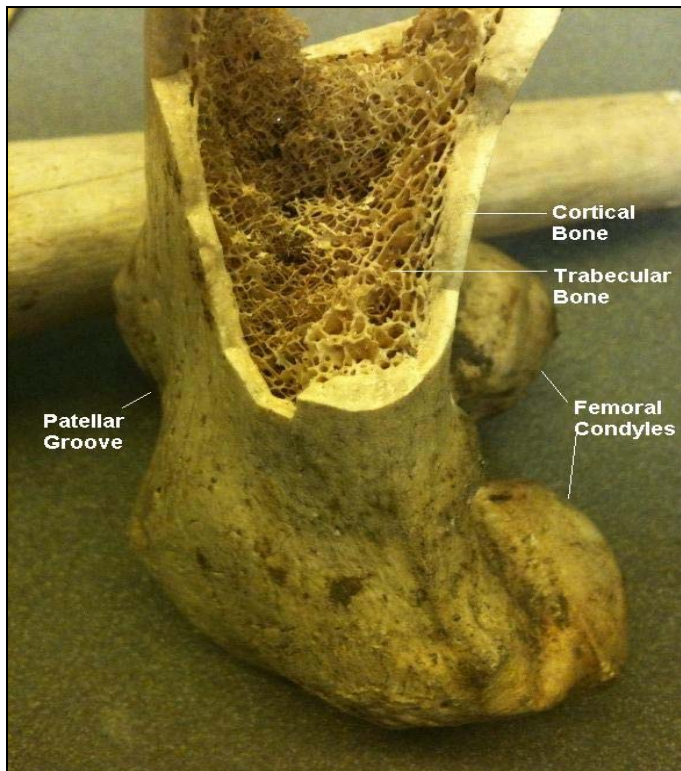


Figure 2.4: Photograph of an archaeological specimen of an adult human femur with a post-mortem break in the distal metaphysis showing the trabecular structure.

atase allows phosphate to be transported into the vesicle where it combines with calcium and crystallizes. This enzyme and the newly created bone crystal are released when the vesicle ruptures, making levels of alkaline phosphatase in the blood stream an important bone formation indicator (Faerk et al., 2002). Osteoblast membranes contain alkaline phosphatase which is important because the presence of this enzyme creates an alkaline environment. Calcium crystallises in an alkaline environment, thereby aiding the osteoblast to produce new bone (Corathers, 2006). Osteoblasts play an important role in haematopoiesis in bone marrow and function as regulators in the haematopoietic environment (Aguila and Rowe, 2005). Much of the activity of osteoblasts occurs at ossification centres and along bone growth plates during childhood and adolescence, but they continue to function to produce new bone throughout life by forming new layers of bone after osteoclasts have removed older bone.

**Osteocytes:** derive from osteoblasts that have become caught up in the matrix they produce. This matrix consists mainly of unmineralised osteoid, collagen and other proteins mentioned previously. The space in which osteocytes become trapped are known as lacunae and the miniscule canals that extend out between osteocytes for removal of waste and the entry of nutrients are known as canaliculi. Osteocytes are also thought to be the major participant in the mechanosensory function of bone, and therefore make a large contribution to the way in which bone adaptation occurs (Aarden et al., 1994, Cowin et al., 1991, Cowin, 2002). Current research suggests that the movement of fluid through the canaliculi and lacunae creates a force strong enough for the osteocytes to sense, and this is the way in which bone is able to sense the mechanical load to which it is subjected (Burger and Klein-Nulend, 1999, Cowin, 2002, Klein-Nulend et al., 2003, You et al., 2001). Osteocytes could then aid in signalling microdamage, disuse and strains to other cells on bone surfaces (Skerry et al., 1989, Marotti et al., 1996, Martin, 2003).

**Osteoclasts:** are bone resorbing cells. They are multinucleated and secrete acids and enzymes that can dissolve the inorganic components of bone, i.e. hydroxyapatite, and the organic components, such as collagen and other proteins. To begin bone resorption, an osteoclast must land, attach and seal to an area of bone. The adhesion of osteoclasts and their progenitor cells are assisted by several attachment proteins called integrins,

which facilitate substrate recognition and allow the formation of a closed microenvironment between the osteoclast and the bone surface called the sealed zone. When the sealed zone is created, a 'ruffled border' is formed inside the sealed zone allowing the bone resorption process to begin (Kölliker, 1889). The ruffled border consists of long tentacle-like projections that permeate the bone matrix. Several biochemical processes essential to bone resorption occur in the sealed zone, such as the formation of hydrochloric acid (Abu-Amer, 2005) and acid hydrolases including protease (Blair et al., 1986). Vesicles transport hydrochloric acid and proteases to the resorption lacuna, which is the area between the bone surface and the ruffled border within the sealed zone where the bone resorption occurs (Vaananen et al., 2000). Osteoclasts are not always active; they must receive a signal indicating how much bone to resorb and from where to resorb it. After an osteoclast has completed resorption, it will either undergo apoptosis or return to an inactive state (Vaananen et al., 2000).

**Bone lining cells:** are present on bone surface areas not undergoing apposition or resorption. Bone lining cells line the medullary cavity on the endosteal surface, line the vascular canals within osteons, and also appear on the periosteal surface. It is believed that they derive from osteoblasts, but are metabolically less active in this terminally differentiated form (Rosen, 2004). Bone lining cells have the ability to secrete collagenases (Meikle et al., 1992), which are necessary to initiate bone resorption. Collagenases are enzymes that digest the endosteal membrane and expose bone mineral, thereby allowing osteoclast attachment (Hill and Orth, 1998, Parfitt, 1994). Bone lining cells can also resorb collagen fibrils protruding from Howship's lacunae, which are left behind by osteoclastic resorption (Everts et al., 2002). The canaliculi allow bone lining cells to deliver signals to and from osteocytes and they also have contact with other types of cells such as those in neighbouring soft tissues and more distant cells through the body's circulation system (Parfitt, 1994). Their location and ability to communicate with a variety of other cells enables them to remain informed of remodelling needs and bring together the necessary components for this process and/or stimulate their activation. It is therefore believed that lining cells are able to signal or 'home' osteoclasts (Khan and Partridge, 1991, Parfitt, 1994, Rosen, 2004).

Fibroblasts are the most common cell type present in connective tissue and they are worth noting because they secrete the elements of the extracellular matrix, including collagen, while also playing a large role in wound healing.

## **2.5 The Origins of Bone Cells and Tissues**

Human bone begins as embryonic tissue called mesoderm. The mesoderm is where the majority of the specialised cells of the musculoskeletal system are derived, including red blood cells and cartilage. In the third week of embryonic development, masses of mesenchymal tissue form adjacent to the notochord (the early developmental stage of the structure that will eventually become the spinal cord) called somites (Müller and O'Rahilly, 2003). Over forty pairs of somites and mesenchymal tissue give rise to different elements i.e. skin, muscle and bone, depending on their position. For example, somites thirteen to twenty-four correspond to the thoracic vertebrae (Müller and O'Rahilly, 1986), located adjacent to the central part of the notochord. Certain skeletal structures derive from pharyngeal arches (pouches that develop in utero adjacent to the pharynx). Some develop in cartilage, which later ossifies, and others develop directly from mesenchymal tissue. Most of the appendicular skeleton develops from the mesenchyme, although muscle cells of the limb have a separate lineage and migrate from somites into limb buds (Wolpert, 1999). Upper limb buds develop slightly before the lower limb buds, around twenty-four to twenty-eight days gestation respectively (O'Rahilly and Gardner, 1975), but they are evident by the end of the third week (Bardeen and Lewis, 1901).

## **2.6 Ossification**

There are two types of bone ossification; intramembranous ossification and endochondral ossification.

**Intramembranous ossification** is defined as the direct mineralisation of a highly vascular connective tissue. This process occurs in the flat bones of the skeleton, such as the facio-maxillary bones. In summary, intramembranous ossification can be considered a four step process:

1. An ossification centre forms.
2. Osteoblasts secrete osteoid elements and the subsequent mineralisation of the osteoid matrix begins working outward from the ossification centre.
3. The early trabeculae form.
4. The periosteum develops. This is the process that creates woven bone.

**Endochondral ossification** is different from intramembranous ossification in that a cartilage precursor (template) to the bone is initially laid down, then the bone begins to take shape in this template. In summary, endochondral ossification can be considered a ten step process:

1. The hyaline cartilage model or template grows and develops. This occurs when chondroblasts (the cartilage equivalent of the osteoblast) begin to secrete collagen and other proteins forming the cartilage matrix. Chondroblasts that become caught in the matrix are subsequently known as chondrocytes. A membrane (perichondrium) surrounds the cartilage model.
2. Blood vessels form in and around the cartilage matrix to bring nutrients and allow the removal of waste.
3. A bone collar and the periosteum form around the diaphysis of the cartilage precursor when the perichondrium develops osteogenic cells.
4. Hypertrophic chondrocytes located at the edges of the primary ossification centres enlarge. The cells eventually degenerate, the matrix becomes compressed and subsequently mineralises. This area is known as the proliferative zone. A representation of the growth plate and adjacent metaphysis during growth is illustrated in Figure 2.5.
5. The original cartilage model is then gradually replaced by woven bone in a complex system of bone apposition, resorption and elongation. This process occurs in the zone of cartilage transformation and the resulting trabeculae form the primary spongiosa.
6. Osteoclasts begin to resorb the woven bone and cartilage remnants, osteoblasts begin to deposit bone matrix and the crystals produced inside the matrix vesicles become organised into the matrix, producing lamellar bone. This process occurs in

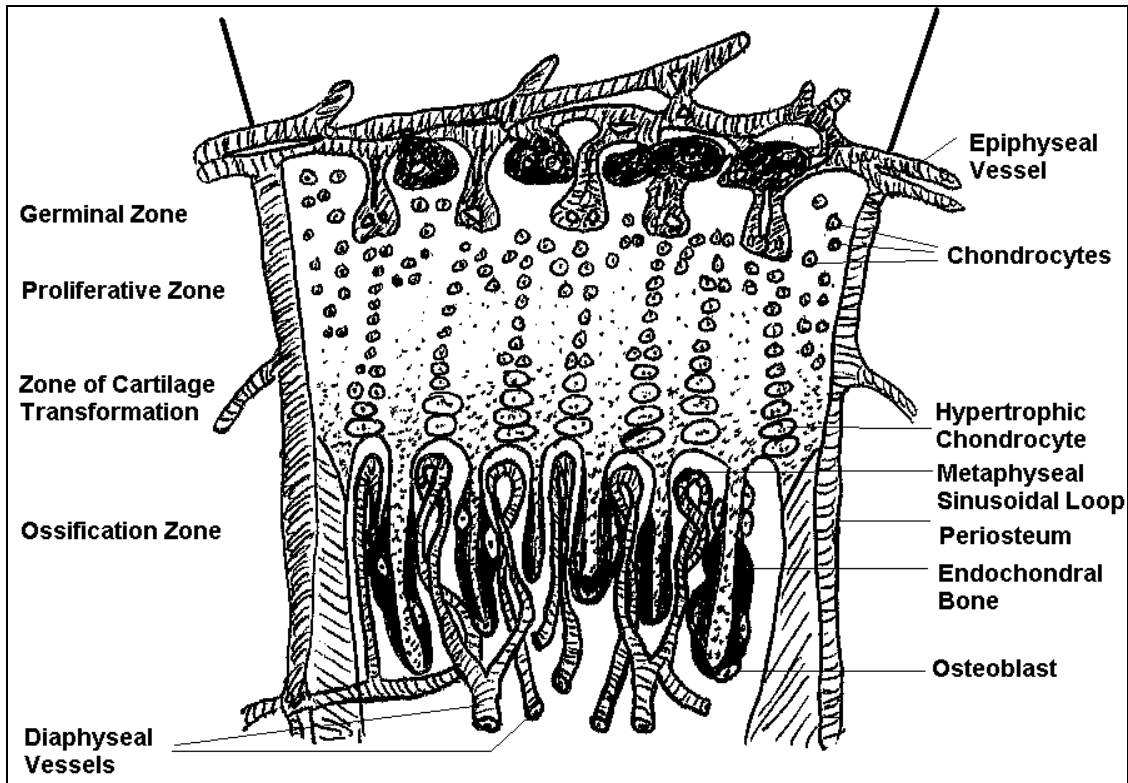


Figure 2.5: A summary of the major features of a diaphyseal growth plate adapted from (Scheuer and Black, 2000).

the zone of ossification and the resulting mature trabeculae form the secondary spongiosa.

7. More blood vessels form during growth because of the constant need to bring nutrients to the newly developing bone.

8. Secondary ossification centres appear at the epiphyses of long bones and more blood vessels form to bring nutrients to these areas. In bones such as the carpals and tarsals, there is a variation in the number and location of secondary ossification centres.

9. The development of a medullary cavity occurs through osteoclastic resorption and the endosteum begins to form. Then bone marrow begins to develop in the newly created cavity. The epiphyses do not have separate medullary cavities. The smaller bones do not develop medullary cavities but all bones have some degree of marrow within their trabecular structure.

10. The articular cartilage forms and remains to form the joint margins.

When the epiphysis and diaphysis of a growing long bone become adjacent to one another, the diaphysis will gradually fuse with the epiphysis via the creation of mineralised bridges until the hyaline-cartilaginous growth plate has been completely replaced by bone and bone marrow (Haines, 1975), making a complete bone. Todd has separated this union process into a nine stage process (Todd, 1930). The articular cartilage remains at joint surfaces to form the joints and prevent attrition.

Long bones must also have a mechanism for increasing their diaphyseal circumference and their length. They do this by subperiosteal addition of bone combined with endosteal resorption. This mechanism ensures that the cortical bone layer does not become too thick, which would therefore make the bone much heavier and mechanically disadvantaged. The size, shape and density of the cortical and trabecular bone will generally develop to a stage at which they are sufficiently strong and light to accommodate loading and activity to which the skeleton is normally exposed.

## **2.7 Mineralisation**

Once the matrix vesicles are produced by osteoblasts and/or chondroblasts, normal mineralisation requires the enzyme alkaline phosphatase, normal pH, calcium and phosphate ions and the active metabolite of vitamin D  $1,25(\text{OH})_2\text{D}$  to enable mineralisation of osteoid and crystal formation. The formation of matrix vesicles is aided by vitamin D and its metabolites and alkaline phosphatase. As the crystals grow and proliferate, the matrix vesicles break down and the crystals are exposed to the matrix. During that process, collagen fibrils and other non-collagenous proteins such as osteopontin and osteonectin help to determine the organisation and orientation of the crystal (Christoffersen and Landis, 1991, Sommerfeldt and Rubin, 2001).

Mineralisation can also occur as the result of crystals forming at sites on collagen fibrils. Although the mechanism for the formation of these crystals outside the vesicle microenvironment is not completely understood, there may be an association of mineral in the collagen matrix with the mineral in vesicles, such as minerals in vesicles serving as a calcium and phosphate ion source to assist early collagen-based mineralisation (Lian et al., 1999, p25). However, one feature the two mineralisation processes have in



common is the need for calcium and phosphate ions (Christoffersen and Landis, 1991, Mundy, 1999).

Vitamin D deficiency reduces the mineral-osteoid ratio and particularly affects endochondral ossification (Mughal, 2002). If the vitamin D deficiency is sufficiently severe it is referred to as rickets in childhood and osteomalacia in adulthood. It results in growth plate expansion and non-mineralised bone matrix, leading to bone deformities (Mundy, 1999) such as abnormal curvature of the spine or bowed legs. Further information regarding vitamin D deficiency and the effects of vitamin D on the growth plate are discussed in Chapter 4.

## **2.8 Bone Modelling and Remodelling**

Modelling is the process by which many bodily tissues, including bone, are grown, developed and organised into an optimally functional structure, which takes place both before and after the birth of an organism (Frost, 2004b). The growth rate of tissues and their elements are genetically determined and highly regulated processes. Remodelling refers to tissue turnover in small areas and this process continues throughout life (Frost, 1966b). Remodelling begins in childhood while bone is still being modelled to change the physical dimensions of bones from those of a child to those of an adult. The mechanism that performs this remodelling/bone turnover is called the Basic Multicellular Unit (BMU) (Frost, 1966a, Frost, 1966b). Osteoclasts, osteoblasts and bone-lining cells are present in a cylindrical structure that is able to burrow through cortical bone or erode a trench in trabecular bone and remodel as it advances. Osteoclasts are located at the burrowing end, osteoblasts are in the middle section and bone-lining cells are at the rear. The end result of each cortical BMU is one new osteon (Parfitt, 1994) and in trabecular bone the end result is a partially remodelled trabecula (Frost, 2004b). The lifespan of a BMU can be from six to twelve months (Parfitt, 1994). The movement of BMUs and the amounts of bone resorbed and formed are directed to achieve an optimum structure. The initial appearance, location and then subsequent disappearance of BMUs, are precisely controlled activities (Frost, 1966b). In order for new BMUs to appear and maintain their activities, new bone cells must form and other elements such as nerves, blood vessels and connective tissue must grow and remodel

alongside (Parfitt, 1994). The main function of remodelling after growth has ceased is to replace older bone that may be fatigued or damaged. On a microscopic level these signs of fatigue are collectively known as microdamage, which was first documented by Frost (Frost, 1960).

Bone remodels due to increased or decreased mechanical loading as demonstrated in experiments performed by Rubin and Lanyon (Rubin and Lanyon, 1984) and explained by the Mechanostat theory introduced by Frost (Frost, 1996). That is, adequate muscle function and normal weight-bearing leads to normal bone development, geometry and mineral content, all of which are constantly evolving to optimise the overall structure of bone to prevent fractures (Frost, 1996). Mechanical loading causes strains on bones, which generate signals detected by osteocytes and to which many other cells respond. These signals have genetically determined threshold ranges that help to regulate modelling and remodelling. Modelling is activated to strengthen load-bearing bones when strains exceed the threshold range and disuse-mode remodelling is activated to reduce bone strength by removing cortical bone adjacent to the marrow cavity (endocortical) and trabecular bone when strains are constantly below the threshold range (Frost, 2004a). This then reduces the amount of trabecular bone by expanding the marrow cavity and thinning cortical bone, which can eventually result in disuse-pattern osteopenia, for example, in those without the use of one or more limbs (Schoenau and Frost, 2002).

During growth, the modelling process dominates, but remodelling begins to dominate when skeletal maturation is reached (Frost, 1966b). An imbalance in the bone formation-resorption cycle can lead to certain disease states due to the fact that as people age, the newly deposited bone is not able to completely replace the amount of resorbed bone. An example of this is post-menopausal and age-related osteoporosis.

### 2.8.1 The Remodelling Cycle

The remodelling cycle has five main phases: activation, resorption, reversal, formation and resting (Fig 2.6).

1. **Activation:** Pre-osteoclasts appear as a result of a signal to activate the remodelling cycle and fuse to create large multinucleated osteoclasts.
2. **Resorption:** Osteoclasts resorb bone, leave behind resorption pits, then undergo apoptosis.
3. **Reversal:** Mesenchymal osteoblast pre-cursors appear near the recently created resorption pit. They proliferate and differentiate into pre-osteoblasts and finally mature osteoblasts, which are then ready to fill in the resorption pit by creating new bone.
4. **Formation:** The osteoblasts begin forming osteoid matrix.
5. **Resting:** The newly deposited matrix gradually becomes mineralised and the site then lies dormant (the resting phase), pending the next cycle of bone remodelling.

Through the remodelling sequence, the human skeleton is able to renew and repair itself and therefore maintain the ability to perform its three primary functions.

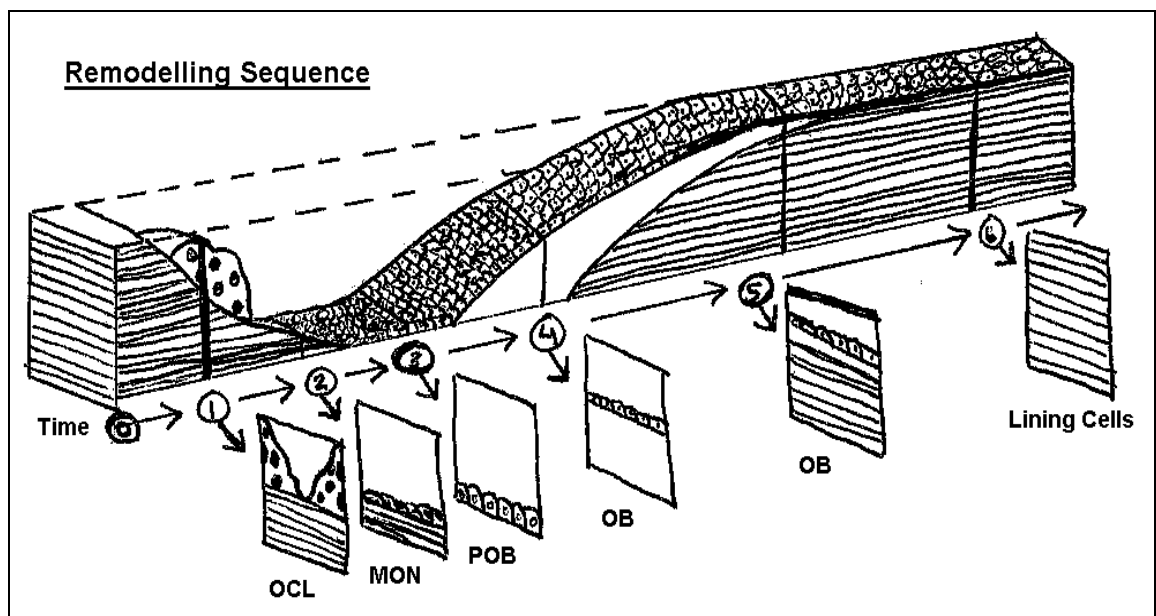


Figure 2.6: Illustration of the stages of trabecular bone remodelling adapted from (Parfitt, 1994). Key: OCL-osteoclasts beginning to resorb bone that was just previously in a resting state. MON-mesenchymal cells appear. POB-osteoblast pre-cursors appear during the reversal phase. OB-Matrix formation by osteoblasts before and during the onset of mineralisation. The last stage shows the completed new 'hemi-osteon', using Parfitt's terminology, covered by bone lining cells.

## **2.9 The Utah Paradigm of Skeletal Physiology and the Mechanostat**

The Utah Paradigm of skeletal physiology is an all encompassing theory that attempts to explain, to the best of current knowledge, how bones grow, develop and adapt. The Paradigm in its initial form was introduced in the 1950's and 1960's over several books and articles (Weinmann and Sicher, 1955, Snapper, 1957, McLean and Urist, 1961), but has since undergone major redevelopments in the 1990's and the millennium by Frost (Frost, 1998, Frost, 2000b, Frost, 2000a, Frost, 2001a, Frost, 2001b, Frost, 2004b, Frost, 2004c). To summarise, the Utah Paradigm states:

1. Bone geometry and strength are partially determined by mechanical forces acting upon bones.
2. Bones can endure normal mechanical usage (levels of 'normal' usage will change throughout life) without failing (fractures).
3. These mechanisms require non-mechanical factors such as vitamins, minerals, hormones, genetic factors and other factors to function appropriately.
4. Mechanical factors guide the non-mechanical factors in terms of generating signals that control the activity (including the activity of bone cells) and levels of non-mechanical factors.
5. These factors together determine bone health. Abnormalities can contribute to bone and associated tissue, such as cartilage, tendon and ligament disorders (Frost, 1997).

The Mechanostat theory is a large part of the Utah Paradigm as it deals with the adaptation of load-bearing bones in response to mechanical forces (Frost, 1987). The Mechanostat consists of four key areas:

1. Genetically determined conditions at baseline.
2. Mechanotransducers (loads that generate signals), which activate or de-activate biologic pathways or mechanisms at tissue level.
3. Minimum effective strain (MES) thresholds for modelling, remodelling, fracture, adaptation and pathology, which are genetically determined.
4. Feedback loops for the MES thresholds (Jee, 2006).

The Mechanostat is important to the current study because loading and strain are important in determining bone shape.

## **2.10 The Functional Muscle-Bone Unit**

The Muscle-Bone Unit or Functional Muscle-Bone Unit is an index that uses bone mineral content (BMC) per unit of cross-sectional muscle area (CSMA) as an index of musculoskeletal adaptation (Schoenau et al., 2002a). Muscle strength and usage have a corresponding effect on bone strength. On average, over 2kg of muscle force is required to move 1kg of body weight, but it is not body weight that exerts the largest voluntary loads on load-bearing bones, it is muscle forces (Schoenau and Frost, 2002). Muscle strength increases from birth to young adulthood and then declines throughout middle and old age until at age 80 years, less than half of the muscle strength present in young adulthood remains (Schoenau and Frost, 2002). Therefore momentary muscle strength (i.e. the muscle strength that is present at any given moment during life), has a profound influence on bone strength. In addition to exercise, these factors include Vitamin D, growth hormone, androgens and calcium (see Chapter 4).

Assessment of muscle strength and bone strength in relation to each other is important. This can be determined in a clinical situation by a dual-energy X-Ray absorptiometry (DXA) scan or a Quantitative Computed Tomography (QCT) / Peripheral Quantitative Computed Tomography (pQCT) scan. Both DXA and QCT/pQCT scans can measure lean body mass, which consists mostly of skeletal muscle. Using algorithms and software provided by the manufacturer, a DXA scan can determine if muscle size is adequate for height and whether bone mineral content (BMC) is normal. If both are normal then the result of the scan is normal. If BMC is too low for muscle size, then a diagnosis of a primary bone defect is made, such as osteoporosis. If muscle size is inadequate for height, but BMC is normal, a diagnosis of a secondary bone defect is made, such as disuse-pattern osteopenia. If both muscle size and BMC are inadequate, then a diagnosis of a mixed bone defect (primary and secondary) is made (Schoenau and Frost, 2002, Fricke and Schoenau, 2007).

## 2.11 Biomechanics of the Human Skeletal System

Biomechanics is the science concerned with forces and their effects, as applied to biological systems. 'Stress' is the term used to describe the force or amount of mechanical loading put onto a bone. There are many types of stress including compressive, tensile, and shear. 'Strain' is the term used to describe the amount of deformation that occurs as a result of the stress. There are 2 types of strain: elastic strain is not permanent. A bone undergoing elastic strain will return to its original shape after the stress is discontinued. Plastic strain is permanent, and bone undergoing plastic deformation will undergo a permanent shape change, or will fail completely (fracture). There are several different types of stress or loading that a long bone can undergo. These include tension, compression, bending, shear and torsion (Fig. 2.7).

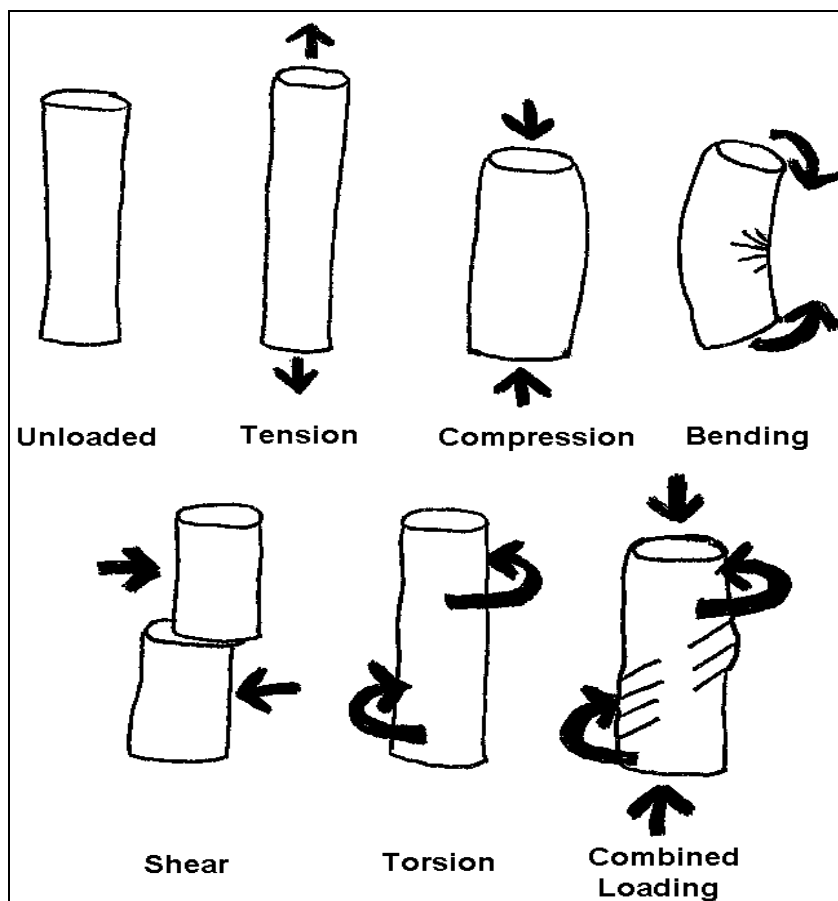
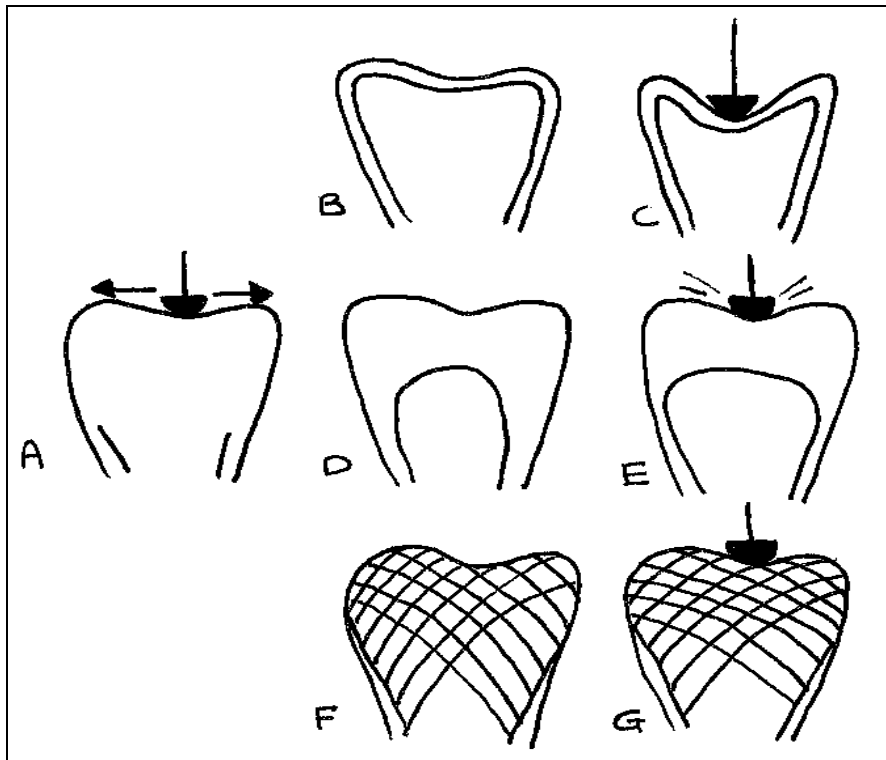


Figure 2.7: Types of stress bones can undergo in vivo, adapted from (Frankel and Nordin, 1980).

The human skeleton has evolved to deal with the stresses to which it is exposed. The structure of the dense outer shell of cortical bone, with an inner lattice framework of trabeculae, is able to adapt to stress in visible patterns. This was first noted by Julius Wolff in 1892 in his First Law: form follows function (Wolff, 1892). The joints connecting long bones are a perfect example of this adaptation. Loading in humans and other vertebrates must be transmitted from one long bone to another through a joint that has a larger articular surface area than the diaphysis of either long bone. The cartilage, along with a thin layer of subchondral bone and trabecular bone in the joint area are designed to spread the load over a larger surface area without allowing the joint surface to undergo large deformations (Curry, 2002). If there was no trabecular bone, the joint surface would undergo large deformations under compression loading, and if the epiphysis/metaphysis was solid i.e. without a trabecular network, a severe compression impact would destroy the articular cartilage (Curry, 2002) and could cause acute microdamage and/or macro-fractures (fractures visible to the naked eye using Radiographs). This is illustrated in Figure 2.8.

The epiphysis and metaphysis can, under certain disease conditions, expand to abnormal dimensions to compensate for a thinner diaphysis; this will be discussed in Chapter 4. Frequency (the number of occurrences of an event per unit of time), duration (the total amount of time for which the event is undertaken), and intensity (how much work, as a percentage of the maximum heart rate, is achieved during the event) will affect bone strength. If frequency, duration and intensity are too high, bone remodelling will not be able to adapt sufficiently rapidly to such increased loading and fatigue fractures will occur (Frankel and Nordin, 2001). Weightlifting is a good example of an activity that subjects the skeleton to compression, bending and combined loading. In contrast, marathon runners improve muscle strength and cardiovascular ability, but bone strength remains more or less unaffected because of the different type of load (intermittent and less intense than weight-lifting) that running places on the skeleton (Schoenau and Frost, 2002).



**Figure 2.8: Examples of metaphyseal design. (A) represents a load being placed on a bone. (B) represents a bone with only a thin cortical shell for support, and when this design undergoes loading (C), there are large bone deformations. (D) represents a metaphysis with a thick cortical shell to prevent large deformations, but when this undergoes loading (E), it produces high local stress on impact, which could damage the articular cartilage. (F) represents a metaphysis with a thin cortical shell and a network of trabeculae. When this design undergoes loading (G), only small deformations occur because the impact is absorbed by the trabecular network. Adapted from Curry, 2002).**

## 2.12 Distal Radial Fractures

Fractures of the distal forearm are the most common fracture site in children (Cooper et al., 2004, Landin, 1983). Risk factors for fracture in children and adolescents include chronic illness, early age of first fracture, endocrine disorders, e.g. Growth Hormone Deficiency (GHD), family history of fractures, genetic disorders e.g. OI, high intake of carbonated drinks, poor overall nutrition with particular emphasis on low calcium, Vitamin D and protein intake, low birth weight, low BMD and/or BMC levels, low levels of physical activity, intake of bone thinning medications e.g. corticosteroids, being overweight or obese and smoking (Goulding, 2007). However, most children presenting with distal forearm fractures are healthy with very few children taking bone-thinning medications such as glucocorticoids, having chronic illness, or being diagnosed



with endocrine/genetic disorders (Goulding, 2007). Why then do apparently healthy children have such a high incidence of fracture around the age of puberty? One pQCT study found that in the metaphysis of younger subjects, although there was an increase in total BMD, there was a much greater increase in cross-sectional area (CSA), leading to an overall decrease in BMC (Rauch et al., 2001b). Therefore the radius was not able to widen sufficiently compared to the rapid longitudinal growth. Ferrari and colleagues did not find significant differences in the BMDa and BMAD levels between fracture and non-fracture groups but they did find lower BMC levels (Ferrari et al., 2006). Numerous other DXA studies have found lower BMC and BMD levels in fracture groups (Black et al., 2002, Davidson et al., 2003, Goulding et al., 1998, Goulding et al., 2000, Goulding et al., 2001, Goulding et al., 2003, Goulding et al., 2004, Jones et al., 2002, Rockell et al., 2005). The increase in strength and mineralisation of the distal radius during growth is not as advanced as the increase in mechanical challenges caused by a fall and because the rate of endocortical apposition is already very high at that site, it appears that it cannot increase further to the levels necessary to keep bone strength adapted to mechanical requirements (Rauch et al., 2001a).

### **2.13 Summary**

Bone functions as part of an adaptive system; bone is able to adapt to the strains or loads placed upon it. Bone does this using a complex interconnected network of cells that are able to sense changes in conditions and deposit or resorb bone where required so that it has the optimum structure, density and mineral content for purpose. Ossification, mineralisation, remodelling and muscle-loading all work together to achieve a normal morphology and are essential parts of the adaptation system. These factors contribute to strain thresholds that allow bone to withstand forces that could cause fracture. Strain thresholds are reduced during puberty at the distal radial metaphysis due to the growth spurt and osteoid not being able to mineralise at a rate fast enough to keep up with the growth rate. The optimum morphology and density in a normal individual will be different for each person based on his/her daily activities, along with genetic, hormonal and nutritional factors, which are discussed in Chapter 4.

### **3. Imaging and Quantitative Assessment of the Skeleton**

#### **3.1 Introduction**

Bone can be quantitatively assessed in vivo using imaging techniques. Clinically, the techniques available for measuring bone mineral in children are the same as those used in adults, but due to the reduced availability of normal values for children, selecting an imaging technique and interpreting the results (Petit et al., 2005) becomes more difficult. This is because growth is non-linear and children of the same age can have different levels of skeletal maturity. Also, children of different ages, heights, weights and ethnicities cannot necessarily be compared to one another easily. This situation is however, beginning to change with the publication of more paediatric reference data (Ward et al., 2007a, Ward et al., 2007b, Zemel et al., 2008).

The beginning of this chapter discusses X-rays in terms of how they form an image and the differences between film-based and modern digital radiography systems. Subsequently, three imaging techniques will be discussed in terms of what they are, how they work and their use in paediatric studies. First: radiogrammetry and digital X-ray radiogrammetry (DXR), second: peripheral quantitative computed tomography (pQCT) and third: dual energy X-ray absorptiometry (DXA). Although not a means of acquiring images, an introduction to bone-ageing has also been included in the section on X-ray imaging due to its relevance to the current study and due to the necessity of having paediatric hand-radiographs in order to carry out a bone-age assessment.

#### **3.2 X-Rays and Radiographs**

##### **3.2.1 Introduction to X-Rays and the Production of Radiographs**

X-rays are a form of high frequency electromagnetic ionising radiation with a range of 0.01 to 10 nanometres in the electromagnetic spectrum. X-ray imaging is a widely used technique that produces radiographs, which are created by passing X-rays through the body to a specially prepared film, or digital receptors, that capture the images. Different tissues attenuate X-rays to different degrees. Relevant topics include resolution, dose, contrast, how radiographs are produced and their use in bone-age assessment, which are discussed below. Further discussion regarding the Photoelectric Effect, the Compton

Effect, attenuation co-efficients and X-ray production and detection are discussed in Appendix 2 (Section 12.2).

### **3.2.2 How Radiographs Are Acquired**

There are two methods of acquiring a radiograph: using radiographic film or using digital detectors. The radiographic film method consists of a base of transparent acetate, one or two coatings of emulsion and normally an intensifying screen. The emulsion consists of small grains of silver bromide suspended in gelatin. When the film is exposed to radiation, the silver grains are sensitised, forming a latent image. The development process causes a darkening of the sensitised silver grains, which are retained and result in the opaque areas seen on a radiograph. The silver grains that are unsensitised are removed, resulting in the transparent areas seen on a radiograph. Intensifying screens are used to enhance the resulting image because on its own, radiographic film only has a certain amount of sensitivity to X-rays. These screens consist of a fluorescent material placed in proximity to the film. When the screens are exposed to radiation, they interact with the fluorescent material, which then emit photons of visible light. The visible light photons then interact with the emulsion and expose the film. Films are kept in sealed cassettes to prevent accidental exposure to ambient light, and are developed in a dark room.

In digital radiography, the latent X-ray image is captured on an image plate. An image plate contains a screen that consists of phosphor crystals embedded in a binding agent and mounted on an underlying layer of plastic (Cowen, 2007). The most common phosphor material is "...barium fluorohalide activated with divalent europium ions (BaFX:Eu<sup>2+</sup> where X typically represents bromine and iodine atoms)" (Cowen, 2007). The image plate is housed in a lightproof container or cassette. When exposed to X-rays, the image plate releases electrons. Over time, the electrons would return to ground-state and release light photons. However that process, if left to occur naturally, would take several hours and cause the image to decay. Instead the image plate and cassette are fed into a computed radiography image reader. Inside the reader, the image plate is passed through a laser scanning bed and is exposed to red laser light from a solid-state laser diode. Exposure to the red laser light causes the electrons to return to

ground-state and the subsequent release of light photons, referred to as laser-stimulated phosphorescence. The emitted light photons are transported to a high-sensitivity photomultiplier tube where they are converted to an electronic current, which is then amplified, filtered, and digitised using an analogue to digital converter. The resulting images can then be accessed and viewed using the Picture Archiving and Communication System (PACS), which is currently replacing plain film radiography (Wiley, 2005). The image plates themselves are re-usable and can pass through several thousand cycles (Cowen, 2007).

### **3.2.3 Resolution, Dose and Contrast**

In plain film radiography, an advantage of the film-screen method is its high sensitivity, which allows radiographic images to be obtained using a very low dose of radiation (Kane, 2005). For example, the Effective Dose Equivalent in the University of Manchester Department of Clinical Radiology for a hand radiograph is 0.00017 mSv (Ashby, 2007). A disadvantage of the method is that the high level of spatial resolution (approximately 0.02 mm) that can be achieved using the film only method, is lost in the film-screen method due to visible photons fanning out when they interact with the film, causing the spatial resolution to be reduced to approximately 0.1 mm (Kane, 2005). The contrast of a radiographic image is dependant on many factors including tissue attenuation, electron scatter, as well as the recording, processing and displaying processes. This is important to bone-age assessment and measurement of the MI. If blurring of bone detail occurs, an incorrect bone-age might be determined. If blurring of the bone-edge occurs, it can be difficult to accurately measure the GPW and MW, therefore giving rise to an incorrect MI.

### **3.3 Radiogrammetry & Digital X-Ray Radiogrammetry (DXR)**

Radiogrammetry utilises radiographs and is a technique in which the dimensions of bones were originally measured with the aid of callipers and a light box. Virtama and Mahonen (Virtama and Mahonen, 1960), and Barnett and Nordin (Barnett and Nordin, 1960) were the first to use hand radiographs to assess cortical bone width as a criterion for bone strength, i.e. if the cortex of a bone thinned over time, this would indicate bone

loss, and bone strength would subsequently be affected. Although this technique was inexpensive and widely used, it had limited reproducibility (coefficient of variation (CV) ~10%), requiring longitudinal studies to extend over longer periods (Adams et al., 1969). With the advent of other densitometry techniques, such as single energy X-ray absorptiometry (SXA) and dual energy X-ray absorptiometry (DXA), radiogrammetry was not widely used for many years (Black et al., 2001). This change was due to the ability of DXA especially, to calculate bone mineral content, fat content and muscle content without requiring body-part thickness. Once radiographs became digitised however, specialised computer software was able to automatically detect bone and quantify bone mineral density and cortical thickness. An example of this is the Sectra Pronosco system (Linköping, Sweden) for evaluating cortical bone thickness in the second, third and fourth metacarpals, and also the radius and ulna (Black et al., 2001) with improved precision compared to manual radiogrammetry (Ward et al., 2007a). Computer-aided radiogrammetry is often referred to as digital X-ray radiogrammetry (DXR). DXR measurements can also be used to help determine whether bone loss is due to a decrease of periosteal surface apposition and/or an increase in endosteal resorption (Shore and Poznanski, 1999). While measurements such as these cannot diagnose a specific disease, any abnormalities detected can then be assessed by other methods. Radiographs of the hand/wrist have an additional advantage that they are often the first diagnostic test taken, in both children and adults, to assess trauma of the hand/wrist in a suspected fracture and for bone-ageing purposes. Another advantage in using hand radiographs is the small absorbed radiation dose received,  $<1\mu\text{Sv}$  (Huda and Gkanatsios, 1998). Even if several radiographs are taken, the dose is unlikely to exceed  $10\mu\text{Sv}$  (Tohill, 1989). With appropriate computer software, DXR can also measure cortical porosity (Nielsen, 2001). The clustering of osteons can subsequently create Haversian canals with excessively large diameters leading to reduced bone strength. This has been reported as a possible cause of femoral neck fracture together with cortical thinning (Bell et al., 1999, Jordan et al., 2000). A disadvantage of radiogrammetry is that it does not quantify trabecular bone (Shore and Poznanski, 1999).

### **3.4 Bone-Age Assessment**

Bone-age assessment encompasses several methods of determining skeletal maturity. Paediatric endocrinologists use bone-age to determine whether skeletal maturity is occurring at the same rate as the chronological ageing process and how far apart the bone-age is from the chronological age. It is not unusual for there to be a slight difference in the two ages because the ageing process will be different in each individual. However, if there is more than a 2 year difference, further investigation may be warranted (Mughal, personal communication). This is important as extremely delayed or advanced bone-age in comparison to chronological age can be a sign of an endocrine disorder or genetic disease (Gilsanz and Ratib, 2005).

There are three well known bone-age assessment methods: Tanner-Whitehouse I, II and III (Tanner et al., 1962, Tanner et al., 1983, Tanner et al., 2001), Greulich-Pyle (Greulich and Pyle, 1950, Greulich and Pyle, 1959) and the Fels (Roche et al., 1988). There is also a relatively new method called the Gilsanz-Ratib method (Gilsanz and Ratib, 2005). All of these methods use hand radiographs to estimate bone-age (which may differ from chronological age) and compare with controls of the same chronological age. The bones used in all of these methods include the distal radius and ulna, the carpals, metacarpals and phalanges (Fig. 3.1). As bone-age assessment involves comparing skeletal age with chronological age, any of the above methods could help to identify whether children are growing and developing normally. The advantage of the Greulich and Pyle (GP) method is that it takes relatively little time in comparison with the Fels method, as the GP method requires comparing one whole hand radiograph with those in an atlas of hand radiographs of American Caucasian males and females ranging in age from birth to middle age (Greulich and Pyle, 1959). The Fels method is computer-assisted and uses 98 statistically weighted age and sex-specific maturity markers of the hand and wrist, to obtain an overall bone age assessment (Roche et al., 1988). This is a very time consuming process, which involves taking numerous measurements. The Tanner-Whitehouse 3 (TW3) method is the most recent development, leading on from the original TW1 and subsequent TW2 methods. In the original method, the bones of the hand and wrist were given ratings with a numerical score. All the scores were summed to give a final score that related to a specific age or

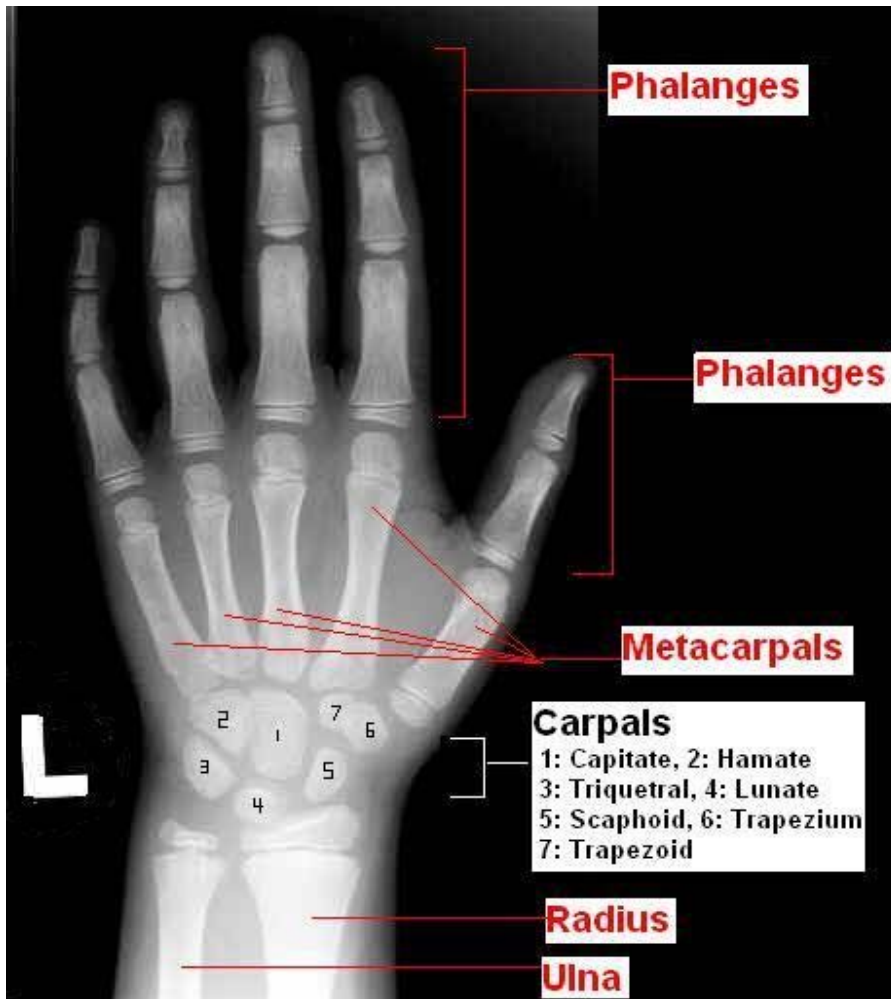


**Figure 3.1:** Paediatric left hand radiograph illustrating the groups of bones used in TW3 bone-ageing. The RUS group is shown in red and the CAR group is shown in black/white. Note the epiphyses of the bones in the RUS group have not fused; their sizes, shapes and degree of fusion to the diaphysis is a large part of bone-age assessment using any method.

age range. In the TW2 and TW3 methods, new reference data were added and slight changes in the scoring methods took place. Also in the TW3, instead of having a single score relating to a single age, the radius, ulna and short bones (RUS) and the carpal bones (CAR) each have separate scores. Therefore, an age range is the more common outcome in the TW3 method rather than a single age. The TW methods are more involved than the GP method, but not as time consuming as the Fels method. TW3 also has the advantage that it was based on a population from Britain, which has been updated from the original TW1 to include more modern population data from a more ethnically diverse background, whereas the Fels method is based on an American

Caucasian population gathered over several decades beginning in the 1930's. There remains a question as to whether the Fels method can be used successfully outside of America on a more ethnically diverse and modern population. TW3 has another advantage in that separate RUS and CAR scores can be useful because the carpal bones often mature earlier than the RUS bones. There is also evidence that the TW method is more reliable than the GP method (Dhar et al., 1993) and that RUS scores correlated more closely with radiograph standards (Wenzel et al., 1984), which is important to the methodology of the current study (see Chapter 5.4.8).

### **3.5 Peripheral Quantitative Computed Tomography (pQCT)**

A pQCT system like the XCT-2000 (Stratec, Pforzheim, Germany) contains hardware that is controlled by specialist computer software and, in a clinical setting, is operated by a radiographer trained in its operation. It uses an older CT technology of rotate/translate radiation beam and detectors to acquire images in  $x$  degree segments and back-projects to make a whole 360 degree representation of the bone. Slices are usually 1-2 mm thick with a voxel size (resolution) of 0.4mm and take approximately one minute to acquire. The newer conventional spiral body CT scanners use more recent CT technology (multiple detectors and continuous spiral rotation of the X-ray tube) to acquire 3 dimensional volume images extremely rapidly, i.e. whole torso in approximately 20 seconds. Both pQCT and central Quantitative Computed Tomography, (QCT) have the unique advantage of being able to quantify separately cancellous bone and cortical bone compartments and can also be used to examine bone size and geometry. Volumetric bone mineral density (BMD  $\text{g}/\text{cm}^3$ ) is less influenced by bone size (Gilsanz, 1998) than a 2-dimensional technique showing areal BMD (BMDa  $\text{g}/\text{cm}^2$ ) such as DXA. pQCT has more of an advantage over central QCT due to a lower radiation dose to the patient, as only the appendicular skeleton is irradiated (Gordon, 2004, Njeh, 2004, Ward et al., 2007a). Muller and colleagues estimated the radiation dose for peripheral scans at 0.1  $\mu\text{Sv}$  (Muller et al., 1989). Because pQCT can measure BMD and bone geometry, this allows the determination of other information such as the polar strength strain index (pSSI) (Ward et al., 2007a), which describes the strength of a bone in terms of bending and torsion and is calculated using the section modulus (the resistance of a bone to



stress) and the volumetric cortical BMD (Schiessl et al., 1996). The axial moment of inertia, which is a measure of the distribution of cortical bone mass around the centre of a cross-section of a tubular-shaped bone, can also be produced by pQCT (Quick et al., 2006). Furthermore, pQCT can be used to examine the cross-sectional area of muscle and therefore be used to examine whether bones have adapted well to the amount of muscle present, i.e. to mechanical loading (Ward et al., 2007a) in terms of the muscle-bone unit (Schoenau, 2005). Figure 3.2 illustrates a pQCT scanogram from which an

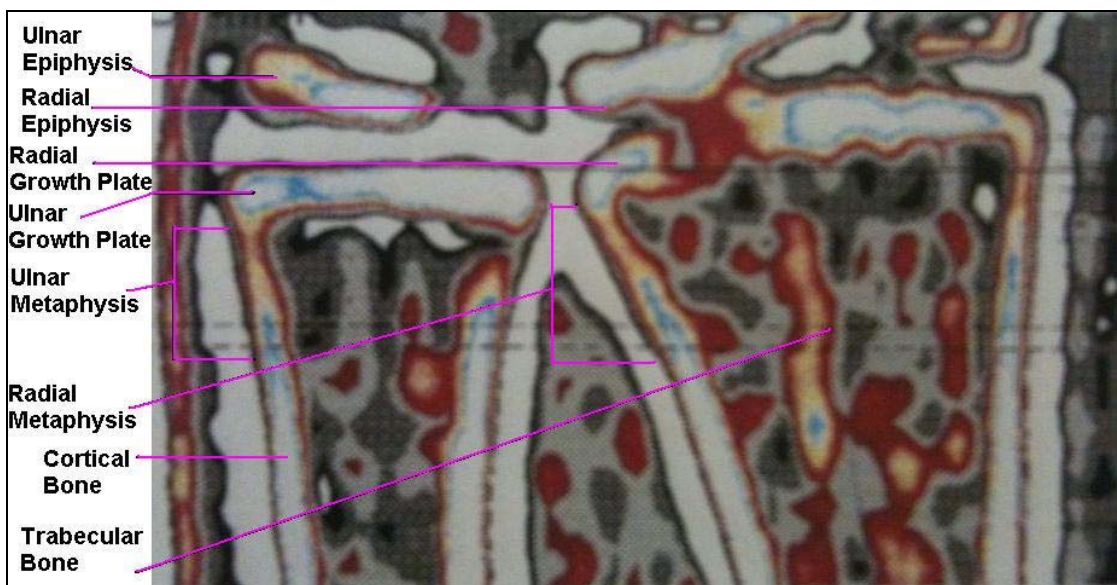


Figure 3.2: Illustration of a pQCT scanogram of the distal radius and ulna.

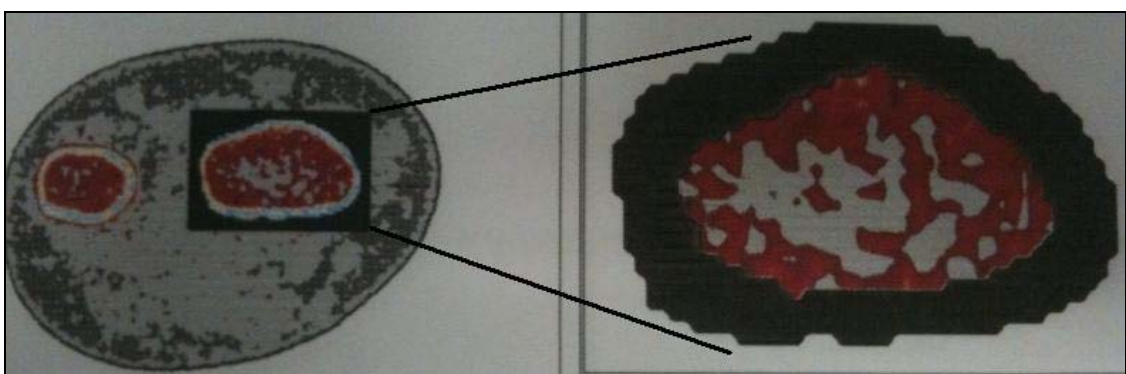


Figure 3.3: Illustration of a pQCT slice through the distal radius and ulna (left) and a close-up of the distal radius (right). The left image illustrates muscle and lean tissue (light grey), intramuscular and subcutaneous fat (dark grey), trabecular bone (red), and cortical bone (bluish white). The close-up image on the right illustrates the threshold used to analyse radial trabecular bone only.

image of the distal radius is obtained. From this scanogram, a reference line for scanning is determined; the forearm length is measured using a tape measure from the olecranon to the ulnar styloid process and then axial sections are measured at selected percentages of the forearm length, i.e. 4% distal and 50% midshaft. Figure 3.3 shows a slice through the distal radius and ulna. It should be noted that the section of the radius scanned for the 4% site is not the same in adults (diaphysis and epiphysis fused) as it is in children (growth plate and epiphysis unfused): the 4% site of the latter will be slightly more proximal, as the upper reference line is placed at the most distal part of the growth plate, while in an adult, the reference line will be adjacent to the articular cartilage (Neu et al., 2001a). pQCT has been used in human studies of adults (Guglielmi et al., 2000, Murray et al., 2006, Nara-Ashizawa et al., 2002, Roldan et al., 2001, Rauch et al., 2001c), children (Dyson et al., 1997, Leonard et al., 2004, MacDonald et al., 2006, Moyer-Mileur et al., 2001, Wang et al., 2005, Ward et al., 2005b) and combinations of adults and children (Neu et al., 2001a, Neu et al., 2001b, Rauch et al., 2001a, Rauch and Schoenau, 2005, Rauch et al., 2001b, Schoenau et al., 2002b). In addition, studies have been performed in animals such as rats (Breen et al., 1996, Ferretti et al., 1995), mice (Jamsa et al., 1998) and goats (Siu et al., 2003). These studies have used pQCT to examine attributes such as BMD, SSI, cross-sectional moment of inertia (CSMI), which is defined as a measure of mass distribution or area of known density, with respect to a given point or axis (Brianza et al., 2006). CSMI is a measure of bone rigidity, cross-sectional bone area (CSA), cross-sectional muscle area (CSMA), and bone strength index (BSI), which is defined as cortical BMD x CSMI (Ferretti, 1995). pQCT scans are performed using a specific threshold. The threshold refers to a mode that separates and disregards all voxels that register below the specified density. For example, in the case of cortical bone, a higher threshold is able to disregard the lower densities of trabecular bone, marrow, fat and muscle. The main advantages of using this technique on both humans and animals are the abilities to assess bone geometry and to differentiate between cortical and trabecular compartments.

There remains a question of adequate precision in terms of locating and reproducing the same regions of interest between institutions with different equipment and operators (Grampp et al., 1995) and the added disadvantage of scan times taking several minutes,

making this technique useful only for those who are able to remain still for the duration of the scan(s) (Ward et al., 2007a).

### **3.6 Dual Energy X-Ray Absorptiometry (DXA)**

DXA was originally referred to as Quantitative Digital Radiography when one of the original DXA machines (the Hologic model QDR-1000) was first described (Kelly et al., 1988). Like pQCT, DXA scans are performed by trained technicians, usually a radiographer. DXA acquires images using beams of two X-ray energies to differentiate bone from soft tissues, hence the name 'dual energy'. Various tissues in the body attenuate these energy beams to different degrees. Bone, muscle and fat are attenuated by high energy photons; muscle and fat are attenuated by low energy photons. BMC is calculated by defining the pixels of bone and multiplying this by the total area of these pixels. Figure 3.4 illustrates how tissues attenuate the beams of energy and how BMC is calculated.

DXA enables measurements of BMD not only at specific sites (i.e. lumbar spine L1-L4, proximal femur, femoral neck and forearm), but also for regional sites (i.e. arms and legs) and the total body. DXA also provides body composition parameters (i.e. lean muscle, BMC and fat mass) (Njeh and Shepherd, 2004). An added advantage is that DXA can calculate these body composition parameters without requiring body-part thickness. Other advantages include relatively fast scan times (1 minute or less), availability of paediatric reference data for > 5 year olds, good precision (CV of approximately 1%), and the low ionising radiation doses received (1-6  $\mu$ Sv) (Ward et al., 2007a). Depending on the site and also the brand of scanner used, the radiation dose will vary (Njeh, 2004). DXA also has some disadvantages. One study has shown that heterogeneous fat distribution in the soft tissues and bone marrow can affect the results, and depending on how the fat is distributed, it can erroneously either increase or decrease bone density (Hangartner and Johnston, 1990). This problem can limit studies not only with obese, but also anorexic children (Gilsanz, 1998).

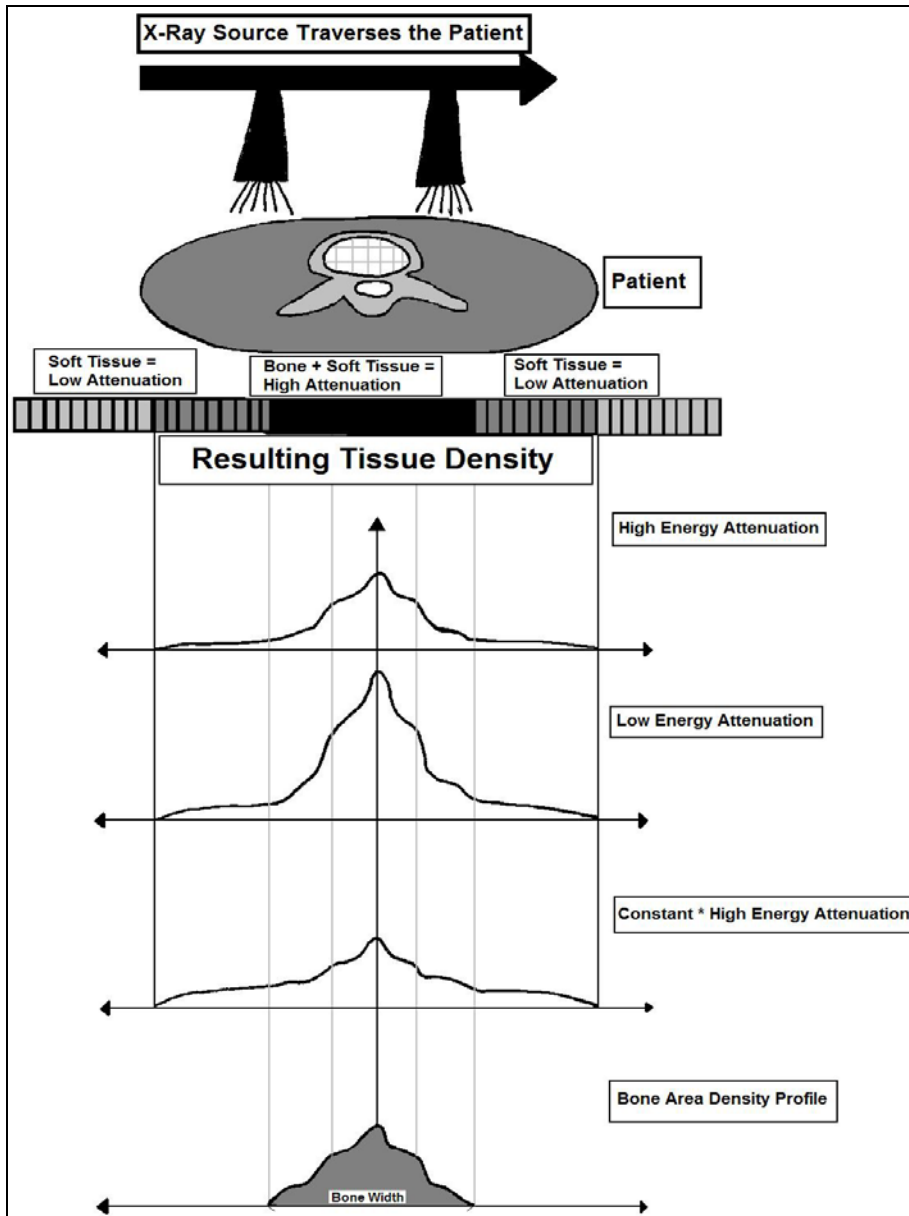


Figure 3.4: Bone profile, observed as the X-ray moves linearly across the patient, and the corresponding tissue density profiles, adapted from (Crabtree et al., 2007b).

Another disadvantage is that DXA provides a measure of integral BMD and cannot distinguish between trabecular and cortical bone (Gilsanz, 1998). DXA measures BMDa in  $\text{g}/\text{cm}^2$ , which is a 2-dimensional area measurement of a 3-dimensional structure. The depth of the bone is not taken into account making this measurement vulnerable to changes in size (Carter et al., 1992). This can be a problem in paediatric studies (Horlick et al., 2004) in which the size of a bone is always changing and the

BMD would be erroneously low in small bones. An advantage is the low ionising radiation doses received (1-6  $\mu\text{Sv}$ ) (Ward et al., 2007a). There are several methods used in an attempt to adjust for this problem, one of which is termed bone mineral apparent density (BMAD). This involves dividing the BMC by the bone volume derived from its projected bone area using a 3-dimensional shape as a model for a bone, e.g. a cube as a model for a vertebra or a cylinder as a model for the femoral neck (Carter et al., 1992, Kroger et al., 1992). Other methods include size adjusted BMC, the Molgaard method (Molgaard et al., 1997), correction using regression models (Prentice et al., 1994) and correction using lean tissue mass (Hagler et al., 2003, Schiessl et al., 1998). There is currently no consensus as to which method is the best, and a comparison of these methods in children showed no significant difference in the abilities of each method to detect children with bone densities that were falsely reported as low using standard adult algorithms (Fewtrell et al., 2005). It is likely that certain methods may be more or less appropriate to individual patients and research hypotheses, however the authors recommend the use of BMC adjusted for height and bone area, and BMAD because the calculations are easier to implement and the results are more straightforward to interpret (Fewtrell et al., 2005).

Other limitations include software that has been specifically developed to help detect low density bone in young children and adults (Crabtree et al., 2007a). Although this development in itself is advantageous, any results obtained using this software must be compared to reference data collected using the same type of software and scanner or the BMD will be artefactually over-estimated. Scanners vary by manufacturer (Njeh and Shepherd, 2004), and although there have been attempts to adjust for this by publishing standardised reference data in adults (Zemel and Petit, 2007), studies involving children and adults must take this into account before comparing results from different scanners. There is also a lack of reference data for ethnic groups (Zemel and Petit, 2007). People of Black African descent generally have larger and stronger bones than Caucasians but reference data exist mainly for Caucasians (Zemel and Petit, 2007).

DXA is currently the most widely used bone densitometry method applied to children in clinical diagnosis (Adams and Shaw, 2004). It has been used in original studies that examine levels of BMC and BMAD in children with relation to fractures (Bailey et al.,

1996, Beck, 2003, Clark et al., 2006, Ferrari et al., 2006), and other fracture risk factors, which include reduced calcium intake, obesity or previous fracture (Goulding et al., 1998, Goulding et al., 2000, Goulding et al., 2001, Goulding et al., 2005, Jones et al., 2002).

### 3.7 The Metaphyseal Index (MI)

Metaphyseal inwaisting is a process of rapid reshaping and remodelling that occurs during growth. Figure 3.5 illustrates the resorption/formation activities that occur. Endocortical drift and periosteal resorption drift serve to both expand the medullary cavity and move the constantly remodelling metaphysis towards its final length during the longitudinal growth of a long bone (Frost, 2004b). One of the aims of this study is to quantify this process by performing a measurement of the distal radial metaphysis called the metaphyseal index (MI). A research group based in Australia has recently published a paper detailing the measurement of the MI of the distal femur (Ward et al., 2005a). Their aim was to quantify the metaphyseal inwaisting process of the distal femur in children being treated with bisphosphonates, for localised disorders not directly affecting the distal femur metaphysis, and compare them to a larger database of age-matched

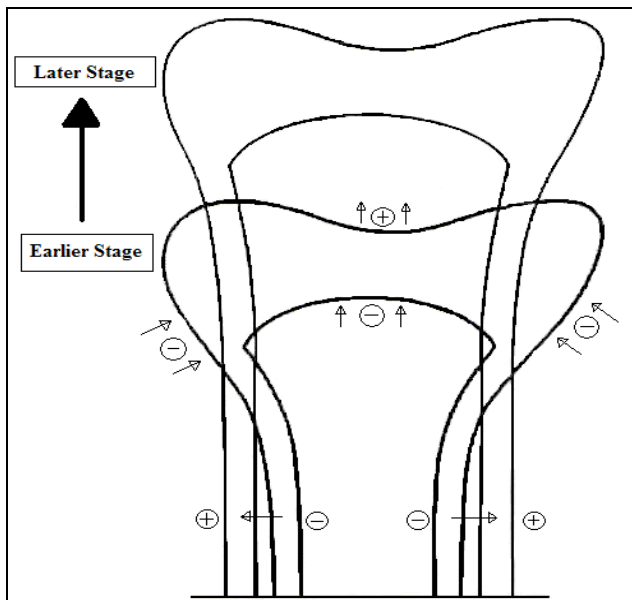


Figure 3.5: Resorption and formation during the growth of long bones, adapted from (Jee, 1983).

controls. Their results show that all twenty children who were being treated with bisphosphonates for localised disorders experienced normal inwaisting of the distal femur when compared with normal controls (Ward et al., 2005a). This was critical to their study as they were investigating whether bisphosphonates could be safely administered to children, and at appropriate doses, without disturbing bone growth and development. Their efforts have also produced a reference range of normal values for the metaphyseal index of the distal femur of children between the ages of five and fifteen (Ward et al., 2005a). They state specifically that although they "...chose to study the femur, similar methodology could be applied to the distal radius once a normative database is known" (Ward et al., 2005a, p1002). The main advantages in examining the distal radius are that it is the most common fracture site in children (Cooper et al., 2004, Landin, 1983) and hand radiographs are easily performed and taken regularly in children for a variety of reasons (i.e. bone-ageing), making it a good choice for study.

Activity levels also have a significant effect on bones. Young gymnasts have a much greater activity level and therefore a larger amount of repetitive stress placed on their bones compared to the average person. There is evidence that the size, shape and density of bone can all be altered due to increased stresses (Haapasalo et al., 2000, Kontulainen et al., 2003, Pettersson et al., 2000, Ward et al., 2005b). Certain diseases such as cerebral palsy (CP) can limit physical activity levels and this in turn has a detrimental effect on bone modelling/remodelling. Studies have shown that increasing physical activity levels can aid in altering bone architecture, thereby reducing bone fragility (Ward et al., 2006).

CP inhibits muscle function, making bone fragility a secondary consequence. But other diseases such as OI (Land et al., 2006), hypophosphatemic rickets (Rauch, 2006), mucopolysaccharidosis (Field et al., 1994), neurofibromatosis (Gupta et al., 1985) as well as drugs/treatments (Ward et al., 2005a) can have a direct effect on bone architecture and remodelling in children, including that of the metaphysis. Although some metaphyseal abnormalities will be obvious upon radiographic analysis (such as the popcorn metaphysis of an OI patient), this method is a way to quantify the results, therefore making it much easier to detect small changes and compare them longitudinally.

To this end, Land and colleagues (Land et al., 2006), have published a more recent study examining children with OI using the same technique. Children with OI can often experience less physical activity than normal children due to the risk of fracture in even the simplest of everyday activities. They found that pamidronate affects metaphyseal inwaisting by decreasing its speed, therefore resulting in an increased metaphyseal width (Land et al., 2006). The difference in results between the Land and Ward studies may be due to the fact that bones with abnormal inwaisting may be more sensitive to the effects of bisphosphonates than bones with normal inwaisting levels, or because the dosage and amount of time over which treatment occurred was higher in the Land study; 9 mg/kg/year over 2 or more years (Land et al., 2006) than in the Ward study, average 3.7 mg/kg/year over a mean of 1.35 years (Ward et al., 2005a).

### **3.8 Puberty and Tanner Pubertal Stages**

The Tanner Pubertal Stages are commonly used to assess the progression through adolescence and puberty for both males and females (Davison et al., 2003). The system rates, over five stages, the development of genitalia and pubic hair in males and pubic hair and breast development in females (Tanner, 1962). Tables 3.1 and 3.2 define these stages. Adolescents are often asked to rate themselves, or self-report, using the Tanner stages for their sex. Black and white drawings of the stages of genital, breast and pubic hair development for females, or genital and pubic hair development combined with an orchidometer (a string of 12 wooden beads approximating the size, shape and volume of the testes) for males are used. The sheets used for self-assessment can be seen in Appendix 12.3. It is important to note that there will always be a certain amount of error in every self-reporting system, however self-assessment is often preferable to being examined by a study investigator (Duke et al., 1980).



**Table 3.1: Descriptions of Tanner Stages for Males**

<b>Stage 1</b>	Pre-adolescent. Testes, scrotum and penis are about the same size and proportion as early childhood. The vellus over the pubes is not further developed than that over the abdominal wall, i.e. no pubic hair.
<b>Stage 2</b>	Enlargement of scrotum and of testes. The skin of the scrotum reddens and changes in texture. Little or no enlargement of the penis at this stage. Sparse growth of long, slightly pigmented downy hair, straight or only slightly curled, appearing chiefly at the base of the penis.
<b>Stage 3</b>	Enlargement of penis, which occurs at first mainly in length. Further growth of testes and scrotum. Pubic hair is considerably darker, coarser and more curled. The hair spreads sparsely over the pubes.
<b>Stage 4</b>	Increased size of penis with growth in breadth and development of glands. Further enlargement of testes and scrotum; increased darkening of scrotal skin. Hair now resembles adult in type, but the area covered by it is still considerably smaller than in the adult. No spread to the medial surface of the thighs.
<b>Stage 5</b>	Genitalia adult in size and shape. No further enlargement takes place after stage 5 is reached. Pubic hair is adult in quantity and type with distribution of the horizontal pattern. Spread to medial surface of thighs but not up linea alba or elsewhere above the base of the inverse triangle.

**Table 3.1: Tanner Stage descriptions of male genital and pubic hair development (Tanner, 1962).****Table 3.2: Descriptions of Tanner Stages for Females**

<b>Stage 1</b>	Pre-adolescent: elevation of papilla only. The vellus over the pubes is not further developed than that over the abdominal wall, i.e. no pubic hair.
<b>Stage 2</b>	Breast bud stage: elevation of breast and papilla as small mound. Enlargement of areolar diameter. Sparse growth of long, slightly pigmented downy hair, straight or only slightly curled, appearing chiefly along the labia.
<b>Stage 3</b>	Further enlargement and elevation of breast and areola, with separation of their contours. Pubic hair is considerably darker, coarser and more curled. The hair spreads sparsely over the pubes.
<b>Stage 4</b>	Projection of areola and papilla to form a secondary mound above the level of the breast. Hair now resembles adult in type, but the area covered by it is still considerably smaller than in the adult. No spread to the medial surface of the thighs.
<b>Stage 5</b>	Mature stage: projection of papilla only, due to recession of the areola to the general contour of the breast. Pubic hair is adult in quantity and type with distribution of the horizontal pattern. Spread to medial surface of thighs but not up linea alba or elsewhere above the base of the inverse triangle.

**Table 3.2: Tanner Stage descriptions of female breast and pubic hair development (Tanner, 1962).**

Epiphyseal fusion occurs earlier in girls than in boys. This is due to females being physically more mature at birth, in utero and throughout the growth period (Tanner, 1962). At birth, females are less than 1 month ahead of males, but by the mid-point between birth and puberty, females have increased their lead by several months, and by puberty the difference is approximately 2 years (Tanner, 1962). Puberty and skeletal maturity are closely related. In fact, puberty is much more related to skeletal maturation than it is to chronological age (Tanner, 1962). In normal circumstances, children who reach maturity faster and begin puberty earlier are often shorter in stature than those who mature at a slower rate (Tanner, 1962). This is because sex-steroids or hormones, which play an essential role in puberty, also play an essential role in determining the timing of the cessation of bone growth, e.g. epiphyseal fusion (Perry et al., 2008). This then leads back to hormonal actions on the normal growth plate and hormonal disorders discussed in Chapter 4.

### **3.9 Summary**

All of the imaging and assessment techniques discussed here are essential for the study of paediatric skeletal and other conditions, both in terms of research and for clinical diagnoses. Radiographs are a front-line imaging technique that can be performed in seconds and doses incurred on peripheral imaging are often less than those incurred on overseas air travel. DXA and pQCT require more scan time and more complex equipment, but they can both provide invaluable quantitative information such as muscle and fat content, as well as bone density and area respectively. Bone-ageing using paediatric hand radiographs are essential for diagnosis of endocrine disorders such as Constitutional Delay of Growth and Puberty (CDGP), and along with Tanner Pubertal Stages, can provide information on whether children are growing and developing properly.

## **4. Factors Affecting the Growth Plate**

### **4.1 Introduction**

Longitudinal bone growth is a dynamic process, which is prone to disturbance by a number of factors. These factors include genetic mutations, hormonal disorders, nutritional deficiencies or excesses and biomechanical forces. The following section will focus on molecular and hormonal actions on bone, followed by a section on how disorders in these mechanisms affect bone and, if applicable, how the MI might be altered.

### **4.2 Genetic and Hormonal Actions in a Normal Growth Plate**

For longitudinal bone growth to occur, the cells of the growth plate must differentiate and form correctly. Two genetic factors play a large part in this process; transcription factors and signalling molecules.

Transcription factors (also known as sequence-specific DNA binding factors) are proteins that bind to specific parts of DNA through binding domains and are also part of the system that controls the transcription of genetic information from DNA to RNA. Transcription factors perform their functions alone or by recruiting other proteins by increasing (activating) or preventing (repressing) the presence of RNA polymerase, which is the enzyme that activates transcription from DNA to RNA (Latchman, 1997).

One of the more important transcription factors involved in chondrocyte cell differentiation in the growth plate is sex reversal Y-related high-mobility group box protein 9 (Sox9). Sox9 is required for the transformation of mesenchymal cells into chondrocytes, proliferation of chondrocytes, suppression of premature transformation of chondrocytes into hypertrophic chondrocytes, and is responsible for direct regulation of the important genes involved in chondrocyte function (de Crombrugghe et al., 2000, Kobayashi and Kronenberg, 2005), like Collagen II alpha1 (Col2a1) (Lefebvre et al., 1997), Collagen XI alpha2 (Col11a2) (Bridgewater et al., 1998), Aggrecan 1 (Agc1) (Sekiya et al., 2000), and cartilage-derived retinoic acid-sensitive protein (CD-RAP) (Xie et al., 1999). Related transcription factors L-Sox5 and Sox6 are important in the commitment and maintenance of chondrocyte phenotypes (Kobayashi and Kronenberg, 2005).

Runx-related transcription factors 2 and 3 (Runx2/Runx3) play important roles in chondrocyte maturation from columnar chondrocytes into hypertrophic chondrocytes (Kobayashi and Kronenberg, 2005). Experiments using mice show that mice lacking Runx2 do not have hypertrophic chondrocytes (Inada et al., 1999) and mice lacking both Runx2 and Runx3 are missing chondrocytes altogether (Yoshida et al., 2004). Runx2 also plays a role in mesenchymal differentiation into pre-osteoblasts (Kobayashi and Kronenberg, 2005).

Osterix (Osx) is a transcription factor that is necessary for osteoblast differentiation during both endochondral and intramembranous ossification (Kobayashi and Kronenberg, 2005). Osx acts with the Beta-catenin/T-cell factor/lymphoid enhancer-binding factor (B-catenin/TCF/LEF) complex aiding pre-osteoblast conversion into osteoblasts as well as working with the aforementioned L-Sox5 and Sox6 in chondrocyte differentiation (Kobayashi and Kronenberg, 2005).

Signaling molecules are involved in transmitting information from one cell to another. They are released from the cell that is sending the signal, cross between cells, then interact with receptors in other cells, which triggers a response. Important signaling molecules include bone morphogenetic proteins (BMP's), fibroblast growth factors (FGF's), insulin-like growth factor 1 (IGF1), Indian hedgehog (Ihh), and parathyroid hormone-related peptide (PTHrP) (de Crombrughe et al., 2000). "These secreted peptides exert their effects by triggering intracellular signaling pathways and their action is likely to be controlled at several levels both extra- and intra-cellularly" (de Crombrughe et al., 2000). BMP signaling is likely to be required for three stages of chondrocyte differentiation; mesenchymal cell to pre-chondrogenic cell, pre-chondrogenic cell to early chondrocyte and columnar chondrocyte to hypertrophic chondrocyte (Kobayashi and Kronenberg, 2005). FGF signaling plays a part in the former two stages, while PTHrP plays a part in the latter stage (Kobayashi and Kronenberg, 2005). FGF's also increase the expression of Sox9 both in undifferentiated mesenchymal cells and chondrocytes, which further aids the differentiation process (de Crombrughe et al., 2000). Growth hormone (GH), which promotes the synthesis of IGF-1 (Venken et al., 2005), and both have critical roles in skeletal growth and maturation. Both GH and IGF-1 stimulate the proliferation of chondrocytes and increase

serum markers for bone turnover (Sjogren et al., 2002). Long-term treatment with GH has been shown to increase BMDa (Johannsson et al., 1996), and IGF-1 has been shown to increase BMD in both mice (Yakar et al., 2002) and human studies (BMDa) (Langlois et al., 1998).

The Hedgehog proteins are a family of secreted intercellular signaling proteins that play essential roles in early embryonic patterning of major organs, including bone and many other tissues. Of the three hedgehog proteins that have been identified in mammals, *Ihh*, along with PTHrP, form a negative feedback loop that controls the proliferation and hypertrophy of chondrocytes, with *Ihh* controlling the width of the proliferative zone along with proliferation and PTHrP controlling the rate of hypertrophy (van Donkelaar and Huiskes, 2007). *Ihh* signaling occurs during the conversion of early chondrocytes to columnar chondrocytes and mesenchymal cell conversion to pre-osteoblasts (Kobayashi and Kronenberg, 2005).

Parathyroid Hormone (PTH) aids longitudinal bone growth. One study found that PTH administration in rats increased total growth plate thickness and increased the rate of longitudinal bone growth by increasing the rate of cell production (Ogawa et al., 2002). When serum calcium levels are too low, the parathyroid glands can produce too much PTH, which results in secondary hyperparathyroidism. This causes osteoclastic bone re-absorption to increase the level of serum calcium and causes more calcium to be re-absorbed in the kidneys and intestines.

The sex steroids androgen and oestrogen play an important role in longitudinal bone growth, particularly at puberty. Oestrogen promotes the pubertal growth spurt and subsequent growth plate fusion to the epiphyses (Perry et al., 2008). This is accomplished by oestrogen's ability to affect GH secretions (Venken et al., 2005). GH secretions are mediated via oestrogen receptors alpha (ER- $\alpha$ ) and beta (ER- $\beta$ ), which are expressed in the hypothalamus and anterior pituitary gland (Perry et al., 2008). Androgens can be placed into two categories: aromatised and non-aromatised, referring to the stability of the ring structure of the compound. The non-aromatised androgens, which include dihydrotestosterone and oxandrolone, stimulate bone growth possibly by acting directly with the androgen receptor in growth plate cartilage (Vanderschueren et al., 2004). One study showed that dihydrotestosterone regulates differentiation and

proliferation of cultured human epiphyseal chondrocytes, most likely by increasing the expression of IGF-I receptor and promoting local IGF-I synthesis (Perry et al., 2008). Testosterone is also able to stimulate GH secretion when it is converted to oestrogen by aromatisation (Perry et al., 2008).

Both sexes show an increase in BMD during puberty. The rate of BMD increase in females in the lumbar spine and femoral neck is approximately 4-fold before puberty and then slows to the stage where BMD changes little thereafter, whereas in males, BMD increases approximately 6-fold during puberty with a slower rate of increase at other skeletal sites thereafter (Prentice et al., 2006). As a result, males have a greater cortical thickness and a larger bone size after puberty than females, but BMD remains similar in both sexes (Prentice et al., 2006).

### **4.3 Genetic and Hormonal Disorders**

There are many possible mutations that can occur in the genes affecting the growth plate. There are also many hormone imbalances that affect skeletal growth. Therefore this thesis will concentrate only on a small number of the most relevant disorders that affect the metaphyses and can be found in children.

#### **4.3.1 Constitutional Delay of Growth and Puberty (CDGP)**

CDGP for a peripubertal child, and Constitutional Growth Delay (CGD), which is diagnosed pre-puberty, are 2 of the most common reasons for children, more often in boys, to be referred to a paediatric endocrinologist (Frank, 2003). Symptoms of CDGP include the following:

1. Short stature with a height below 2 standard deviations for chronological age.
2. Growth rate below the 25<sup>th</sup> percentile for chronological age.
3. Delayed bone-age.
4. No indications of chronic illness, endocrine disorder or genetic disease.
5. Onset of puberty at an age greater than 2 standard deviations above average (girls >13 years and boys > 14 years) (Frank, 2003).

When natural puberty occurs in CDGP, both insulin-like growth factor (IGF-1) and GH levels increase normally, but final height is often still slightly below average (Frank,

2003). Some CDGP children have been found to have below average levels of GH (Bierich and Potthoff, 1979, Clayton et al., 1988, Longas et al., 1996), but while treatment with GH can increase the child's growth rate, it does not improve final height (Clayton et al., 1988, Longas et al., 1996). In one study, the bone-age, rate of mineralisation and bone turnover markers such as AP of pre-pubertal children were shown to be similar to those in children with CDGP (Doneray and Orbak, 2008). Findings in the literature differ regarding whether BMD is altered in adult males with a previous history of CDGP. Some studies have reported reduced radial and lumbar spine BMDa in adult males with a history CDGP (Finkelstein et al., 1992, Moreira-Andres et al., 1998), but because they used the DXA measurement areal BMD (BMDa), which is vulnerable to size bias (because it is a 2-dimensional estimate of a 3-dimensional measurement), the results of these studies should be viewed with scepticism. However, Finkelstein and colleagues re-examined their original data using an algorithm to determine BMAD, and stated that their original results remained significant (Finkelstein et al., 1999). This is not in agreement with the findings of Bertelloni and colleagues who also used BMAD but found that although BMDa was reduced, BMAD was normal (Bertelloni et al., 1998). The difference may be due to the use of different algorithms to calculate BMAD, and although QCT would provide more accurate measurements of BMD, the higher radiation exposure would be a concern (Bertelloni et al., 1999). Finkelstein and colleagues also compared radial width at the 65% site in both men with a history of CDGP and controls, and no significant difference was found (Finkelstein et al., 1992), though perhaps a width measurement (obtained from total cross-sectional area) as well as a BMD measurement using pQCT would have been informative. In a follow-up study to the original, BMDa was measured at the femoral neck and was found to be lower in men with a history of CDGP, along with radial and spinal BMDa, suggesting that BMDa men with a history of CDGP fails to improve over time and that the appropriate timing of puberty is important for bone accrual, BMD levels and fracture risk later in life (Finkelstein et al., 1996, Saggese et al., 2001).

There is nothing in the current literature detailing whether metaphyseal dysplasia in any long bone occurs as a result of CDGP, however with reduced mineralisation and BMD it

is conceivable that a degree of dysplasia may occur to compensate for loading under these conditions.

#### **4.3.2 Neurofibromatosis Type I (NF1)**

NF1 is an autosomal dominant condition occurring in 1 out of every 3000 births (NIH, 1988). It is caused by a mutation in the neurofibromatosis gene located on chromosome 17 that codes for the neurofibromin protein. Neurofibromin is a negative regulator of RAS; RAS being an important protein subfamily of GTPases controlling intracellular signaling and regulation of cell growth and survival (Declue et al., 1992). Specifically, neurofibromin limits cell growth and therefore represses tumour growth (Williams et al., 2009). Individuals who have no expression or only partially expressed neurofibromin, often exhibit multiple benign dermal tumours, or occasionally malignant peripheral nerve sheath tumours (Williams et al., 2009). An individual is diagnosed with NF1 if they present with any 2 of the following features:

1. Intertriginous freckling (freckles in areas of skin that rub together such as the armpit).
2. Café-au-lait spots (small areas of skin that are light brown in colour; several usually clustered in one area).
3. Neurofibromas (tumours of the nerve sheath, either cutaneous or subcutaneous, which are localised tumours affecting only one peripheral nerve, or plexiform, which can affect peripheral nerve bundles and more internal nerve bundles).
4. Lisch nodules (small pigmented benign tumours, specifically hamartomas that project from the surface of the iris, but do not typically affect vision).
5. Optic pathway gliomas (mainly benign tumours affecting the optic nerves, tracts, radiations, chiasm or hypothalamus, which collectively form the optic pathway).
6. Skeletal abnormalities including osteopaenia, long-bone dysplasia and bowing, pseudoarthroses, sphenoid wing hypoplasia and fibrous cortical defects.
7. An immediate family member with a diagnosis of NF1 (Williams et al., 2009).

There are several reports of congenital pseudoarthrosis of the radius and radial dysplasia with confirmed or suspected NF1 (Kohler et al., 2005, Ramelli et al., 2001, Sprague and



Brown, 1974), but the tibia, fibula and vertebrae are significantly more common sites for this to occur (Alwan et al., 2007, Stevenson et al., 1999). The radius is often shortened showing irregular development in these cases (Sprague and Brown, 1974). It is noteworthy that tibiae, fibulae and vertebrae are all weight-bearing bones, but this does not explain the lack of lesions in other weight-bearing bones such as calcanei, tali and femora (Alwan et al., 2007). It is possible that the dysplasia in particular is a result of neurofibromin-insufficient bone reacting to loading (Alwan et al., 2007). This would not explain dysplasia in non weight-bearing bones, however the combination of irregular development including a reduction in chondrocyte proliferation and abnormal collagen synthesis, lesions and altered mineralisation (Yu et al., 2005) would explain why the growth plate would expand to compensate for these conditions.

Figure 4.1 is a radiograph of a Caucasian male aged 8 months, exhibiting a congenital pseudoarthrosis of the radius (Sprague and Brown, 1974), which is possibly a case of NF1. The father of this patient had NF1 and the patient also exhibited other effects such as café-au-lait spots. This figure also illustrates the grossly expanded growth plate of the distal radius, which would result in an altered MI.

### 4.3.3 Other Disorders

**Chondrodysplasias** present with many indicators, some of which are metaphyseal defects. They include disorders such as achondroplasia (dwarfism), hypochondroplasia, thanatophoric dysplasia type I and II, and the more recently discovered disorder severe achondroplasia with developmental delay and acanthosis nigricans (SADDAN) dysplasia. All of these conditions result from a mutation in the fibroblast growth factor receptor 3 gene (FGFR3) (Shiang et al., 1994, Tavormina et al., 1995, Bellus et al., 1995, Tavormina et al., 1999). FGFR3 mutations are extremely variable (Vajo et al., 2000), as mutations located in different domains of the FGFR3 receptor can cause different phenotypes and various mutations in the same codon can also cause clinically distinct disorders. Therefore mutations in what is normally a lysine codon within the cytoplasmic tyrosine kinase activation loop of FGFR3 can result in hypochondroplasia when the lysine residue is replaced by asparagine or glutamine, thanatophoric dysplasia

occurs when the lysine residue is replaced by glutamic acid or methionine and SADDAN when the lysine is replaced by methionine (Zelzer and Olsen, 2003).



**Figure 4.1: Possible case of NF1 in an 8 month old male with a congenital pseudoarthrosis of the distal radius. Note the expanded radial metaphysis, which would cause a smaller MI than normal. Reproduced and adapted with permission and copyright © of the Journal of Bone and Joint Surgery (Sprague and Brown, 1974).**

Achondroplasia arises from a sporadic (as opposed to inherited) mutation in over 90% of affected individuals and is caused by a single nucleotide substitution in more than 95% of cases (Ballock and O'Keefe, 2003). Symptoms include small body size with shortened limbs, bowed lower legs, frontal bossing, depressed nasal bridge and lordosis. Features of hypochondroplasia are similar to those of achondroplasia but tend to be

milder and include rhizomelia (a disproportion in the length of the proximal limbs). The features of SADDAN are more severe and include structural abnormalities of the brain that can cause severe developmental delay, seizures and mental retardation. Acanthosis nigricans (AN) is a term which describes patches of dark, thick, velvet-like skin hyperpigmentation that appear in these patients, although AN can occur separately from SADDAN. Patients with these conditions exhibit varying degrees of metaphyseal 'flaring', therefore the MI may be in the normal range, or may be decreased due to expansion of the growth plate.

The **metaphyseal chondro-dysplasias** (MCD) include disorders such as cartilage-hair hypoplasia (CHH), also known as McKusick type MCD, Schmid type MCD and Jansen type MCD0. All of these conditions are characterised by metaphyseal changes evident on radiographs. McKusick type MCD is the result of a mutation of the ribonuclease mitochondrial RNA processing (RMRP) gene, which is the RNA component of the RMRP ribonuclease complex (Ridanpaa et al., 2001). The RMRP complex is involved in multiple cellular and mitochondrial processes, but the mechanism of impairment that causes the disease remains unknown (Ridanpaa et al., 2003). Schmid type MCD is the result of a mutation of the collagen X gene, specifically the collagen 10 alpha-1 chain (COL10A1). This affects the chondrocytes in the hypertrophic zone: histological examination of this area shows thickening and disorganisation (Ho et al., 2007). Jansen type MCD is caused by a mutation in the receptor for PTH or PTHrP. Genetic studies in mice confirm that the primary role of PTHrP is to control the transition between chondrocyte proliferation and differentiation (Ballock and O'Keefe, 2003). Transgenic mice that lack either the PTH/PTHrP receptor or PTHrP itself demonstrate dwarfism, which results from accelerated differentiation and premature chondrocyte hypertrophy, whereas mice in which PTHrP is over-expressed in the growth plate exhibit a dwarfism that is due to a distinct slowing of chondrocyte differentiation (Ballock and O'Keefe, 2003).

The features of all three MCD's include dwarfism and the characteristic flared metaphysis, but more specifically, the features of McKusick type MCD can also include an outward splaying of the lower ribcage, immunodeficiencies, Hirschprung's disease, shortening of the tibia compared to the fibula, light-coloured brittle hair, and an

increased risk of developing certain cancers. The features of Schmid type MCD are very similar to McKusick type MCD and can include an outward splaying of the lower ribcage, leg pain, bowed legs and hip deformities. The features of Jansen type MCD are the most severe and can include stiffening and swelling of the joints, facial and skull deformities that can result in blindness or deafness, benign bone masses, clubbed fingers and mental retardation. Patients with an MCD are far more likely to have a decreased MI as metaphyseal flaring is the primary feature of MCD's. There is also a group of disorders known as the spondylometaphyseal dysplasias (SMD). This group however will not be discussed in depth because of the similarities to the MCD's. The SMD's have vertebral deformities that can result in scoliosis and/or kyphosis in addition to many of the symptoms of MCD's.

The following two disorders are characterised by excessive bone formation and can result in severe deformities; they are **Osteoectasia with Hyperphosphatasia (OwH)**, sometimes referred to as Juvenile Paget's Disease, and **Braun-Tinschert type MCD**. The latter presents with significantly different radiographic findings than other MCD's and has a similar phenotype to OwH, which is why the Nosology Group of the International Skeletal Dysplasia Society have grouped these (among several others) disorders together (Superti-Furga et al., 2007). Braun-Tinschert type MCD was first described by Braun and colleagues after studying a German family who exhibited expanded metaphyses (without a widened growth plate) due to undermodelling known as the Erlenmeyer flask deformity, bowing of the distal radii (often sickle-shaped) combined with shortening of the ulnae, flat exostoses in the metaphyses, thin cortices and trabecular irregularities (Braun et al., 2001). Braun and colleagues have done extensive genetic testing in an attempt to localise the gene responsible but have not as yet been successful, although they have determined that it is an autosomal dominant condition, which distinguishes it from the autosomal recessive Pyle's Disease (Braun et al., 2001). Until recently this disease had only been observed in Braun's German cohort, but has now been observed in a young Japanese girl, indicating that the disease is not restricted to the German population (Takata et al., 2006). Figure 4.2 illustrates the expanded distal radial metaphyses seen in this case (Takata et al., 2006). The MI in this

group would be larger compared to normal as the GPW would not be significantly larger than the MW.

OwH is an inherited autosomal recessive disorder caused by a mutation in the gene that encodes for osteoprotegerin (OPG). OPG is a receptor that is released from osteoblasts and pre-osteoblasts to suppress bone resorption (Whyte et al., 2007). Features of hyperphosphatasia include raised serum AP due to increased osteoclastic activity, cortical thickening leading to hearing and vision loss, and muscular weakness (Cundy et al., 2002). Osteoectasia refers to the bowing of long bones (Osman and Girdany, 1973).



**Figure 4.2: Radiograph of a 7 year-old Japanese girl exhibiting the expanded distal radial metaphyses characteristic of Braun-Tinschert type MD. Reproduced and adapted with permission and copyright © of the American Journal of Medical Genetics Part A (Takata et al., 2006).**

Radiographically, the phalangeal joints are expanded and the trabeculae are thickened and distorted. Although this disease is sometimes referred to as Juvenile Paget's disease (JPD), JPD refers to hyperphosphatasia only. Juvenile Paget's is not to be confused with Paget's disease; Paget's is a metabolic disease resulting in lytic and sclerotic regions often affecting many bones of the skeleton (Whitehouse, 2002). It is caused by a mutation in the SQSTM1 gene encoding sequestosome-1 and always begins in middle

age (Whyte et al., 2007). The MI of an OwH or hyperphosphatasia patient would be increased because there is reduced remodelling of the metaphyses.

#### **4.3.4 Hormonal Disorders**

**Oestrogen** promotes the pubertal growth spurt and subsequent epiphyseal fusion by its ability to affect GH secretions (Venken et al., 2005). Precocious puberty results from a premature increase in sex steroid production, which leads to a reduced final height due to an early growth spurt and epiphyseal fusion (Smith et al., 1994). A case of a 28 year old male with a homozygous mutation of ER- $\alpha$  resulted in continued longitudinal bone growth well beyond puberty (Smith et al., 1994). The mutation resulted in the patient having higher than normal serum oestradiol concentrations, but the mutated gene contained no binding sites, which made treatment with oestrogen ineffective and only served to increase serum estradiol levels (Smith et al., 1994). This patient had a delayed bone age of 15 years, osteoporosis, and an increased serum AP level indicating increased bone resorption (Smith et al., 1994).

**Androgens** are also important sex steroids, as men who lack androgens often have osteoporosis (Foresta et al., 1984) and men who have had CDGP experience low bone density and an increased risk of fracture in adulthood (Finkelstein et al., 1992). Although the patient with ER- $\alpha$  knockout had normal serum androgen concentrations, androgens were not able to compensate for a lack of oestrogen, demonstrating that oestrogen has a vital role in normal pubertal growth and bone maturation in both males and females (Smith et al., 1994). A lack of either androgens or oestrogen would not affect the MI directly. The ratio would most likely be in the normal range because it is not the fundamental shape of the bone that is being altered, but the growth rates.

**GH deficiency** (GHD) results in impaired longitudinal growth while an excess of GH results in gigantism (Nilsson et al., 2005). By examining IGF-1 null mice, Wang and colleagues determined that IGF-1 has an impact on chondrocyte size in the hypertrophic zone of the metaphysis; mice who lacked IGF-1 still had the same number of chondrocytes and columns, the same chondrocyte proliferation rate and the same differentiation rate, and an equal proportion of cells in the hypertrophic and proliferative zones of the metaphysis (Wang et al., 1999). Therefore the only feature of growth plate

expansion that was clearly disturbed was the extent of chondrocyte hypertrophy; the degree of attenuation of chondrocyte hypertrophy corresponds to the degree of reduction in longitudinal growth (Wang et al., 1999). As with androgen and oestrogen, an excess or deficiency of GH/IGF-1 would not affect the MI directly; the ratio would most likely be in the normal range because again it is not the fundamental shape of the bone that is being altered but the growth rate.

**Thyroid hormone** (T3) is one of the major systemic hormones that influence growth during childhood. Left untreated, hypothyroidism (reduced/absent T3) can result in delayed skeletal maturation (i.e. younger bone-age) and extreme growth retardation, but this condition can be treated with thyroxine (T4) (Williams et al., 1998). Animals with hypothyroidism display a disorganized growth plate with a decreased hypertrophic zone that lacks bone resorption in this region resulting in no new metaphyseal bone formation and reduced subchondral primary spongiosa in the metaphyseal area (Williams et al., 1998). Congenital hypothyroidism, due to hypoplasia or thyroid dysgenesis, is the result of mutations in the paired box 8 (PAX8) gene and is inherited as an autosomal recessive condition. Hyperthyroidism or thyrotoxicosis (abnormally high levels of T3) in childhood causes growth acceleration and advanced bone age, which can lead to craniosynostosis, premature closure of growth plates and shortened stature (Williams et al., 1998). The autosomal dominant condition of hereditary hyperthyroidism is caused by a mutation in the thyroid stimulating hormone receptor (TSH-R) gene, though there are other causes of hyperthyroidism including cancerous adenomas (Duprez et al., 1994). If either hypo- or hyperthyroidism resulted in a change in shape of the metaphysis or a change in length of the growth plate then the MI would be altered, but if they resulted in smaller bones with no fundamental change in shape, then the MI would not be altered, the latter being most likely. It is important to note that both hyper- and hypothyroidism can occur as secondary conditions and in those cases could have other factors that affect growth plate architecture.

#### **4.4 Nutrition**

A large number of vitamins and minerals together with proteins, fats and carbohydrates play a role in maintaining bone health. Some of the most important vitamins and

minerals for bone health are vitamins A, B, C, D, K and the minerals calcium, phosphorus, magnesium, zinc, copper, manganese, potassium and iron (Palacios, 2006, Prentice et al., 2006).

**Protein** intake aids longitudinal bone growth by increasing levels of IGF-1 and it increases calcium absorption (Palacios, 2006, Prentice et al., 2006). Fat has the potential to inhibit calcium absorption but a certain amount of fat intake is necessary to ensure overall body health (Prentice et al., 2006). Fat provides calories for movement and exercise, which places a loading force on the skeleton, which in turn ensures normal bone growth. A certain amount of carbohydrates are also necessary to ensure general health, although to increase carbohydrate intake at the expense of other nutrients can be damaging to general health, including bone health. For example, a case-control study conducted in Greece showed that a high consumption of cola-type drinks was positively associated with increased fracture risk in children aged 7 to 14 years (Petridou et al., 1997). Several studies have shown how milk and other dairy products have been 'replaced' by nutritionally deficient sugary drinks and foods in the Western diet compared to 50 years ago (Kennedy and Goldberg, 1995, Morton and Guthrie, 1998, Gerrior et al., 1998), leading to a calcium and phosphorous dietary imbalance (Johnson and Frary, 2001). This in turn has a detrimental effect on bone health which is discussed further in the next section.

#### **4.4.1 Minerals – Calcium and Phosphorus/Phosphate**

**Calcium** is one of, if not the most important mineral for bone growth. In adults, 99% of total body calcium content, which consists of approximately 1000g, exists as hydroxyapatite  $\text{Ca}_5(\text{PO}_4)_3\text{OH}$ , while the remainder is located in other tissues and extra cellular fluid (Favus et al., 2006). Hydroxyapatite crystals contribute to the mechanical weight-bearing properties of bone and also serve as a calcium reservoir for other systems that may require calcium (Favus et al., 2006). Chondrocyte maturation in vitro is induced by high concentrations of extracellular calcium (Bonen and Schmid, 1991), by increasing phosphate uptake (Mansfield et al., 2003), and by regulating the expression of, among other things, collagen type X and PTHrP (Burton et al., 2005, Wu et al., 2003, Zuscik et al., 2002). Calcium concentrations in the fetal growth plate increase from the



resting zone to the zone of proliferation, and again from the zone of proliferation to the zone of hypertrophy (van Donkelaar et al., 2007). Calcium concentrations in the growth plate increase even further once a secondary ossification centre has developed (van Donkelaar et al., 2007) to aid in the mineralisation process. It has also been shown that vesiculation or ectocytosis of the plasma membrane, which occurs during the creation of matrix vesicles, is reliant on an influx of calcium into the cytoplasm from several cell types including chondrocytes (Wang and Kirsch, 2002). Proteins called annexins form  $\text{Ca}^{2+}$  channels in the chondrocytes of the hypertrophic zone in the growth plate and the altered  $\text{Ca}^{2+}$  homeostasis leads to the release of annexin-containing, mineralisation-competent matrix vesicles (Wang and Kirsch, 2002).

**Phosphorus and phosphate** ( $\text{PO}_4$ ) are also very important in the growth plate. Hydroxyapatite crystals account for 85% of the total  $\text{PO}_4$  in the body, and the rest is located in other tissues, with a very small amount being contained in extracellular fluids (Favus et al., 2006). Phosphorus aids chondrocyte maturation and subsequent matrix mineralisation. In the cartilage mineralisation area, an increase in local  $\text{Ca}^{2+}$  ions and  $\text{PO}_4$  concentrations regulates oxidative metabolism and causes apoptosis of terminally differentiated chondrocytes to initiate (Mansfield et al., 2003). The body of a healthy individual can adapt well to a variety of different levels of phosphorus consumption, whereas the ability to adjust to a low calcium intake appears to be limited. Therefore the absolute intake of phosphorus seems to be less important for bone health than the ratio of calcium to phosphorus intake (Palacios, 2006). Conditions that cause low serum calcium levels (hypocalcemia), or hinder phosphate metabolism or removal, such as renal failure, can lead to secondary hyperparathyroidism (Slatopolsky et al., 1999). The increase in PTH secretion leads to an inhibition of vitamin D, specifically  $1,25(\text{OH})_2\text{D}$  synthesis in the kidneys (Hruska, 2006), see Fig 4.3. The reduction in vitamin D could lead to growth plate expansion in the growing skeleton. Hypophosphataemia can lead to rickets/ osteomalacia (Hruska, 2006), which is treatable with oral vitamin D supplements or injections.

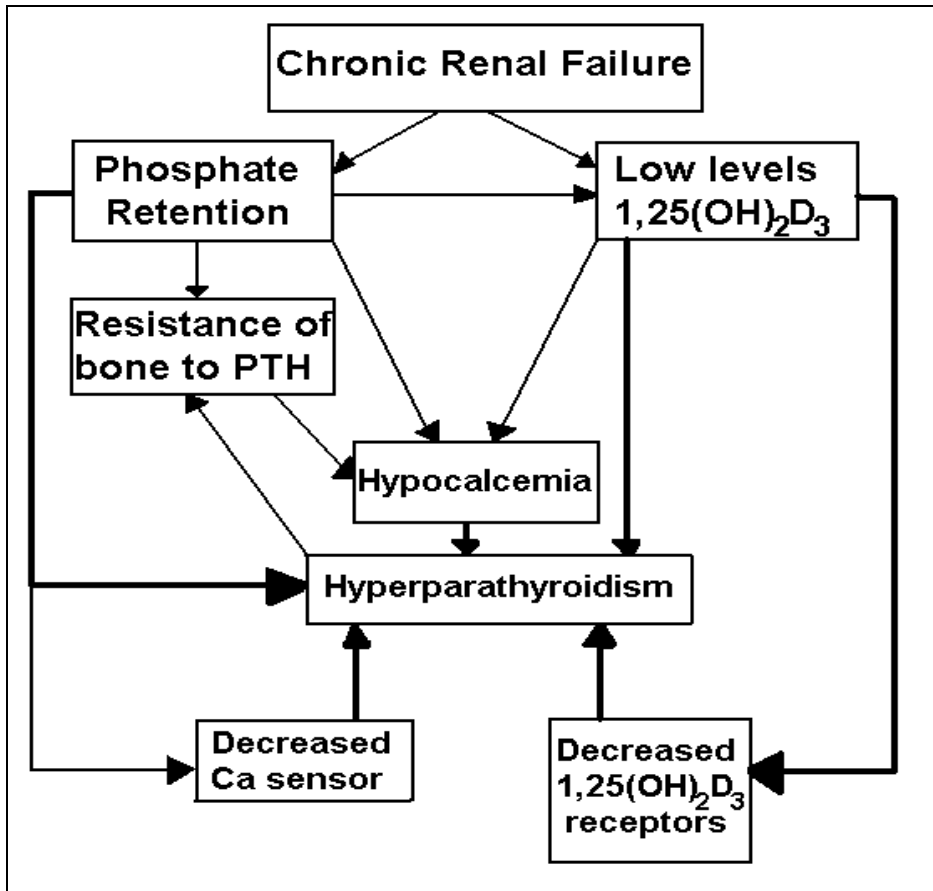


Figure 4.3: Factors involved in the pathogenesis of secondary hyperparathyroidism, adapted from (Slatopolsky et al., 1999).

#### 4.4.2 Other Minerals

The adult body contains approximately 25g of **magnesium**, about two thirds of which is located in the skeleton, one third is intracellular and a minute percentage is located in extracellular compartments (Favus et al., 2006). Around 60% of intracellular magnesium is located within the mitochondria, where its function is to act as a cofactor in hundreds of enzyme systems relating to use of ATP, transcription and translation, and phosphate transport (Favus et al., 2006, Palacios, 2006). Magnesium also acts to decrease hydroxyapatite crystal size, which prevents larger crystals from forming that can result in brittle bone (Palacios, 2006). A study using mice demonstrated that magnesium deficiency resulted in osteoporosis, increased skeletal fragility, a decrease in growth plate width of 33%, a decrease in metaphyseal trabecular bone volume and chondrocyte column decreases in number and length, which all suggested that a

magnesium deficiency reduced bone growth (Rude et al., 2003). Studies in humans have also shown that magnesium deficiency is linked to increased bone resorption (New et al., 2000).

The adult body contains approximately 2.3g of **zinc** (IRCP, 1975). Zinc is also found in other bodily tissues such as the prostate, pituitary, liver, red blood cells and skeletal muscle (Aitken, 1976). Zinc is a fundamental micronutrient for many enzymes both as a cofactor and as a stabiliser of their molecular structure (Rossi et al., 2001). Zinc aids chondrocyte activity at the growth plate and has an effect on the synthesis and degradation of all types of collagen (Wallwork and Sandstead, 1990). Zinc is also needed for osteoblastic and AP activity (Palacios, 2006). Zinc deficiency exhibits similar manifestations in most animal species; these include alopecia, dermatitis, testicular atrophy, ocular lesions, anorexia and growth retardation (Rossi et al., 2001). A study using rats demonstrated that a zinc-deficient diet resulted in reduced activity at the growth plate, leading to reduced growth plate width and hypertrophic cartilage decreases, lower BMD and a reduced bone growth rate (Rossi et al., 2001).

The adult body contains approximately 50-120mg (80mg average) of **copper**, the largest amount being contained in the skeleton, but smaller amounts are located in the brain, liver, kidneys and heart (Barceloux, 1999). Copper aids mineralisation of bone, influences the integrity of connective tissue (Palacios, 2006) and is an important catalyst for iron absorption (Barceloux, 1999). A copper-containing enzyme, lysyl oxidase, is essential for collagen fibril cross-linking, which then increases collagen's mechanical strength to form strong and flexible connective tissue (Palacios, 2006). Increased levels of copper were shown to increase differentiation and proliferation of mesenchymal stem cells into both osteoblasts and adipocytes (Rodriguez et al., 2002). In an in-vitro experiment using human mesenchymal stem cells, increased copper levels decreased AP activity, and AP reached its maximum value in increasingly shorter culture times, which caused deposition of hydroxyapatite crystals to occur earlier than normal (Rodriguez et al., 2002). Copper deficiency has been reported to decrease mineralisation in the growing skeleton of animals (Strause et al., 1986) and has been found to significantly alter mineralisation in the mature skeleton (Smith et al., 2002). Copper deficiency can result in cortical thinning, growth plate splaying, irregular matrix deposition and

osteoporosis associated with reduced osteoblast activity in rats (Parry et al., 1993). Osteoporosis leading to fractures is one of the features of Menke's disease, which is an X-linked disorder of copper transport (Danks, 1995).

An adult human body contains approximately 12-20mg of **manganese**, most of which is located in the skeleton, however there is also a large concentration in mitochondria due to the role of manganese in mitochondrial enzyme function (Reynolds et al., 1998). Increased levels of manganese in chondrocytes isolated from the growth plates of 6 to 8 week old hybrid broiler-strain chickens have been shown to inhibit proteoglycan synthesis and inhibit mineralisation in cell cultures at levels of 50µm, while double that level caused a 50% reduction in protein levels (Litchfield et al., 1998). There was however no affect on AP (Litchfield et al., 1998). Studies examining manganese deficient animals found disproportionate skeletal growth including the shortening of long bones and the absence of epiphyses (Hurley et al., 1961). Inhibition of mineralisation has the potential to affect the MI because the undermineralised bone can become soft and can expand at the growth plate.

**Potassium** is important for bone growth because it promotes an alkaline environment, which reduces the demand for skeletal salts to balance endogenous acid generated from acid producing food such as meat (New et al., 2000, Palacios, 2006) thereby helping to prevent osteoporosis by preserving calcium in the skeleton that might otherwise be utilised to maintain normal pH (Palacios, 2006). Increased intakes of potassium have been associated with an increased BMDa in perimenopausal women, while decreased intakes were associated with lower BMDa (New et al., 2000). Potassium is also associated with decreased urinary calcium excretion, improved calcium balance, reduced bone resorption, and increased bone formation (New et al., 2000). There is a lack of literature as to the effect of potassium on the growth plate.

The adult human body contains approximately 2-3g of **iron**, most of which is contained in red blood cells with a smaller concentration in the liver as ferritin (Beard, 2001). Iron is an important factor in bone growth because it serves as a cofactor for enzymes involved in collagen synthesis (Ilich-Ernst et al., 1998, Palacios, 2006). Iron also serves as a cofactor for 25-hydroxycholecalciferol hydroxylase, which is an enzyme involved in transforming vitamin D into its active form, which if deficient would then have

repercussions on calcium absorption (Palacios, 2006). In studies using nephrectomised rats (to cause renal failure), increased levels of iron have been shown to inhibit endochondral ossification (Mandalunis et al., 2002, Mandalunis and Ubios, 2005). Decreased levels of iron can result in anaemia, which has been shown to increase bone fragility in rats (Medeiros et al., 1997). In another study, two groups of rats were fed either a control diet or an iron-deficient diet (Katsumata et al., 2009). They found lower BMC and BMDa of the femur, lower trabecular number, a significantly reduced bone formation rate and osteoclast surface area in the lumbar vertebrae, and decreased levels of serum 1,25(OH)<sub>2</sub>D, serum total protein, albumin, globulin, IGF-1, C-terminal telopeptide of type I collagen (CTx), deoxypyridinoline (DPD) and osteocalcin in the iron-deficient group (Katsumata et al., 2009). CTx and DPD are excreted in urine as a by-product of osteoclastic bone resorption and are therefore good markers for bone turnover. These results suggest that severe iron deficiency decreases protein synthesis and the conversion of cholecalciferol to 1,25(OH)<sub>2</sub>D, affecting bone formation and inhibiting osteoclast number, which reduces bone resorption (Katsumata et al., 2009). Although it would be improbable to have the severe level of iron-deficiency in humans as induced in the Katsumata experiment (Katsumata et al., 2009), the results suggest that it is possible for the MI to be altered if iron-deficiency is severe and prolonged.

#### **4.4.3 Vitamins**

Vitamins are defined as essential organic compounds with a low molecular weight, required in trace amounts for normal growth and metabolic processes, which usually act as components of coenzyme systems. The importance of vitamin D in relation to bone growth has already been described in several sections. However, because vitamin D is one of the most important vitamins in relation to bone growth, this section will highlight the importance of vitamin D and of vitamins A, C, K and the B vitamins.

**Vitamin D** is something of a misnomer, as vitamin D is in fact a steroid hormone that exists in two main forms: D<sub>3</sub> (also known as cholecalciferol), which is the form of vitamin D that is ingested in foods such as cod liver oil and egg yolks, and generated in the skin when ultraviolet (UV) light is absorbed by 7-dehydrocholesterol (7-DHC); and D<sub>2</sub> (also known as ergosterol), which is the form found in plants. Neither D<sub>3</sub> nor D<sub>2</sub> are

biologically active. They must be metabolised first in the liver to 25-hydroxy vitamin D (25OHD) and then in the kidneys to 1,25-dihydroxy vitamin D (1,25(OH)<sub>2</sub>D). Both D<sub>3</sub> and D<sub>2</sub> undergo this metabolism, therefore D represents both D<sub>3</sub> and D<sub>2</sub> (Fig. 4.4). The vitamin D receptor (VDR) binds to several forms of vitamin D, but its affinity for 25OHD is approximately one thousand times less than for 1,25(OH)<sub>2</sub>D, therefore making 1,25(OH)<sub>2</sub>D the most biologically active form (Bowen, 2007). The half-life of 1,25(OH)<sub>2</sub>D is less than a day, whereas the half-life of 25OHD is several weeks, therefore levels of serum 25OHD are what is measured to determine vitamin D status. There has been some question in the literature as to whether D<sub>2</sub> is as effective as D<sub>3</sub> at maintaining the serum levels of calcium and phosphorus at an optimal level. In a double blind trial in which subjects were given either placebo, 1000 IU/day D<sub>2</sub> (equivalent to 25µg), 1000 IU/day D<sub>3</sub> or 500 IU D<sub>2</sub> combined with 500 IU D<sub>3</sub> daily for 11 weeks (Holick et al., 2008), all three groups had significant increases in 25OHD levels (Holick et al., 2008). This is in contrast to previous studies in which D<sub>2</sub> was less effective than D<sub>3</sub> in maintaining serum 25OHD levels (Armas et al., 2004, Trang et al., 1998). Furthermore, a single dose of 50,000 IU D<sub>2</sub> given to healthy adults decreased the serum 25OHD levels more rapidly than in the placebo group, suggesting D<sub>2</sub> was not only less effective in maintaining serum 25OHD levels, but also increased the degradation of D<sub>3</sub> (Armas et al., 2004). Although it is possible that a single dose of 50,000 IU D<sub>2</sub> increased the degradation of D<sub>3</sub>, D<sub>2</sub>, and caused a decrease in levels of 25OHD as a result, a similar weekly (Malabanan et al., 1998), or twice weekly (Adams et al., 1999) dose resulted in an average 100% increase in serum 25OHD levels, and in a significant BMDa increase in the spine and hip (Adams et al., 1999). Possible reasons for these discrepancies include the carrier (lactose, ethanol, oil) in which the vitamin D was dissolved, that may influence catabolism or bioavailability, but more studies are required (Holick et al., 2008). An important function of vitamin D is mineralisation of the skeleton, but vitamin D does not act on the skeleton directly. Instead vitamin D aids bone mineralisation by elevating serum phosphorus and calcium concentrations, the levels of which also prevent hypocalcaemic tetany (DeLuca, 1979). Vitamin D does this in two ways: it enables the active transport of both calcium and phosphate in the enterocytes, which are intestinal absorptive cells of the small intestine (DeLuca, 1979).

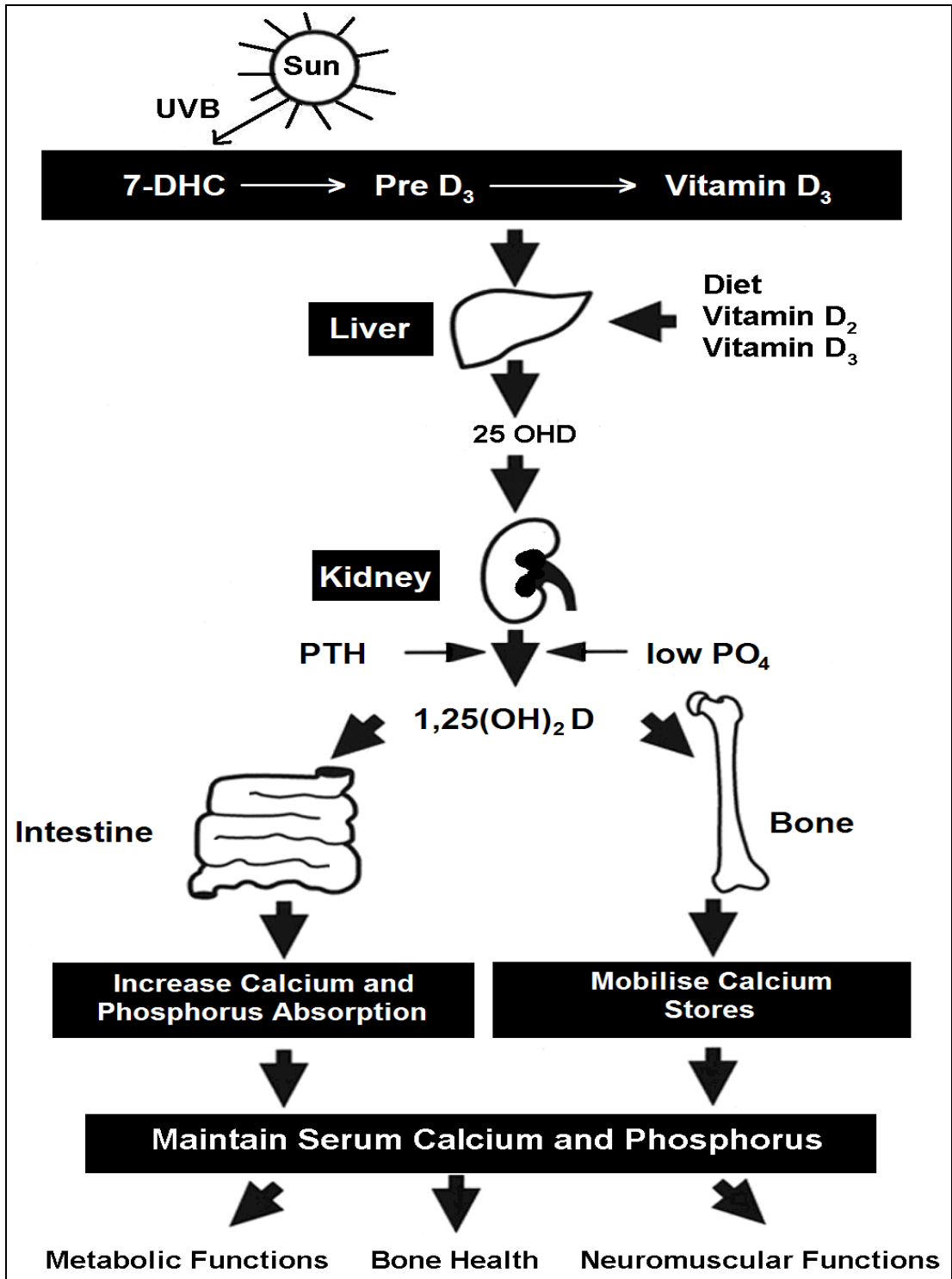


Figure 4.4: Illustration of Vitamin D metabolism. Adapted from (Holick, 2006).

Also, when there is insufficient dietary calcium intake, vitamin D, along with PTH, stimulates the formation of osteoclasts, and thus bone resorption, to maintain normal serum calcium levels (Garabedian et al., 1974). These indirect effects are supported by the results of Brooks et al., who studied children with vitamin D resistant rickets type II, who presented with high circulating levels of 1,25(OH)<sub>2</sub>D (Brooks et al., 1978). Treatment with any form of vitamin D was unsuccessful because there was a genetic fault with the VDR; either a complete lack of a VDR, or a defective, or partially defective VDR (Brooks et al., 1978). Effective treatment is available in the form of calcium and phosphorus infusions (Brooks et al., 1978), therefore supporting the indirect actions of vitamin D on mineralisation. PTH stimulates osteoclasts to resorb bone in order to raise levels of serum calcium. As this occurs, BMD decreases and as a result, the risk of fractures increases (Wagner and Greer, 2008). In the more severe cases of vitamin D deficiency (rickets in children and osteomalacia in adults), the following features occur: enlargement of joints, curvature of the spine and femora, general muscle weakness and osteopenia (Wagner and Greer, 2008). The stages of vitamin D deficiency are outlined in Table 4.1. The metaphyses of long bones in children are abnormal in severe vitamin D deficiency. There is also evidence that vitamin D toxicity could also cause an altered MI (discussed further in a subsequent section).

**Table 4.1: Stages of Vitamin D Deficiency**

	<b>25OHD Levels</b>	<b>Ca Levels</b>	<b>PO<sub>4</sub> Levels</b>	<b>PTH Levels</b>
<b>Stage 1</b>	↓	↓	--	--
<b>Stage 2</b>	↓	↑	↓	↑
<b>Stage 3</b>	↓	↓	↓	↑

**Table 4.1: In the first stage, 25OHD and Ca levels decrease but PO<sub>4</sub> and PTH remain unchanged. In the second stage, 25OHD levels decrease further but PTH acts to raise Ca levels. PO<sub>4</sub> levels decrease. In the most severe third stage, 25OHD levels continue to decrease but even the raised levels of PTH are not able to keep Ca levels normal so they begin to decrease along with PO<sub>4</sub>. (‘↑’ = Increase, ‘↓’ = Decrease, ‘--’ = Unchanged). Adapted from Wagner and Greer, 2008.**



**Vitamin A** is important in the formation of matrix vesicles and the subsequent mineralisation process. Proteins called annexins facilitate the influx of calcium into chondrocyte cytoplasm by creating  $\text{Ca}^{2+}$  channels (Wang and Kirsch, 2002). Growth plate chondrocytes treated with retinoic acid (RA) (i.e. vitamin A), result in the induction of their terminal differentiation and subsequent mineralisation (Kirsch et al., 2000). This initiates an increase that regulates a series of events, which leads to matrix mineralisation of growth plate chondrocytes (Wang and Kirsch, 2002). Vesicles isolated from cultures that were not treated with RA, were unable to take up significant amounts of  $\text{Ca}^{2+}$  (Wang and Kirsch, 2002). RA negatively regulates longitudinal bone growth by inhibiting chondrocyte proliferation, hypertrophy and matrix synthesis at the growth plate through retinoic acid receptors (RAR's) to prevent bone overgrowth (De Luca et al., 2000). The growth-inhibiting effects of RA were completely reversed by an RAR antagonist; in the absence of exogenous RA, the RAR antagonist accelerated bone growth to an abnormal level (De Luca et al., 2000). Both excess vitamin A (Pease, 1962, Standeven et al., 1996, Wolbach, 1947) and vitamin A deficiency (Wolbach, 1947, Harris et al., 1978, Fan and Zhu, 1999) have negative effects on the growth plate. Excess vitamin A has been associated with premature closure of the growth plate (Standeven et al., 1996) while vitamin A deficiency has been associated with incomplete skeletal development and reduced body length in rats (Fan and Zhu, 1999) and an overgrowth of bone through osteoblast activity, with decreased calcium content in guinea pigs (Harris et al., 1978). There is no published evidence of metaphyseal splaying resulting from either a deficiency or excess vitamin A. Therefore it seems unlikely that either of these conditions would cause a significant alteration to the MI ratio.

The water soluble **B vitamins**, have at various points in time, included approximately 30 different substances. However only 8 are currently classified as B vitamins: B<sub>1</sub> – thiamine, B<sub>2</sub> – riboflavin, B<sub>3</sub> – niacin, B<sub>5</sub> – pantothenic acid, B<sub>6</sub> – pyridoxine, B<sub>7</sub> – biotin, B<sub>9</sub> – folic acid and B<sub>12</sub> – cobalamin. This section will concentrate on the effects of those that have been studied most in relation to bone: B<sub>6</sub>, B<sub>9</sub> and B<sub>12</sub>.

**Vitamin B<sub>6</sub>** (pyridoxine) assists in balancing potassium and sodium levels and promotes the production of red blood cells. In addition, it serves as an important coenzyme in

many biochemical reactions including the biosynthesis of dopamine and serotonin (neurotransmitters), and is most likely important for normal perinatal development of the central nervous system (Spector, 1978). There are differing opinions as to the effects of vitamin B<sub>6</sub> on the mineralisation process. Dodds and colleagues examined the growth plate and fracture healing in rat metatarsals and found that rats fed on a B<sub>6</sub> deficient diet showed metaphyseal, epiphyseal and diaphyseal changes as well as growth plate abnormalities that resembled osteoporotic bone (i.e. contained large cavities lined with osteoclasts), that were only exacerbated by the presence of a fracture (Dodds et al., 1986). The amount of new bone formed in the fracture callus was diminished compared to controls, and fractures took longer to unite in the B<sub>6</sub> deficient rats (Dodds et al., 1986). Abnormalities were also observed by Rodda and colleagues, who described the metaphyseal changes as similar to those seen in starvation, including reduced, irregularly shaped and degraded trabeculae (Rodda, 1975, Dodds et al., 1986). A study using tissue non-specific alkaline phosphatase (TNAP) null mice examined how vitamin B<sub>6</sub> affected mineralisation (Narisawa et al., 2001). The mineralisation of TNAP null mice did not improve with administration of vitamin B<sub>6</sub>, suggesting that vitamin B<sub>6</sub> metabolism does not affect mineralisation in TNAP null hypophosphatasia (Narisawa et al., 2001). It is possible that the MI could be altered in a vitamin B<sub>6</sub> deficient environment, although the only evidence for this in the literature are the effects one study observed in rats (Dodds et al., 1986). Because the B vitamins are water soluble, excesses are excreted in urine, therefore there is currently a lack of evidence on B vitamin excess and bone.

**Vitamin B<sub>9</sub>** (folic acid) is an important substance, particularly for expectant mothers, as it can prevent birth defects. Calcification in baby rats whose mothers were chronically folic acid deficient, was delayed and disordered (Jaffe and Johnson, 1973). Studies concerning the effects of folic acid on bone growth are relatively rare, however there is currently no data to suggest that the MI of long bone would be altered as a result of folic acid deficiency.

**Vitamin B<sub>12</sub>** (cobalamin), acts as a cofactor for osteoblast-related proteins such as osteocalcin and AP, and is therefore important for osteoblast function (Palacios, 2006). In a study of osteoblast specific proteins, AP and osteocalcin levels were lower in cobalamin deficient patients compared to controls, suggesting that osteoblast activity is

dependant on cobalamin and that bone metabolism is affected by cobalamin deficiency (Carmel et al., 1988). In children fed a mainly vegetarian diet, cobalamin levels were found to be low compared to controls on an omnivorous diet (Dhonukshe-Rutten et al., 2005). This deficiency was subsequently found to be associated with low BMC and BMDa compared to controls (Dhonukshe-Rutten et al., 2005). B<sub>12</sub> deficiency also causes neurological effects (e.g. memory loss and neuropathy) and haematological effects (e.g. anaemia) (Carmel et al., 1988). As with folic acid, there is no information in the literature to suggest that the MI would be altered in a case of cobalamin deficiency.

**Vitamin C** (ascorbic acid) is a water soluble vitamin that is an essential nutrient for humans. A deficiency in vitamin C causes scurvy, which has symptoms that include cutaneous bleeding, bleeding from mucous membranes, haemorrhaging from the gums and in some cases, tooth loss. Vitamin C is required for the process of cross-linking collagen fibrils in bone by functioning as a cofactor in the hydroxylation of proline and lysine (Palacios, 2006). If vitamin C is not present in sufficient quantities, poor quality collagen will be synthesised, which leads to poor quality dentine formation, resulting in the dental symptoms listed above (Rajakumar, 2006). The following events in bone formation occur in the metaphyseal area, between the growth plate cartilage and the end of the diaphysis:

- Osteoblasts are unable to form bone matrix, resulting in cessation of endochondral ossification.
- However the calcification of growth plate cartilage in long bones continues, leading to a thickening of the growth plate.
- The typical invasion of capillaries into growth plate cartilage fails to occur.
- Consequently pre-existing bone becomes brittle because it is undergoing a normal rate of resorption.
- This leads to the formation of microscopic fractures in the spicules between the diaphysis and calcified cartilage (Rajakumar, 2006).

The periosteum becomes loosened because of these fractures, resulting in subperiosteal haemorrhage in the metaphyseal area of long bones, however intra-articular haemorrhage is rare because the attachment of the periosteum to the growth plate is very

strong (Rajakumar, 2006). A case study of an infant with both rickets and scurvy showed marked under-mineralisation of the skeleton and metaphyses were cupped and splayed (Lewis et al., 2007). Although the metaphyseal splaying could be explained in this case by rickets, metaphyseal splaying has also been observed in animals being fed a vitamin C deficient diet (Sabin, 1939). Therefore there is evidence suggesting that the MI could be altered in cases of vitamin C deficiency.

**Vitamin K** is a fat soluble vitamin with two molecular forms, designated K<sub>1</sub> (phylloquinone) and K<sub>2</sub> (menaquinone). Vitamin K is an important cofactor of  $\gamma$ -carboxylase, an enzyme necessary for the  $\gamma$ -carboxylation of glutamic acid residues in certain proteins such as osteocalcin (Palacios, 2006, Booth, 2003). The presence of glutamic acid residues facilitates the calcium binding of osteocalcin to the hydroxyapatite bone matrix (Shearer, 1995). Vitamin K deficiency increases the amount of under-carboxylated osteocalcin, which is a less functional form and found in osteoporotic patients (Palacios, 2006). Also, warfarin, which is a commonly prescribed anticoagulant and vitamin K antagonist, has been shown to increase the amount of under-carboxylated osteocalcin (Bach et al., 1996). Studies in both children and adults, particularly postmenopausal women, have shown that an increase in vitamin K is associated with; increases in BMC (Knapen et al., 2007, van Summeren et al., 2008), increased width of the femoral neck (Knapen et al., 2007) and increased BMDa in peripubertal children (van Summeren et al., 2008). There are however conflicting results concerning the association of vitamin K with BMD (Cashman, 2005). Some studies have reported no association (Knapen et al., 2007), while others have reported that a low intake of vitamin K is associated with decreased BMD (Booth et al., 2003). There is speculation that a relative lack of vitamin K in growing children could lead to reduced bone strength, quality or suboptimal bone mineralisation, leading to an increased fracture risk (van Summeren et al., 2008). This is in addition to the increased fracture risk already present in peripubertal children, due to bone mineralisation not being able to keep up with the height increase (van Summeren et al., 2008). There are few studies examining bone geometry in relation to vitamin K in children. However, an intriguing hypothesis has been proposed relating to the interrelationship of actions of vitamins A, D and K on the growth plate and pathological soft tissue calcification

(Masterjohn, 2007). He proposed that inducing a vitamin K deficiency is the mechanism by which vitamin D becomes toxic (Masterjohn, 2007). In this model he states that "...vitamin D up-regulates the expression of certain proteins that must be activated by the vitamin K-dependent process of carboxylation" (Masterjohn, 2007), such as osteocalcin (Palacios, 2006), and matrix gamma-carboxyglutamic acid protein (MGP) (Cancela et al., 1990). When the amount of vitamin K available to carboxylate these proteins has been exhausted, the "...vitamin K-dependent processes that support the nervous system, retain minerals in the bone matrix, and protect the soft tissues from calcification, cannot be performed" (Masterjohn, 2007). Warfarin (Bach et al., 1996) causes an overabundance of under-carboxylated proteins, which overcome the quantity of carboxylated proteins, so the under-carboxylated proteins themselves may assist the liberation of calcium from the bone matrix, leading to the accumulation of calcium into other soft tissues (Masterjohn, 2007). He also proposed that the method by which vitamin A protects against vitamin D toxicity is the ability of vitamin A to down-regulate the previously mentioned vitamin K-dependent protein MGP (Masterjohn, 2007). It was also noted that the methods in which vitamins A and D alter vitamin K concentrations need further study (Fu et al., 2008). As the demand for carboxylation reduces, the resulting effect is the counteraction of (vitamin D-induced) vitamin K depletion (Masterjohn, 2007). There have been studies showing that the consequences of overdoses in vitamin D strongly resemble the symptoms of vitamin K deficiency, or a deficiency in vitamin K-dependent proteins (e.g. MGP) (Proudfoot and Shanahan, 2006, Munroe et al., 1999, Fu et al., 2008, Masterjohn, 2007). Animals with vitamin D toxicity develop soft tissue calcification in the arteries, lungs and trachea, and develop growth retardation, bone demineralisation and in severe cases, suffer death due to calcification of the aorta and its branches (Masterjohn, 2007). Similar symptoms, though not exactly the same phenotype, have been observed in humans with MGP mutations (Keutel Syndrome) (Munroe et al., 1999). The mechanism by which vitamin D is able to cause growth retardation is unknown, however a similar effect is present in MGP knockout mice, which exhibit widespread calcification of the proliferative zone and zone of provisional calcification in metaphyses (Masterjohn, 2007). MGP knockout mice have disorganised hypertrophic chondrocytes, which are not organised into normal

columns, and consequently the scaffolding usually provided for the deposition of bone matrix is not present, leading to short stature (Luo et al., 1997). This indicates that an alteration in the MI during growth is certainly possible in cases of vitamin K deficiency.

#### **4.5 Exercise**

Exercise causes muscles to exert stress and strains on long bones, particularly at weight-bearing sites. This influences longitudinal bone growth. Bones must adapt to the stress being placed upon them by increasing properties such as BMD and cross-sectional bone area in order to prevent exceeding fracture thresholds. Conversely, if a person is immobilised, osteocytes will sense this and facilitate the appearance of osteoclasts, which remove bone that is not required due to reduced loading. Some studies using rats have shown that stress increases certain properties such as BMD, BMC and cross-sectional area (Umemura et al., 1995, Gunter et al., 2008, Isaksson et al., 2009), while others have shown that the stress associated with intensive treadmill exercise suppresses bone growth (Bourrin et al., 1994, Li et al., 1991). These differences can most likely be explained by various types and magnitudes of stress. For example, some studies using animals have concluded that the stress/strain rate is more significant than the magnitude (Judex and Zernicke, 2000b, Judex and Zernicke, 2000a, Skerry and Peet, 1997). In a study of post-menopausal women, BMDa at the hip and lumbar spine was increased over a year in participants that undertook a higher level stress/strain exercise program, than those who undertook more aerobic low level (walking, running) exercise (Stengel et al., 2005). In a study using pQCT to examine child gymnasts and controls, the gymnasts exhibited a higher total BMD at the distal tibia, greater cross-sectional bone and muscle area at the 50% radius, higher strength strain index (SSI) at the 50% radius and greater total and trabecular BMD at the distal radius (Ward et al., 2005b). Crucially however, the total cross-sectional area of the bone at the 4% distal radius was not significantly different between the gymnasts and controls, indicating that although much larger amounts of muscle stress were occurring at the 4% distal radius of gymnasts, it was not sufficient to cause a significant change in metaphyseal area at this site. A study of both child and adult tennis players showed that children who started playing around the time of puberty showed a significant difference in BMC, BMD and bone area differences at

the distal radius (Ducher et al., 2006). This indicates that the irregular stress on the playing arm of tennis players was sufficient to cause significant morphological changes in the metaphysis. These results were supported in another study in female tennis players who had begun playing before the onset of puberty, in which total cross-sectional area of the distal radius was significantly different between dominant and non-dominant forearms, and between athletes and controls (Kontulainen et al., 2003). Interestingly, both studies found that the differences between dominant and non-dominant forearms was much more apparent at the mid-radial diaphysis (Ducher et al., 2006) and the mid-humerus (Kontulainen et al., 2003) in adult tennis players. The response of the distal radial metaphysis to stress may be limited after epiphyseal fusion, and because bone turnover in cortical sites (e.g. mid-diaphysis of a long bone), takes longer than in trabecular sites (e.g. metaphysis), this may explain the site-specific differences observed in both studies (Ducher et al., 2006, Kontulainen et al., 2003). Both studies also confirm the link between increased high-level intermittent mechanical stress and increased bone strength (Ducher et al., 2006, Kontulainen et al., 2003). Some advocate beginning stress-inducing activities such as tennis before puberty to reduce fracture risk (Ducher et al., 2006), which is particularly relevant considering fractures of the distal radius are the most common type of fracture in peri-pubertal age groups (Rauch et al., 2001a). This evidence indicates that stress and exercise are able, under certain circumstances, to alter the MI.

#### **4.6 Bisphosphonates**

Bisphosphonates are a type of drug that inhibits osteoclastic activity. They do this in two ways: clodronate and etidronate, which are older types of bisphosphonate, cause the formation of ATP analogues that accumulate in osteoclasts and are cytotoxic, causing apoptosis (Shaw and Bishop, 2005). The newer generation of bisphosphonates, which include pamidronate, olpandronate, ibandronate, aledronate, risendronate and zoledronate, inhibit the production of farnesyl pyrophosphate and geranylgeranyl pyrophosphate (Luckman et al., 1998). This causes a subsequent prenylation failure of several GTP-binding proteins, leading to a failure in the translocation of these proteins

into the cell membrane, inducing severe cellular interference and eventually apoptosis (Luckman et al., 1998).

Many studies have been conducted on the use of bisphosphonates (both oral and intravenous) for the treatment of a variety of paediatric conditions such as juvenile idiopathic osteoporosis (Bachrach and Ward, 2009, Brumsen et al., 1997, Brown and Zacharin, 2009), OI (Land et al., 2006, Madenci et al., 2006, Chevrel et al., 2006, DiMeglio and Peacock, 2006, Pizones et al., 2005, DiMeglio et al., 2005, Rauch et al., 2007, Senthilnathan et al., 2008), fibrous dysplasia (Kitagawa et al., 2004, Plotkin et al., 2003), idiopathic juvenile hyperphosphatasia (Cundy et al., 2004), Menke's disease (Kanumakala et al., 2002) and cerebral palsy (Henderson et al., 2002). These conditions mainly result in metaphyseal splaying, however bisphosphonates could act to reverse this effect and over the course of time cause the MI to become closer to normal. This change can proceed too far and eventually cause drug-induced osteopetrosis, such as was seen in a case report of a 12 year old male (Fig. 4.5) by Whyte and colleagues (Whyte et al., 2003). Osteopetrosis is an umbrella term that consists of many disorders, both autosomal dominant and autosomal recessive, which differ in onset and severity. It is often characterised by increased bone opacity as seen on a radiograph, increased bone mass, fractures, and impaired longitudinal bone growth resulting in short stature (Stark and Savarirayan, 2009). The fractures occur because the bone is not remodelled due to inhibition of osteoclast differentiation or, in the case of bisphosphonates, function. Bisphosphonate use in children has been a widely debated topic due to reports of brittle bones and increases in numbers of fractures (Marini, 2003) Bisphosphonates have a half-life of several years in the skeleton, depending on the bone turnover rate, which caused the symptoms of the 12 year old male to persist over 18 months after bisphosphonate treatment had been discontinued (Whyte et al., 2003). The ratio of GPW to MW in this case appears almost 1 to 1, and since the MI is equal to the  $0.5MW/GPW$ , a ratio of 1 to 1 would produce an MI of 0.5. Once osteoclast function returned after discontinuation of treatment, the bone would gradually remodel until the increased bone mass and radio-opacity disappeared. Therefore bisphosphonates do have an affect on MI.





**Figure 4.5: Progression from normal femur to bisphosphonate induced osteopetrosis. A: Normal distal femur (age 8 years); B: radio-opaque banding in the distal metaphysis indicating a modelling failure (age 9 years – 1.25 years of pamidronate therapy); C: radio-opaque banding expanding further into the metaphysis (age 12 years – 1.5 years after last infusion of pamidronate). Reproduced with permission and copyright © of the NEJM (Whyte et al., 2003).**

#### 4.7 Summary

There are many different types of dysplasias and other conditions that can cause an alteration in the MI ratio. NF1 is such a condition, while CDGP is a possibility. There are also several vitamins, minerals and drugs that have an effect on the MI including vitamin C, D, calcium, phosphate, copper, manganese, and bisphosphonates. Several vitamins and minerals could have an effect on the MI including vitamin B6, K, magnesium zinc and iron. Exercise may also affect MI. Table 4.2 summarises the vitamins, minerals, bisphosphonates and exercise effects on the MI.

**Table 4.2 – Summary of Actions on the Growth Plate**

	<b>Could Alter MI?</b>	<b>In What Way?</b>	<b>Comments</b>
Vitamin A	Unlikely		Negatively affects growth plate in terms of fusion times but not overall morphology
Vitamin B <sub>6</sub>	Possibly	Deficiency = reduced diaphyseal size	Only 1 reference (from 1986) to suggest possible effects
Vitamin B <sub>9</sub>	No evidence in literature to support an MI effect		
Vitamin B <sub>12</sub>	No evidence in literature to support an MI effect		
Vitamin C	Yes	Deficiency = metaphyseal splaying	
Vitamin D	Yes	Severe deficiency and toxicity = metaphyseal splaying	
Vitamin K	Possibly	Deficiency = metaphyseal splaying	
Calcium	Yes	Deficiency = metaphyseal splaying	Severe deficiency and toxicity can result in death
Phosphorus/PO <sub>4</sub>	Yes	Deficiency = metaphyseal splaying	
Magnesium	Possibly	Deficiency = narrowed growth plate height, which may in turn cause metaphyseal splaying	
Zinc	Possibly	Deficiency could result in splaying or more likely overall reduction in bone size meaning MI ratio would remain in proportion	
Copper	Yes	Deficiency = metaphyseal splaying	
Manganese	Yes	Deficiency = metaphyseal splaying	
Potassium	No evidence in literature to support an MI effect		
Iron	Possibly	Deficiency = metaphyseal splaying	If severe & prolonged
Exercise (loading of the distal radius)	Possible		More likely to cause changes in BMD and BMC rather than morphology. If morphology were affected, it is more likely to be proportional, therefore the MI ratio would remain similar.
Bisphosphonates	Yes	Will increase MW compared to GPW (the opposite effect to splaying).	An overdose can mimic osteopetrosis.

**Table 4.2: Summary of external forces that could affect the distal radial GPW and MW.**

## **5. Methods - Original Study Groups**

### **5.1 Introduction**

The MI study is a retrospective work using the data from two ongoing studies and two previously completed studies. The two ongoing studies are the NF1 and CDGP studies and the two completed studies are the B16N2 Normal Children study and the Gymnast study. The bone-age assessment study using DXA hand images and hand radiographs is also a retrospective study using data collected as part of the B16N2 Normal Children Study. Sections 5.2 through 5.5 of this chapter outline these four studies and include information such as the original inclusion and exclusion criteria, age ranges, what techniques were used and what data was collected. These studies were all carried out in accordance with the Declaration of Helsinki (1964).

### **5.2 The B16N2 Normal Children Study**

The aim of the B16N2 Normal Children study was as follows: to provide a comprehensive cross-sectional and longitudinal database of paediatric reference data (aged 5 to 20 years) for DXA, pQCT and radiographic examinations, taking into account pubertal stage, diet, exercise and lifestyle information (Ashby et al., 2008, Ward et al., 2007b).

The justification for generating data from normal children was as follows: paediatric studies are more difficult to design and recruit for and although there is a wealth of normal adult reference data, there is a paucity of normal paediatric reference data. It can be difficult to assess whether a child is “normal” when comparing him or her to adult reference data.

The B16N2 Normal Children’s Study was originally approved in 1998 by the Central Manchester Local Research Ethics Committee (Reference No. CEN/98/036) and was later approved by the North West Multi-Centre Research Ethics Committee (Reference No. MREC 04/8/006) in 2004. It was also approved and registered with the University of Manchester Ethics Committee (Dr Tim Stibbs, personal communication) and recruited from 1998 to 2008. The data gathered examining bone growth and development in normal children included:

- DXA hand image for bone-age assessment.
- BMDa of the proximal femur (total hip and femoral neck) and lumbar spine (L1 – L4).
- BMAD of lumbar spine and femoral neck.
- Whole body total and regional BMC, BMDa and fat and lean muscle mass.
- pQCT at the 4% forearm and 50% forearm.
- Radiographs of the hand/forearm (for subjects examined in the Stopford building only – mobile units were equipped with DXA and pQCT only).
  - DXR measures (MCI, BMDa and CrTThick) were subsequently obtained from hand radiographs.
- Grip strength.
- Height.
- Weight.
- Tanner pubertal stage.
- Food and exercise diaries.

Inclusion criteria included being of white Caucasian ancestry and being aged between 5 and 20 years from baseline and throughout all follow-up scans (follow-up scans refer to subjects that returned for additional examinations over the course of several years for the purpose of gathering longitudinal data). Exclusion criteria included being of non-white/Caucasian ancestry, inability to give informed consent, weight and/or height outside the minimum (0.4<sup>th</sup> centile) or maximum (99.6<sup>th</sup> centile) weight or height reference curves for the UK (Freeman et al., 1995b), fracture within the previous 12 months, history of recurring low-trauma fractures, presence of systemic disease, any periods of prolonged immobilisation within the previous 12 months, undertaking any procedure involving ionising radiation within the previous 12 months, the use of drugs or presence of any condition known to affect skeletal health, a first-degree relative diagnosed with primary osteoporosis, and in the case of females, pregnancy or the possibility of pregnancy (Ashby, 2007).

### **5.3 The Gymnast Study**

The aim of the original study was as follows: to examine BMC, BMD, CSMA and bone area and the effects of calcium supplementation in young gymnasts using DXA, pQCT and anthropometric measurements and compare the data with that of normal controls (Ward et al., 2005b).

The justification for this study was as follows: previous studies have reported beneficial effects of gymnastics on the skeleton (Nichols et al., 1994, Nickols-Richardson et al., 1999), as the amount of stress placed on the skeleton during gymnastics will cause the bones to adapt by increasing BMD and or BMC, but bone geometry and the uptake of calcium (whether gymnasts will respond differently when supplemented with calcium than normal controls), had not been investigated.

The Gymnast group were part of a 12 month randomised control trial investigating calcium supplementation in pre-pubertal children who participated in 6 or more hours of competitive gymnastics per week (Ward et al., 2005b). The study was approved by the Central Manchester Local Research Ethics Committee (Reference No. CEN/00/144) and the Liverpool Children's Research Ethics Committee (Reference No. 01/27/E). Subjects were randomised to either calcium supplementation or placebo and examined at baseline and at 12 months (Ward et al., 2005b). A total of 44 gymnasts (17 male, 1 mixed ancestry, 1 Chinese ancestry) aged 5 to 12 years (mean age 9 years) were originally recruited from schools within the Greater Manchester Area (Ward et al., 2005b). The inclusion and exclusion criteria for the gym study were very similar to the B16N2 Normal study except that participants were not excluded based on race or ethnic background. The additional exclusion criteria were allergy to dairy products or a personal or family history of nephrocalcinosis or kidney stones (Ward et al., 2005b). All subjects were confirmed as pre-pubertal by self-assessment (and parental aid if necessary) at baseline using the Tanner criteria and an orchidometer (Tanner, 1962).

#### **5.4 The NF1 Study**

The aim of this study is as follows: to investigate spinal abnormalities including spinal cord dural ectasia, spinal neurofibromas, and meningoceles with dysplastic osseous abnormalities, dystrophic scoliosis and general bone health in individuals aged 6 to 9 years of age with NF1.

The justifications behind this study were as follows:

- Dysplastic radiographic findings may be useful clinical screening tools for scoliosis, which would allow preventative strategies for the development and progression of scoliosis to be investigated.
- Changes to vertebral body and canal area lead to rapid progression of neurological complications; therefore a screening tool/technique to detect these changes would be clinically useful.
- There may be indications of future complications of the disease when bone health (as studied using DXA, pQCT, radiographs and urinary examination of pyridinium cross-links) is investigated.

Manchester is one of the centres in the NF1 study, which is a multi-centre and multi-national (other centres are Cincinnati USA, Utah USA and Vancouver Canada) study that was originally approved in 2006 by the South Manchester Research Ethics Committee (Reference No. 06/Q1403/107) and continues until 2011. The original inclusion criteria include meeting the National Institute of Health criteria for diagnosing NF1 (in subjects aged 6 to 9 years at time of enrolment and Tanner stage not greater than 1 at time of enrolment). All subjects were confirmed as pre-pubertal by self-assessment (and parental aid if necessary) using the Tanner criteria and an orchidometer (Tanner, 1962). The original exclusion criteria include prior surgical repair of the spine, short-segment (4-6 vertebrae) curve with a Cobb angle of 45° or more, taking hormone replacement therapy, chronic glucocorticoid use, presence of tibial pseudoarthrosis, or presence of other chronic medical problems known to influence general bone health (i.e. diabetes mellitus, cerebral palsy etc). Subjects are examined once per year over four years with a hand radiograph taken at years one and four for bone-age assessment.

## 5.5 The CDGP Study

The aims of the original study were as follows:

- To investigate BMD and body mass index (BMI) in CDGP and compare this group with normal controls.
- To investigate whether biochemical markers are useful in identifying children with CDGP who have a low BMDa.
- To investigate genetic polymorphisms associated with lower BMDa in children with CDGP.

The justification for the study was: bone health may be affected in children with CDGP, therefore quantitative imaging and biochemical analysis may provide further insight into identifying children with CDGP and assess whether any adverse affects to bone health may persist into adulthood.

The CDGP study is an ongoing study that began recruiting in 2003 and has been ethically approved by the CMMCUH (Reference No. 00137) and the North West 9 Research Ethics Committee – Greater Manchester West (Reference No. 07/H1009/66). The principal investigator is Dr Indraneel Banerjee of the Manchester Royal Children's Hospital. Subjects were recruited between ages 5 to 17 years; a diagnosis of CDGP is made if there are no signs of puberty by age 12 in girls and 13 in boys and a diagnosis of constitutional growth delay (CGD) may be made in girls aged <12 years and boys aged <13 years. Inclusion criteria were a diagnosis of CDGP or CGD. Subjects were not excluded due to race, ethnic origin, other chronic disease(s), systemic diseases or use of drugs that could affect bone health. The exclusion criterion was being unable to give informed consent.

## **6. Methods – Study Groups, Subjects and Quantitative Assessment**

### **6.1 Introduction**

The following chapter describes how the data from the original study groups (described in the previous chapter) were used in the MI study. Sections 6.2 through 6.6 describe the subjects, inclusion and exclusion criteria, methods used and information obtained. Section 6.7 contains two tables that summarise the methods and information obtained from the original study groups, as well as the author contribution. Sections 6.8 through 6.13 are in-depth descriptions of the methods used. As this was a retrospective study, the ethics approval was already granted in the ethics approvals of the original studies.

### **6.2 Normal Group Data**

All subjects in the Normal group, or described as Normal controls, were part of the B16N2 Normal Children's Study discussed in section 5.2. Inclusion criteria for the current study, for examination of the MI and TW3 bone-age assessment, were: subjects were required to be aged between 5 and 20 years and have minimum 1 hand radiograph. Exclusion criteria for the MI study were as follows: subjects were excluded if, subsequent to the original examination, one of the original exclusion criteria for the B16N2 study was found to apply, such as low BMD, abnormal bone geometry or presence of systemic disease. There were eight subjects excluded from the original B16N2 database, and were therefore excluded from the present study. Subjects were excluded from the MI study if the radiographs were not of sufficient quality or had poor positioning so that the MI, MW, GPW or bone-age could not be determined; 1 subject was excluded on this basis as only a few millimetres of the distal radius was visible. Subjects examined only on the mobile osteoporosis vans for the B16N2 study were excluded from the MI study because no hand radiographs were available for these participants. This was due to the lack of mobile radiographic equipment on the vans, which were equipped only with a Hologic QDR Discovery (Bedford, USA) and a Stratec XCT-2000 pQCT (Phorzeim, Germany), for the period this study was recruiting. The total number of subjects that met the inclusion criteria for the MI study was 378 (155 male). Of the 378 subjects, 11 did not have an available baseline pQCT scan due to movement artefacts and 17 did not have a follow-up pQCT scan, but did have a follow-



up hand radiograph. Of the 378 subjects, 16 refused to complete the self-assessed Tanner pubertal stage, leaving 362 subjects that provided at least one (baseline) Tanner pubertal stage. MI, MW, GPW, TW3 and GP bone-age were assessed using hand radiographs. Three DXR measures (MCI, BMDa and metacarpal cortical thickness) were assessed using hand radiographs and the Sectra Pronosco DXR system (Linköping, Sweden). Only 159 subjects within this group had DXR results available for comparison in the MI study. Chronological age, height, weight, arm length and pQCT values were obtained from the original study and compared to the MI, MW and GPW.

### **6.3 Gymnast Group Data**

At baseline, 37 (15 male) gymnasts aged 5 to 12 years (mean 9 years) had hand radiographs available for examination in the MI study. Inclusion criteria for the MI study included meeting the original inclusion criteria and having a minimum of one hand radiograph available for analysis. Subjects were excluded from the MI study if the radiographs were not of sufficient quality or had poor positioning so that the MI, MW, GPW or bone-age could not be determined; one subject was excluded for this reason, leaving 36 subjects (15 male). MI, MW and GPW were assessed from hand radiographs. Chronological age, height, weight, arm length and pQCT values were obtained from the original study and compared to the MI, MW and GPW values.

### **6.4 NF1 Group Data**

The inclusion criteria of the MI study included meeting the original inclusion criteria and having one hand radiograph minimum available for analysis. Subjects were excluded from the MI study if the radiographs were not of sufficient quality or had poor positioning so that the MI, MW, GPW or bone-age could not be determined, however neither of these situations occurred. MI, MW and GPW were assessed using hand radiographs. By September 2008, 23 subjects had been recruited and had a baseline radiograph on hard-copy film; when the NF1 study began recruiting, it pre-dated PACS. PACS replaced the use of radiograph film after 17 (7 male) subjects were recruited. Because the subjects who had PACS hand radiographs could not have calibration markers placed on the image retrospectively to determine the absolute GPW and MW

values, any subject with a PACS hand radiograph was excluded from the MI study. Chronological age, height, weight, arm length and pQCT values were obtained from the original study and compared to the MI, MW and GPW. Two of the 17 subjects did not have pQCT scan data and one subject did not have a forearm length measurement.

### **6.5 CDGP Group Data**

The inclusion criteria of the MI study included meeting the original inclusion criteria and having one hand radiograph minimum available for analysis. Subjects were excluded from the MI study if the radiographs were not of sufficient quality or had poor positioning so that the MI, MW, GPW or bone-age could not be determined, however neither of these situations occurred. MI, MW, GPW and TW3 bone-age were assessed using hand radiographs. Height, weight and chronological age were obtained from the original study. However, the majority subject case-notes were stored in a secure NHS location and were not available to the author for the MI study. Only 25 subjects (22 male) were available for the MI study that had a height and weight measurement on the same day as their hand radiograph was taken. It should be noted that some of the illnesses suffered by the CDGP subjects included gynecomastia, Hodgkin's lymphoma, Leri-Weill syndrome, congestive heart disease, unspecified allergies, clinical obesity, asthma (some subjects taking unspecified steroids, some not), coeliac, anaemia, and renal failure. The author did not have access to case notes, therefore it was not possible to associate these conditions with any particular subject.

### **6.6 DXA Bone-Age Data**

Subjects from the B16N2 database were included in the MI study if they fit the original inclusion criteria and had a DXA hand scan and hand radiograph taken at the same visit. Ninety-nine children fit the inclusion criteria. Subjects were excluded if either the hand radiograph or DXA hand scan were of insufficient quality or exhibited poor positioning such that bone-age could not be determined. One subject was excluded due to an incomplete DXA hand scan in which only half of the hand was visible due to poor placement, which meant an accurate bone-age could not be determined. Therefore 98 subjects (38 male) aged 6 to 20 (mean 13.27; SD 3.78) years, had a postero-anterior

(PA) DXA image and radiograph (96 left, 2 right) of the non-dominant hand, at the same visit. GP bone-age was determined for each radiograph and each corresponding DXA hand scan.

### **6.7 Data and Methods Summary**

The retrospective nature of the MI study and the use of two ongoing and two previously completed studies, all with different inclusion and exclusion criteria, age ranges and some with follow-up visits, may lead to ambiguity. Therefore two summary tables attempt to clarify what information was obtained from the original studies and how many subjects (both total and baseline) were examined (Table 6.1) and what information the author collected for the MI study (Table 6.2).

### **6.8 Quantitative Assessment**

Hand radiographs produced in the B16N2 Normal, Gymnast and the NF1 subjects were taken in the University of Manchester Medical School and those obtained in the CDGP study were taken at Booth Hall Children's Hospital, Greater Manchester.

<b>Table 6.1 – Subject Summary</b>	<b>B16N2 Normal</b>	<b>Gymnast</b>	<b>NF1</b>	<b>CDGP</b>
<b>Chronological Age</b>	542 Total 378 Baseline	68 Total 36 Baseline	17 Total & Baseline	161 Total 108 Baseline
<b>TW3 Bone-Age</b>	542 Total 378 Baseline	N/A	N/A	161 Total 108 Baseline
<b>GP Bone-Age</b>	98 Radiograph 98 DXA Image	N/A	N/A	N/A
<b>MW</b>	542 Total 378 Baseline	68 Total 36 Baseline	17 Total & Baseline	161 Total 108 Baseline
<b>GPW</b>	542 Total 378 Baseline	68 Total 36 Baseline	17 Total & Baseline	161 Total 108 Baseline
<b>Height</b>	542 Total 378 Baseline	68 Total 36 Baseline	17 Total & Baseline	25 Total & Baseline
<b>Weight</b>	542 Total 378 Baseline	68 Total 36 Baseline	17 Total & Baseline	25 Total & Baseline
<b>Tanner Pubertal Stage</b>	499 Total 362 Baseline	68 Total 36 Baseline	17 Total & Baseline	Unavailable to Author
<b>Arm Length</b>	541 Total 377 Baseline	66 Total 36 Baseline	16 Total & Baseline	Less than 10 subjects had pQCT scans when the analysis was being done for the MI study. Due to subject number being too small to obtain reliable statistical output, none were analysed.
<b>Total Bone Density 4%</b>	541 Total 377 Baseline	66 Total 36 Baseline	15 Total & Baseline	
<b>Total Bone Area 4%</b>	541 Total 377 Baseline	66 Total 36 Baseline	15 Total & Baseline	
<b>CSMA 50%</b>	538 Total 374 Baseline	65 Total 35 Baseline	15 Total & Baseline	
<b>pSSI 50%</b>	538 Total 374 Baseline	65 Total 35 Baseline	15 Total & Baseline	
<b>Total Bone Area 50%</b>	538 Total 374 Baseline	65 Total 35 Baseline	15 Total & Baseline	
<b>Cortical Bone Density 50%</b>	538 Total 374 Baseline	65 Total 35 Baseline	15 Total & Baseline	
<b>Metacarpal Index DXR</b>	148 Total & Baseline	N/A	N/A	N/A
<b>BMDa DXR</b>	148 Total & Baseline	N/A	N/A	N/A
<b>Cortical Thickness DXR</b>	148 Total & Baseline	N/A	N/A	N/A

**Table 6.1: Data summary across all four studies outlining number of subjects examined in each group and using what technique.**

<b>Table 6.2 – Data Summary</b>	<b>Data Obtained from Original Studies Used for MI Study</b>	<b>Data Calculated by Author for MI Study</b>
<b>Chronological Age</b>	X	
<b>TW3 Bone-Age</b>		X
<b>GP Bone-Age</b>		X
<b>Height</b>	X	
<b>Weight</b>	X	
<b>Hand Radiograph</b>	X	
<b>DXA Hand Image</b>	X	
<b>40% &amp; 60% MI/MW</b>		X
<b>MI Z Scores</b>		X
<b>MW</b>		X
<b>GPW</b>		X
<b>Arm Length</b>	X	
<b>pQCT Measures</b>	X	
<b>DXR Measures</b>	X	
<b>Statistical Analyses</b>		X

Table 6.2: Summary of data obtained from previous studies and data calculated by the author for the MI study.

### 6.8.1 Image Acquisition - Radiographs

Hand radiographs were performed by several radiographers in the department of Clinical Radiology at the University of Manchester, using Philips Medical Systems Super 80 CP X-ray equipment (Philips, Eindhoven, The Netherlands). X-ray exposure was 55–60 kV, 5 mAs, film focus distance 1m, and fine focal spot 0.6 mm. The radiographic film used was either high-resolution Kodak MinR 2000 (Kodak, Rochester, N.Y.) single-sided emulsion mammography film (SF), with Kodak MinR screens, or Konica MGSR fine-grain DF, with Kodak Lanex fine screens (all 24cm by 30cm). All films were processed on a standard processing cycle in a Kodak X-OMAT M35 processor.

Shortly after the CDGP group hand radiographs were completed at Booth Hall Hospital, this hospital was permanently closed and many records were moved to off-site NHS storage facilities, to which the author was not able to obtain access. Therefore the author was not able to obtain the specifics of the radiographic processing for this group.

### 6.8.2 Digitising Radiographs

To obtain the optimum method for digitising the radiographs to make the MI/MW/GPW assessments was problematic and required several approaches.

a) The initial protocol involved using a digital camera (Canon model EOS 20D with Canon Macro lens set at medium quality .jpg 2544 x 1696 pixels, file size 1.2MB) mounted on a stand at 60cm above the film. The films were illuminated using a light box to which a clear plastic ruler was attached both to give a straight edge with which to align the radius for computer analysis, and to give the images calibration markers. The viewfinder of the camera was equipped with square boxes which were used to align the camera to the straight edge of the ruler. The radiographs were then placed underneath the ruler with the widest part of the distal radial growth plate aligned to the straight edge of the ruler. This practice ensured that the image of the radial growth plate would be horizontal, which was essential to the computer assisted measurement process. The camera was set with a timer so that the camera placement would not be accidentally altered when the images were captured.

The advantages of this protocol were the speed at which the images could be acquired; approximately 30 to 45 seconds to place the film and capture the digital image, and the resulting digital images did not require alignment alterations. This protocol was discontinued after approximately 60 test images because access to this specific camera became difficult. Another camera of this quality was not easily accessible, therefore the protocol was changed and a dedicated radiographic digitiser was used.

b) The second method of digitising the radiographs involved using the VIDAR DiagnosticPro *Advantage* film digitiser (Vidar, Herndon, USA). The digitiser was set at the following settings: depth 12, resolution 300dpi, pixels 3000 x 3600, scan size 10 x 12 and the power was set at 5. Power is the level of light/dark. Power 1 is the lightest and power 10 is the darkest, therefore power 5 is in the midrange. Although this often resulted in the middle and distal phalanges being too dark to distinguish clearly (unimportant in an MI assessment), it also kept the background around the radius from being too light, which interfered with the ability of the author to judge the edges of the bone. The advantage of this method was that the scan time for a 300dpi image was short at approximately 30 seconds. However, this resolution resulted in an image of

significantly reduced quality compared to Method 1 and it was often difficult to judge the edges of the bone. This method was abandoned after approximately 70 test images.

c) The third protocol also used the VIDAR *DiagnosticPro Advantage* film digitiser. The digitiser was set at the following settings: depth 12, resolution 570dpi, pixels 5700 x 6840, scan size 10 x 12 and power set at 3 (which is the default power setting). The image quality was excellent at this resolution but the file size was very large. The Vidar has the advantages of being able to scan up to 25 radiographs in one batch and has scan-settings of up to 570dpi resolution. The disadvantages are the time it takes to scan one radiograph at 570dpi (approximately 4 minutes) and the large file sizes at that resolution (approximately 75MB .tiff files for the scan settings in this protocol). Another disadvantage specific to this study is that for the computer-based measurements to be accurate, the widest part of the radial growth plate must be a completely straight horizontal line. This meant that to prepare a digitised radiograph for computer-based measurement, the image would have to be opened in Adobe Photoshop and rotated until the radial growth plate of the image was horizontal. Unfortunately this process changed the size of the image: the more the image had to be rotated, the higher the increase in file size, which could have undetermined effects on the image. This also resulted in the image files often exceeding 100MB and the software used to perform the computer-assisted measurements often experienced difficulties opening the files or would crash during the measurement process. The issues of file size being too large to be opened/measured, image rotation file size differences and a malfunction in the VIDAR that was causing damage to the films lead to a final change in protocol back to the original digital camera method after completing approximately 25 test images.

d) The final protocol was as described for a) the initial protocol, using the same Canon model EOS 20D digital camera and Canon Macro lens. A 1.2MB file size was easily managed by the program used to perform the computer assisted measurements (further detail in section 6.10), and provided excellent resolution for bone-edge detection. The final method is illustrated in Figure 6.1.

### 6.8.3 Image/Data Acquisition – pQCT

All pQCT scans for the original B16N2 study were performed by a radiographer in the department of Clinical Radiology at the University of Manchester using a Stratec XCT-2000 pQCT scanner (Phorziem, Germany). The length of the forearm to be scanned



**Figure 6.1: Photograph of setup used to digitise radiographs, optimised for measurement of MI.**

(arm length) was measured by placing the subject's elbow on a table with the arm resting vertically and using a tape-measure to measure from the ulnar styloid process to the olecranon, and was performed by a radiographer. The arm of the subject was placed within the bore of the pQCT where their hand rested on a hand-grip. This allowed the subject to keep his/her arm still, thus avoiding movement artefact (Fig 6.2). Scans were taken at the 3.5%, 4% and the 50% midshaft radius. Generally the 3.5% slice is not used but two subjects experienced movement artefacts on the 4% slice, therefore the 3.5% was used in those cases. The measurements used were total bone mineral density





**Figure 6.2:** The Stratec XCT-2000 pQCT machine at the Manchester Royal Infirmary (formerly housed at the department of Clinical Radiology, University of Manchester).

(toBMD), cross-sectional muscle area (CSMA), polar strength-strain index (pSSI), radius cortical area (50%) and radius bone density (50%). The cortical scans at the 4% site were performed using a  $710 \text{ mg/cm}^3$  threshold. The cortical scans at the 50% site were performed using a  $960 \text{ mg/cm}^3$  threshold, except the cortical SSI threshold, which was performed at  $480 \text{ mg/cm}^3$ . Contour mode 1 peel mode 1 was the standard loop analysis used for bone and contour mode 3 peel mode 1 was used for muscle and bone analysis. The contour mode works by identifying a voxel on the edge of the region of interest (e.g. radius) and comparing it to several other voxels surrounding it. This process is repeated around the circumference of the radius until the starting voxel is reached. Voxels not meeting the required threshold are excluded, leaving the region of interest. Peel mode 1 peels away 55% of the outer bone layers (cortical bone) leaving 45% of trabecular bone. Bone area is the total cross-sectional area of a bone calculated

before the peel mode takes effect. The standard Phorzeim pQCT phantoms were used to perform quality assurance daily. Although there are no precision calculations for pQCT scans of children, the CV for adults in the Department of Clinical Radiology = 1.27% for trBMD and 2.1% for toBMD at the 4% distal radius and 1.7% for tBA, 2.4% for csBA, and 3.7% for CSMA at the 50% radius (Ashby, 2007).

#### **6.8.4 Image Acquisition – DXA Hand Images**

All DXA scans were performed by a radiographer in the department of Clinical Radiology at the University of Manchester using Hologic QDR 4500 Discovery DXA scanner, software version 12.4 (Hologic Inc. Bedford, MA) (Fig 6.3), using the lumbar spine protocol. The standard Hologic phantom was used to perform quality assurance daily. During lumbar spine lateral morphology scans, a single-energy scout scan is used in order to determine if the patient is in the correct position. It is this single energy scan



**Figure 6.3: Hologic QDR 4500 Discovery DXA scanner in the Bone Densitometry suite at the Manchester Royal Infirmary (formerly housed in the department of Clinical Radiology, University of Manchester).**

that was used to produce the DXA hand images. To simulate soft tissue and improve image quality, a piece of polystyrene of uniform thickness (PUT), which measured 3 cm in thickness, was placed under the hand before the scan commenced. Subjects placed their pronated forearm and hand, with fingers together, on the PUT. Scanning then commenced a few centimetres distal to the finger-tips and stopped after approximately 1/3 of the distal forearm was scanned. Data regarding DXA BMDa were disregarded as the images obtained were the focus of this study. Although no studies of precision were conducted on DXA hand image scans, the department of Clinical Radiology had a CV = 1.1% for adult lumbar spine scans, and for whole body and lumbar spine scans combined, the maximum estimated dose equivalent was 0.0055 mSv (Ashby, 2007).

### **6.9 Anthropometric Data**

Height to the nearest 0.1 cm was measured in the B16N2 normal, gymnast and NF1 studies using a Leicester Height stadiometer (Child Growth Foundation, UK). Weight to the nearest 0.1 kg was measured in all studies using Seca digital scales (Autoweigh Scales, UK). Subjects were clothed but without shoes when height and weight were assessed. Tanner pubertal stage was assessed using the Tanner criteria (Tanner et al., 1962) and a Prader orchidometer (Pharmacia and Upjohn, Sweden). Subjects were provided with a private changing room and parental assistance was permitted when needed.

### **6.10 Calculating the Metaphyseal Index**

The method for calculating the MI is the same as that originated by Ward and colleagues (Ward et al., 2005a). It is defined as the ratio of half the metaphyseal width (0.5MW) to the growth plate width (GPW) (Fig 6.4). Two measurement techniques were employed: manual and computer assisted measurement. The manual measurement technique was performed using a hard copy film radiograph, a Lineartools Electronic Digital Calliper (Middlesex, UK), and a light box.

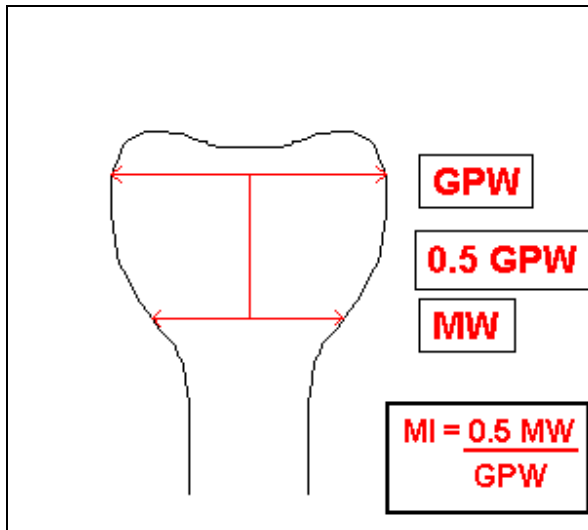


**Figure 6.4: Method for calculating the MI.**

The computer assisted technique used the program Qwin© by Leica Microsystems (Milton Keynes, UK). The Stopford numbers (used to anonymise images) of each radiograph were matched with the file name that the camera automatically assigned to each image. Each time the setup was dismantled, the number of images taken was recorded in order to ensure that the calibration was checked on the first image of a new batch and on other randomly selected images. The calibration was achieved by selecting two points on the image, usually points on the ruler between 10mm and 30mm apart. The operator would enter the appropriate distance in millimetres into the calibration menu. After entering the distance, QWin would provide a calibration. The calibration was checked approximately 50 times over the course of analysing the images. In every case the calibration used was 0.0449mm. This meant that despite the setup being dismantled and set up several times, the repeatability was excellent (see section 8.2) as the calibration given by QWin was always the same. The digital images appeared approximately quadruple the size of what was visible using a hard-copy film for the manual measurements. The pointer (controlled by the computer's mouse) combined with the size and quality of the image, allowed for a very finely detailed selection of the edge of the radial growth plate. Once the widest edge of the radial growth plate was selected (usually beginning with the left edge), the pointer was moved across to the opposite edge of the radial growth plate. As the pointer moved, the distance (in number

of pixels) would change accordingly and appeared in a function menu at the side of the screen. Once the opposite edge of the radial growth plate was reached, the number of pixels was noted. This number, when converted by the computer to millimetres, was the GPW measurement. GPW was then divided by two to obtain the 0.5GPW measurement. Once the GPW was divided by two, the pointer was moved downwards until it reached the number of pixels equivalent to 0.5GPW. The resulting image was a box in the shape of a rectangle. To obtain the 0.5MW measurement, the pointer was used to select the edges of the bone and the excess portions of the rectangle were removed. QWin converted the length of these lines from pixels to millimetres and produced information for each image. To make this process faster and more user friendly, a QUIP was written within Qwin to automate certain actions. QUIP is an interactive macro-programming facility that allows the operator to create semi-automatic routines for repetitive tasks. Once the QUIP was running, the image folder containing the digitised radiographs opened. After the operator selected a radiograph, the calibration toolbar appeared, which allowed a calibration check to occur on every image if the operator so chose. Once the operator accepted the calibration, a box-drawing toolbar appeared that allowed the operator to mark the GPW and MW. Once the operator accepted the box, the 'erasure' toolbar appeared allowing the user to erase the parts of the box that extended beyond the bone edge. When the operator accepted the bone-edge detection, the measurements of the two remaining lines (GPW and MW) appeared (in millimetres) in a Microsoft Office compatible table that could easily be copied and pasted into a master document or spreadsheet. Once the operator copied and pasted the values for that image into another document and the 'continue' button was clicked, the process began again. Figure 6.5 is an illustration of the computer assisted measurement method. Table 6.3 is an example of the information produced by QWin. Feature number 1 is the GPW measurement and Feature number 2 is the MW measurement, both given in millimetres. The other statistical information (X FCP and Y FCP) is defined as the feature count point for the X and Y axes, which are pixel co-ordinates. This information is currently, along with the descriptive statistical information i.e. the mean, standard deviation etc., irrelevant for the purposes of this project but has been saved. By dividing the MW by 2

( $21.611 / 2 = 10.806$ ) we obtain the 0.5MW measurement. MI is calculated by  $0.5MW / GPW$ . Therefore the MI for the example in Table 6.3 is  $10.806 / 29.289 = 0.369$ .

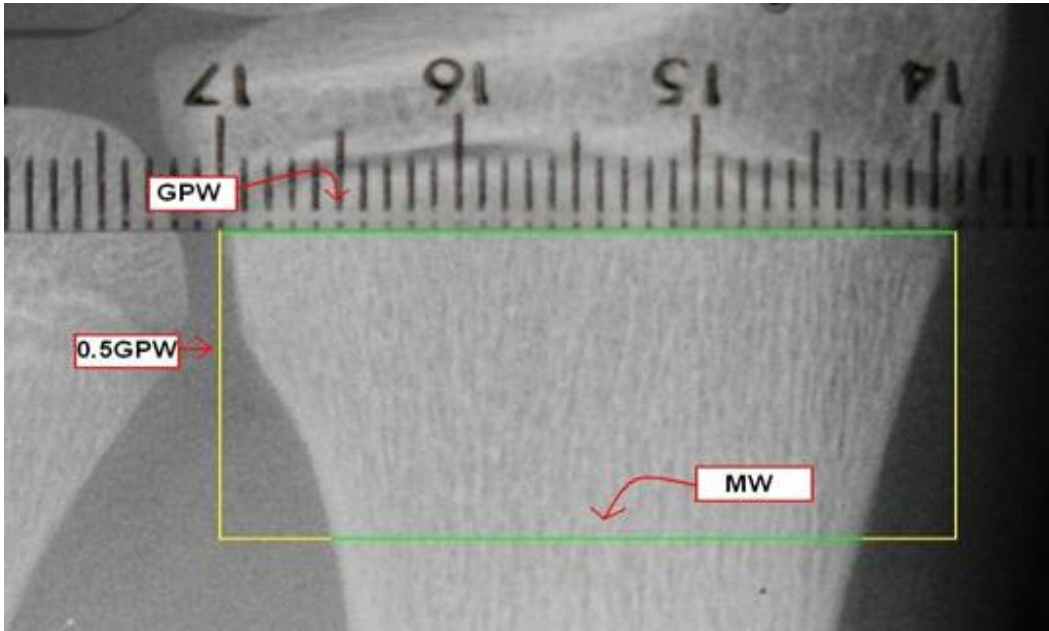


**Figure 6.5:** An example of the measurement process using Leica QWin. Bone edge detection was performed by the operator. The green lines were measured and the yellow lines were discarded.

<b>Table 6.3 – QWin Data Output</b>			
Features	2		
Number	X FCP	Y FCP	Width (mm)
1	1062	469	29.289
2	992	779	21.611
Total	2054	1248	50.901
Mean	1027	624	25.45
Std Dev	35	155	3.839
Std Err	24.749	109.602	2.714
Max	1062	779	29.289
Min	992	469	21.611
2-s Ran	140	620	15.355

**Table 6.3:** Example of output produced by Leica QWin. Width number 1 is the GPW and width number 2 is the MW.

### 6.10.1 Assessing the Metaphyseal Index

The formula for calculating the MI is  $0.5\text{MW}/\text{GPW}$ . The metaphyseal site at which the MW is measured is calculated by taking 50% of the GPW. However, taking 50% of the GPW is an arbitrary percentage chosen by Ward and colleagues (Ward et al., 2005a) and it is possible that using 40% or 60% of the GPW would result in a statistically more useful area of the metaphysis being measured, though the choices to take measurements at 40% and 60% of the GPW were also arbitrary. When 40% of the GPW was chosen, it resulted in a slightly more distal site of the metaphysis being measured. When 60% of the GPW was chosen, it resulted in a more proximal site of the metaphysis being measured (Fig. 6.6). This meant the MW would be at a different site and therefore a different width depending on how much of the GPW was used to calculate the MW site. The term '40% MI' was used to describe an MI where 0.4 GPW was used to determine the MW site, and the term '60% MI' was used to describe an MI where 0.6 GPW was used to calculate the MW site. Twenty-five randomly selected males and 25 randomly selected females from the normal group were assessed using the 40% MI and the 60% MI. Both the 40% MI and 60% MI were plotted against age and the plots compared to the original MI. The minimum, maximum and mean were calculated and also compared with the original MI results.

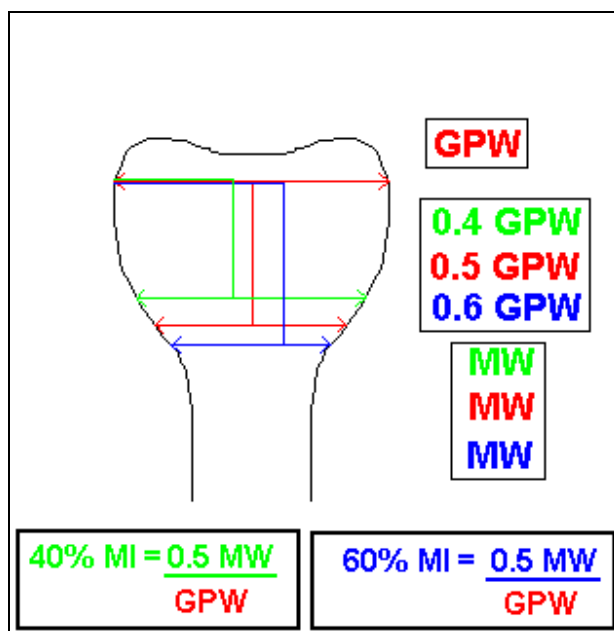


Figure 6.6: An illustration the methods for calculating the 40% and 60% MI.

### 6.11 TW3 Bone-Age Assessment Using Hand Radiographs

The bone-ageing method chosen for the MI study was the TW3 (Tanner et al., 2001), which is the most current of the TW series and all hand radiographs were assessed using this method. This method involves designating each relevant bone with a letter of the alphabet along with its corresponding numerical score. The letters range from *B* to *I*; *B* being the most skeletally immature category and *I* being the most skeletally mature category. Once the bone was assigned a letter based on maturity level, it was assigned a corresponding numerical score, which is different for every bone and is sex specific, as the female skeleton matures earlier than the male skeleton. Some bones, such as the radius and ulna, are weighted higher in the scoring system than phalanges or metacarpals. Therefore, having a more mature radius ensures a higher overall score than having a mature phalanx. A higher overall score therefore corresponds to a higher bone age. The TW3 method has two scoring systems, one for the radius, ulna and short bones (RUS), and one for the carpal bones (CAR). The specific bones included in the RUS group are the radius, ulna and the metacarpals and phalanges of the first, third and fifth digits. The bones included in the CAR group are the capitate, hamate, triquetral, lunate, scaphoid, trapezium and trapezoid (Fig. 6.7). Separating the scores in this way means that there is one bone age for the RUS group and one for the CAR group. The highest overall score attainable for both the RUS and CAR groups for both sexes is 1000. An overall score of 1000 for a male RUS is equivalent to a bone age of 16.5 years and an overall score of 1000 for a male CAR is equivalent to a bone age of 15+ years. For females, an overall score of 1000 for an RUS is equivalent to a bone age of 15 years and an overall score of 1000 for a CAR is equivalent to a bone age of 13+ years. RUS bones are shown in red and CAR bones are shown in black. Each radiograph was assessed using this method. The RUS scores were then plotted on graphs comparing them to the value of the MI. Only the RUS scores were used because the radius is the most relevant bone to compare to the radial MI. The carpals often have a bone-age that is more advanced than both the RUS age and chronological age because they mature at a faster rate (Dhar et al., 1993) and a single age rather than an age range is needed for statistical comparisons.



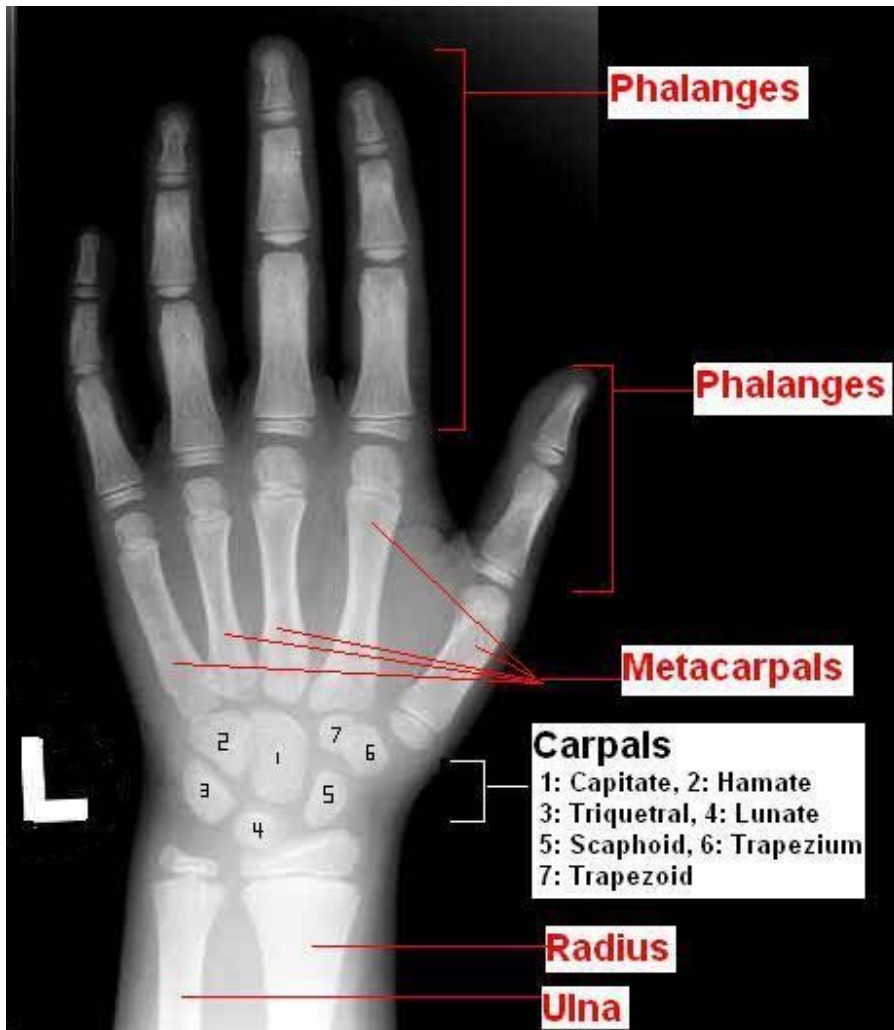


Figure 6.7: The bones used in TW3 bone-age assessment. The 1<sup>st</sup>, 3<sup>rd</sup> and 5<sup>th</sup> metacarpals and phalanges are used in this method. Although not visible in this radiograph, the pisiform (one of the carpal bones) is also not used in this method.

### **6.12 GP Bone-Age Assessment Using Radiographs and DXA Hand Images**

In the B16N2 Normal study, the Mobile Osteoporosis Research Scanning Units owned by the University of Manchester were frequently taken to schools to obtain scans from children to improve recruitment. However, this mobile unit did not contain any X-ray equipment (for taking hand radiographs), due to availability and the cost of making such devices portable. In a previous study, a set of images of the left hand made using a Hologic 4500 DXA scanner (Hologic Inc., Bedford, MA, USA) were used to investigate whether bone-age assessments could be performed by DXA to replace standard radiographs (Ashby et al., 2002a). In 2004 the software for the DXA scanner was upgraded to Hologic QDR 4500 Discovery (Bedford, USA) software version 12.4, resulting in improved image quality from that obtained in the original study. Beginning in October 2004, DXA hand images of children participating in the B16N2 study were taken using the new DXA software. The aim of this study is to evaluate bone age assessment using the GP method from hand radiographs and compare the results with hand/wrist images generated by DXA using a cross-sectional approach. The primary hypothesis is that bone-age assessment from hand radiographs will differ significantly from those made using DXA hand images. The inclusion criteria were as follows: Each child was required to have both a hand radiograph and a viable DXA hand scan, which were performed on the same day, available for comparison. Some children had multiple hand radiographs and DXA hand scans in the longitudinal study so where there was more than one option, the base-line hand radiograph and DXA hand scan were preferred for consistency, but not utilised exclusively in order to obtain a more varied age range. All scans were performed using the lumbar spine algorithm on software version 12.4. Twenty repeat bone-age measurements were performed to calculate bone-age assessment precision; 10 males and 10 females, both randomly selected. Figure 6.8 illustrates a conventional hand radiograph taken using radiographic film and a DXA hand image.



**Figure 6.8: A comparison of a conventional hand radiograph (A) and a DXA hand image (B).**

### **6.13 DXR Measures**

All DXR measures (BMDa, cortical thickness the Metacarpal Index (MCI)), were obtained using baseline hand radiographs of the Normal group by a previous PhD student using the Sectra Pronosco system (Linköping, Sweden) and have been published previously (Ashby, 2007). The Sectra Pronosco system consists of a flatbed scanner linked to a computer with the Pronosco software. A hand radiograph is placed on the scanner and the system automatically detects the regions of interest, which are the diaphyses of the second, third, and fourth metacarpals (Adams, 2010).

## **7. Methods - Analysis**

### **7.1 Statistical Analyses and Data Handling**

All statistical calculations were performed using SPSS (Statistical Package for the Social Sciences) (Chicago, USA) using software version 16.0, StatsDirect software version 2.6.2 (Altrincham, UK) and Analyse-It (Leeds, UK) attachment for Microsoft Excel 2003 (Washington, USA). All subject data were stored in SPSS files (.sav, .spv) and/or in Microsoft Excel and Word 2003 spreadsheets in .xls, and .doc files respectively. Graphical representations of the data were made using StatsDirect or SPSS. Digital images were analysed using Leica Qwin© (Milton Keynes, UK). DXA hand images were stored using Hologic QDR Discovery software version 12.4. Data were stored securely on password protected hard drives within the University of Manchester's Imaging Science Department. Stopford numbers were assigned to each subject to ensure anonymisation during the analyses.

### **7.2 Precision**

Precision or co-efficient of variation (CV) was calculated using Equation 7.2:

Equation 7.2: 
$$CV\% = (\textit{within subject standard deviation} / \textit{mean}) \times 100$$

(Gluer et al., 1995). The within subject standard deviation equals the square root of the within subject variance, or mean square in SPSS, which was calculated using a one-way ANOVA. The CV% was calculated using repeat MI measurements of 30 subjects (9 male). Thirty-five subjects (14 male) were used to calculate the precision of the TW3 bone-age assessment using radiographs and GP bone-age assessment using radiographs.

### **7.3 Normal Group**

Distributions of variables were examined using histograms to check for normal distributions. The baseline MI, MW and GPW values for the Normal group were compared to chronological age, height, weight, arm length, toBMD (4% site), CSMA (50% site), radius bone area (50% site), radius cortical density (50% site), MCI, BMDaDXR and CrtThickDXR in males and females using simple linear regressions and

the relationships were compared using Spearman's rank correlation. MI and chronological age were compared using a polynomial regression. MI, MW and GPW were plotted against chronological age and height using simple linear and polynomial regressions. Mean MI, MW and GPW values of males and females (adjusted for age) were compared using a one-way analysis of variance (ANOVA) with Tukey's HSD. Where statistically significant differences or large differences in minimum and maximum values were detected between males and females, Tukey's HSD and descriptive statistics were used to guide the adjustment of values so that the values in each category matched or overlapped significantly. A stepwise multiple linear regression was performed to examine the relationships of MI, MW and GPW using the anthropometric, pQCT measures and DXR measures as covariates, the results of which determined the covariates used in the analysis of co-variance (ANCOVA) analysis. ANCOVA was used to compare the slopes of the above data in males and females. MI values were also plotted against Tanner pubertal stage and Tanner group using box and whisker plots. To increase the number of subjects in each group for statistical purposes, the Tanner stages were grouped together; Tanner stage 1 comprised Tanner group A (136, 67 male) Tanner stages 2 and 3 comprised Tanner group B (100, 48 male), and Tanner stages 4 and 5 comprised Tanner group C (127, 36 male). Tanner stages were not available to the author for 15 Normal group subjects. Tukey's HSD was used to compare the means between the MI, MW and GPW in Tanner groups A, B and C. To visually examine the distribution, the MI values were transformed into Z scores using Equation 7.3:

$$\text{Equation 7.3: } MI \text{ Z score} = \frac{(\text{subject MI value} - \text{mean MI value for that Tanner group})}{\text{the SD of the mean MI for that Tanner group}}$$

Male and female means and SD's were calculated separately.

### **7.3.1 TW3 Bone-Age Assessments**

All Normal radiographs, including longitudinal radiographs, had a TW3 bone-age assessment. Repeats were performed to assess precision as discussed in section 7.2. Bone-age was used instead of chronological age for the CDGP and to compare them with the Normal group as discussed in sections 7.6 and 7.7.

### **7.3.2 40% and 60% MI and MW**

The 40% and 60% MI and MW were compared to chronological age using 25 randomly selected females and 25 randomly selected males. The 40% MI and MI, the 60% MI and MI, the 40% MW and MW, and the 60% MW and MW were plotted against each other using simple linear regressions to examine the relationships between these variables.

### **7.3.3 Longitudinal Analysis**

Many subjects in the Normal group attended multiple visits. In the Normal group, 63 subjects attended for 2 visits, 36 subjects attended for 3 visits and 9 subjects attended for 4 or more visits. The minimum time elapsed between visits was approximately 1 year and the maximum was approximately 6 years. The MI values of all Normal group subjects with a visit at Tanner pubertal stage 3 and Tanner pubertal stage 4 (21 subjects, 7 male), were plotted against each other using both a simple linear regression and a grouped linear regression separating males and females.

#### **7.4 Gymnast Group**

The baseline MI, MW and GPW values for the Gymnast group were compared with chronological age, height, weight, arm length, toBMD, CSMA, radius bone area (50% site) and radius cortical density (50% site) in males and females using Spearman's rank correlations and the relationships were compared using simple linear regressions. Mean MI, MW and GPW values of males and females (not adjusted for age) were compared using a one-way ANOVA with Tukey's HSD. The regression lines of chronological age and height in males and females were compared using grouped multiple linear regressions and ANCOVA. To visually examine the distribution, the MI values were transformed into Z scores using Equation 7.3, but male and female means and SDs were not calculated separately due to insufficient subject numbers.

##### **7.4.1 Longitudinal Analysis**

Most subjects in the Gymnast group attended multiple visits: 32 (12 male) of 36 subjects attended for 2 visits and no subjects attended for more than 2 visits. The time elapsed between visits was approximately 1 year ( $\pm$  1 month) in each case. The data for each subject with 2 or more visits was examined. The MI value from the first visit was plotted against the MI value from the second visit using simple and grouped linear regressions to examine the relationship between the 2 visits.

#### **7.5 NF1 Group**

The MI, MW and GPW values for the NF1 group were plotted against chronological age, height, weight, arm length, toBMD, CSMA, radius bone area (50% site) and radius cortical density (50% site) in males and females using Spearman's rank correlations. Where statistically significant differences or large differences in minimum and maximum values were detected between males and females, Mann-Whitney U-tests and descriptive statistics were used to guide the truncation of values so that the values in each category matched or overlapped. Mean MI, MW and GPW values of males and females (not adjusted for age) were compared using a one-way ANOVA with Tukey's HSD. The relationships of these variables were compared using non-parametric linear regressions, where the value of the median slope (ms) is reported in place of an r value.

The regression lines of males and females were compared using ANCOVA. To visually examine the distribution, the MI values were transformed into Z scores using Equation 7.3. Male and female means and SDs were not calculated separately due to insufficient subject numbers. A Shapiro-Wilk test was used to test for non-normal distribution of the MI Z scores.

## 7.6 CDGP Group

Shapiro-Wilk tests were used to test for non-normal distribution of the variables. The MI, MW and GPW values for the NF1 group were plotted against TW3 bone-age (using a polynomial regression), height and weight in males and females using simple linear and polynomial regressions and the relationships were compared using Spearman's rank correlations. Mean MI, MW and GPW values of males and females (not adjusted for age) were compared using a one-way ANOVA with Tukey's HSD. The regression lines of males and females were compared using ANCOVA. For the height and weight calculations, only 25 subjects (22 male) of the total number of subjects examined (108, 89 male) were used due to height and weight information only being available to the author for those 25 subjects. Height values were not truncated despite the large differences between the minimum and maximum values of male and female heights because there were only 3 female heights available for comparison. To visually examine the distribution, the MI values were transformed into Z scores using Equation 7.6.

$$\text{Equation 7.6: } MI \text{ Z score} = \frac{(\text{subject MI value} - \text{mean MI value for that bone-age year})}{SD \text{ of the mean MI for that bone-age year}}$$

where 'that bone-age year' refers to groupings of subjects within 1 bone-age year (e.g. 6.0 – 6.9 years, 7.0 to 7.9 years etc). Male and female means and SDs were not calculated separately due to an insufficient number of female subjects in this group. A Shapiro-Wilk test was used to test for non-normal distribution of the MI Z scores. A paired t-test and a box and whisker plot were used to illustrate the differences between chronological age values and TW3 bone-age values. All CDGP subjects, including longitudinal radiographs, had a TW3 bone-age assessment. TW3 bone-age was used in



place of chronological age in all CDGP assessments and a comparison between MI and TW3 bone-age and MI and chronological age using polynomial regressions was made to illustrate the purpose of this.

### **7.6.1 Longitudinal Analysis**

Many subjects in the CDGP group attended multiple visits: 23 subjects attended for 2 visits, 10 subjects attended for 3 visits and 3 subjects attended for 4 or more visits. The minimum time elapsed between visits was approximately 1 year and the maximum was approximately 4 years. The data for each subject with 2 or more visits was examined for visits that were approximately 18 months apart ( $\pm$  4 months). These 2 MI values were plotted against each other using simple and grouped linear regressions to examine the relationship between the 2 visits (15, 9 male).

### **7.7 Comparison of All Groups**

Visual comparisons of the MI, MW and GPW were made using box and whisker plots illustrating the means, standard deviations and range of all 4 groups. The differences in mean height were analysed by comparing the mean height of the Gymnast group, NF1 group and CDGP group compared to the Normal group using three unpaired t-tests. The baseline MI values for the Normal, Gymnast and NF1 groups were plotted against age using a grouped linear regression plot and the means were compared using a one-way ANOVA with a Dunnett's test. The baseline values of the Normal, Gymnast and CDGP groups were truncated to match the chronological age distribution of the smallest group (NF1), therefore all subjects aged between 5.9 years and 9.9 years (or with a TW3 bone-age of 5.9 to 9.9 years in the case of the CDGP group) were used in the one-way ANOVA with Dunnett's t test (107 Normal, 26 Gymnast, 17 NF1 and 32 CDGP). As the only consistent interval variable throughout all 4 groups was age, the only covariate used in the ANCOVA analysis was age (chronological for Normal, Gym and NF1 and the equivalent TW3 bone-age for CDGP). Levene's test was used to examine the groups for homogeneity of variance. Dunnett's t test is the only test that specifically requires a control group to be chosen so that all other groups are compared only to the chosen control, therefore the results section (8.7) concentrated on the results of the Dunnett's t

test. Each subject in the Gymnast group was matched for height (within 1.5cm) with one control from the Normal group. A paired t-test was performed on both height and MI to determine the any mean differences. The MI Z scores using “chronological age groups” were used to compare the Normal, Gymnast and NF1 groups. The MI Z scores using “bone-age groups” were used to compare the Normal and CDGP groups.

### **7.8 DXA Bone-Age Study**

Statistical analyses were performed using SPSS (Statistical Package for the Social Sciences) (Chicago, USA), software version 14.0 and Med-Calc software version 9.5.2.0 (Mariakerke, Belgium). The CV% was calculated using the equation 7.3. The within subject standard deviation equals the square root of the within subject variance, or mean square in SPSS, which was calculated using one-way ANOVA. A Bland and Altman plot (Bland and Altman, 1986) was used to test the agreement between the two methods (radiograph and DXA). The  $r^2$  value was calculated to indicate the correlation between DXA bone-age and radiograph bone-age. Twenty repeat measurements (10 male) each were performed to calculate the precision of GP bone-age assessment using DXA hand images and GP bone-age assessment using radiographs. The repeat bone-age assessments were performed approximately one month after the original assessments and were performed by the same assessor (the author).

## 8. Results

### 8.1 Introduction

This chapter has three parts containing the results of the work presented in this thesis. The first part contains the results of the four groups studied and is organised into four sections: results within the Normal group, within the Gymnast group, within the NF1 group and within the CDGP group. The second part compares the results of each study group to the Normal group. The third part outlines the results of the DXA bone-age assessment study. For abstracts and posters with descriptions of preliminary experiments and results of the MI study, see Appendix 12.1. There are significant numbers of figures referred to in this chapter that may impede readability if they were to all be placed within this chapter. Therefore any figures with an asterisk placed next to the figure reference in the text (e.g. Fig 8.1A\*) are located in Appendix 12.4.

### 8.2 Precision

Table 8.2A represents the CVs of the MW, GPW and MI measurements.

<b>Table 8.2A: Precision of MI Measurements – Comparison of Manual and Computer Assisted Techniques</b>	<b>CV %</b>
Manual MW	<b>1.81%</b>
Manual GPW	<b>2.35%</b>
Manual MI	<b>2.91%</b>
Computer Assisted MW	<b>0.92%</b>
Computer Assisted GPW	<b>1.28%</b>
Computer Assisted MI	<b>1.05%</b>

**Table 8.2A: CVs of manual compared to computer-assisted measurement techniques.**

This table shows that all the computer-assisted measurements (0.92% MW, 1.28% GPW and 1.05% MI) have a higher repeatability than the manual measurements (1.81% MW, 2.35% GPW and 2.91% MI), therefore the computer-assisted measurements were used for subsequent work.

<b>Table 8.2B: Precision of Bone-Age Assessment - Comparison of TW3 and GP Methods</b>	<b>CV %</b>
Radiograph Bone-Age Assessments (TW3)	<b>1.61%</b>
Radiograph Bone-Age Assessments (GP)	<b>2.68%</b>

**Table 8.2B: CVs of bone-age assessment methods comparing the precision of the TW3 method to the GP method.**

Table 8.2B shows the CV of the TW3 bone-age assessment method compared to the CV of the GP bone-age assessment method. This table shows that the CV of TW3 bone-age assessments indicate a higher repeatability than the CV of GP bone-age assessments.

### 8.3 Normal Group

Each pQCT and anthropometric variable exhibited normal distribution. When the baseline MI values were compared with the baseline values of each anthropometric measure (chronological age, TW3 bone-age, height, weight, Tanner stage and arm length), each pQCT measure (toBMD, CSMA, pSSI, radius bone area 50% and cortical bone density 50%), and each DXR measure (MCI, BMDaDXR and CrtThickDXR) Spearman's rank and Pearson's r correlations showed that the MI was not significantly correlated with any DXR measures (all  $p > 0.297$ ) or toBMD (4%) ( $p = 0.181$ ). MI was significantly correlated with all other variables (all  $p < 0.0009$ ), with no r values above 0.305 (Tanner stage). If one squared the highest significant r value and multiplied it by 100; ( $0.305^2 = 0.093$ ), ( $0.093 \times 100 = 9.3$ ), this would indicate that although the correlation was significant, only 9.3% of variation in the MI could be explained by Tanner stage.

MI was not compared to toBA (4%) because bone width, which is a component of the MI, will always be correlated with toBA. When MI was compared to chronological age using baseline values, the MI was lower in early age groups, and increased through the pre-teenage and teenage years where it reached a plateau (Fig 8.3A). A similar result occurred when MI was compared to height using baseline values (Fig 8.3B). Using grouped linear regressions to examine the MI in males and females compared with chronological age (Fig 8.3C) and height (Fig 8.3D), with age and height values adjusted so that the minimum and maximum values were the same for both males and females, there were no statistically significant differences in the slopes for either MI compared to chronological age ( $p = 0.240$ ), or MI compared to height ( $p = 0.092$ ).

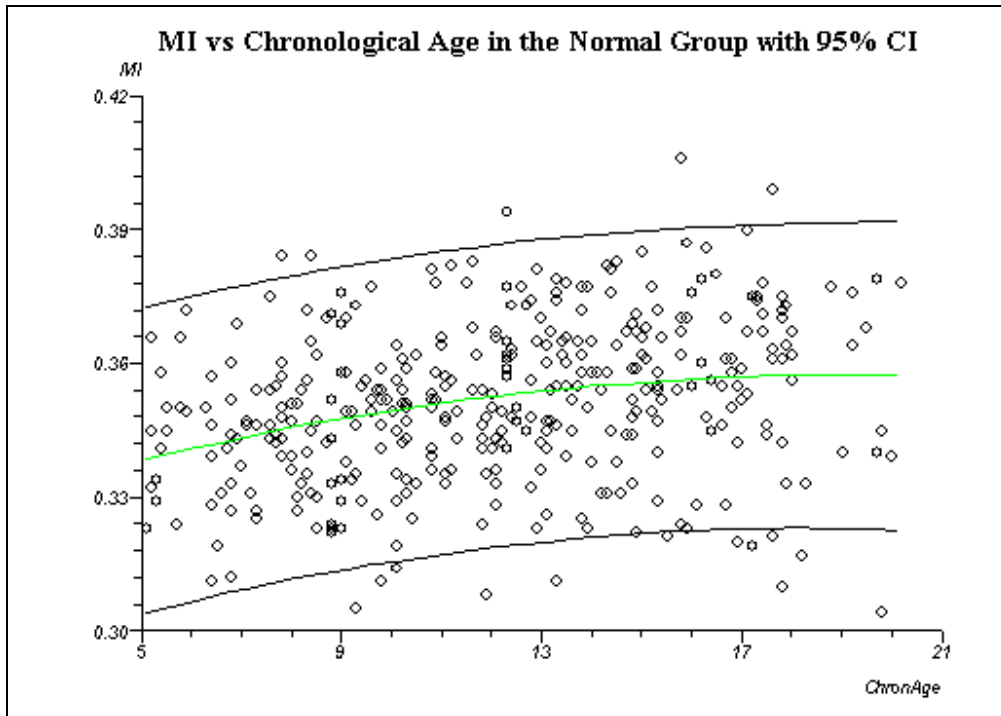


Figure 8.3A: MI vs chronological age (years) in the Normal group (baseline values). This cross-sectional plot illustrates that the MI increases with age.

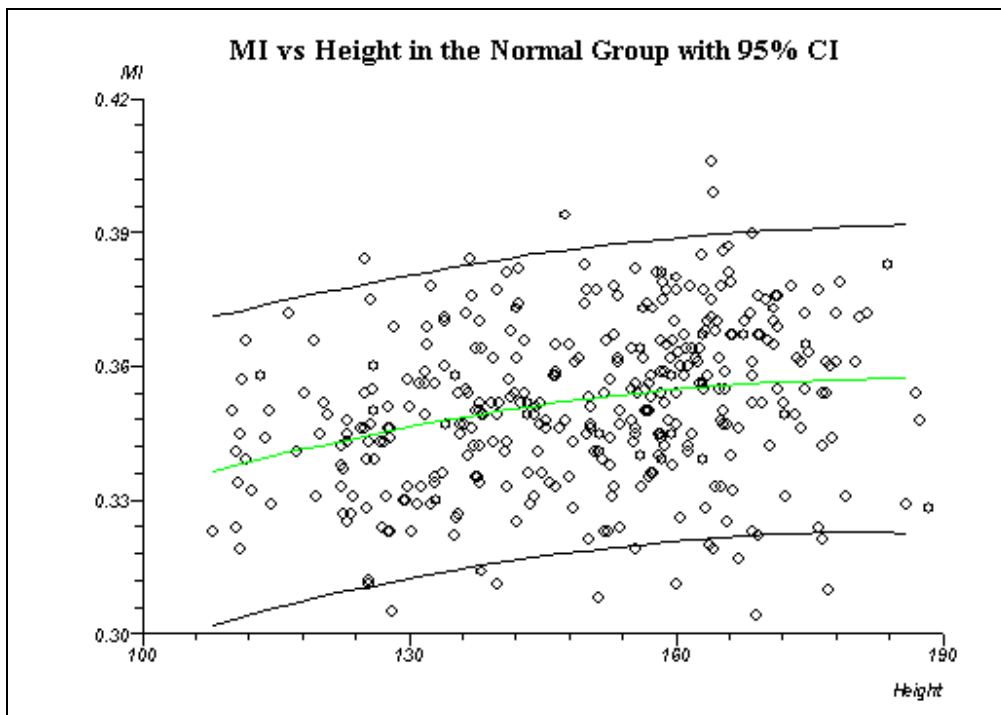


Figure 8.3B: MI vs height (cm) in the Normal group (baseline values). This cross-sectional plot illustrates that the MI increases with height.

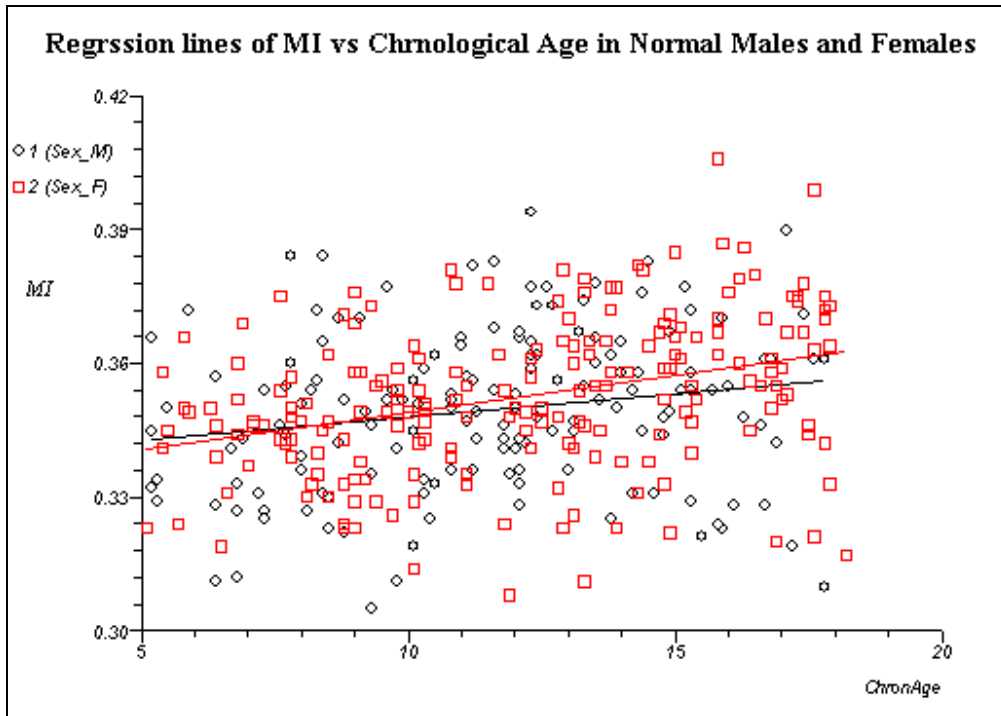


Figure 8.3C: MI vs chronological age (years) in Normal males and females. This plot illustrates the slightly different regression lines of males and females, but there is no statistically significant difference.

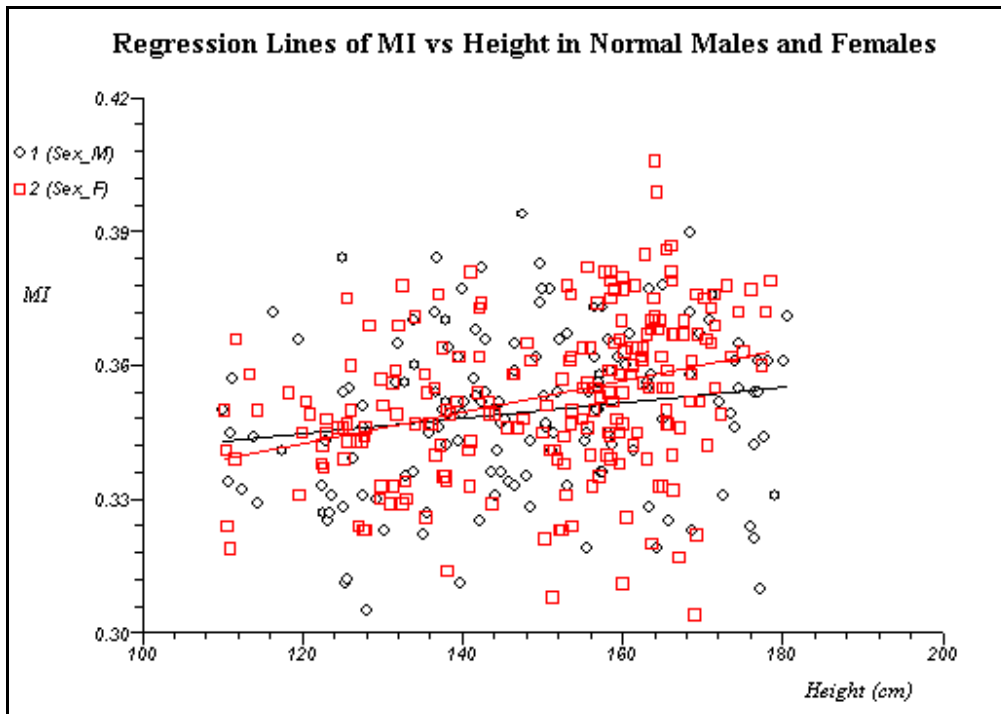


Figure 8.3D: MI vs height (cm) in Normal males and females. This plot illustrates the slightly different regression lines of males and females, but there is no statistically significant difference.

The common slopes were both significantly different from zero (both  $p < 0.0001$ ).

The MW was compared with the same variables discussed previously and most Spearman's rank and Pearson's  $r$  values were significant ( $p < 0.0001$ ) except those for toBMD, MCI, BMDaDXR and CrtThickDXR, which showed insignificant correlations (all  $p > 0.9$ ). The lowest significant  $r$  value was cortical bone density (50%);  $r = 0.273$  with a 95% CI of 0.174 to 0.366, and the highest was pSSI;  $r = 0.815$  with a 95% CI of 0.777 to 0.847. Therefore cortical bone density explained 7.5% of the variation in MW and pSSI explained 66.4% of the variation in MW. MW was compared to chronological age in the Normal group using baseline values. This showed a similar result to the MI, but exhibited a tighter concentration of values around the regression line (Fig 8.3E). The Spearman's rank correlation for chronological age compared to MW (baseline values) was  $r = 0.673$  ( $p < 0.0001$ ), with a 95% CI for  $r = 0.614$  to 0.725, which indicated a statistically significant positive correlation between MW and chronological age. A similar result occurred when MW was compared to height (baseline values) (Fig 8.3F);  $r = 0.763$ , ( $p < 0.0001$ ) with a 95% CI of 0.718 to 0.803, indicating that height was also significantly positively correlated with MW.

GPW was compared to all variables discussed previously, and all Spearman's rank and most Pearson's  $r$  values were statistically significantly correlated (all  $p < 0.007$ ) except for toBMD (4%), MCI, BMDaDXR and CrtThickDXR, which were insignificantly correlated (all  $p > 0.1$ ). The lowest significant  $r$  values was cortical bone density (50%);  $r = 0.251$  with a 95% CI of 0.151 to 0.345, and the highest  $r$  value was CSMA;  $r = 0.806$  with a 95% CI of 0.767 to 0.840. Therefore cortical bone density explained 6.3% of the variation in GPW and CSMA explained 65.0% of the variation in GPW. GPW compared with chronological age in the Normal group (baseline values) showed a similar result to MW vs chronological age; a tight concentration of values around the regression line (Fig 8.3G),  $r = 0.657$  ( $p < 0.0001$ ) with a 95% CI of 0.596 to 0.711, indicating a statistically significant correlation between GPW and chronological age. GPW compared with height showed a similar result (Fig 8.3H),  $r = 0.751$  ( $p < 0.0001$ ) with a 95% CI of 0.703 to 0.792, also indicating a statistically significant positive correlation between GPW and height. Outliers will be discussed in section 9.3.



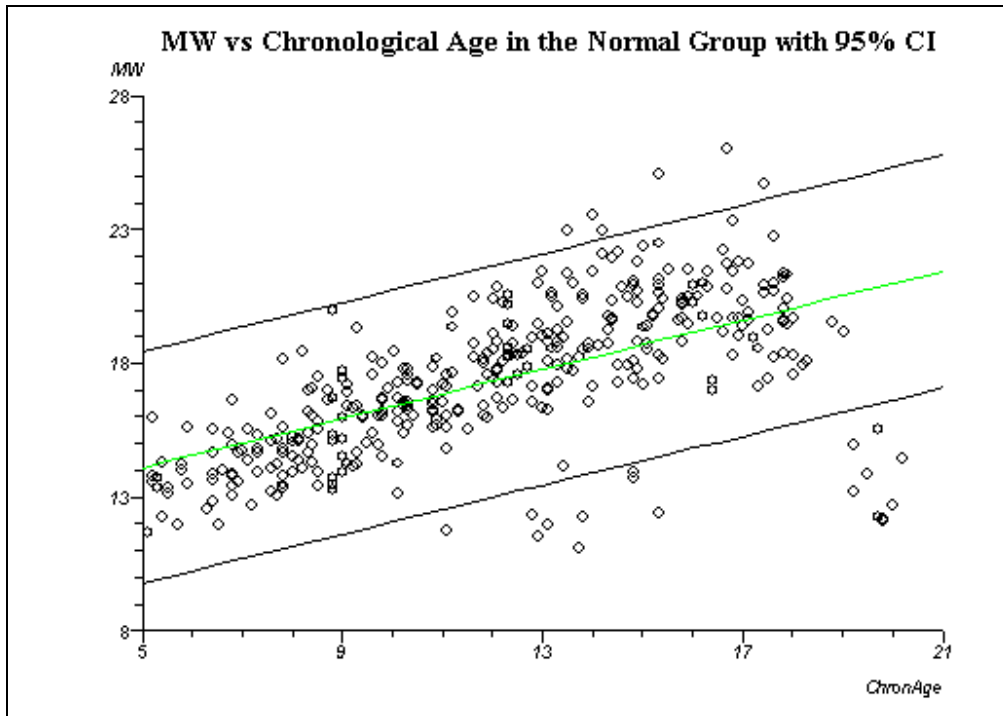


Figure 8.3E: MW (mm) vs chronological age in the Normal group (baseline values). This cross-sectional plot illustrates that the MW increases with age.

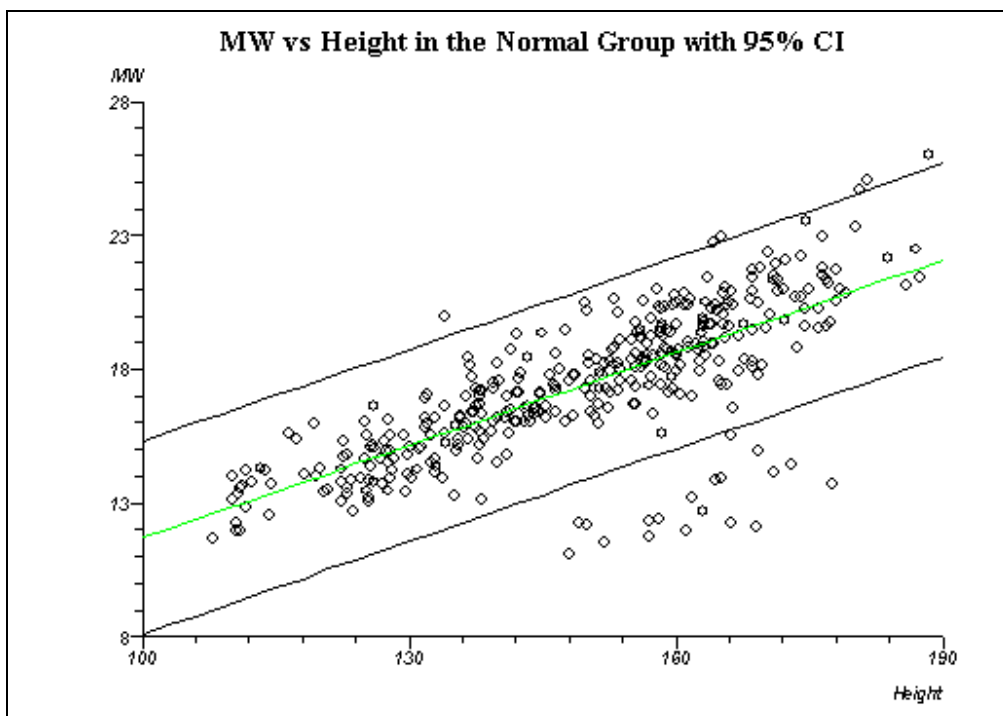


Figure 8.3F: MW (mm) vs height (cm) in the Normal group (baseline values). This cross-sectional plot illustrates that the MW increases as height increases.

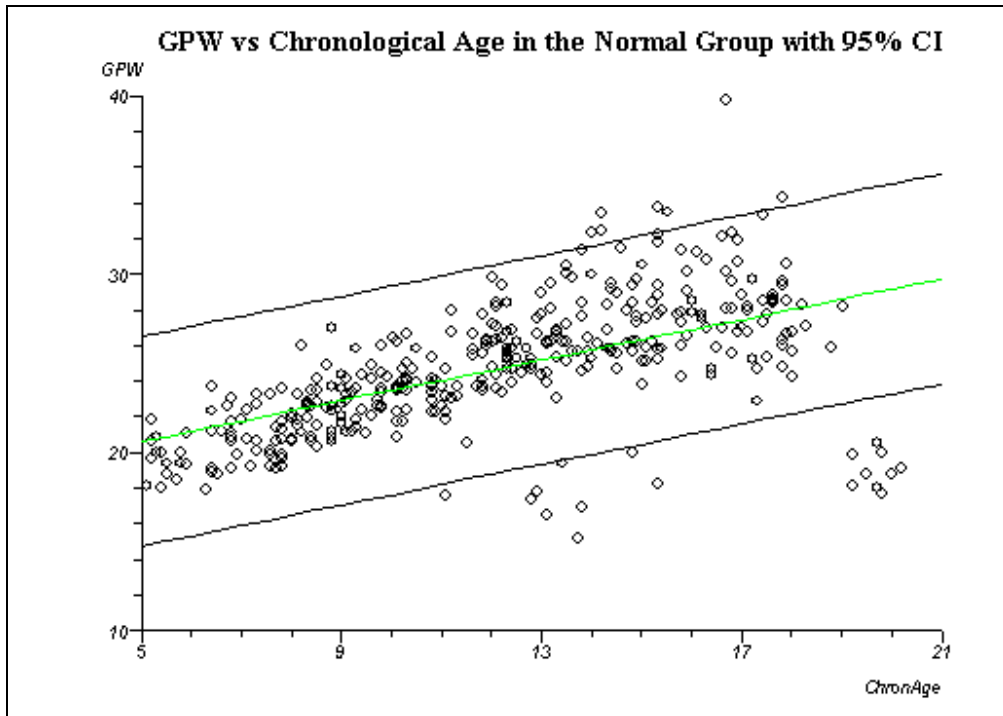


Figure 8.3G: GPW (mm) vs chronological age in the Normal group (baseline values). This cross-sectional plot illustrates a similar result to the MW plot - that the GPW increases with age.

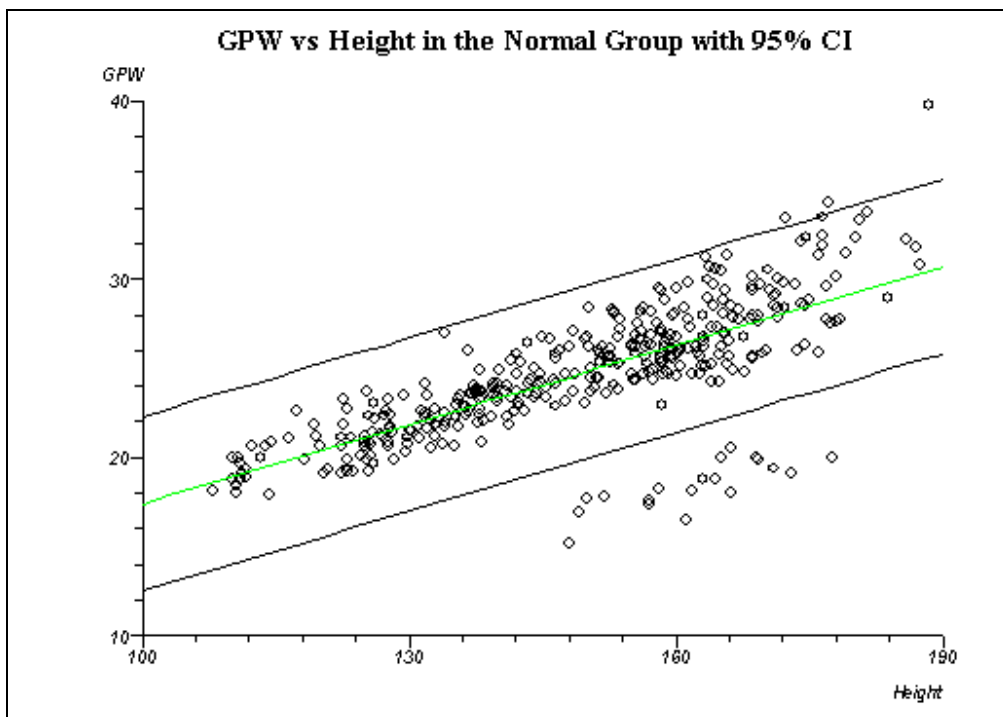


Figure 8.3H: GPW (mm) vs height in the Normal group (baseline values). This cross-sectional plot illustrates a similar result to the MW plot - that the GPW increases as height increases.

A comparison of mean MI, MW and GPW values of males and females Tukey’s HSD revealed that there were no significant differences between the MIs ( $p = 0.734$ ) or MWs ( $p = 0.129$ ) of males and females, but there was a significant difference between the GPWs of males and females ( $p = 0.007$ ).

Tanner pubertal stage was also assessed in the Normal group. The means of each MI, MW and GPW in the 5 Tanner stages (rounded to 3 decimal points) are shown in Table 8.3A. The MI in Tanner stages 1 through 5 showed that the MI increased through puberty (Fig 8.3I\*). Using Tukey’s HSD test, the only significant differences in the MI means were found between Tanner stages 1 and 4 ( $p = 0.001$ ) and Tanner stages 1 and 5 ( $p < 0.0001$ ). The MW means (Fig 8.3J\*) showed significant differences between Tanner stages 1 and each other Tanner stage (all  $p < 0.0001$ ). There were also significant differences between MW Tanner stages 2 and 4 ( $p < 0.0001$ ) and 2 and 5 ( $p < 0.0001$ ). There were significant differences between the GPW mean at Tanner stage 1 and each other Tanner stage (1 and 2,  $p = 0.001$ ; 1 and 3/4/5,  $p < 0.0001$ ) (Fig 8.3K\*). As in the MW means, the GPW means showed significant differences between Tanner stage 2 and 4 ( $p = 0.001$ ) and 2 and 5 ( $p < 0.0001$ ).

<b>Table 8.3A – Means of MI, MW and GPW in Tanner Stages 1 through 5</b>		<b>Mean MI</b>	<b>Mean MW</b>	<b>Mean GPW</b>
Tanner Group A	Tanner Stage 1	0.347	15.342	22.130
Tanner Group B	Tanner Stage 2	0.352	17.096	24.297
	Tanner Stage 3	0.352	18.284	25.997
Tanner Group C	Tanner Stage 4	0.358	19.094	26.705
	Tanner Stage 5	0.358	19.442	27.184

**Table 8.3A: Means of MI in the Normal group by Tanner pubertal stage and Tanner group.**

Table 8.3C shows the mean MI  $\pm$  2SD values (males and females combined) for Tanner Groups A, B and C.

<b>Table 8.3B – Tukey’s HSD Comparisons of the Mean Values of MI, MW and GPW in Tanner Groups A, B and C</b>			
<u>Tukey’s HSD Comparison</u> MI: TannerA vs. TannerB MI: TannerB vs. TannerC MI: TannerA vs. TannerC	<u>Mean difference (95% CI)</u> 0.005701 (0.0003 to 0.0111) 0.006082 (0.0007 to 0.0115) 0.011783 (0.0067 to 0.0168)	<u>S.E.</u> 3.529327 3.739872 7.778573	<u>Sig.</u> p = 0.0347 p = 0.0232 p < 0.0001
<u>Tukey’s HSD Comparison</u> MW: TannerA vs. TannerB MW: TannerB vs. TannerC MW: TannerA vs. TannerC	<u>Mean difference (95% CI)</u> 2.402921 (1.7252 to 3.0806) 1.55322 (0.8710 to 2.2355) 3.956141 (3.3206 to 4.5916)	<u>S.E.</u> 11.80238 7.57744 20.72048	<u>Sig.</u> p < 0.0001 p < 0.0001 p < 0.0001
<u>Tukey’s HSD Comparison</u> GPW: TannerA vs. TannerB GPW: TannerB vs. TannerC GPW: TannerA vs. TannerC	<u>Mean difference (95% CI)</u> 3.080363 (2.1636 to 3.9971) 1.783681 (0.8607 to 2.7067) 4.864044 (4.0043 to 5.7238)	<u>S.E.</u> 11.1839 6.43235 18.8317	<u>Sig.</u> p < 0.0001 p < 0.0001 p < 0.0001

**Table 8.3B: Tukey’s HSD Comparisons of the Mean Values of MI, MW and GPW in Tanner Groups A, B and C. Note there is a significant difference in MI, MW and GPW between Tanner groups indicating that MI, MW and GPW change significantly as puberty develops in the Normal group.**

<b>Table 8.3C – Values of the Means and SDs for Tanner Groups A, B and C</b>	<b>Mean MI -2 SD</b>	<b>Mean MI</b>	<b>Mean MI +2 SD</b>
<b>Tanner Group A</b>	0.313	0.348	0.383
<b>Tanner Group B</b>	0.320	0.354	0.387
<b>Tanner Group C</b>	0.316	0.353	0.390

**Table 8.3C: Values of the means and standard deviations for Tanner groups A, B and C in the Normal group.**

A stepwise multiple linear regression was performed to determine the most significant covariates to use in an ANCOVA analysis. Within the Normal group, the most significant covariates for the MI were chronological age and toBMD (4%). This meant that chronological age and toBMD were the most important predictors of MI. This model had the highest  $r^2 = 0.120$  with an F-ratio of 23.315 ( $p < 0.00001$ ), meaning that chronological age and toBMD (4%) explain 12% of the variance in MI values. The negative  $\beta$  value of toBMD (Table 8.3D) meant the relationship between MI and toBMD was a negative one; as MI increased, toBMD decreased. The results of the ANCOVA

analysis for MI indicated that both the male and female slopes as a whole (common slope), were not significantly different from zero ( $p = 0.735$ ) and there was no statistically significant difference between the slopes of males and females ( $p = 0.643$ ), meaning that once the covariates were accounted for, the slope of the lines was flat.

<b>Table 8.3D Covariates for MI Normal</b>	<b>r<sup>2</sup></b>	<b>F-ratio</b>	<b>p</b>	<b>β</b>	<b>p</b>
<b>Chronological Age</b>	0.120	23.315	< 0.00001	0.348	< 0.0001
<b>toBMD (4%)</b>				-0.231	< 0.0001

**Table 8.3D: Summary of results of the multiple linear regression with MI as the dependent variable in the Normal group.**

Within the Normal group, the most significant covariates for the MW were height, chronological age, CSMA, pSSI and toBMD (4%), meaning that these were the most important predictors for MW. This model had the highest  $r^2 = 0.663$  with an F-ratio of 144.911 ( $p < 0.0001$ ), meaning that height, chronological age, CSMA, pSSI and to BMD explain 66.3% of the variance in MW values. The negative  $\beta$  value of chronological age and toBMD (Table 8.3E) meant that the relationship between MW and those variables was a negative one; as MW increased, chronological age and toBMD decreased. In the case of chronological age, this is most likely a statistical anomaly and the  $\beta$  value of chronological age was not significant ( $p = 0.070$ ).

<b>Table 8.3E Covariates for MW Normal</b>	<b>r<sup>2</sup></b>	<b>F-ratio</b>	<b>p</b>	<b>β</b>	<b>p</b>
<b>Height</b>	0.663	144.911	< 0.0001	0.540	< 0.0001
<b>Chronological Age</b>				-0.132	= 0.070
<b>CSMA</b>				0.274	< 0.0001
<b>pSSI</b>				0.194	< 0.0001
<b>toBMD</b>				-0.152	= 0.001

**Table 8.3E: Summary of results of the multiple linear regression with MW as the dependent variable in the Normal group.**

The results of the ANCOVA analysis for MW indicated that both the male and female slopes as a whole (common slope), were significantly different from zero ( $p < 0.0001$ )

but there was no statistically significant difference between the regression lines of males and females ( $p = 0.134$ ). This meant that despite the covariates included in the model, the common slope was still rising, but there was no statistically significant difference between the slopes of males and females.

Within the Normal group, the most significant covariates for the GPW were height, chronological age, CSMA, arm length, pSSI and toBMD (4%), meaning that these were the most important predictors for GPW. This model had the highest  $r^2 = 0.644$  with an F-ratio of 110.626 ( $p < 0.0001$ ), meaning that height, chronological age, CSMA, arm length, pSSI and toBMD explain 64.4% of the variance in GPW values. There were negative  $\beta$  values (Table 8.3F) for chronological age, CSMA and toBMD but the value for CSMA was not significant ( $p = 0.062$ ).

<b>Table 8.3F Covariates for GPW Normal</b>	<b><math>r^2</math></b>	<b>F-ratio</b>	<b>p</b>	<b><math>\beta</math></b>	<b>p</b>
<b>Height</b>	0.644	110.626	< 0.0001	0.817	< 0.0001
<b>Chronological Age</b>				-0.270	< 0.0001
<b>Arm Length</b>				0.346	< 0.0001
<b>CSMA</b>				-0.201	= 0.062
<b>pSSI</b>				0.136	= 0.028
<b>toBMD</b>				-0.085	= 0.018

**Table 8.3F: Summary of results of the multiple linear regression with GPW as the dependent variable in the Normal group.**

The results of the ANCOVA analysis for GPW indicated that both the male and female slopes as a whole (common slope), were significantly different from zero ( $p < 0.0001$ ), but again there was no statistically significant difference between the regression lines of males and females ( $p = 0.198$ ). This meant that despite the covariates included in the model, the common slope was still rising, but there was no statistically significant difference between the slopes of males and females.

The chronological ages of females extend further than that of males: 15 females were recruited from ages 18-20 (baseline values), compared to zero males in the 18-20 age categories at baseline. In order to take this into account, the female age range was adjusted when comparing the means of the MI in males and females. Using an unpaired t-test to compare the means of MI in females (0.353) and MI in males (0.350) ( $p =$

0.123, 95% CI = -0.007 to 0.00008) showed no significant difference in the MI of females and males. All MI values were transformed into Z scores and the results were plotted in two histograms, one for males (Fig 8.3L) and one for females (Fig 8.3M). The MI values of both males and females exhibit a normal distribution around the mean of zero, which were both confirmed by Shapiro-Wilk tests; male  $W = 0.955$  ( $p = 0.927$ ), female  $W = 0.992$  ( $p = 0.404$ ).

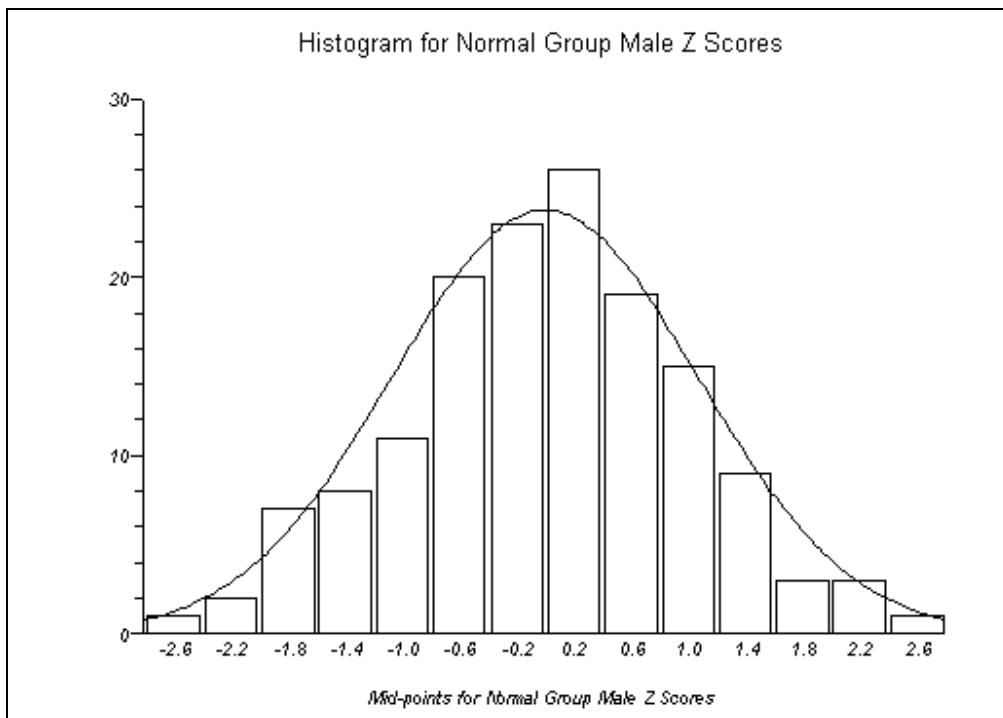


**Figure 8.3L: MI values for males in the Normal group as Z scores illustrating a normal distribution around the zero mean.**

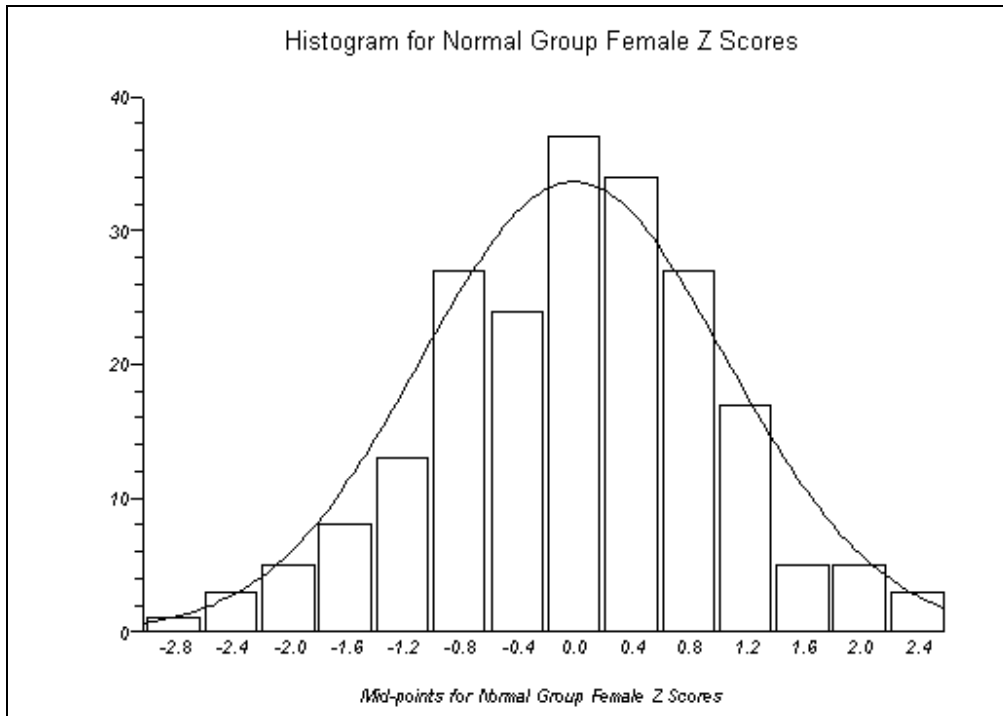


**Figure 8.3M: MI values for females in the Normal group as Z scores illustrating a normal distribution around the zero mean.**



### 8.3.1 TW3 Bone-Age Assessments

The results of comparing MI with TW3 bone-age in the Normal group (baseline values) were similar to those obtained in the comparison of MI and chronological age (Fig 8.3.1A). MI was lower in early ages then increased through the pre-teenage and teenage years where it reached a plateau. The concentration of females at age 15 and males from 15 to 16.5 is due to 15 and 16.5 being the maximum bone-ages for female and males respectively using the TW3 technique. Therefore any females with a bone-age similar to, or advanced than their chronological age, will reach the maximum TW3 bone-age in their early teens and will remain at the maximum from that point onwards, hence the large concentration of females at TW3 bone-age 15. A TW3 bone-age of 15 includes a

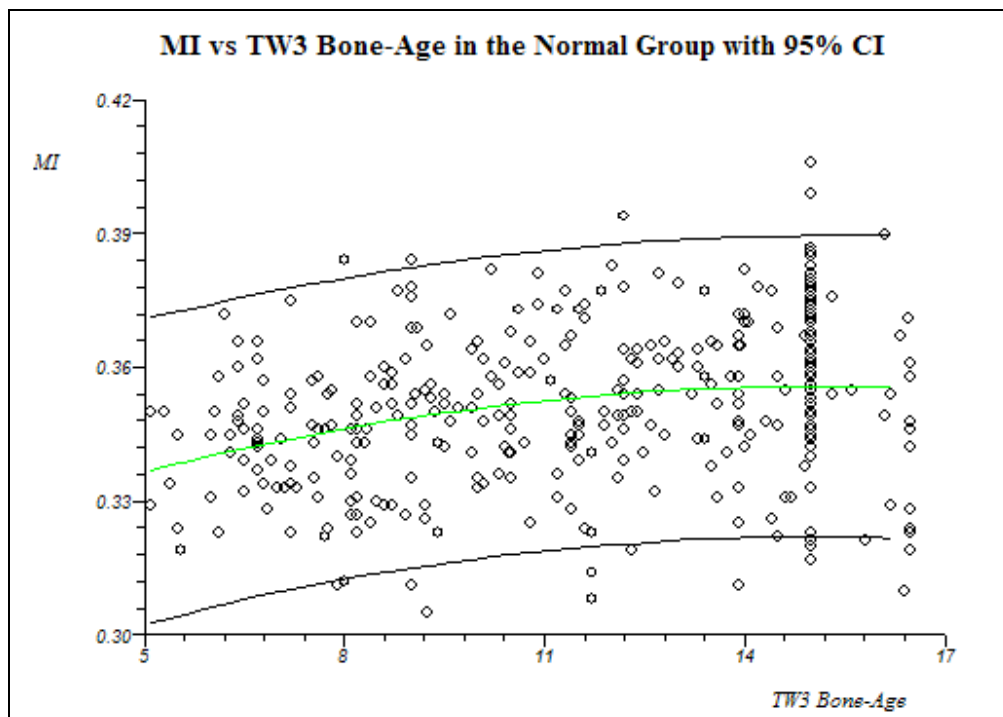


**Figure 8.3.1A: MI vs chronological age (years) in the Normal group (baseline values).** This cross-sectional plot illustrates that the MI increases with age. The large concentration of values at TW3 bone-age 15 is due to that being the maximum bone-age given to a skeletally mature female.

wide range of female chronological ages from 13 to 20 years. The same phenomenon occurs in males approximately 1.5 years later. The Spearman's rank correlation  $r = 0.285$  ( $p < 0.0001$ ), with a 95% CI = 0.190 to 0.375, indicating that there is a statistically significant positive correlation between MI and TW3 bone-age. MW and GPW showed

a similar relationship to those seen when they were plotted against chronological age (results not shown).

### 8.3.2 40% and 60% MI and MW

The slopes of the 40% MI, 40% MW, and 60% MW exhibited similar results as illustrated using the MI and chronological age. The 40% MI compared with chronological age (Fig 8.3.2A) shows that the 40% MI was lower in younger age groups, then rose through pre-teenage and teenage years where it reached a plateau. A simple linear regression showed the 40% MI was statistically significantly correlated with chronological age,  $r = 0.785$  ( $p < 0.0001$ ) with a 95% CI of 0.649 to 0.873. The 60% MI however showed a completely flat regression line when compared with chronological age (Fig 8.3.2B), which is unlike the MI and 40% MI. A simple linear regression showed the 60% MI was not statistically significantly correlated with chronological age,  $r = 0.002$  ( $p = 0.99$ ) with a 95% CI of -0.277 to 0.280. Outliers will be discussed in section 9.3.2.

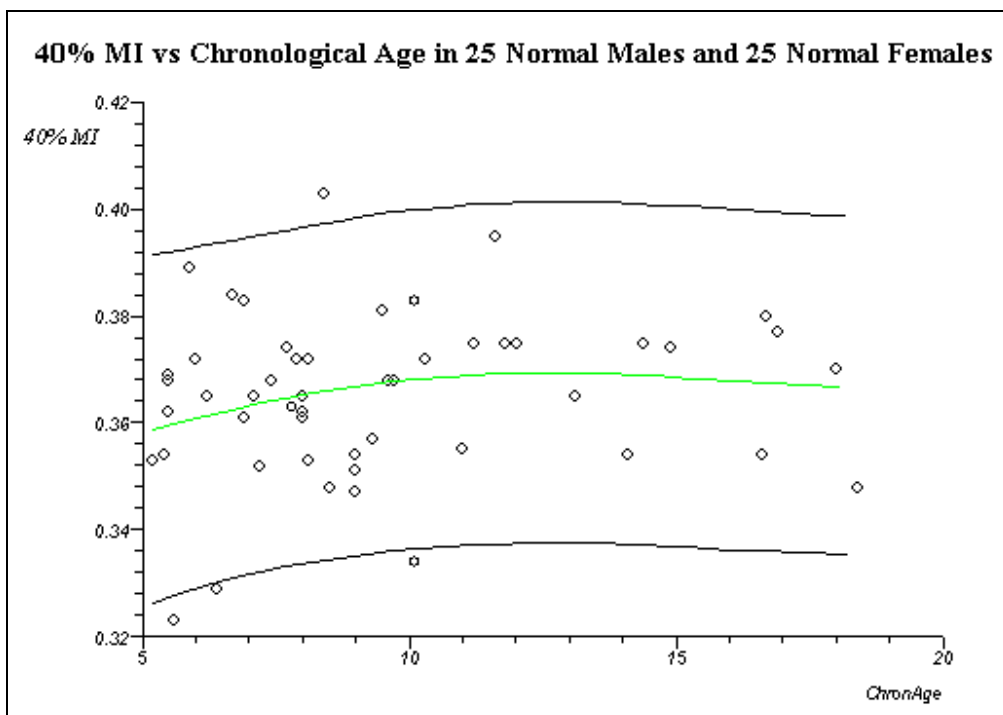
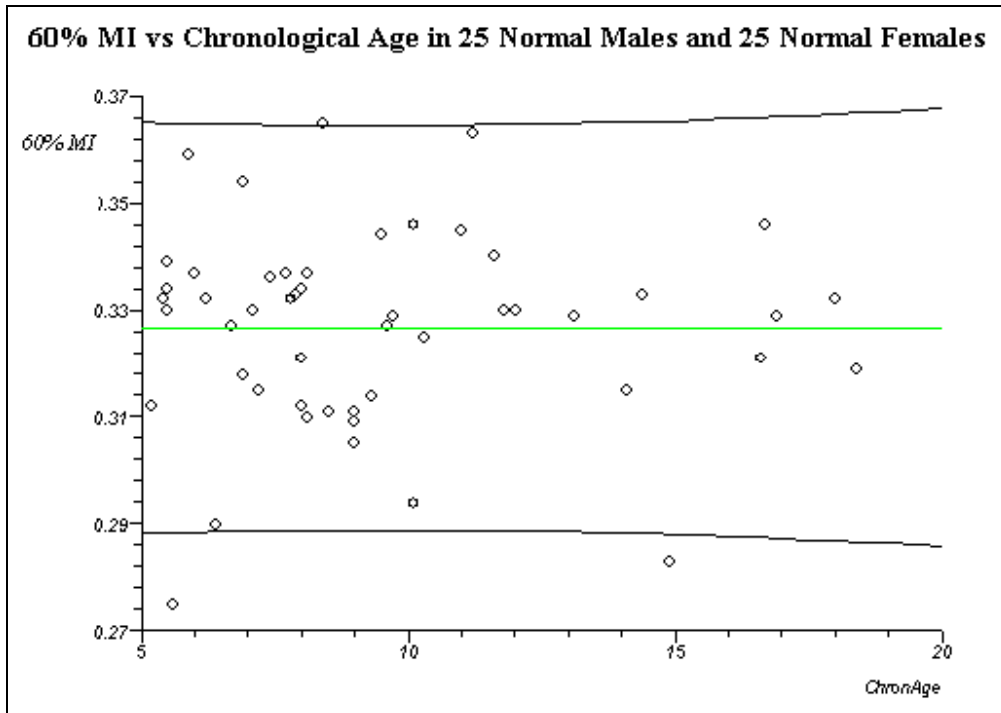


Figure 8.3.2A: 40% MI compared to chronological age using 25 males and 25 females from the Normal group (baseline values). This plot illustrates that the 40% MI increases with age.



**Figure 8.3.2B: 60% MI vs chronological age (years) using 25 males and 25 females from the Normal group (baseline values). This cross-sectional plot illustrates that the 60% MI appears not to increase with age.**

The 40% MW (Fig 8.3.2C\*) and the 60% MW (Fig 8.3.2D\*) both showed a tight concentration of values around the regression line, 40% MW  $r = 0.834$  ( $p < 0.0001$ ) with a 95% CI of 0.723 to 0.903, and 60% MW  $r = 0.809$  ( $p < 0.0001$ ) with a 95% CI of 0.684 to 0.887, indicating a statistically significant correlation between both the 40% and 60% MW's and chronological age. Outliers will be discussed in section 9.3.2.

The MI, 40% MI and 60% MI were plotted against each other in 3 simple linear regression plots to examine how well these variables correlate with each other. All 3 plots showed similar results with values distributed close to the regression lines, had high corresponding  $r$  values and statistically significant  $p$  values. This indicates each variable correlated well with the other variables. The MI compared to the 40% MI (Fig 8.3.2E\*) had an  $r = 0.880$  ( $p < 0.0001$ ) with a 95% CI of 0.798 to 0.931. The MI compared with the 60% MI (Fig 8.3.2F\*) had an  $r = 0.883$  ( $p < 0.0001$ ) with a 95% CI of 0.802 to 0.932. The 40% MI compared to the 60% MI (Fig 8.3.2G\*) had an  $r = 0.785$

( $p < 0.0001$ ) with a 95% CI of 0.649 to 0.873. Outliers will be discussed in section 9.3.2.

### 8.3.3 Longitudinal Analysis

The results of the comparison MI values of Normal group subjects with visits at both Tanner stage 3 and Tanner stage 4 (Fig 8.3.3A) were that  $r = 0.913$  ( $p < 0.0001$ ) with a 95% CI of 0.795 to 0.965. This indicates a very high correlation between MI values at Tanner stages 3 and 4. When males and females were examined separately (Fig 8.3.3B), there was very little difference between the slopes and this was confirmed by the statistical output. The common slope was statistically significantly different from zero ( $p < 0.0001$ ), but there was no statistically significant difference between the slopes of males and females ( $p = 0.400$ ).

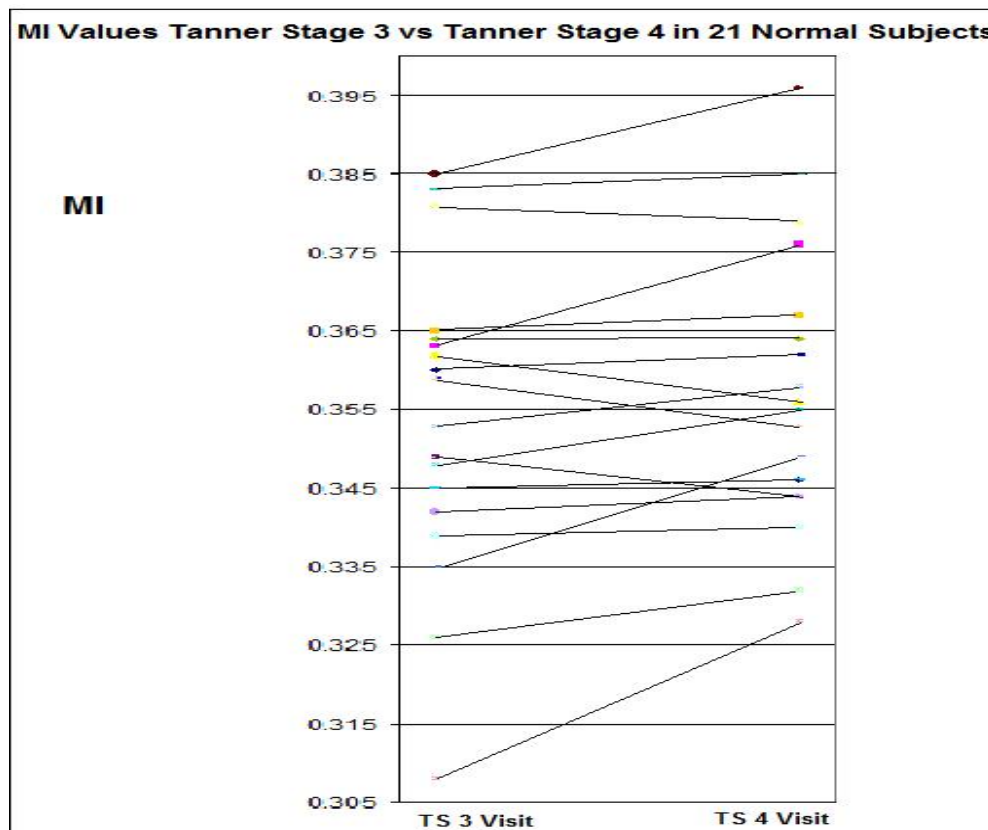
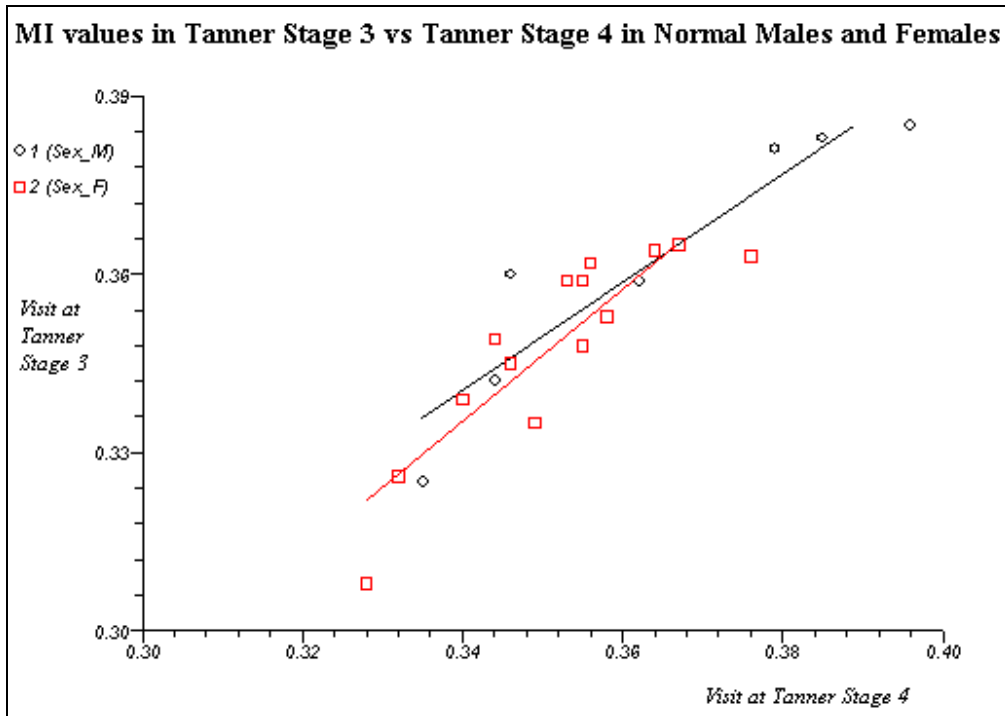


Figure 8.3.3A: A plot comparing MI values of 21 Normal group subjects with visits at Tanner stage 3 and Tanner stage 4. Most subjects have a higher MI at Tanner stage 4 but not all.



**Figure 8.3.3B:** A grouped linear regression plot comparing MI values of 21 Normal group subjects (7 male) with visits at Tanner stages 3 and 4. This plot appears to show a slight difference between the slopes of males and females, but there is no statistically significant difference ( $p = 0.400$ ).

#### 8.4 Gymnast Group

Each pQCT and anthropometric variable exhibited normal distribution. When the baseline MI values were compared with the baseline values of each anthropometric measure (chronological age, height, weight and arm length) and each pQCT measure (toBMD, CSMA, radius bone area 50% and cortical bone density 50%), Spearman's rank correlations showed that the MI was not significantly correlated with most of the variables (all  $p > 0.300$ ), except for toBMD,  $r = -0.383$  ( $p = 0.022$ ). The negative value of  $r$  denotes an inverse relationship between MI and toBMD, so as toBMD decreases, MI increases. MI was not compared to toBA (4%) because bone width, which is a component of the MI, will always be correlated with toBA. A simple linear regression comparing MI to chronological age using baseline values (Fig 8.4A) does not show a growth curve as it did in the Normal group. Although the graph appears to show a slight decrease in MI as Gymnasts age, this relationship is not statistically significant,  $r = -0.034$  ( $p = 0.843$ ) with a 95% CI of -0.359 to 0.298. Another simple linear regression

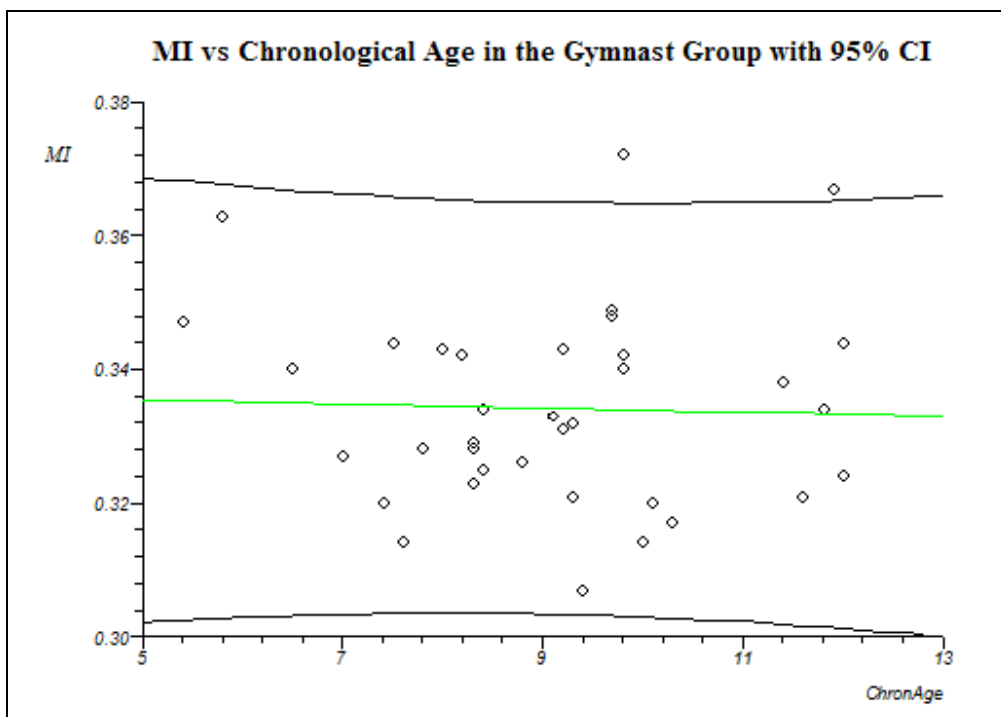


**Figure 8.4A:** MI compared to chronological age in the Gymnast group using baseline values. This cross-sectional plot appears to show a slight decrease in MI values as gymnasts age, but there is no statistically significant relationship ( $p = 0.843$ ).

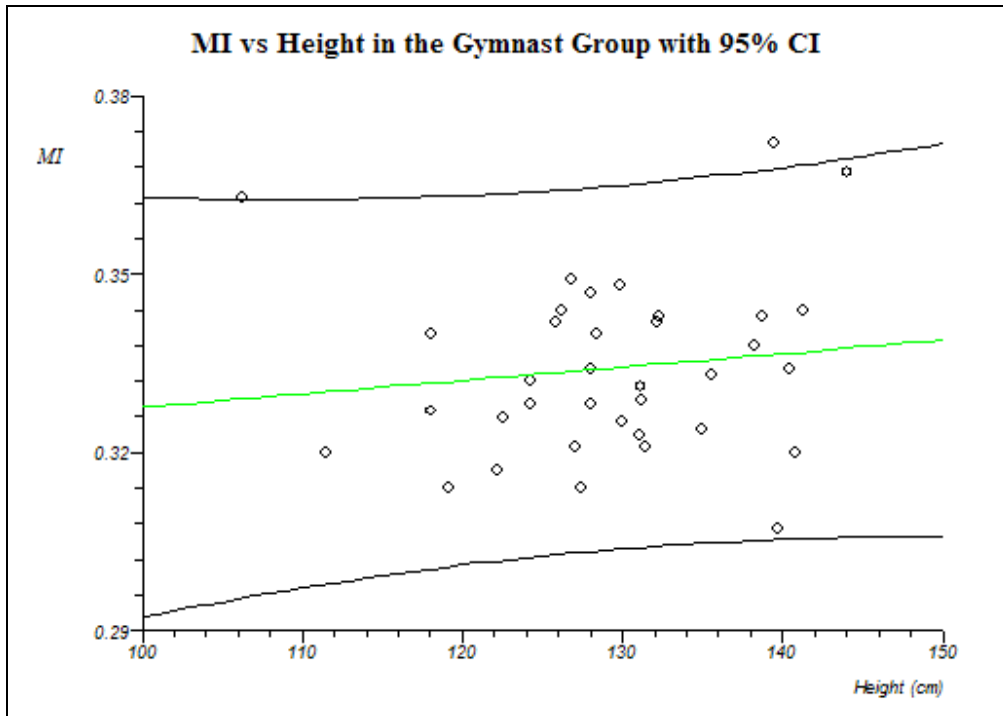


**Figure 8.4B: MI compared to height in the Gymnast group (baseline values).** This cross-sectional plot shows a slight increase in MI as Gymnast height increases, but it was not significant ( $p = 0.452$ ).

was used to compare MI to height using baseline values (Fig 8.4B) using adjusted height values due to a difference of maximum and minimum heights between males and females. This graph illustrated a slight increase in MI as Gymnasts grew in height, but again the relationship was not statistically significant,  $r = 0.129$  ( $p = 0.452$ ) with a 95% CI of -0.208 to 0.439. Using grouped linear regressions to examine the MI in Gymnast males and females compared with chronological age (Fig 8.4C\*) and MI compared with height (Fig 8.4D\*) when the age and height values are adjusted so the minimum and maximum values were the same for both males and females, there were no statistically significant differences in the regression lines for either MI compared to chronological age ( $p = 0.502$ ), or MI compared to height ( $p = 0.959$ ). Neither of the common slopes was significantly different from zero (both  $p > 0.225$ ).

The MW was compared with the same variables discussed previously and showed all Spearman's rank and Pearson's  $r$  values were significant ( $p < 0.0001$ ) except those of toBMD (4%) (Spearman's  $r = 0.179$ ,  $p = 0.295$ , Pearson's  $r = 0.196$ ,  $p = 0.130$ ). MW compared to chronological age in the Gymnast group using baseline values (Fig 8.4E\*)

showed a similar result to the same analysis in the Normal group. The  $r = 0.833$  ( $p < 0.0001$ ), with a 95% CI for  $r = 0.694$  to  $0.912$ . This indicates a statistically significant positive correlation between MW and chronological age. Similar results occurred when MW was compared to height. MW was compared to height using baseline values in the Gymnast group (Fig 8.4F\*)  $r = 0.770$ , ( $p < 0.0001$ ) with a 95% CI of  $0.590$  to  $0.877$ , indicating that height is also significantly positively correlated with MW.

GPW was compared to all variables discussed previously, and all Spearman's rank and Pearson's  $r$  values were statistically significantly correlated (all  $p < 0.05$ ). GPW compared with chronological age in the Gymnast group using baseline values in a simple linear regression (Fig 8.4G\*), showed a similar result to MW compared to the Normal group;  $r = 0.872$  ( $p < 0.0001$ ) with a 95% CI of  $0.761$  to  $0.933$ , indicating a statistically significant correlation between GPW and chronological age. GPW compared with height showed a similar result (Fig 8.4H\*),  $r = 0.735$  ( $p < 0.0001$ ) with a 95% CI of  $0.535$  to  $0.857$ , also indicating a statistically significant positive correlation between GPW and height. Outliers will be discussed in section 9.4.

A comparison of mean MI, MW and GPW values of males and females Tukey's HSD revealed that there were no significant differences between the MIs, MWs or GPWs of males and females (all  $p > 0.995$ ).

A stepwise multiple linear regression was performed to determine the most significant covariates to use in an ANCOVA analysis. Within the Gymnast group, the only significant covariate for the MI was toBMD (4%). This meant that toBMD was the most important predictor of MI. This model had the highest  $r^2 = 0.151$  with an F-ratio of  $5.847$  ( $p = 0.021$ ), meaning toBMD (4%) explains 15.1% of the variance in MI values. The negative  $\beta$  value (Table 8.4A) meant that the relationship between toBMD and MI is negative; as MI increased, toBMD decreased.

<b>Table 8.4A Covariates for MI Gym</b>	<b><math>r^2</math></b>	<b>F-ratio</b>	<b>p</b>	<b><math>\beta</math></b>	<b>p</b>
<b>toBMD (4%)</b>	0.151	5.847	= 0.021	-0.388	= 0.021

**Table 8.4A: Summary of results of the multiple linear regression with MI as the dependent variable in the Gymnast group.**



The results of the ANCOVA analysis for MI indicated that both the male and female slopes as a whole (common slope), were not significantly different from zero ( $p = 0.454$ ) and there was no statistically significant difference between the slopes of males and females ( $p = 0.989$ ), meaning that once the covariate was accounted for, the slopes of both males and females were not significantly different from a flat line.

Within the Gymnast group, the most significant covariates for the MW were chronological age, toBMD (4%) and pSSI, meaning that these were the most important predictors for MW. This model had the highest  $r^2 = 0.858$  with an F-ratio of 62.418 ( $p < 0.0001$ ), meaning that chronological age, toBMD and pSSI explain 85.8% of the variance in MW values. The negative  $\beta$  value (Table 8.4B) for toBMD indicated that the relationship between toBMD and MW was negative; as MW increased, toBMD decreased.

<b>Table 8.4B Covariates for MW Gym</b>	<b><math>r^2</math></b>	<b>F-ratio</b>	<b>p</b>	<b><math>\beta</math></b>	<b>p</b>
<b>Chronological Age</b>	0.858	62.418	< 0.0001	0.493	< 0.0001
<b>toBMD</b>				-0.264	= 0.002
<b>pSSI</b>				0.576	< 0.0001

**Table 8.4B: Summary of results of the multiple linear regression with MW as the dependent variable in the Gymnast group.**

The results of the ANCOVA analysis for MW indicated that both the male and female slopes as a whole (common slope), were not significantly different from zero ( $p = 0.454$ ) and there was no statistically significant difference between the regression lines of males and females ( $p = 0.989$ ). This means that despite the covariates included in the model, the common slope is still rising, but there is no statistically significant difference between the slopes of males and females.

Within the Gymnast group, the most significant covariates for the GPW were chronological age, arm length and pSSI, meaning that these were the most important predictors for GPW. This model had the highest  $r^2 = 0.882$  with an F-ratio of 77.460 ( $p < 0.0001$ ), meaning that height, chronological age, arm length and pSSI explain 88.2% of the variance in GPW values. There are no negative  $\beta$  values (Table 8.4C) in this

model meaning that each covariate has a positive relationship with GPW. Though arm length is technically not significant at  $p = 0.052$ , it is very close to being significant.

<b>Table 8.4C Covariates for GPW Gym</b>	<b>r<sup>2</sup></b>	<b>F-ratio</b>	<b>p</b>	<b>β</b>	<b>p</b>
<b>Chronological Age</b>	0.882	77.460	< 0.0001	0.321	= 0.010
<b>Arm Length</b>				0.237	= 0.052
<b>pSSI</b>				0.447	= 0.001

**Table 8.4C: Summary of results of the multiple linear regression with GPW as the dependent variable in the Gymnast group.**

The results of the ANCOVA analysis for GPW indicated that both the male and female slopes as a whole (common slope), were not significantly different from zero ( $p = 0.055$ ), and there was no statistically significant difference between the regression lines of males and females ( $p = 0.856$ ). This indicates that the common slope is not significantly different from zero, though with a  $p = 0.052$  this remains very close to a significant relationship.

Using an unpaired t-test, neither the chronological ages of females and males (baseline values) were statistically different ( $p = 0.241$ ), nor were the means of the MI in Gymnast females (0.336) and Gymnast males (0.331) ( $p = 0.361$ , 95% CI = -0.015 to 0.006). A Mann-Whitney U-test confirmed these results (not shown). All MI values were transformed into Z scores and shown in a combined histogram (Fig 8.4I) due to an insufficient number of subjects in the Gymnast group available to calculate the mean MI of each age group in each sex. This group shows a normal distribution around the zero mean.

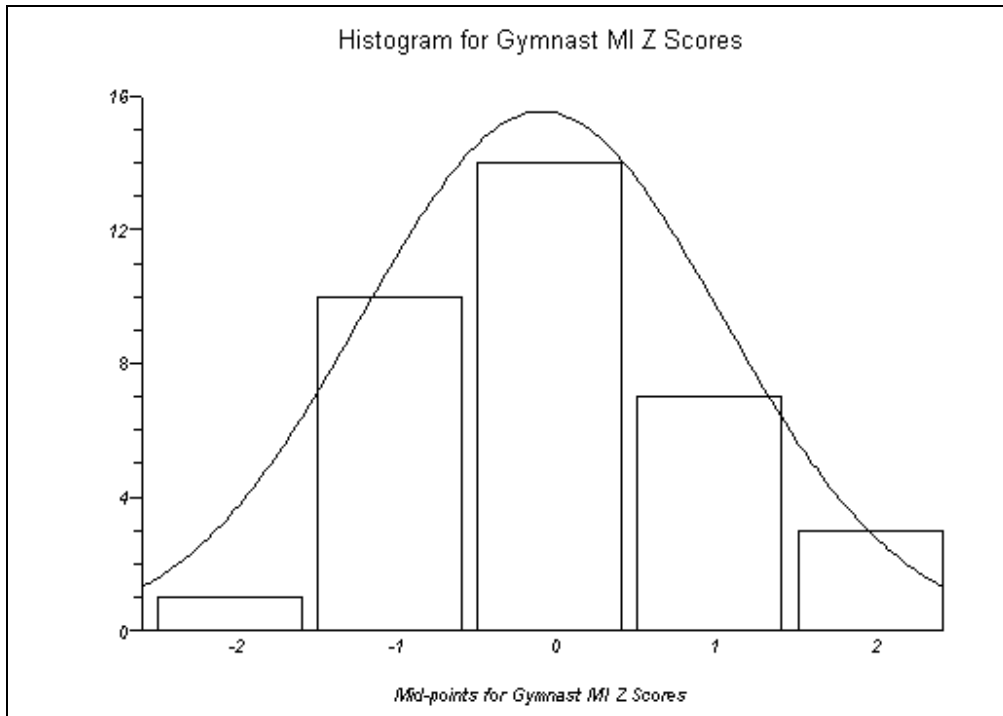


**Figure 8.4I: MI Z score values for the Gymnast group. These Z scores show a normal distribution and a mean of zero.**

### 8.4.1 Longitudinal Analysis

The results of the comparison of MI values of the Gymnast group subjects (Fig 8.4.1A) with 2 visits at approximately 1 year apart (32, 12 male) were that  $r = 0.787$  ( $p < 0.0001$ ) with a 95% CI of 0.604 to 0.891. This indicates a very high correlation between MI values at visit 1 and visit 2. When males and females were examined separately (Fig 8.4.1B), there was very little difference between the slopes and this was confirmed by the statistical output. The common slope was statistically significantly different from zero ( $p < 0.0001$ ), but there was no statistically significant difference between the slopes of males and females ( $p = 0.122$ ). Fig 8.4.1C shows how the MI changes between visits in males and females (male changes are indicated by red lines).

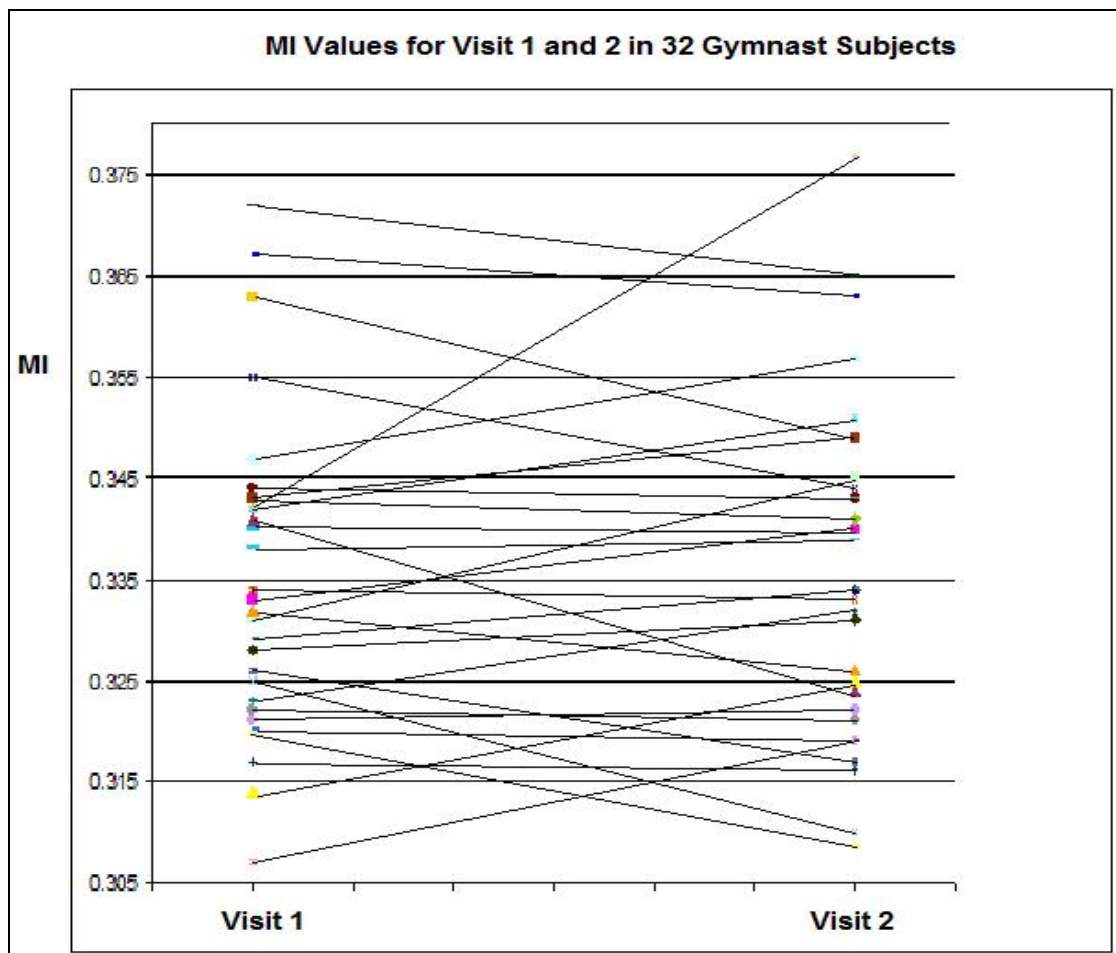


**Figure 8.4.1A:** A simple linear regression plot comparing MI values of 32 Gymnast subjects with visits approximately 1 year apart. This plot shows all but 1 value is within the 95% CI.

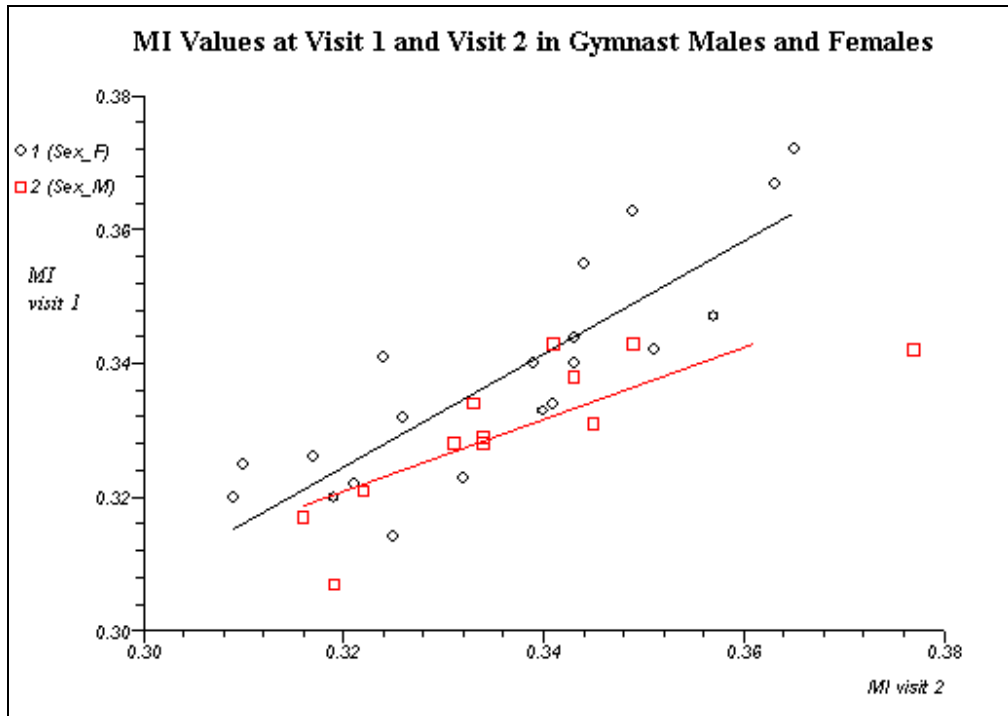


Figure 8.4.1B: A grouped linear regression plot comparing MI values of 32 Gymnast subjects (12 male) with visits approximately 1 year apart. This plot appears to show a slight difference between the slopes of males and females, but there is no statistically significant difference ( $p = 0.122$ ).

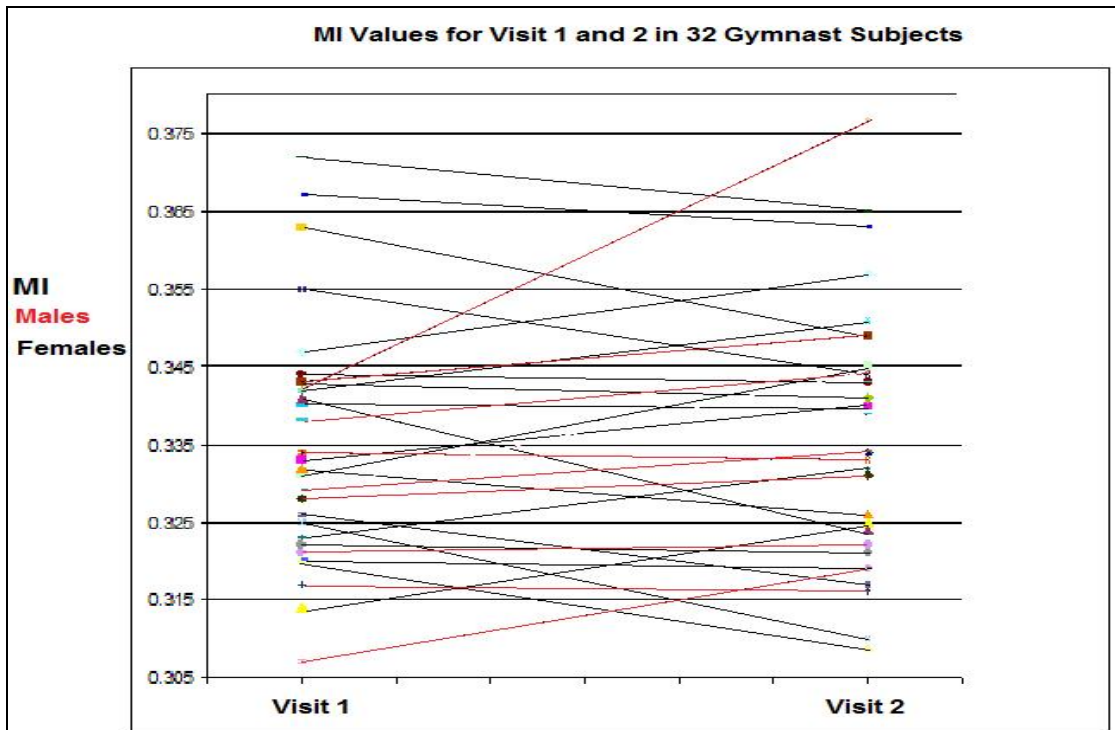


Figure 8.4.1C: A plot comparing MI values of 32 Gymnast subjects (12 male) with visits approximately 1 year apart.

## 8.5 NF1 Group

Unlike the Normal and Gymnast groups, there were only 17 subjects in the NF1 group, meaning that not all variables exhibited a normal distribution. Therefore a combination of non-parametric and parametric tests was used. When the MI values were compared with the baseline values of each anthropometric measure (chronological age, height, weight and arm length) and each pQCT measure (CSMA, pSSI, radius bone area 50% and cortical bone density 50%), Spearman's rank correlations showed that the MI was not significantly correlated with any of these variables (all  $p > 0.072$ ). A Spearman's rank correlation comparing MI to toBMD showed an  $r = -0.513$  ( $p = 0.052$ ) with a 95% CI of -0.812 to -0.001, which is on the border of achieving statistical significance. The negative value of  $r$  denotes an inverse relationship between MI and toBMD, so as toBMD decreases, MI increases, though not significantly in this group. MI was not compared to toBA (4%) because bone width, which is a component of the MI, will always be correlated with toBA. A simple linear regression comparing MI to chronological age using baseline values (Fig 8.5A) does not show a growth curve as it did in the Normal group. Although the graph appears to show a slight increase in MI as NF1 subjects age, this relationship is not statistically significant;  $ms = -0.001$  ( $p = 0.868$ ) with a 95% CI of -0.010 to -0.013. Another non-parametric linear regression was used to compare MI to height (Fig 8.5B). This graph illustrated a slightly steeper increase in MI as NF1 subjects grew in height, but again the relationship was not statistically significant;  $ms = 0.0005$  ( $p = 0.509$ ) with a 95% CI of -0.001 to 0.002.

Using grouped linear regressions to examine the MI in NF1 males and females compared with chronological age (Fig 8.5C\*) and MI compared with height (Fig 8.5D\*), there were no statistically significant differences in the regression lines for either MI compared to chronological age ( $p = 0.802$ ), or MI compared to height ( $p = 0.840$ ). Neither of the common slopes was significantly different from zero (both  $p > 0.287$ ). The height values for this regression were adjusted due to a statistically significant difference between the mean height of males and females (Mann-Whitney U test  $p = 0.05$ ).

The MW was compared with the same variables discussed previously using Spearman's rank correlations. MW compared with chronological age, toBMD and cortical density

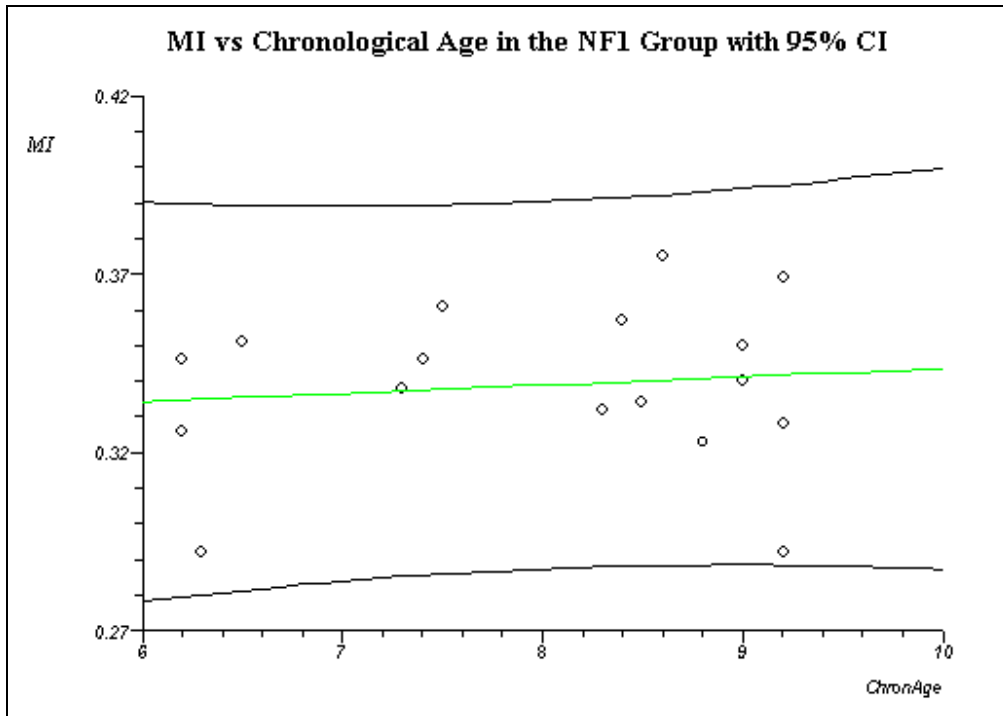


Figure 8.5A: MI compared to chronological age in the NF1 group. This cross-sectional plot appears to show a slight increase in MI values as NF1 subjects age, but there is no statistically significant relationship ( $p = 0.868$ ).

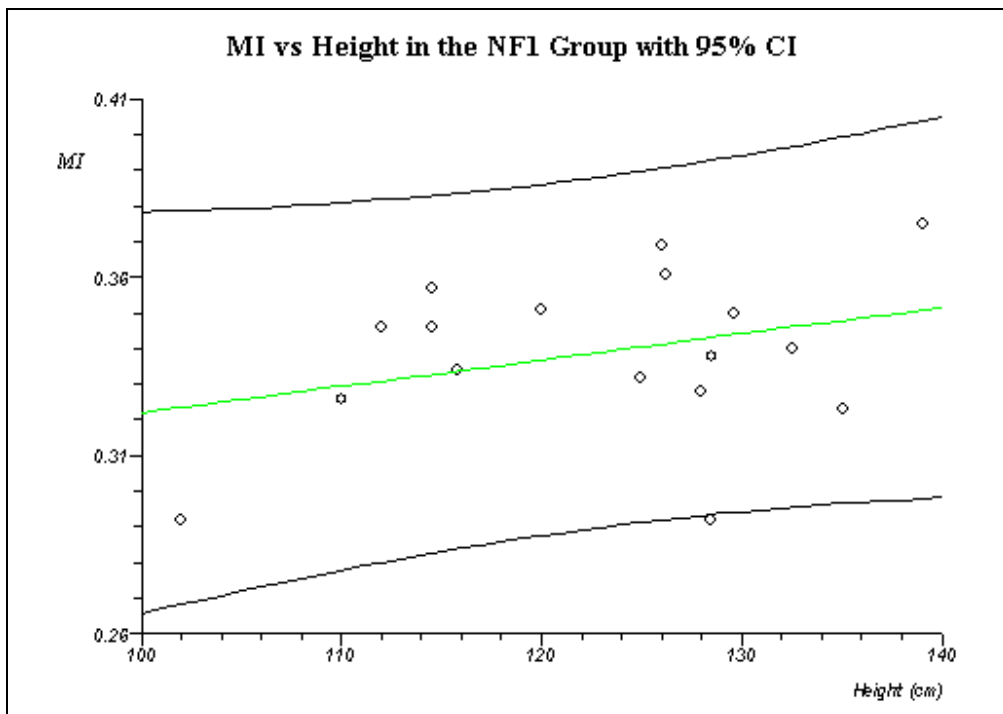


Figure 8.5B: MI compared to height in the NF1 group. This plot shows a slightly steeper increase in MI than in Fig 8.5A as NF1 height increases, but it was not significant ( $p = 0.509$ ).

(50%) were not significantly correlated (all  $p > 0.115$ ). MW compared with height ( $p = 0.003$ ), weight, ( $p = 0.0003$ ), arm length ( $p = 0.005$ ), CSMA ( $p = 0.008$ ), pSSI ( $p = 0.0002$ ) and radius bone area (50%) ( $p = 0.001$ ) were all significantly correlated. MW compared to chronological age in the NF1 group (Fig 8.5E\*) showed a dissimilar result to the same analysis in the Normal group;  $ms = 0.614$  ( $p = 0.159$ ), with a 95% CI for  $ms = -0.405$  to  $1.364$ . This indicates that MW and chronological age are not significantly correlated. All age values were within the 95% CI. MW was compared to height in the NF1 group (Fig 8.5F\*)  $ms = 0.115$ , ( $p = 0.005$ ) with a 95% CI of  $0.041$  to  $0.169$ , indicating that MW increased as height increased. Outliers will be discussed in section 9.5.

GPW was compared to all variables discussed previously using Spearman's rank correlations. GPW compared with chronological age ( $p = 0.082$ ), toBMD (4%) ( $p = 0.071$ ), CSMA ( $p = 0.057$ ), pSSI ( $p = 0.084$ ) and radius cortical density (50%) ( $p = 0.928$ ) were not significantly correlated. GPW compared with height ( $p = 0.013$ ), weight ( $p = 0.004$ ), arm length ( $p = 0.018$ ) and radius bone area (50%) ( $p = 0.013$ ) were all significantly correlated. GPW was compared with chronological age (Fig 8.5G\*) in the NF1 group using a simple linear regression and this showed a similar result to the same comparison in the Normal group;  $r = 0.872$  ( $p < 0.0001$ ) with a 95% CI of  $0.761$  to  $0.933$ , indicating a statistically significant correlation between GPW and chronological age. GPW compared with height showed a similar result to the previous comparison (Fig 8.5H\*),  $r = 0.735$  ( $p < 0.0001$ ) with a 95% CI of  $0.535$  to  $0.857$ , also indicating a statistically significant positive correlation between GPW and height. There are no outliers in these plots.

A comparison of mean MI, MW and GPW values of males and females Tukey's HSD revealed that there were no significant differences between the MIs, MWs or GPWs of males and females (all  $p > 0.492$ ).

Two linear regressions were performed to determine the most significant covariates to use in an ANCOVA analysis. Within the NF1 group, there were no variables with significant Pearson correlations, so due to that and the small number of subjects in the NF1 group, only the results of the Spearman's rank correlations were used. This meant that toBMD (4%) was the only covariate used in the first linear regression. However,



this resulted in a very low  $r^2$  value = 0.083,  $\beta$  = -0.288 ( $p$  = 0.297). Therefore a second linear regression (multiple) was performed using all of the previously mentioned variables. This regression indicated that the best model was one that included all covariates;  $r^2$  = 0.839 with an F ratio of 2.314 ( $p$  = 0.218,  $df$  = 9, 4), meaning that this model accounts for 83.9% of variation in the MI values. Most of the  $\beta$  values did not have significant,  $p$  values except for toBMD (4%) ( $p$  = 0.026), meaning toBMD (4%) was the most statistically significant predictor in the model (Table 8.5A).

Two ANCOVA analyses for MI were performed, one with toBMD (4%) as the only covariate, and one with all variables in Table 8.5A used as covariates. The results were very similar in that both indicated that the common slopes were not significantly different from zero, and there was no significant difference between male and female slopes.

<b>Table 8.5A Covariates for MI NF1</b>	<b><math>r^2</math></b>	<b>F-ratio</b>	<b>p</b>	<b><math>\beta</math></b>	<b>p</b>
<b>toBMD (4%)</b>	0.839	2.314	= 0.218	-1.100	= 0.026
<b>Chronological Age</b>				-0.327	= 0.687
<b>Height</b>				1.530	= 0.197
<b>Weight</b>				0.145	= 0.814
<b>Arm Length</b>				-0.682	= 0.216
<b>CSMA</b>				-0.590	= 0.573
<b>pSSI</b>				0.072	= 0.887
<b>Radius Area (50%)</b>				0.603	= 0.311
<b>Cortical Density (50%)</b>				0.572	= 0.139

**Table 8.5A: Summary of results of the multiple linear regression with MI as the dependent variable in the NF1 group.**

Using only the  $p$  values from the latter ANCOVA, the common slope was not significantly different from zero ( $p$  = 0.602) and there was no significant difference between the slopes of males and females ( $p$  = 0.919), meaning that once the covariates were accounted for, the slopes of both males and females were not significantly different from a flat line.

Within the NF1 group, the most significant covariates for the MW were pSSI and radius bone area (50%), meaning that these were the most important predictors for MW. Although a model using all possible covariates resulted in a higher  $r^2$  value, the model using pSSI and radius bone area (50%) had a much higher and statistically significant F-

ratio;  $r^2 = 0.857$ , F ratio = 32.895 ( $p < 0.0001$ ). This meant that pSSI and radius bone area (50%) explained 85.7% of the variance in MW values (Table 8.5B). There were no negative  $\beta$  values in this model meaning that each covariate had a positive relationship with GPW.

<b>Table 8.5B Covariates for MW NF1</b>	<b><math>r^2</math></b>	<b>F-ratio</b>	<b>p</b>	<b><math>\beta</math></b>	<b>p</b>
<b>pSSI</b>	0.857	32.895	< 0.0001	0.494	= 0.013
<b>Radius Bone Area (50%)</b>				0.502	= 0.012

**Table 8.5B: Summary of results of the multiple linear regression with MW as the dependent variable in the NF1 group.**

Two ANCOVA analyses for MW were performed, one using pSSI and radius bone area (50%) as covariates, and one using all possible covariates. The former indicated that the common slope was statistically significant from zero ( $p < 0.0001$ ), while the latter indicated the common slope was not statistically different from zero ( $p = 0.508$ ). Neither indicated a statistically significant difference between the regression lines of males and females (both  $p \geq 0.117$ ). These results will be discussed further in section 9.5.

Within the NF1 group, the most significant covariate for the GPW was height, meaning that height was the most important predictor for GPW variation. This model had the highest  $r^2 = 0.340$  with an F-ratio of 6.187 ( $p = 0.029$ ), meaning that height explained 2.9% of the variance in GPW values. There were no negative  $\beta$  values (Table 8.5C) in this model meaning that each covariate has a positive relationship with GPW. Though arm length is technically not significant at  $p = 0.052$ , it is very close to being significant.

<b>Table 8.5C Covariate for GPW NF1</b>	<b><math>r^2</math></b>	<b>F-ratio</b>	<b>p</b>	<b><math>\beta</math></b>	<b>p</b>
<b>Height</b>	0.340	6.187	= 0.029	0.321	= 0.029

**Table 8.5C: Summary of results of the multiple linear regression with GPW as the dependent variable in the NF1 group.**

The results of the ANCOVA analysis for GPW indicated that the common slope was not significantly different from zero ( $p = 0.144$ ), and there was no significant difference between the regression lines of males and females ( $p = 0.917$ ).

Using a Mann-Whitney U-test, the chronological ages of females and males were not significantly different;  $U = 20.5$  ( $p = 0.168$ ) with a 95% CI of -2.3 to 0.2, but the MI in females (median = 0.349) and males (median = 0.328) were significantly different;  $U = 55.5$  ( $p = 0.046$ ) with a 95% CI of 0 to 0.04. There were not enough subjects to separate males and females when transforming the MI values into Z scores. Therefore they are

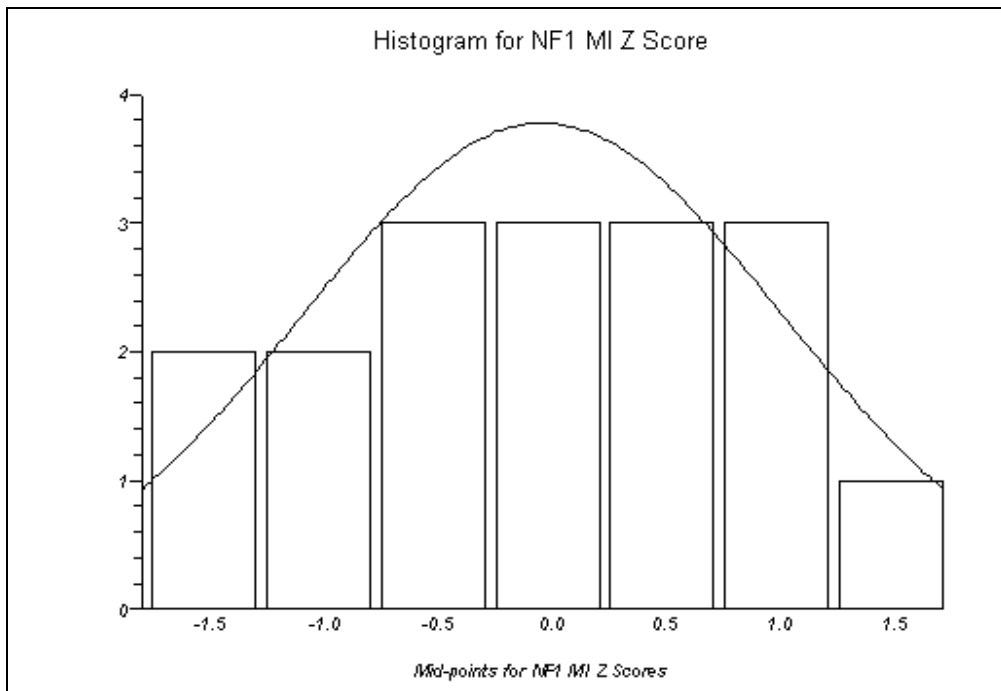


**Figure 8.5I: MI Z score values for the NF1 group. These Z scores show a normal distribution around the zero mean.**

shown in a combined histogram (Fig 8.5I). The histogram looks to be fairly normally distributed around the zero mean, but in order to determine this statistically, a Shapiro-Wilk W-test was performed to test for non-normality;  $W = 0.970$  ( $p = 0.815$ ). The p value was not significant indicating there was no evidence for non-normality.

## 8.6 CDGP Group

In this group, height and TW3 bone-age exhibited a normal distribution, but weight did not; Shapiro-Wilk  $W = 0.895$  ( $p = 0.015$ ). When the baseline MI values were compared with the baseline values of TW3 bone-age, height and weight using Spearman's rank correlations, they showed that the MI was not significantly correlated with height or weight (all  $p > 0.092$ ), but was significantly correlated with TW3 bone-age;  $r = 0.242$  ( $p = 0.012$ ). A polynomial regression was used to compare MI with TW3 bone-age (Fig 8.6A) and revealed that  $r = 0.238$  with a 95% CI of 0.051 to 0.408 ( $p = 0.013$ ). This plot showed a similar growth curve to the Normal group. A simple linear regression was used to compare MI to height using 25 baseline values (Fig 8.6B). This plot illustrated a slight increase in MI as the CDGP subjects grew in height and the relationship was statistically significant,  $r = 0.396$  ( $p = 0.050$ ) with a 95% CI of 0.0008 to 0.684.

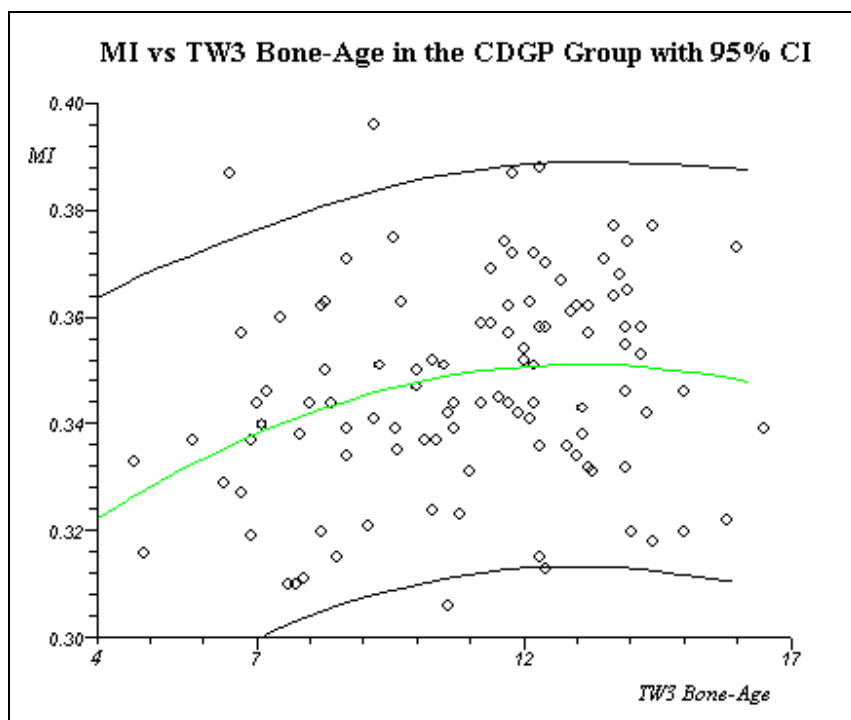


**Figure 8.6A:** MI compared to TW3 bone-age in the CDGP group using all baseline values. This cross-sectional plot shows a similar growth curve to the Normal group. The MI increases as bone-age increases.

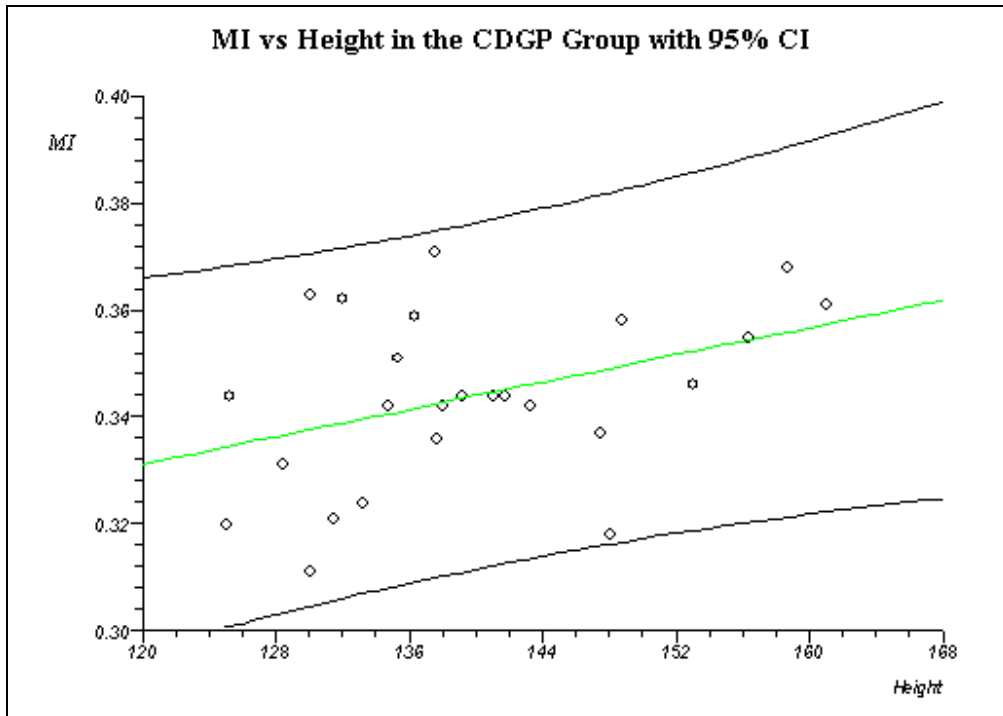


**Figure 8.6B: MI compared to height in the CDGP group using 25 baseline values. This plot shows a slight increase in MI as CDGP subject height increases, which was significant ( $p = 0.050$ ).**

Grouped linear regressions were used to examine the MI in CDGP males and females and compared with TW3 bone-age (Fig 8.6C\*) and with height (Fig 8.6D\*). Figure 8.6C\* shows a statistically significant common slope ( $p = 0.017$ ), but there was no significant difference between the regression lines of males and females ( $p = 0.550$ ). Figure 8.6D\* appears to show a large difference in the slopes of males and females, but the difference was not significant ( $p = 0.812$ ). The common slope was also not significantly different from zero ( $p = 0.062$ ).

The MW was compared to TW3 bone-age, height and weight. The results showed all Spearman's rank  $r$  values were significant; MW compared to TW3 bone-age ( $p < 0.0001$ ), MW compared to height ( $p = 0.0001$ ) and MW compared to weight ( $p = 0.0009$ ). MW compared to TW3 bone-age in the CDGP group using all baseline values (Fig 8.6E\*) showed a similar result to the same analysis in the Normal group;  $r = 0.778$  ( $p < 0.0001$ ), with a 95% CI for  $r = 0.601$  to  $0.822$ . This indicates a statistically significant positive correlation between MW and TW3 bone-age. A similar result occurred when MW was compared to height using baseline values in this group (Fig

8.6F\*)  $r = 0.751$ , ( $p < 0.0001$ ) with a 95% CI of 0.507 to 0.884, indicating that height is also significantly positively correlated with MW.

GPW was compared to all variables discussed previously, and all Spearman's rank values were statistically significantly correlated (all  $p < 0.003$ ). When GPW was compared to chronological age in the CDGP group using all baseline values in a simple linear regression (Fig 8.6G\*), this showed a similar result to the same test in the Normal group;  $r = 0.822$  ( $p < 0.0001$ ) with a 95% CI of 0.749 to 0.875, indicating a statistically significant correlation between GPW and TW3 bone-age. GPW compared with height showed a similar result (Fig 8.6H\*),  $r = 0.714$  ( $p < 0.0001$ ) with a 95% CI of 0.444 to 0.865, also indicating a statistically significant positive correlation between GPW and height. Outliers will be discussed in section 9.6.

In a comparison of mean MI, MW and GPW values of males and females Tukey's HSD revealed that there were no significant differences between the MIs, MWs or GPWs of males and females (all  $p > 0.452$ ).

A multiple linear regression was performed to determine the most significant covariates to use in an ANCOVA analysis. Within the CDGP group there were no significant covariates, but the model using TW3 bone-age, height and weight as independent variables was the model with the highest  $r^2 = 0.047$  with an F-ratio of 0.341 ( $p = 0.795$ ), meaning TW3 bone-age, height and weight only explain 4.7% of the variance in MI values.

<b>Table 8.6A Covariates for MI CDGP</b>	<b><math>r^2</math></b>	<b>F-ratio</b>	<b>p</b>	<b><math>\beta</math></b>	<b>p</b>
<b>TW3 Bone-Age</b>	0.047	0.342	= 0.795	-0.289	= 0.366
<b>Height</b>				0.115	= 0.750
<b>Weight</b>				0.014	= 0.965

**Table 8.6A: Summary of results of the multiple linear regression with MI as the dependent variable in the CDGP group.**

The results of the ANCOVA analysis for MI using all three variables, despite their statistical insignificance, indicated that the common slope was not significantly different from zero ( $p = 0.753$ ) and there was no statistically significant difference between the slopes of males and females ( $p = 0.998$ ).

Within the CDGP group, the most significant covariate for the MW was TW3 bone-age, meaning that this was the most important predictor for MW. This model had the highest  $r^2 = 0.696$  with an F-ratio of 52.550 ( $p < 0.0001$ ), meaning that TW3 bone-age explained 69.6% of the variance in MW values. The positive  $\beta$  value (Table 8.6B) indicated a positive relationship between TW3 bone-age and MW; as TW3 bone age increased, MW increased.

<b>Table 8.6B Covariates for MW CDGP</b>	<b><math>r^2</math></b>	<b>F-ratio</b>	<b>p</b>	<b><math>\beta</math></b>	<b>p</b>
<b>TW3 Bone-Age</b>	0.696	52.550	< 0.0001	0.834	< 0.0001

**Table 8.6B: Summary of results of the multiple linear regression with MW as the dependent variable in the CDGP group.**

The results of the ANCOVA analysis for MW indicated that the common slope was significantly different from zero ( $p < 0.0001$ ), but there was no statistically significant difference between the regression lines of males and females ( $p = 0.607$ ). This means that despite the covariates included in the model, the common slope is still rising, but there is no statistically significant difference between the slopes of males and females.

Within the CDGP group, the most significant covariate for GPW was again TW3 bone-age, meaning that this was the most important predictor for GPW. This model had the highest  $r^2 = 0.746$  with an F-ratio of 67.597 ( $p < 0.0001$ ), meaning that TW3 bone-age explained 74.6% of the variance in GPW values. The positive  $\beta$  value (Table 8.6C) indicated a positive relationship between TW3 bone-age and GPW; as TW3 bone age increased, GPW increased.

<b>Table 8.6C Covariates for GPW CDGP</b>	<b><math>r^2</math></b>	<b>F-ratio</b>	<b>p</b>	<b><math>\beta</math></b>	<b>p</b>
<b>TW3 Bone-Age</b>	0.746	67.597	< 0.0001	0.864	< 0.0001

**Table 8.6C: Summary of results of the multiple linear regression with GPW as the dependent variable in the CDGP group.**

The results of the ANCOVA analysis for GPW indicated that the common slope was significantly different from zero ( $p < 0.0001$ ), but there was no statistically significant difference between the regression lines of males and females ( $p = 0.550$ ).

Using an unpaired t-test, neither the TW3 bone-ages of females and males (all baseline values) were statistically different ( $p = 0.507$ ), nor were the means of the MI in CDGP females (0.342) and Gymnast males (0.348) ( $p = 0.218$ , 95% CI = -0.004 to 0.016). As there were no differences between males and females in the CDGP group, all MI values were transformed into Z scores and shown in a combined histogram (Fig 8.6I). This was due to the small number of females (19) in this group. A Shapiro-Wilk W-test was performed to confirm normality;  $W = 0.983$  ( $p = 0.189$ ), indicating there is no evidence of non-normality. The CDGP group Z scores show a normal distribution around the zero mean.

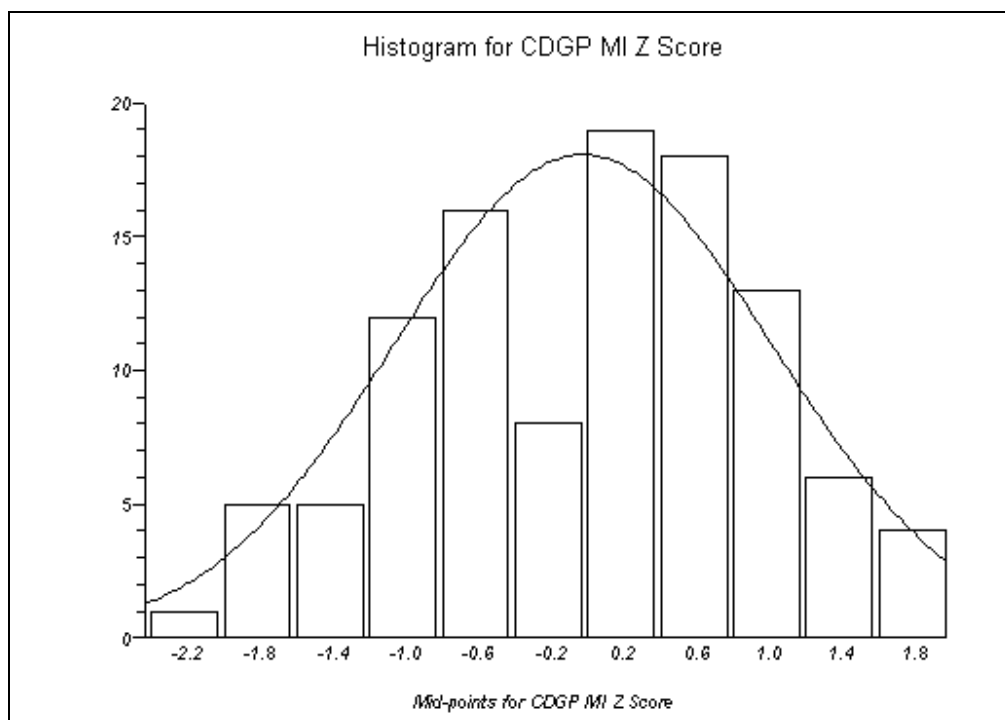


**Figure 8.6I: MI Z score values for the CDGP group. These Z scores show a normal distribution around the zero mean (approximately).**



A comparison was made between the means of chronological age compared with TW3 bone-ages of this group using a paired t-test and plotted using a box and whisker plot (Figure 8.6J). The results indicate the means are significantly different ( $p < 0.0001$ ); specifically the chronological ages of the group are much higher (mean = 12.872) than the TW3 bone-ages (mean = 11.056), in part due to their CDGP condition.

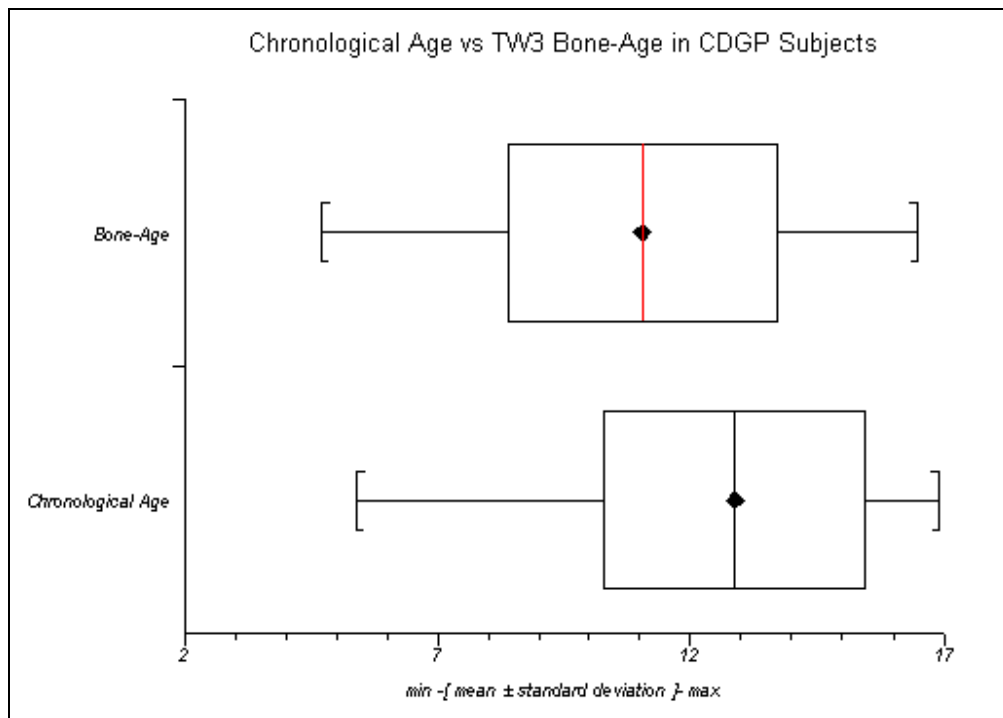


**Figure 8.6J:** A box and whisker plot illustrating the difference in means, SD's, minimum and maximum values when chronological age values are compared to TW3 bone-age values in the CDGP group ( $p < 0.0001$ ).

Because the skeletal maturity of the CDGP group is not as advanced as their chronological age, chronological age would not be an appropriate measure to use. This is illustrated in Figure 8.6K where MI is plotted against TW3 bone-age (A) and MI is plotted against chronological age (B). The figures are both similar but note the  $x$  axes in both plots; the curve of the regression line and plateau happen earlier in the TW3 bone-age plot (A) because the TW3 bone-age values are lower than their chronological age values.

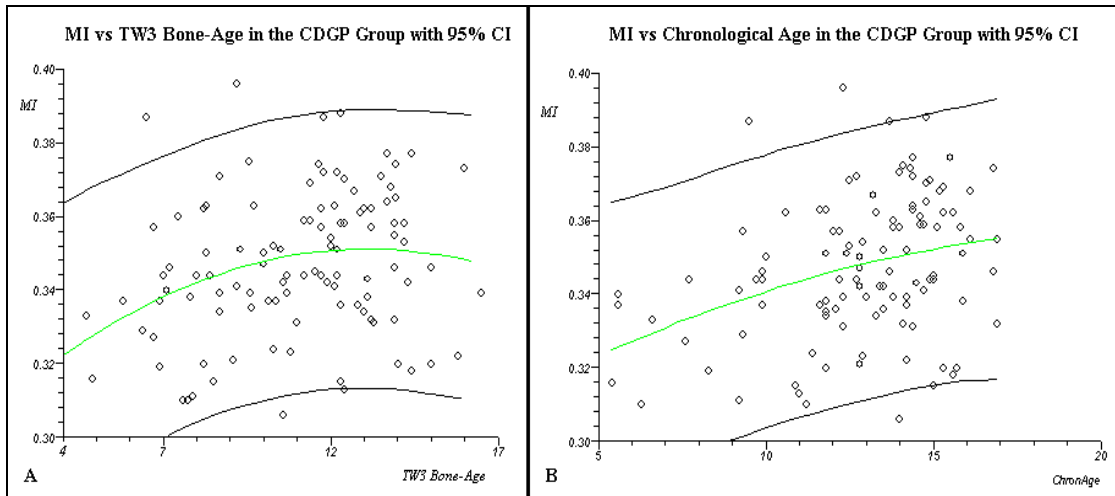


**Figure 8.6K: Comparison of two plots – MI vs TW3 bone-age (A) and MI vs chronological age (B). Note the x axes and the regression line. The curve of the regression line and the plateau happen earlier in A because the TW3 bone-age values are lower than their chronological age.**

### 8.6.1 Longitudinal Analysis

The results of the simple linear regression of MI values of 15 CDGP group subjects (9 male) with 2 visits at approximately 18 months apart  $\pm$  3 months (Fig 8.6.1A) were that  $r = 0.789$  ( $p = 0.0005$ ) with a 95% CI of 0.464 to 0.927. This indicates a very high positive correlation between MI values at visit 1 and visit 2. When males and females were examined separately (Fig 8.6.1B), there was very little difference between the slopes, which was confirmed by the statistical output. The common slope was statistically significantly different from zero ( $p = 0.002$ ), but there was no statistically significant difference between the slopes of males and females ( $p = 0.380$ ).

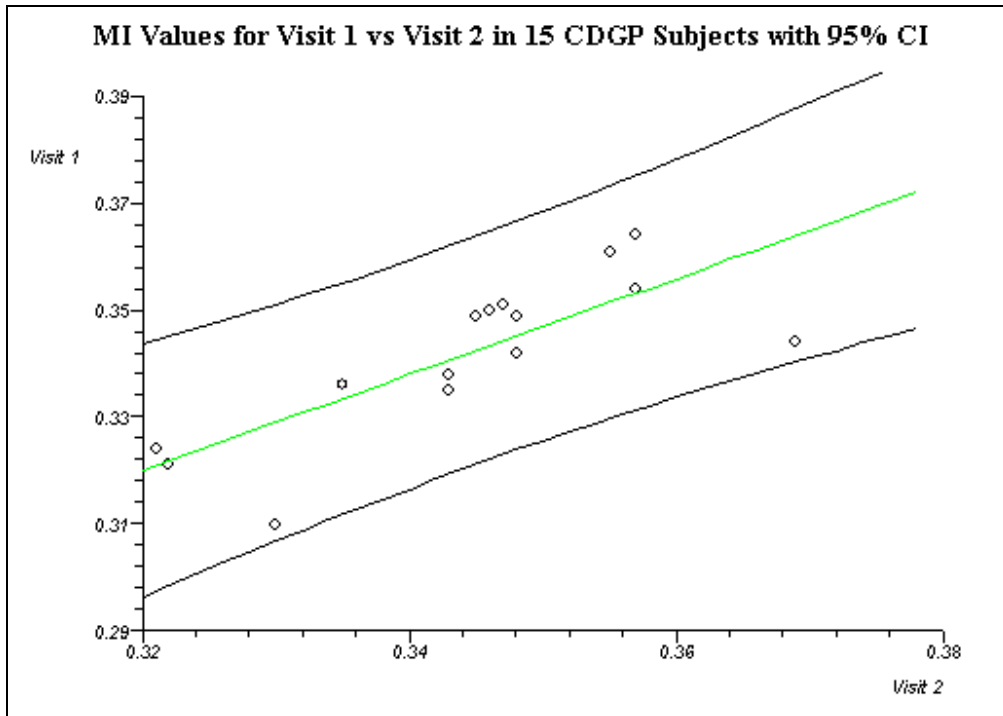


Figure 8.6.1A: A simple linear regression plot comparing MI values of 15 CDGP subjects with visits approximately 18 months apart. This plot shows all values are within the 95% CI.

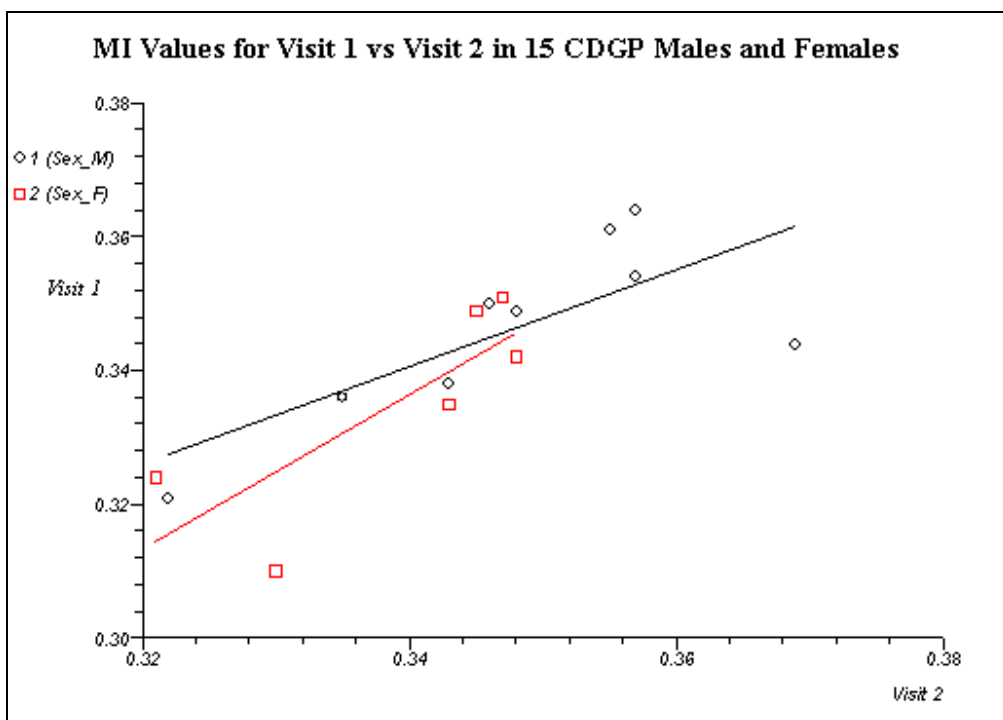


Figure 8.6.1B: A grouped linear regression plot comparing MI values of 15 CDGP subjects (9 male) with visits approximately 18 months apart. This plot appears to show a slight difference between the slopes of males and females, but there is no statistically significant difference ( $p = 0.380$ ).

## 8.7 Comparison of All Groups

A visual comparison of the means, standard deviations and ranges of the MI, MW and GPW of all 4 groups using box and whisker plots was performed (Fig 8.7A\*, B\*, C\*), with the means highlighted in Table 8.7A. The results of the MI means in all 4 groups showed the Normal group had the highest mean and the Gymnast group had the lowest.

<b>Table 8.7A: Means of Normal, Gymnast, NF1 and CDGP MI, MW and GPW</b>	<b>Normal</b>	<b>Gymnast</b>	<b>NF1</b>	<b>CDGP</b>
<b>Mean MI</b>	0.346	0.334	0.339	0.342
<b>Mean MW</b>	15.210 mm	15.339 mm	14.488 mm	14.711 mm
<b>Mean GPW</b>	21.980 mm	22.988 mm	21.412 mm	21.471 mm
<b>Difference in Mean Heights Adjusted for Chronological Age‡ compared to Normal Group</b>		4.8cm shorter than Normal (p = 0.005)	5.6cm shorter than Normal (p = 0.009)	4.9cm shorter than Normal (p = 0.037)

**Table 8.7A: Summary table of means for MI, MW and GPW in all 4 groups with highest values in red and lowest values in blue. (‡ The CDGP group was adjusted for TW3 bone-age compared to the Normal group).**

The results of the MW means in all 4 groups showed that the Gymnast group had the highest mean and the NF1 group had the lowest mean. It should be noted that even after adjusting for age in each group, there was a statistically significant difference in heights between the Normal group and the other groups. Figure 8.7A\* also showed that the standard deviations for MW values were smaller across each group than they were for the MI means plot. The results of the GPW means in all 4 groups showed that the Gymnast group had the highest mean (22.988 mm) and the NF1 group had the lowest mean (21.412 mm), which was only slightly less than the CDGP group mean (21.471 mm). All plots showed the standard deviation and ranges overlapping.

The grouped linear regression plot for MI values (Fig 8.7D) compared with age indicated the common slope was not significantly different from zero (p = 0.311) and the difference between the regression lines was not significant (p = 0.975).

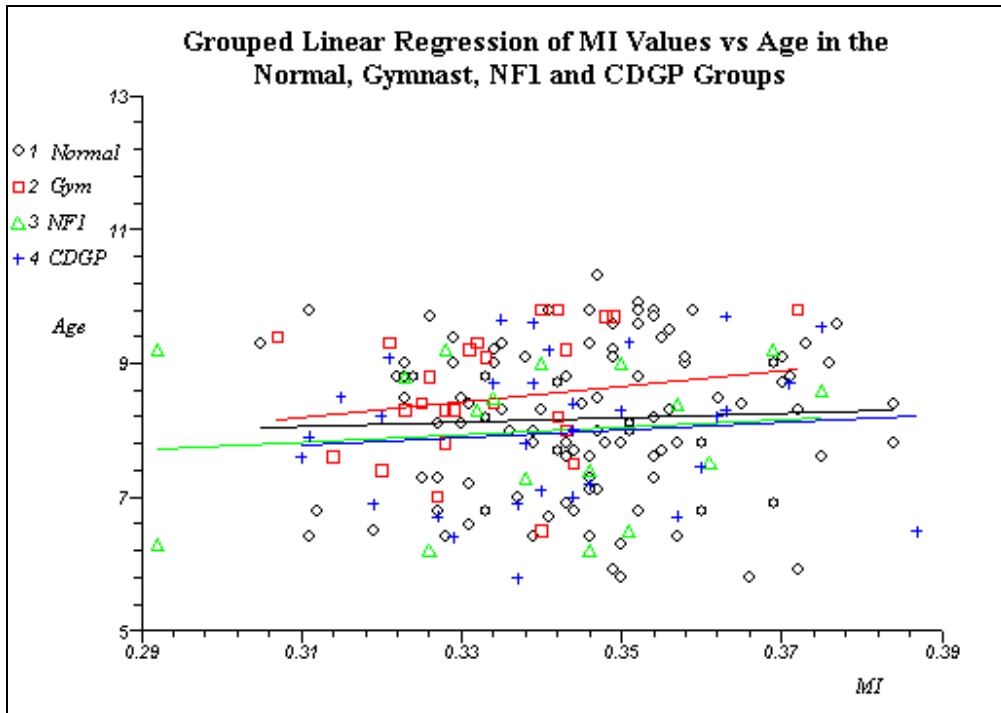


**Figure 8.7D:** A grouped linear regression plot illustrating MI values compared to age in the Normal, Gym, NF1 and CDGP groups using adjusted ages (5.9 – 9.9 years). Neither the common slope nor the differences between slopes were significant ( $p = 0.311$ ,  $p = 0.975$  respectively).

The Levene statistic = 1.551 ( $p = 0.203$ ), meaning that there was no evidence for heterogeneity of variance. The ANOVA indicated the F-ratio (between groups) = 3.467 ( $p = 0.017$ ) meaning that the experimental group that a subject was in had an effect on MI values, and the effect was significant. Bonferonni's test, Gabriel's procedure, the Hochberg GT2 test and Dunnett's  $t$  (2-sided) all gave very similar results, therefore this section has concentrated on the results of Dunnett's  $t$  (Table 8.7B). These results indicated that the Gymnast group MI was significantly different from the Normal group, but the NF1 and CDGP groups were not.

Each Gymnast baseline subject was matched for height with a control from the Normal group and a paired  $t$ -test was performed to ensure the heights were not significantly different, which they were not ( $p = 0.210$ ). The MI was compared between Gymnast cases and Normal controls using a paired  $t$ -test, which was significant ( $p = 0.038$ ). This indicates that the significant difference seen when these groups were matched for chronological age is not due to the difference in height between the two groups.

<b>Table 8.7B – Results of Dunnett’s t (2-sided) Test for MI Comparisons Between Groups (Adjusted for Age)</b>							
Group X	Group Y	r	Mean Difference (X-Y)	Std. Error	Sig.	95% CI	
						Lower Bound	Upper Bound
Gymnast	Normal	0.223	-.011379*	.003725	.008	-.02034	-.00242
NF1	Normal	0.112	-.006709	.004448	.341	-.01741	.00399
CDGP	Normal	0.071	-.003251	.003433	.710	-.01151	.00500

**Table 8.7B: Results of Dunnett’s t (2-sided) test for MI compared to age using the Normal group for comparison with the other 3 groups. The results indicate that the Gymnast group has a significant difference to Normal, but the other groups do not.**

The grouped linear regression plot for MW values (Fig 8.7E) compared with age indicated the common slope was significantly different from zero ( $p < 0.0001$ ), but the difference between the regression lines was not significant ( $p = 0.342$ ). The Levene statistic = 1.109 ( $p = 0.307$ ), meaning that there was no evidence for heterogeneity of variance. The ANOVA indicated the F-ratio (between groups) = 2.106 ( $p = 0.101$ ) meaning that the experimental group that a subject was in did not have a significant effect on MW values. For reasons mentioned previously, this section has concentrated on the results of Dunnett’s t (Table 8.7C). The results of the Dunnett’s t test indicated that no group was significantly different from the Normal group.

<b>Table 8.7C – Results of Dunnett’s t (2-sided) Test for MW Comparisons Between Groups (Adjusted for Age)</b>							
Group X	Group Y	r	Mean Difference (X-Y)	Std. Error	Sig.	95% CI	
						Lower Bound	Upper Bound
Gymnast	Normal	0.030	.128887	.324189	.969	-.65069	.90846
NF1	Normal	0.139	-.722538	.387120	.275	-1.65344	.20837
CDGP	Normal	0.125	-.499496	.298739	.256	-1.21817	.21858

**Table 8.7C: Results of Dunnett’s t (2-sided) test for MW compared to age using the Normal group for comparison with the other 3 groups. The results indicate that none of the 3 groups have a significant difference to the Normal group.**

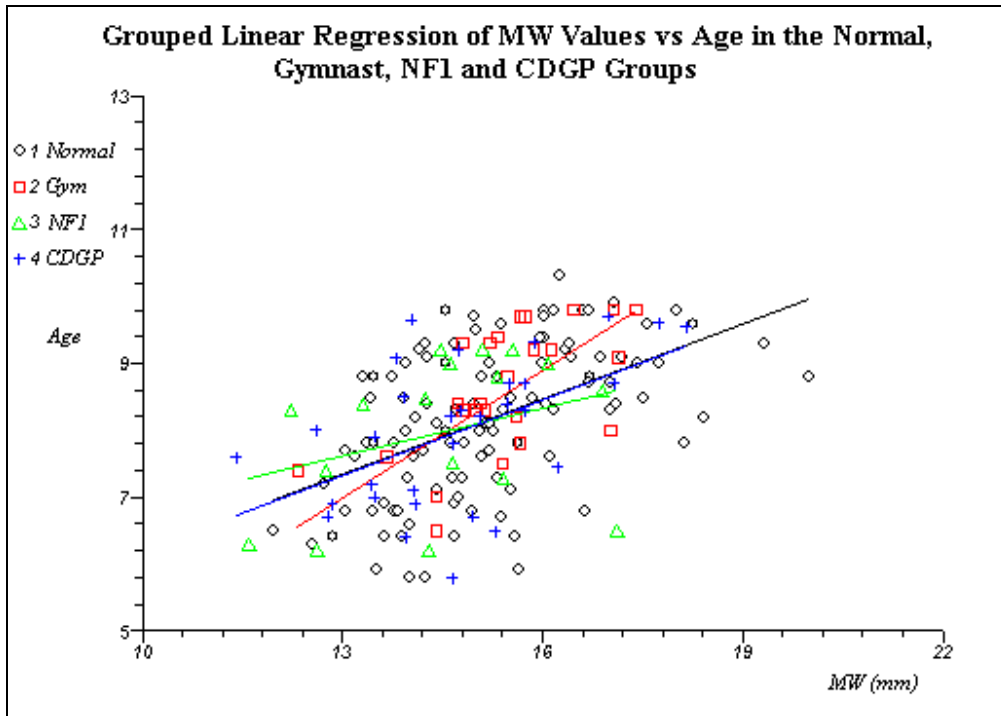


**Figure 8.7E:** A grouped linear regression plot illustrating MW values compared to age in the Normal, Gym, NF1 and CDGP groups using adjusted ages (5.9 – 9.9 years). The common slope was significantly different from zero ( $p < 0.0001$ ), but the differences between slopes were not significant ( $p = 0.342$ ).

The grouped linear regression plot for GPW values (Fig 8.7F) compared with age indicated the common slope was significantly different from zero ( $p < 0.0001$ ), but the difference between the regression lines was not significant ( $p = 0.210$ ). The Levene statistic = 1.491 ( $p = 0.219$ ), meaning that there was no evidence for heterogeneity of variance. The ANOVA indicated the F-ratio (between groups) = 4.268 ( $p = 0.006$ ), meaning that the experimental group that a subject was in had a significant effect on GPW values. For reasons stated previously, this section concentrated on the results of Dunnett's *t* (Table 8.7D). The results of the Dunnett's *t* test indicated that the Gymnast group had a significant difference from the Normal group ( $p = 0.029$ ), but the other groups did not have a significant difference from the Normal group. Each Gymnast baseline subject was matched for height with a control from the Normal group and a paired *t*-test was performed to ensure the heights were not significantly different, which

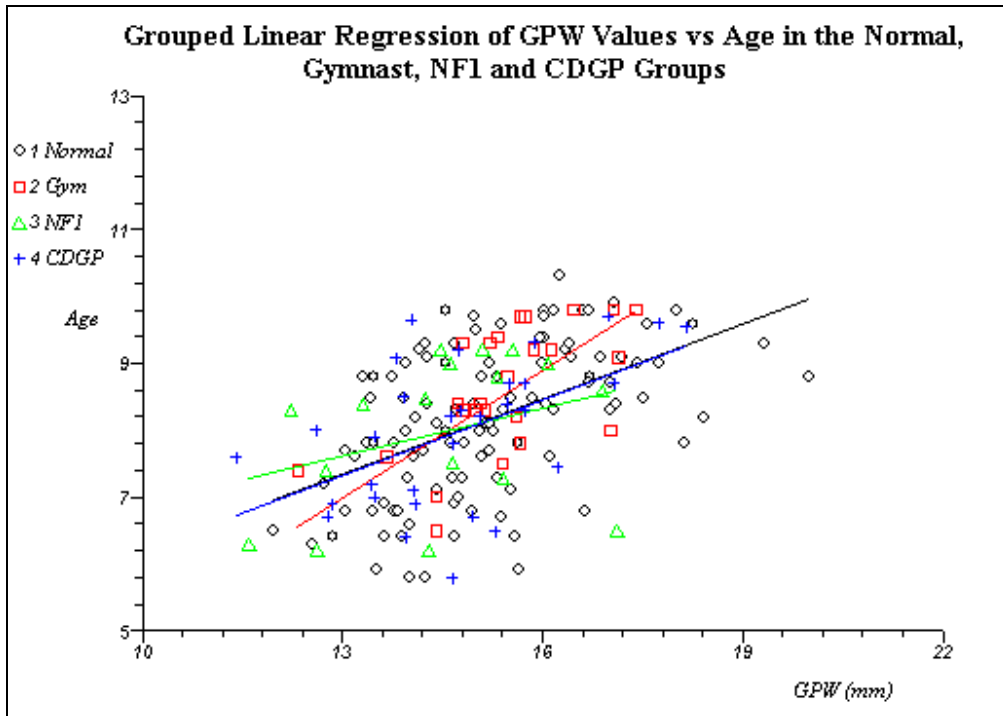


Figure 8.7F: A grouped linear regression plot illustrating GPW values compared to age in the Normal, Gym, NF1 and CDGP groups using adjusted ages (5.9 – 9.9 years). The common slope was significantly different from zero ( $p < 0.0001$ ), but the differences between slopes were not significant ( $p = 0.210$ ).

Table 8.7D – Results of Dunnett’s t (2-sided) Test for GPW Comparisons Between Groups (Adjusted for Age)							
Group X	Group Y	r	Mean Difference (X-Y)	Std. Error	Sig.	95% CI	
						Lower Bound	Upper Bound
Gymnast	Normal	0.191	1.008379	.387446	.029	.07669	1.94007
NF1	Normal	0.092	-.568048	.462657	.518	-1.68060	.54450
CDGP	Normal	0.106	-.508657	.357030	.319	-1.36720	.34989

Table 8.7D: Results of Dunnett’s t (2-sided) test for GPW compared to age using the Normal group for comparison with the other 3 groups. The results indicate that Gymnasts have a significant difference to the Normal group ( $p = 0.029$ ), but the other groups do not.

they were not ( $p = 0.210$ ). The GPW was compared between Gymnast cases and Normal controls using a paired t-test, which was significant ( $p < 0.0001$ ). This indicates



that the significant difference seen when these groups were matched for chronological age was not due to the difference in height between the two groups.

A visual comparison of the distributions of MI Z scores (Fig 8.7G) showed all groups are normally distributed. A combined histogram of Normal males and females (Fig 8.7G) also showed a normal distribution with the centre around +1 SD. Separate histograms for Normal males (Fig 8.3L) and Normal females (8.3M) are shown in section 8.3.

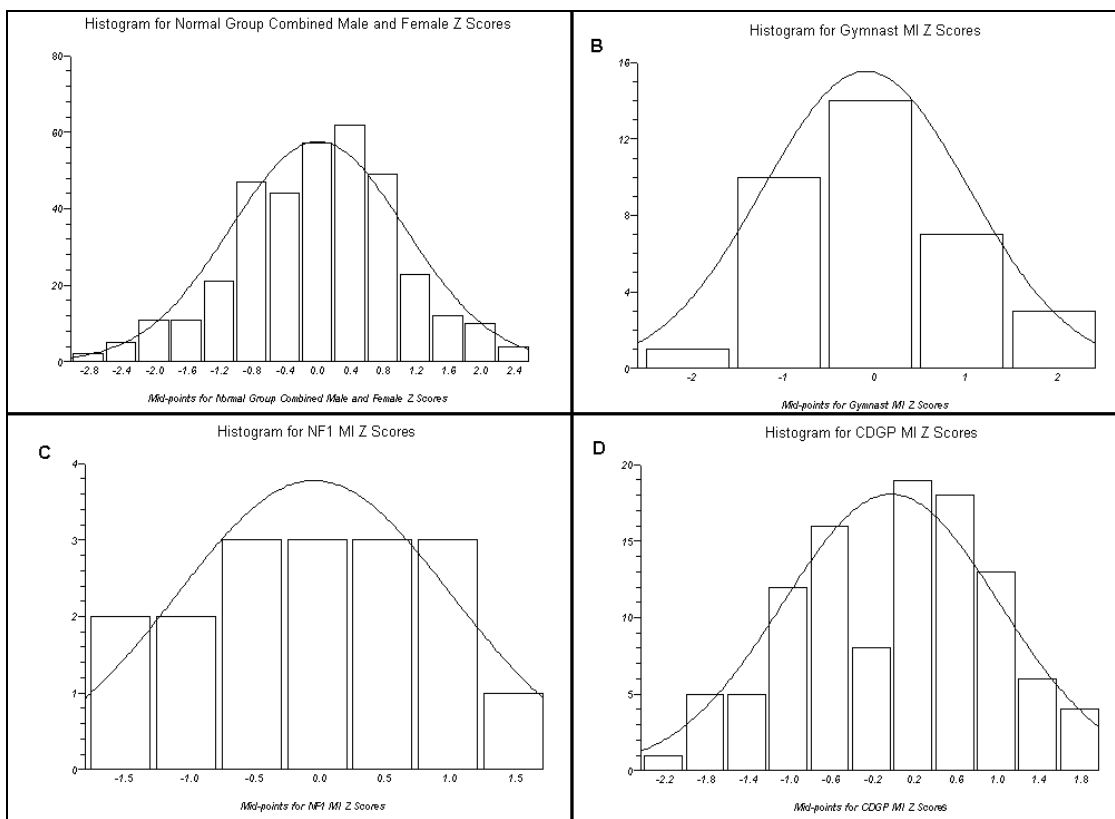


**Figure 8.7G: A visual comparison of the distribution of all MI Z Scores. A – Normal, B – Gymnast, C – NF1, D – CDGP. These graphs show normal distributions for all groups, but the Normal group shows positively skewed result (+1 SD).**

## 8.8 Comparison of DXA Images and Radiographs using GP Bone-Age

Table 8.8A shows the CVs of GP bone-age assessments using radiographs and DXA hand images. The CVs in this table indicate that radiographic bone-age assessments have

<b>Table 8.8A: Precision of Bone-Age Assessment - Comparison of DXA Images and Radiographs using the GP Method</b>	<b>CV %</b>
Radiograph Bone-Age Assessments (GP)	<b>2.68%</b>
DXA Bone-Age Assessments (GP)	<b>2.95%</b>

Table 8.8A: The CVs of bone-age assessments using the GP methods showing radiographs compared to DXA images.

a higher repeatability than the CV of DXA bone-age assessments. The relation between bone-age assessed from radiographs and DXA images is shown in Fig 8.8A,  $r^2 = 0.986$  ( $p < 0.001$ ). There was no significant difference between the mean bone ages of the two

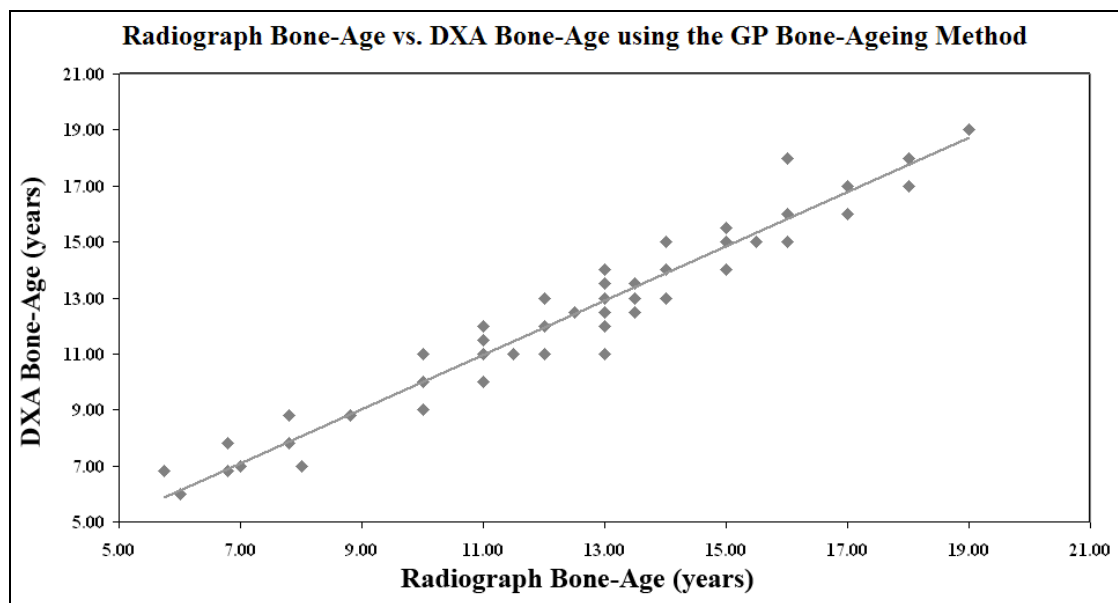


Figure 8.8A: A plot comparing DXA bone-ages to radiograph bone-ages, which indicates a strong positive relationship ( $p < 0.0001$ ).

methods ( $p = 0.114$ ) and the upper and lower 95% confidence intervals include zero. There was a significant overlap in results (e.g. 5 subjects have a bone-age of 10 years by both radiographs and DXA images). A Bland and Altman plot of the differences

between the two bone-age assessments compared to the means of the two ages (Fig 8.8B) shows 96 of the 98 subjects (98%) had no more than a 1 year difference in bone-age when comparing assessment from hand radiographs and DXA. There were two subjects outside the 95% prediction interval (Fig 8.8B), one with a +2 year difference and one with a -2 year difference between the radiograph and DXA bone-ages. In the first subject (-2 year difference), both the radiograph and DXA bone-ages were within 2 years of the chronological age. In the second subject (+2 year difference), the DXA bone-age was within 2 years of the chronological age but the radiograph bone-age had a >2 year difference. One further subject also showed a >2 year difference between chronological age and radiograph bone-age, but the DXA bone-age was within 2 years and both bone-ages were within 2 years of each other. Fifty-nine subjects (60%) had bone-age assessments that were identical as assessed by radiographs and DXA. Sixty-seven subjects (68%) had a radiograph bone-age that was within 1 year of their chronological age and 68 subjects (69%) had a DXA bone-age that was within 1 year of their chronological age. One subject had a >2 year difference between chronological age and both radiograph and DXA bone-age. However, this was due to the methodological issue stated in the GP Bone-Age Method section, as the subject in question was a female aged 20.2 years.

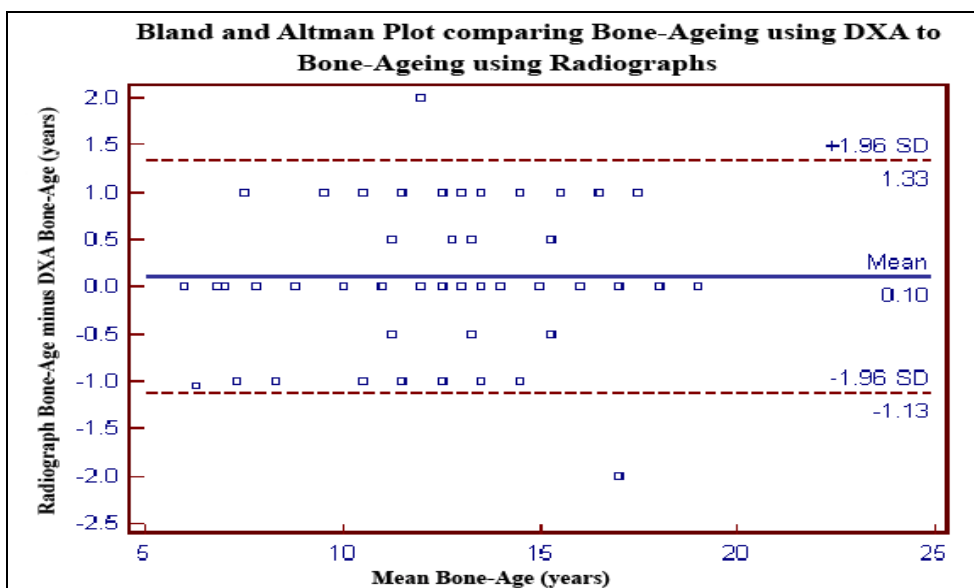


Figure 8.8B: Bland and Altman plot showing the differences in ages between the DXA hand images and the hand radiographs plotted against the means of the two ages.

## **9. Discussion**

### **9.1 Introduction**

This chapter has four parts; the first three correspond with the first three parts in Chapters 7 and 8. The first part is organised into four sections: a discussion of results and statistical analyses conducted within the Normal group, within the Gymnast group, within the NF1 group and within the CDGP group. The second part discusses the results of the statistical analyses performed in the comparison of the latter three groups to the Normal group. The third part discusses the results of the DXA Bone-age study. The chapter ends with sections discussing the challenges, study limitations, comparisons with the literature and potential future work involving examinations of the MI and DXA bone-age assessment.

### **9.2 Precision**

It was not surprising to observe that the manual method of measuring the MW, GPW and therefore the MI, was less repeatable than the computer-assisted method. As discussed in section 7.2, the computer-assisted method allowed the user to zoom in on a radiograph to many times its normal size, while still maintaining resolution, aiding the user to detect the bone edges more accurately, thus its greater repeatability.

It is also unsurprising to find that the TW3 bone-age assessment method is more repeatable than the GP method. The TW3 method allows the user to examine each relevant bone and/or epiphysis for specified size and shape changes. The GP method of examining a whole radiograph with that of standards in an atlas cannot be as accurate (if accuracy is measured as obtaining a bone-age similar to the subject's chronological age in a normal subject) or precise as if each bone was examined individually. Not all bones/epiphyses mature at exactly the same rate, therefore it is more desirable to examine bones individually to obtain a result that is more likely to be closer to the individual's actual level of skeletal maturity. Although the GP method is quicker to perform for the novice, once an assessor becomes familiar with the TW3 method (as the author has during this study), it is possible to perform an assessment in less than 3 minutes. Those radiographs that indicate full skeletal maturity in every bone can be assessed in less than 30 seconds.

### 9.3 Normal Group

In the Normal group, the correlation co-efficients (r values) and associated p values indicated significant correlations between MI and chronological age, TW3 bone-age, height, weight, Tanner stage, arm length, CSMA, pSSI, radius bone area (50%) and cortical bone density (50%). However the highest r value was for Tanner stage;  $r = 0.305$ . This indicates that although the correlations were significant, a maximum of only 9.3% of the variation in the MI could be explained by a significantly correlated variable. This leaves 90.7% of the variation in MI values to be explained by other variables. These results are expected because the MI is a ratio that attempts to measure the same area of a bone irrespective of bone size. Variables like height, weight, Tanner stage, arm length, CSMA, pSSI, radius bone area (50%) and cortical bone density (50%) all increase with age during the growth period under normal conditions. Even cortical bone density (50%), which is measured in  $\text{g}/\text{cm}^3$ , is a volumetric measurement and volume correlates with both components of the MI (MW and GPW). The low r values confirm that the MI is successful at eliminating the issue of bone size when measured at the distal radius.

Both plots comparing MI with chronological age and MI with height showed a typical growth curve. Most of the values were within the 95% CI but there were outliers. In the plot that compared MI with chronological age (Fig 8.3A), the outliers occurred from age 7 to age 19 and, by definition, consisted of those with a high MI (closer to 0.5 maximum) and those with a low MI (closer to zero). The fact that MI values had outliers in the majority of age groups and on either side of the CI, meant that although MI increased with age, younger subjects were not more likely to have an MI outside the lower 95% CI and older subjects were not more likely to have an MI outside the higher 95% CI. In the plot that compared MI with height (Fig 8.3B), the outliers occurred from heights 125 cm to 170 cm. The fact that MI values had outliers in the majority of height groups and on either side of the CI, meant that although MI increased with height, shorter subjects were not more likely to have an MI outside the lower 95% CI and taller subjects were not more likely to have an MI outside the higher 95% CI. The plots comparing the regression lines of males and females showed no statistically significant difference between them when comparing MI with chronological age (Fig 8.3C) and MI

with height (Fig 8.3D). The MI increased slightly as both chronological age and height increased but it was not a statistically significant rise. This indicated that by using the MI (a ratio of  $0.5\text{MW}/\text{GPW}$ ), that the age of the subject and the height of the subject (surrogates for bone size) were affecting the results, but not significantly. This combined with the low  $r$  values confirmed that MI was not significantly dependent on bone size when measured at the distal radius.

The  $r$  values and associated  $p$  values indicated significant correlations between MW and chronological age, TW3 bone-age, height, weight, Tanner stage, arm length, CSMA, pSSI, radius bone area (50%) and cortical bone density (50%). However, the  $r$  values ranged from 0.287 to 0.814, indicating that up to 66.3% of the variation in the MW could be explained by a single significant variable. This leaves 33.7% of the variation to be explained by other variables. These  $r$  values are much higher than the  $r$  values obtained using the MI. This is expected because the MW is a width measurement, which will obviously be related to bone size; width increases as bone size increases. Variables such as height, weight, Tanner stage, arm length, CSMA, pSSI, radius bone area (50%) and cortical bone density (50%) all increase with age during the growth period under normal conditions. Therefore all of the above variables would correlate significantly with a bone width measurement. The high  $r$  values confirm that the MW is dependent on bone size and correlates well with several variables when measured at the distal radius.

The plots comparing MW with chronological age and height each showed outliers in approximately the same areas. Examination of the outliers revealed that those individuals with values below the 95% CI in the chronological age plot were more likely to be shorter for their age, and those individuals with values above the 95% CI were more likely to be taller for their age. It is interesting to note that 9 of the 15 females aged 18 to 20 years measured from 150cm to 162cm (Fig 9.3A purple), the range of which is below the mean height for an adult British female (Nettle, 2002). In UK females aged 18 years, a height of 162cm is below the 50<sup>th</sup> centile and a height of 150cm is below the 3<sup>rd</sup> centile (Freeman et al., 1995a). Nine of the 15 females aged 18 to 20 years in this study group had MW values below 15.0, which is outside the 95% CI. However only 5 of the 9 females in question both measured under 162cm and had an

MW below 15.0mm. This indicated that individuals who are short for their age are more likely to have a smaller MW. This trend was confirmed when MW was compared to height. Those individuals with values above the 95% CI were taller for their age, and those individuals below the 95% CI were shorter for their age. The outlier with an MW of 26.0mm was a male aged 16 measuring 188.4cm (Fig 9.3A red), which is well above the mean height of British males (177.4cm) (Nettle, 2002) and is above the 97<sup>th</sup> centile for UK males aged 16 years (Freeman et al., 1995a). These results were expected because chronological age and height are related; bones increase in length as individuals age, therefore the MW will increase in proportion with height and bone length. Indeed MW compared to height showed a smaller 95% CI than MI indicating that MW width exhibits less variation when compared to height than age, and is a tightly controlled process during growth. The greatest variation in height was seen from ages 12 to 16 years when the pubertal growth spurt occurs, although these outliers had a spread of Tanner stages ranging from 1 to 3. Although the outliers exhibited small MWs, none of them exhibited abnormal MIs.

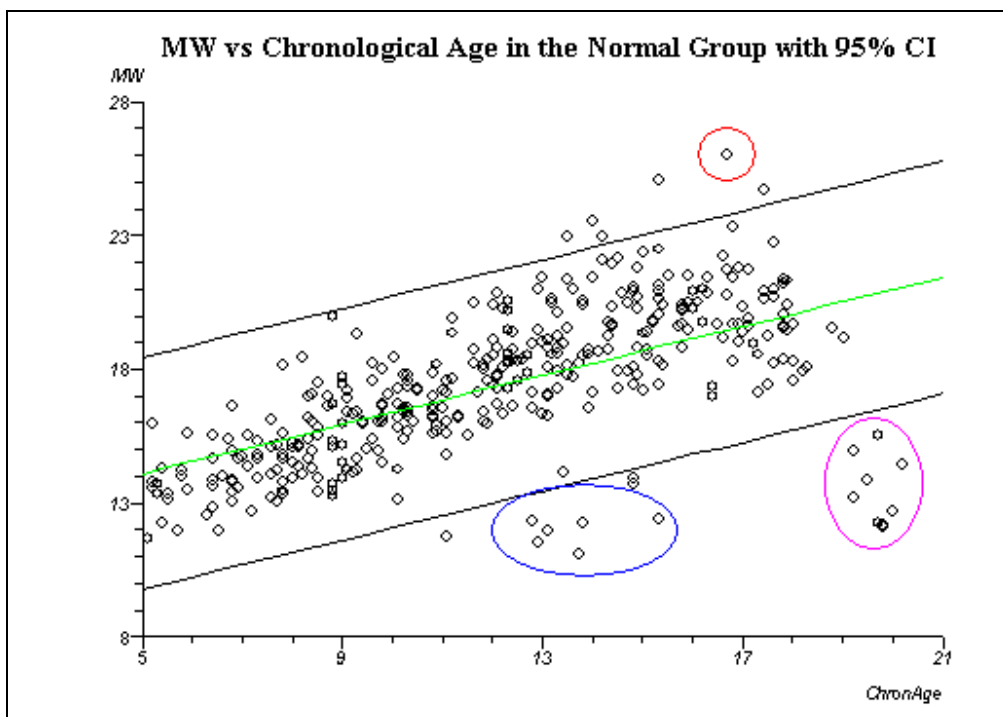


**Figure 9.3A: MW compared to chronological age in the Normal group (baseline values) with outliers highlighted.**

The r values and associated p values indicated significant correlations between GPW and chronological age, TW3 bone-age, height, weight, Tanner stage, arm length, CSMA, pSSI, radius bone area (50%) and cortical bone density (50%). However, the r values ranged from 0.251 to 0.806, indicating that up to 65.0% of the variation in the GPW could be explained by a single significant variable. This leaves 35.0% of variation left to be explained by other variables. These r values are much higher than the r values obtained using the MI. This is expected because as with the MW, GPW is a width measurement, which will be related to bone size; width increases as bone size increases. Variables like height, weight, Tanner stage, arm length, CSMA, pSSI, radius bone area (50%) and cortical bone density (50%) all increase with age during the growth period under normal conditions. Therefore all of the above variables would correlate significantly with a bone width measurement. The high r values confirm that the GPW is dependent on bone size and correlates well with several variables when measured at the distal radius.

The plots comparing GPW with chronological age and height each showed outliers in approximately the same areas (Fig 9.3B). Examination of the outliers revealed that those individuals with values below the 95% CI in the chronological age plot were more likely to be shorter for their age, and those individuals with values above the 95% CI were more likely to be taller for their age. It is interesting to note that 9 of the 15 females aged 18 to 20 years measured below 162cm (Fig 9.3B purple), which is below the mean height for an adult British female (Nettle, 2002) and 9 of the 15 females aged 18 to 20 years had GPW values below 20.0, which is outside the 95% CI. As mentioned previously, in UK females aged 18 years, a height of 162cm is below the 50<sup>th</sup> centile and a height of 150cm is below the 3<sup>rd</sup> centile (Freeman et al., 1995a). However only 5 of the 9 females in question measured both under 162cm and had a GPW below 20.0mm. This indicated that individuals who are short for their age are more likely to have a smaller GPW. This trend was confirmed when GPW was compared to height. Those individuals with values above the 95% CI were taller for their age, and those individuals below the 95% CI were shorter for their age. The outlier with a GPW of 39.6mm was a male aged 16 years measuring 188.4cm (Fig 9.3B red), which is well above the mean



height of British males (177.4 cm) (Nettle, 2002) and is above the 97<sup>th</sup> centile for UK males aged 16 years (Freeman et al., 1995a). These results were expected because chronological age and height are related; bones increase in length as individuals age, therefore the width of the GPW will increase in proportion with height and bone length. Indeed GPW compared to height showed a smaller 95% CI indicating that GPW width exhibits less variation when compared to height than age and is a tightly controlled process during growth. Discounting the purple outliers, the greatest variation in height is seen from ages 12 to 16 years when the pubertal growth spurt occurs, although these

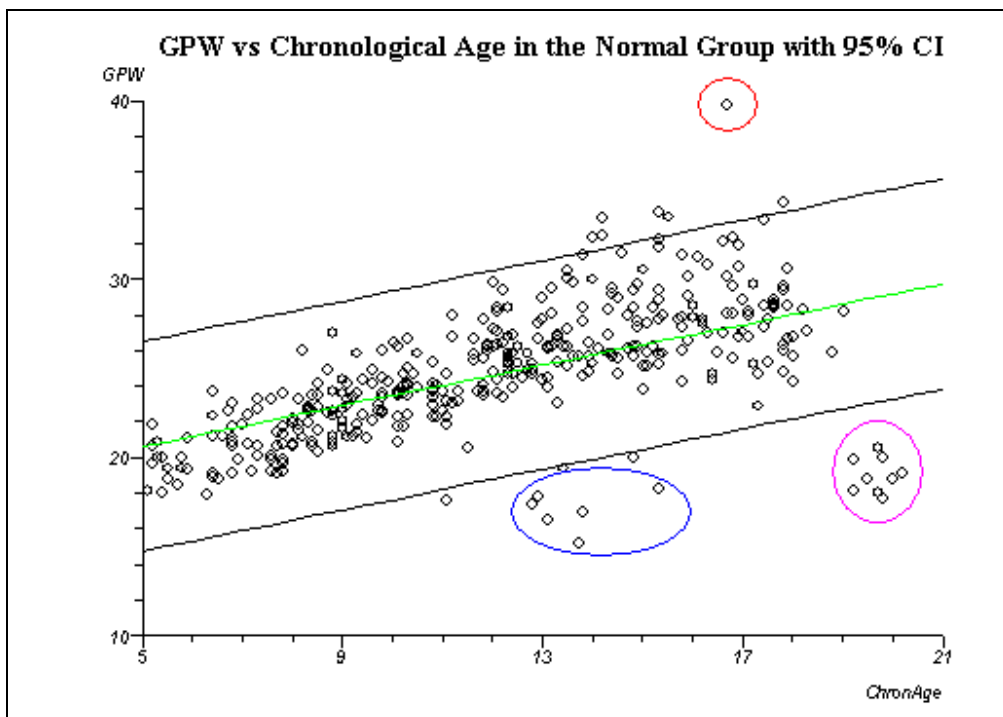


**Figure 9.3B: GPW compared to chronological age in the Normal group (baseline values) with outliers highlighted.**

outliers had a spread of Tanner stages ranging from 1 to 3 (Fig 9.3B blue). Although the blue outliers exhibited small GPWs, none of them exhibited abnormal MIs.

The Tukey's HSD test comparing mean MI or MW values between males and females revealed no significant differences between MI or MW values, but there was a significant difference between the male and female GPWs (males have a larger mean GPW than females). The Normal group is the only group with an age range that extends

through puberty and beyond, therefore it is not surprising that GPWs are larger in males as adult males generally have larger bones than females (Nieves et al., 2005). The combination of a difference in GPW values in males and females combined with no significant difference in MW values in males and females could have produced MI values outside the 95% CI but as stated above, this was not the case. This indicates that the proportions of the MW and GPW remain very similar in normal males and females.

It has already been shown that the MI, MW, and GPW increase with age, therefore it follows that they all increase with each Tanner stage. The MW and GPW exhibit the same statistically significant differences between Tanner groups indicating that the MW and GPW stay in proportion to each other during growth.

Stepwise multiple linear regressions were performed to discover the most significant variables to use in ANCOVA analyses for the MI, MW and GPW. However growth is not a linear process. As mentioned previously there is a growth spurt around puberty and then the increase plateaus in the teenage years. Linear analyses of growth may thus have limited utility. However non-linear growth analyses are complex requiring major statistical input and collaboration, which is beyond the purview of a PhD thesis (Roberts, personal communication). It was considered that multiple linear regressions were the most appropriate alternative.

The results of the MI multiple linear regression showed the most significant variables in the model were chronological age and toBMD (4%). Although MI does increase slightly with age, this increase is not significant. The  $r^2$  value and associated F-ratio for the MI model is much lower than those of the MW and GPW indicating that although the MI model is statistically significant, the MI model does not have the same predictive power as the MW and GPW models. The negative  $\beta$  value of toBMD is signifying that metaphyseal bone density at the 4% site decreases, or rather the rate of bone mineralisation slows around the pubertal growth spurt when longitudinal bone growth is proceeding more quickly than the mineralisation process. A non-linear growth analysis would be helpful in determining the intricacies of this relationship, as it is very probable the relationship is not linear. Therefore after adjusting for all the confounding variables, the MI common slope no longer shows as being significantly different from zero,

meaning that MI continued to eliminate bone size as a confounder when another variable was taken into account.

The models for MW and GPW were very similar. The significant variables in both of these models were height, chronological age, CSMA, pSSI and toBMD. The model for GPW had an additional significant variable; arm length. In the MW model, chronological age did not have a significant  $\beta$  value, but the other variables did. The model shows the same negative  $\beta$  value for toBMD, indicating a similar relationship as discussed previously in the MI model. In the GPW model, CSMA did not have a significant  $\beta$  value, but the other variables did. Again toBMD has a negative  $\beta$  value, but in this model chronological age does also. This is an interesting result as it has already been determined that GPW increases with age. This result may indicate that chronological age has a similar type of relationship to GPW as toBMD; as chronological age increases, the GPW expansion rate plateaus, at which point the relationship ceases to be linear. Although chronological age did not have a significant  $\beta$  value in the MW model, the fact that the  $\beta$  value was negative indicates the same trend as in the GPW model.

The ANCOVA analysis for MI indicated that once chronological age and toBMD were added as covariates, the regression lines for both males and females were neither significantly different from flat, nor significantly different from each other. This is to be expected as it has already been confirmed that the MI successfully eliminates the issue of bone size. However, though the ANCOVA analyses for MW and GPW did not show a significant difference between the male and female regression lines, the common slope showed a significant difference from flat. This could indicate that even after adjusting for the covariates, there is still a significant rise in MW and GPW as height increases or it could mean that there are variables that have not been accounted for that are causing the slope of the model to rise. Since the main predictor in each model is height, it is more likely that even after adjusting the model using the covariates, there is still a significant relationship between MW and height, and GPW and height.

The histograms illustrating the Z scores of males (Fig 8.3L) and females (Fig 8.3M) both showed a normal distribution. To create Z scores for each chronological age year (5.0 to 5.9 years, 6.0 to 6.9 years...etc.), would have been the ideal, however when the subjects

in the Normal group were divided by sex and chronological age year, there were not enough subjects to maintain a normal distribution within each group. Because Z scores require taking means and SD's, the separate groups from which the data belong must also be normally distributed. When a calculation of Z scores was attempted using this method (results not shown), a skewed Z score histogram resulted due to this statistical flaw. This could be remedied by examining more Normal subjects in the future and adding them to the dataset.

### **9.3.1 TW3 Bone-Age Assessments**

MI was plotted against TW3 bone-age and the results showed a similar growth curve to that seen when MI was plotted against chronological age. Although the r value and associated p value indicated TW3 bone-age and MI were significantly correlated, TW3 bone-age was not used in the multiple linear regressions or in the ANCOVA analyses because chronological age was a more appropriate variable to use in the Normal group. MW and GPW also showed a similar relationship to the plots against chronological age (results not shown).

### **9.3.2 40% and 60% MI and MW**

The 40% MI plotted against chronological age showed a similar growth curve to the MI plot, however the 60% MI plotted against chronological age showed an almost flat line (Fig 8.3.2B). This may indicate that the 60% MW, which is a component of the 60% MI was not a suitable place to measure in order to see a significant change over time because the 60% MW did not change enough with age. A more in depth study may indicate whether larger changes are easier to detect using the 40% MW/MI. The 40% (Fig 8.3.2C\*) and 60% (Fig 8.3.2D\*) MW plotted against chronological age showed that both increased as age increased. The outlier is the same outlier discussed in section 9.3 (red circle). This male measured 188.4 cm in height, therefore it was unsurprising to find that his radius was larger as a consequence. The next three plots showed the MI, 40% MI and 60% MI plotted against each other (Figs 8.3.2E\*, F\* and G\*). These plots

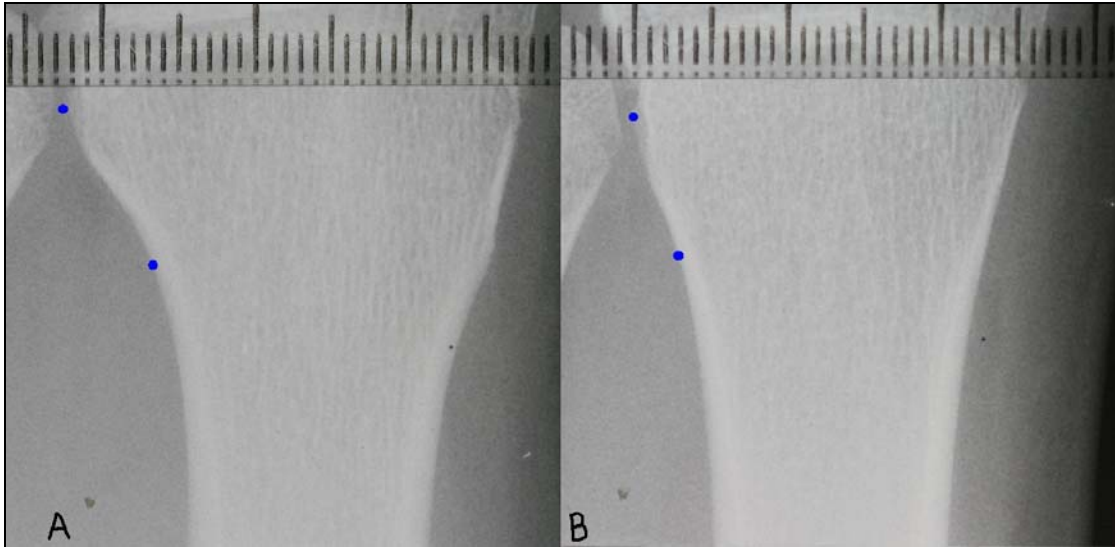


**Figure 9.3.2A:** Two radiographs of a distal radius; one showing a large change in bone width moving distally from the diaphysis towards the epiphysis (A) and the other showing a smaller change in bone width moving distally from the diaphysis towards the epiphysis (B). The blue dots have been placed to highlight the areas in question.

show that subjects with a low or high MI / 40% MI / 60% MI are likely to have low or high MI / 40% MI / 60% MI respectively (i.e. all MI's increase with age). The outliers are those subjects with significantly different indices in the two measurements, which indicated a significant shape change in the metaphysis as the measurement proceeded distally along the metaphysis (Fig 9.3.2A).

### 9.3.3 Longitudinal Analyses

Two plots were constructed plotting subjects with a visit at Tanner stage 3 against their visit at Tanner stage 4 (Fig 8.3.3A, B), the latter separating males and females. These plots confirm that subjects with a low/high Tanner stage 3 score were likely to have a low/high Tanner stage 4 score, respectively, and there was no statistically significant difference between males and females. However, 6 of the 21 subjects showed a lower MI value at Tanner stage 4 than at Tanner stage 3. Although it is possible that this is due to measurement error or a difference in hand positioning in each radiograph, it is also possible that the growth process in certain individuals causes the GPW to expand more relative to the expansion rate of the MW at near the end of the pubertal growth spurt. This process may then reverse itself by Tanner stage 5, but there are insufficient

subjects to examine this hypothesis. There were also insufficient subjects to construct a plot with Tanner stage 2 plotted against Tanner stage 3, or Tanner stage 3 plotted against Tanner stage 5. Although there were sufficient numbers to construct a plot with subjects that had a visit at Tanner pubertal stages 1 and 5, the purpose was to examine the effects of MI during puberty.

#### 9.4 Gymnast Group

The  $r$  values and associated  $p$  values indicated only one significant correlation; between MI and toBMD (4%);  $r = -0.383$ . This showed that although the correlation was significant, a maximum of only 14.7% of the variation in the MI could be explained by toBMD (4%). This result indicates a similar result to that in the Normal group and is expected because the MI is a ratio that attempts to measure the same area of a bone irrespective of bone size and bone width is a component of BMD ( $BMD = BMC / \text{bone width}$ ). The low  $r$  value confirms that the MI is successful at eliminating the issue of bone size when measured at the distal radius in the Gymnast group. The negative  $r$  value indicates that as MI increases, toBMD (4%) decreases. As in the Normal group, this relationship is describing the decrease in metaphyseal bone density at the 4% site, or rather the rate of bone mineralisation slowing around the pubertal growth spurt when longitudinal bone growth is proceeding more quickly than the mineralisation process.

Neither the plot comparing MI with chronological age (Fig 8.4A), nor the plot comparing MI with height (Fig 8.4B) showed typical growth curves as did the plots in the Normal group. This may be an indication that there were not enough subjects in the Gymnast group to illustrate such a curve in graphical form or it may indicate that the increased load bearing at the distal radius experienced by gymnasts causes the MI to remain stable throughout growth. The oldest gymnast subjects were aged 12 years at baseline, so it was not possible to determine if a change in MI exists beyond age 12 in the Gymnast group. Most of the values in Figs 8.4A and B were within the 95% CI but there were outliers. In the plot that compared MI with chronological age (Fig 9.4A), the outliers were both female aged 9.8 years (red) and 11.9 years (blue). The blue outlier was the tallest subject in the Gymnast group by 2.7 cm (144cm). The red outlier was also one of the tallest subjects measuring 139.4cm. However both of these heights were approximate to the 50<sup>th</sup> centile for their respective ages for UK females (Freeman et al., 1995a). As there was a statistically significant difference between the mean height of Gymnast group and the mean height of the Normal group adjusting for age (gymnasts were shorter), this confirms that shorter subjects are more likely to have a lower MI.

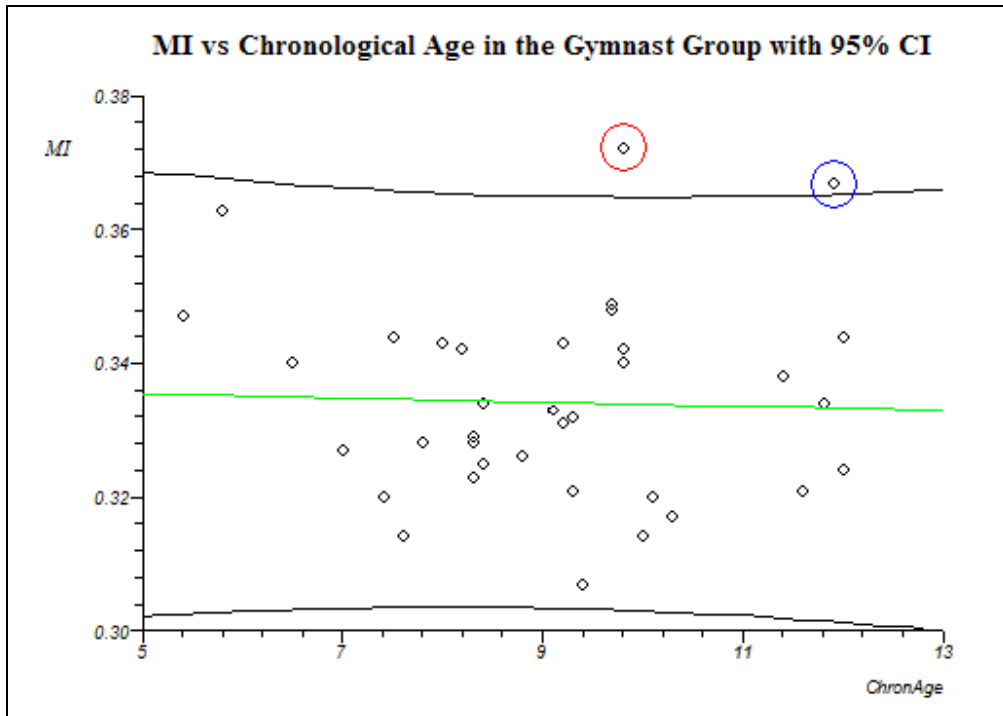


Figure 9.4A: MI compared to chronological age in the Gymnast group using baseline values with outliers highlighted.

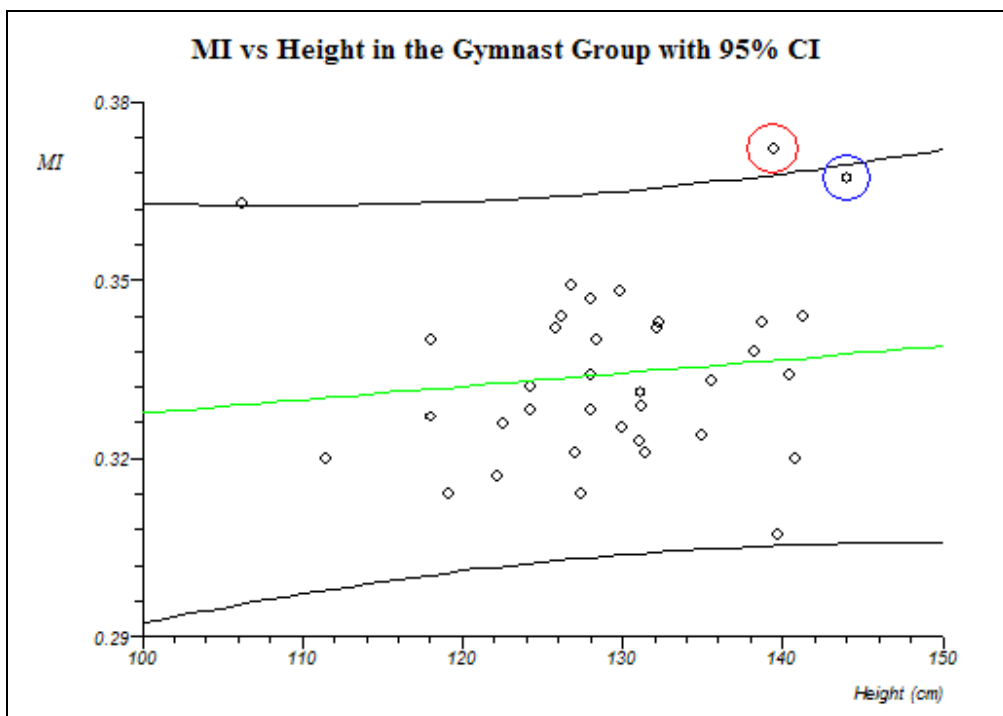


Figure 9.4B: MI compared to height (cm) in the Gymnast group using baseline values with outliers highlighted.



The higher MIs of the outliers indicate that their distal radii are less flared in shape, which corresponds more to the shape seen in Figure 9.3.2A, photo B. In the plot that compared MI with height (Fig 9.4B), the blue outlier is now within the 95% CI, but the red outlier remains outside the 95% CI. It is interesting to note that neither of these subjects would be outliers if they were included in the Normal plots; they simply have a less flared distal radius for their age and height than average for the Gymnast group, but not to the point that they show any other abnormalities. The plots comparing the regression lines of males and females showed no statistically significant difference between them when comparing MI with chronological age (Fig 8.3C\*) and MI with height (Fig 8.3D\*). Although the MI increased slightly as both chronological age and height increased, it was not a statistically significant rise. These results were similar to those seen in the Normal group and indicated that by using the MI (a ratio of 0.5MW/GPW), that the size of the bone was not significantly affecting the results. The low  $r$  value of toBMD (4%) and the fact that no other variables such as height or weight had a statistically significant correlation with the MI (which can be seen in the regression plots), confirmed that MI was independent of bone size when measured at the distal radius in the Gymnast group.

The  $r$  values and associated  $p$  values indicated significant correlations between MW and chronological age, TW3 bone-age, height, weight, Tanner stage, arm length, CSMA, pSSI, radius bone area (50%) and cortical bone density (50%). Like the Normal group, the significant  $r$  values were much higher than those seen in the MI correlations and ranged from 0.712 to 0.858, indicating that up to 73.6% of the variation in the MW could be explained by a single significant variable. This is expected because the MW is a width measurement, which will obviously be related to bone size; width increases as bone size increases. Variables such as height, weight, Tanner stage, arm length, CSMA, pSSI, radius bone area (50%) and cortical bone density (50%) all increase with age during the growth period under normal conditions. Therefore all of the above variables would correlate significantly with a bone width measurement. The high  $r$  values confirm that the MW is dependent on bone size and correlates well with several variables during growth when measured at the distal radius in the Gymnast group.

The plots comparing MW with chronological age (Fig 8.4E\*) and height (Fig 8.4F\*) showed no significant outliers. These results were expected for the same reasons they were expected in the Normal group, because chronological age and height are related; bones increase in length as individuals age, therefore the MW will increase in proportion with height/bone length. Indeed MW compared to height showed a smaller 95% CI indicating that MW width exhibits less variation when compared to height than age, and is a tightly controlled process during growth in the Gymnast group.

The  $r$  values and associated  $p$  values indicated significant correlations between GPW and chronological age, TW3 bone-age, height, weight, Tanner stage, arm length, CSMA, pSSI, radius bone area (50%) and cortical bone density (50%). The  $p$  value for toBMD ( $p = 0.047$ ) was just below the significance level. The  $r$  values ranged from 0.334 to 0.866, indicating that up to 75.0% of the variation in the GPW could be explained by a single significant variable. These  $r$  values are much higher than the  $r$  values obtained using the MI. This is expected because as with the MW, GPW is a width measurement, which will be related to bone size; width increases as bone size increases. Variables like height, weight, Tanner stage, arm length, CSMA, pSSI, radius bone area (50%) and cortical bone density (50%) all increase with age during the growth period under normal conditions. Therefore all of the above variables would correlate significantly with a bone width measurement. The high  $r$  values confirm that the GPW is dependent on bone size and remains in proportion with several variables when measured at the distal radius in the Gymnast group.

The plot comparing GPW with chronological age showed no outliers (Fig 8.4G\*). The plot comparing GPW with height showed two outliers, highlighted in red and blue (Fig 9.4C). An examination of the outliers revealed that the red outlier was one of the oldest subjects in the study at age 11.6 years, while the blue outlier was the youngest at age 5.4 years. Neither of the outliers exhibited abnormal MIs. This result was also similar to the corresponding result in the Normal group and indicated that individuals who are short for their age are more likely to have a smaller GPW. This was expected because chronological age and height are related; bones increase in length as individuals age, therefore the width of the GPW will increase in proportion with height/bone length.

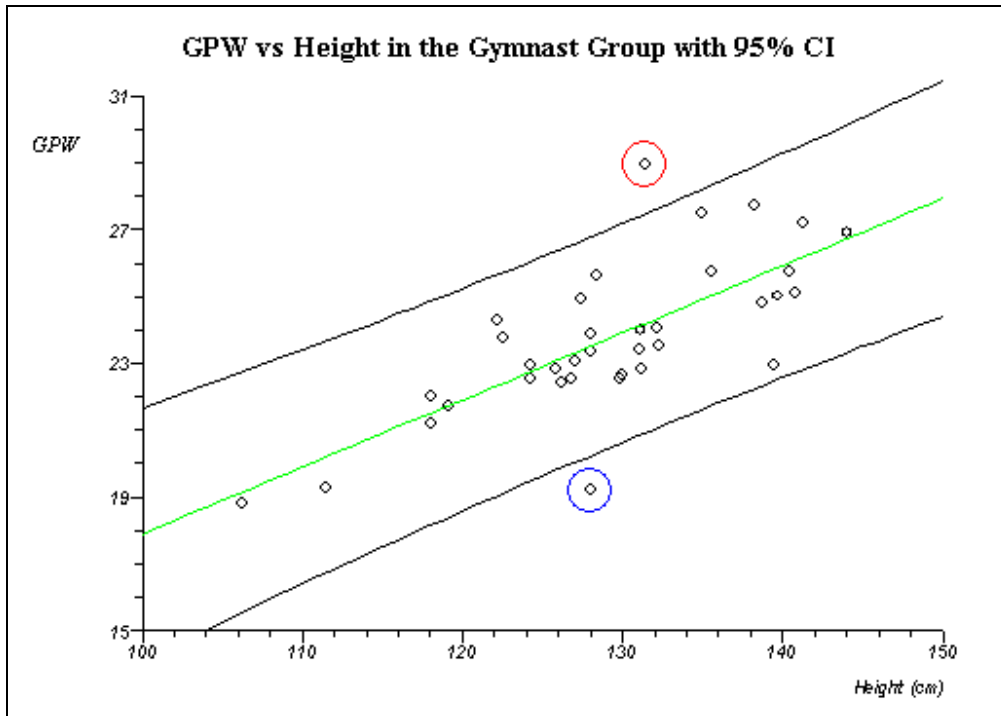


**Figure 9.4C: GPW (mm) compared to height in the Gymnast group (baseline values) with outliers highlighted.**

Indeed GPW compared to height showed a smaller 95% CI indicating that GPW width exhibits less variation when compared to height than age and is a tightly controlled process during growth.

The Tukey's HSD test comparing mean MI, MW and GPW values between males and females, revealed no significant differences between MI, MW or GPW values in the Gymnast group. This group does not have an age range that extends through puberty and beyond, therefore it is not surprising that there is no significant difference in GPW values in this group as there was in the Normal group. A previous study of the Normal group found that toBA (4%) was greater in males at all Tanner pubertal stages (Ashby, 2007). This was in contrast to the results of this study, which found that toBA (4%) was not significantly different between the sexes at Tanner stages 1, 2 or 3, was borderline significant at Tanner stage 4, and highly significantly different at Tanner stage 5. Using the results in this thesis, it is unsurprising that there was no significant difference in GPW values (as there was in the Normal group) in the Gymnast group as all baseline subjects were confirmed as Tanner stage 1. The difference seen between the Ashby study (Ashby, 2007) and this study may be due to the inclusion of over 100 more

subjects in Ashby's study than were available for this study. The results presented in this thesis show that the proportions of the MW and GPW remain very similar in Gymnast males and females.

Stepwise multiple linear regressions were performed to discover the most significant variables to use in ANCOVA analyses for the MI, MW and GPW. However growth is not a linear process. As mentioned previously there is a growth spurt around puberty and then the increase plateaus in the teenage years. So once again the use of a linear analysis, whilst not ideal, is presented as a pragmatic alternative to more complex non-linear methods.

The results of the MI multiple linear regression showed the only significant variable in the model was toBMD (4%). Although MI does increase slightly with age, this increase was not significant. The  $r^2$  value and associated F-ratio for the MI model is much lower than those of the MW and GPW indicating that although the MI model is statistically significant, the MI model does not have the same predictive power of the MW and GPW models. The negative  $\beta$  value of toBMD is signifying that metaphyseal bone density at the 4% site decreases, or rather the rate of bone mineralisation slows around the pubertal growth spurt when longitudinal bone growth is proceeding more quickly than the mineralisation process. A non-linear growth analysis would be helpful in determining the intricacies of this relationship, as it is very probable the relationship is not linear, as with the Normal group.

The models for MW and GPW are very similar. The significant variables in both of these models were height, chronological age, toBMD and pSSI. In the model for GPW, the significant variables were chronological age, arm length and pSSI. In the MW model all of the  $\beta$  values were significant and again toBMD showed a negative  $\beta$  value. In the GPW model, arm length did not quite achieve statistical significance, but the other variables did, showing that GPW can be predicted using chronological age and pSSI.

The ANCOVA analysis for MI indicated that once chronological age, toBMD and pSSI were added as covariates, the regression lines for both males and females were neither significantly different from flat, nor significantly different from each other. This is to be expected as it has already been confirmed that the MI successfully eliminates the issue

of bone size. However, though the ANCOVA analyses for MW and GPW did not show a significant difference between the male and female regression lines, the common slope showed a significant difference from flat. This could indicate that even after adjusting for the covariates, there is still a significant rise in MW and GPW over time or it could mean that there are variables that have not been accounted for that are causing the slope of the model to rise. Since the main predictors in each model were chronological age and pSSI, it is more likely that even after adjusting the model using the covariates, there is still a significant relationship between MW and chronological age/pSSI, and GPW and chronological age/pSSI.

Due to an insufficient number of subjects, it was not possible to calculate separate male and female Z scores, but overall the histogram illustrating the Z scores of males and females combined (Fig 8.4I) showed a normal distribution centred around the zero mean.

#### **9.4.1 Longitudinal Analysis**

Two plots were constructed plotting the first visit of a subject against their second visit (Fig 8.4.1A, B), the latter separating males and females. These plots confirm that those with a low/high first visit score were likely to have a low/high second visit score, respectively, and there was no statistically significant difference between males and females. However, 16 of the 32 subjects showed a lower MI value at the second visit than at the first visit. Although it is possible that this is due to measurement error or a difference in hand positioning in each radiograph, it is also possible that the growth process in certain individuals causes the GPW to expand more relative to the expansion rate of the MW at near the end of the pubertal growth spurt, especially considering the weight-bearing nature of a gymnast's distal radius. This process may then reverse itself to a certain degree by Tanner stage 5, but all subjects in this group were confirmed as Tanner stage 1 at baseline, therefore this hypothesis could not be tested.

## 9.5 NF1 Group

The  $r$  values indicated that none of variables were significantly correlated with MI, though the correlation between MI and toBMD (4%) was on the verge of achieving statistical significance;  $r = -0.513$  ( $p = 0.052$ ). This result is similar to the Gymnast group and is expected because the MI is a ratio that attempts to measure the same area of a bone irrespective of bone size. The low  $r$  values confirm that the MI is successful at eliminating the issue of bone size when measured at the distal radius. The correlation between MI and toBMD (4%) is so close to achieving statistical significance, it may indicate that the result could change if more subjects aged 6 to 9 were added to the study. Another explanation is that the oldest subjects in the NF1 study are aged 9.2 and were confirmed as Tanner stage 1 by self-assessment before being examined. Although the onset of puberty in these subjects had not yet begun, the negative  $r$  value (which indicates that as MI increases, toBMD (4%) decreases), may indicate the beginning of the decrease in metaphyseal bone density at the 4% site, or rather the rate of bone mineralisation slowing around the pubertal growth spurt when longitudinal bone growth is proceeding more quickly than the mineralisation process. Based on the results of other groups, statistical significance may have been achieved if older subjects had been included in the study.

Neither the plot comparing MI with chronological age (Fig 8.5A) nor the plot comparing MI with height (Fig 8.5B) showed typical growth curves like those in the Normal group. Although they both showed a slight rise in MI as age and height increased, the rise was not significant. This may be an indication that there were not enough subjects in the NF1 group to illustrate such a curve in graphical form. Also, the oldest NF1 subjects were aged 9.2 years, so it was not possible to determine if a change in MI existed beyond this age in the NF1 group, which could also account for the lack of a visible growth curve in the plot. Most of the values in Figs 8.5A and B were within the 95% CI, although there was one point that could be considered an outlier on the border of the 95% CI in Figure 8.5B.

The plots comparing the regression lines of males and females showed no statistically significant difference between them when comparing MI with chronological age (Fig 8.5C\*) and MI with height (Fig 8.5D\*). Although the MI increased slightly as both

chronological age and height increased, it was not a statistically significant rise. These results were similar to those seen in the Normal group and indicated that by using the MI (a ratio of 0.5MW/ GPW), that the size of the bone was not affecting the results. Although the r value of MI and toBMD (4%) was not particularly low, the fact that no other variables such as height or weight had a statistically significant correlation with the MI (which can be seen in the regression plots), confirms that MI is independent of bone size when measured at the distal radius in the NF1 group.

The r values and associated p values indicated significant correlations between MW and height, weight, arm length, CSMA, pSSI and radius bone area (50%). Like the Normal group, the significant r values were much higher than those seen in the MI correlations and ranged from 0.678 to 0.842, indicating that up to 70.9% of the variation in the MW could be explained by a single significant variable. This is expected because the MW is a width measurement, which will be related to bone size; width increases as bone size increases. Variables such as height, weight, arm length, CSMA, pSSI, radius bone area (50%) all increase with age during the growth period under normal conditions. Therefore all of the above variables would correlate significantly with a bone width measurement. The high r values confirm that the MW is dependent on bone size when measured at the distal radius in the NF1 group. MW and cortical bone density (50%) showed significant correlations in both the Normal and Gymnast groups, but did not in this group. This may indicate that the age range of the NF1 study prohibited a correlation and/or the total number of subjects in the study was not sufficient to determine a level of correlation.

The plot comparing MW with chronological age (Fig 8.5E\*) showed no significant outliers and the plot comparing MW with height (Fig 8.5F\*) showed only one outlier, which was not significantly outside the 95% CI. These results were expected for the same reasons they were expected in the Normal group, because chronological age and height are related; bones increase in length as individuals age, therefore the width of the MW will increase in proportion with height/bone length. Indeed MW compared to height showed a smaller 95% CI indicating that MW width exhibits less variation when compared to height than age, and is a tightly controlled process during growth in the NF1 group.

The r values and associated p values indicated significant correlations between GPW and height, weight, arm length and radius bone area (50%). However the p values for chronological age, CSMA, pSSI and radius cortical density (50%) were close to achieving statistical significance. The significant r values ranged from 0.590 to 0.677, indicating that up to 45.8% of the variation in the GPW could be explained by a single significant variable. These r values are much higher than the r values obtained using the MI. This is expected because as with the MW, GPW is a width measurement, which will be related to bone size; width increases as bone size increases. Variables like height, weight, arm length and radius bone area (50%) all increase with age during the growth period under normal conditions. Therefore all of the above variables would correlate significantly with a bone width measurement. Although the CSMA, pSSI and radius cortical density also increase during growth, there are too few subjects in this group to for these variables to achieve statistical significance, though there are strong trends. The high r values confirm that the GPW is dependent on bone size and remains in proportion with several variables when measured at the distal radius in the NF1 group.

The plots comparing GPW with chronological age (8.5G\*) and GPW with height (8.5H\*) showed no outliers, and a significant rise in GPW values as both age and height increase. This result was also similar to the Normal group and indicated that individuals who are short for their age are more likely to have a smaller GPW. This was expected because chronological age and height are related; bones increase in length as individuals age, therefore the width of the GPW will increase in proportion with height/bone length. Again GPW compared to height showed a smaller 95% CI indicating that GPW width exhibits less variation when compared to height than age and is a tightly controlled process during growth.

The Tukey's HSD test comparing mean MI or MW values between males and females, revealed no significant differences between MI, MW or GPW values in the NF1 group. As seen in the Gymnast group, this group does not have an age range that extends through puberty and beyond, therefore it is not surprising that there is no significant difference in GPW values in this group as there was in the Normal group. A previous study of the Normal group found that toBA (4%) was greater in males at all Tanner



pubertal stages (Ashby, 2007). This is in contrast to the results presented in this thesis, which found that toBA (4%) was not significantly different between the sexes at Tanner stages 1, 2 or 3, was borderline significant at Tanner stage 4, and highly significantly different at Tanner stage 5. Using the results obtained in this thesis, it is unsurprising that there was no significant difference in GPW values (as there was in the Normal group) in the NF1 group as all baseline subjects were confirmed as Tanner stage 1. As stated previously, this may be due to the larger number of subjects in the Ashby study (Ashby, 2007). The current results show that the proportions of the MW and GPW remain very similar in NF1 males and females.

Stepwise multiple linear regressions were performed to discover the most significant variables to use in ANCOVA analyses for the MI, MW and GPW; once again their use is affected by the pubertal growth spurt, but they provide a practical alternative to more complex non-linear models.

The results of the MI multiple linear regression showed the only significant variable in the model was toBMD (4%). The  $r^2$  value, F-ratio and associated p value for the second multiple linear regression ANOVA are interesting in that although the  $r^2$  value is high (0.839) and the F-ratio is  $> 1$  (2.314), the p value ( $p = 0.218$ ) indicates the model is not significant. Using the  $df$  (9,4) and an F-distribution critical values table for significance at  $p \leq 0.05$  (Hill and Lewicki, 2005), the critical F-value for a model exhibiting  $df = 9,4$  is 5.998. The F-value of the MI multiple linear regression ANOVA is less than the critical value, meaning there is a 21.8% chance of an F-ratio this size happening chance. Therefore this model is not a significantly better predictor of NF1 MI values than the mean, which again may be a result of too few subjects in the NF1 group. The negative  $\beta$  value of toBMD is signifying that metaphyseal bone density at the 4% site decreases, or rather the rate of bone mineralisation slows around the pubertal growth spurt when longitudinal bone growth is proceeding more quickly than the mineralisation process. A non-linear growth analysis would be helpful in determining the intricacies of this relationship, as it is very probable the relationship is not linear, which is a very similar result compared to the Normal group.

The model for MW showed the significant predictors to be pSSI and radius bone area (50%). The only significant variable in the GPW model was height. In the MW model

both of the  $\beta$  values were significant and both showed positive values, meaning that as they increased, the MW increased. In the GPW model, the  $\beta$  value for height was also positive and significant and meaning as height increased, GPW increased. These results show that MW and GPW are more easily predicted than MI in the NF1 group. The results also indicate that in the NF1 group, GPW remains more in proportion to height than the MW.

Section 8.5 stated that two multiple linear regressions were performed; one with toBMD (4%) as the only variable and one with toBMD (4%), chronological age, height, weight, arm length, CSMA, pSSI, radius bone area (50%) and cortical bone density (50%) as the variables. The ANCOVA analyses for MI indicated that both models produced similar results; the regression lines for both males and females were neither significantly different from flat, nor significantly different from each other. This is to be expected as it has already been confirmed that the MI successfully eliminates the issue of bone size. However, though the ANCOVA analyses for MW and GPW did not show a significant difference between the male and female regression lines, the common slope showed a significant difference from flat. This could suggest that even after adjusting for the covariates, there is still a significant rise in MW and GPW over time or it could mean that there are variables that have not been accounted for that are causing the slope of the model to rise. Since the main predictor in each model differs, therefore it is likely that even after adjusting the model using the covariates, there is still a significant relationship between MW and pSSI, and GPW and height.

When the result of the Mann-Whitney U-test comparing MI between NF1 males and females, was compared to the results of an unpaired t-test, the results of which were not presented in the results section; ( $p = 0.110$ ) with a 95% CI of -0.005 to 0.041, the unpaired t-test indicated that the mean MIs were not significantly different. The 95% CI of the Mann-Whitney U-test was 0 to 0.04. Note that the zero lower CI was a marginal result and it was possible the null hypothesis would not have been accepted if the unpaired t-test had been used. The significant difference between the mean NF1 male and female MIs differs from the Normal group result. Considering that the age range of this study did not include pubertal ages, it is likely that this difference is due to an insufficient number of subjects. Because of the limited number of subjects, it was not

possible to calculate separate male and female  $Z$  scores, but overall the histogram illustrating the  $Z$  scores of males and females combined (Fig 8.4I) showed a normal distribution centred around the zero mean, with no evidence of non-normality.

## 9.6 CDGP Group

The  $r$  values and associated  $p$  values indicated only one significant correlation; between MI and TW3 bone-age;  $r = 0.242$  ( $p = 0.012$ ). All 108 subjects had baseline bone-age assessments, and if applicable bone-age assessments were performed for subsequent examinations. However, only 25 subjects had height and weight values available to the author. The  $r$  value for the comparison of MI and TW3 bone-age was not significant when only 25 subjects were used (results not shown), which suggests that had there been more height and weight values available to the author, significant correlations between MI and height and/or MI and weight may have been found. The  $r$  value indicated that although the correlation was significant, only 5.9% of the variation in the MI could be explained by TW3 bone-age. This result indicated a similar result to the Normal group and was expected because the MI is a ratio that attempts to measure the same area of a bone irrespective of bone size. The low  $r$  value confirms that the MI is successful at eliminating the issue of bone size when measured at the distal radius in this group. As less than 10 subjects had pQCT data available to the author, the results were not analysed, however it would be reasonable to assume that there would be other significant correlations in this group, such as a correlation between MI and toBMD (4%), which was seen in the other groups (borderline in the NF1 group).

The plot comparing MI with TW3 bone-age (Fig 8.6A) showed a typical growth curve like that seen in the Normal group where MI was compared to chronological age. There were three outliers, but because of the lack of height values for this group, it was not possible to determine whether these three subjects were very tall for their age (upper outliers) or very short for their age (lower outlier). The plot comparing MI with height (Fig 8.6B) did not show a typical growth curve like those in the Normal group, but this is most likely due to an insufficient number of subjects. Nevertheless the rise was borderline significant. This result is to be expected as the CDGP group is essentially normal but for the retardation in growth and the delay of puberty. It is interesting to note that all three outliers would also be outliers if they were included in the Normal plots; the upper outliers may simply have a less flared distal radius for their age and height than average, and the lower outlier may simply have a more flared distal radius

for their age and height than average, but not to the point of significant abnormality. Though, as previously stated, height values for the outliers were not available.

The plots comparing the regression lines of males and females showed no statistically significant difference between them when comparing MI with chronological age (Fig 8.6C\*). However, the plot comparing MI with height (Fig 8.6D\*) did show a significant difference ( $p = 0.050$ ), which does not correlate well with the results of the other groups. Since this analysis only included 25 subjects, it is likely that the difference is not actually significant. A non-parametric linear regression may have produced a different result, especially in a group of this size, but that test does not allow for the selection of identifying variables (in this case male and female).

The  $r$  values and associated  $p$  values indicated significant correlations between MW and chronological age, TW3 bone-age, height and weight. Like the Normal group, the significant  $r$  values were much higher than those seen in the MI correlations and ranged from 0.630 to 0.785, indicating that up to 61.6% of the variation in the MW could be explained by a single significant variable. This is expected, even in the CDGP group, due to reasons discussed in the results of the other groups. Therefore all of the above variables would correlate significantly with a bone width measurement. The high  $r$  values confirm that the MW is dependent on bone size and remains in proportion with several variables when measured at the distal radius in the CDGP group.

The plot comparing MW with TW3 bone-age (Fig 8.6E\*) showed one outlier. No height or weight values were available for this subject but based on outliers in other groups, it is possible the subject is tall for his age. The outlier showed the largest MW of all 108 subjects and was also an outlier in the plot comparing MI with TW3 bone-age (Fig 8.6A) with an abnormal MI of 0.396. This outlier is discussed further in the GPW comparisons. The plot comparing MW with height (Fig 8.6F\*) showed no significant outliers. These results were expected for the same reasons they were expected in the Normal group, because chronological age and height are related; bones increase in length as individuals age, therefore the width of the MW will increase in proportion with height/bone length. Indeed MW compared to height showed a smaller 95% CI indicating that MW width exhibits less variation when compared to height than age, and is a tightly controlled process during growth in the CDGP group.

The  $r$  values and associated  $p$  values indicated significant correlations between GPW and TW3 bone-age, height and weight. The  $r$  values ranged from 0.515 to 0.819, indicating that up to 67.1% of the variation in the GPW could be explained by a single significant variable. These  $r$  values are much higher than the  $r$  values obtained using the MI. This is expected because as with the MW, GPW is a width measurement, which will be related to bone size; width increases as bone size increases. Variables like TW3 bone-age, height and weight all increase with age during the growth period under normal conditions and under CDGP conditions. Therefore all of the above variables would correlate significantly with a bone width measurement. The high  $r$  values confirm that the GPW is dependent on bone size and correlates with several variables when measured at the distal radius in the CDGP group.

The plots comparing GPW with TW3 bone-age (Fig 8.6G\*) and height (Fig 8.6H\*) both showed one outlier each. As mentioned previously, there was no height information for most of the subjects in this group, but it possible that the outlier in Fig 8.6G\* was tall for his age. The outlier in Figure 8.6H\* was the youngest (aged 7.7 years with a TW3 bone-age of 7 years) of the 25 subjects with height values by 1.5 chronological years. This confirms that outliers are often due to subjects being either very tall or very short for their age, which is also seen in the Normal group. The outlier in Figure 8.6H\* did not show an abnormal MI but the outlier in Figure 8.6G\* did show an abnormal MI and was also one of the outliers in the plot comparing TW3 bone-age to MI (Fig 8.6A). This may indicate the presence of another condition that alters the metaphyseal modelling. Although individual case notes were not available to the author, some of the concomitant diseases in this group included asthma (including subjects not taking and taking steroids), Hodgkin's lymphoma, congestive heart disease and renal dialysis. These conditions combined with CDGP and potential bone modelling interference caused by medications may be responsible for this outlier. In other groups, GPW compared to height showed smaller 95% CI's but in this group, the 95% CI for GPW compared to height was large. This is most likely due to fewer numbers of subjects with height values available.

The Tukey's HSD test comparing mean MI or MW values between males and females, revealed no significant differences between MI, MW or GPW values in the CDGP

group. Although this group does not have an age range that extends through puberty, the nature of CDGP means that chronological age and Tanner stage do not correlate as they would in normal subjects. A previous study of the Normal group found that toBA (4%) was greater in males at all Tanner pubertal stages (Ashby, 2007). This was in contrast to the results of the current study, which found that toBA (4%): was not significantly different between the sexes at Tanner stages 1, 2 or 3; was borderline significant at Tanner stage 4; and was highly significantly different at Tanner stage 5. Tanner stages for the CDGP group were not available to the author, but it would be reasonable to assume that most if not all of the subjects in this group had yet to reach Tanner stage 4 to 5. Therefore it is unsurprising that there is no significant difference in GPW values in this group as there was in the Normal group. The difference seen between the Ashby study (Ashby, 2007) and the current study may once again be due to the inclusion of more Normal subjects in Ashby's study. The current results show that the proportions of the MW and GPW remain very similar in CDGP males and females.

Stepwise multiple linear regressions were performed to discover the most significant variables to use in ANCOVA analyses for the MI, MW and GPW. However, once again, it is important to note that while linear analyses have their limitations in non-linear situations such as growth, they have been presented as a pragmatic alternative.

The results of the MI multiple linear regression showed that none of the 3 available variables were significant leading to an insignificant overall model. Again the  $r^2$  values and associated F-ratio for the MI model were much lower than those of the MW and GPW indicating that the MI model does not have the same predictive power of the MW and GPW models and is no better than using the mean as a predictor. However, this most likely had to do with the use of only 25 subject values in the model. Although TW3 bone-age had 108 baseline values, height and weight only had 25 values each. Therefore during a multiple linear regression, the predictive power of the other 83 TW3 bone-age values was lost, as it was a significant predictor when all 108 values were used in a simple linear regression.

The models for MW and GPW are very similar. The significant variable in both the MW and GPW models was TW3 bone-age. Both models had high  $r^2$  values, high F-ratios and high  $\beta$  values all with highly significant p values. Although height was often a significant predictor for MW and GPW models in other groups, there were only 25 subjects with height values available in this group, therefore the relationship may be even more significant than the borderline result seen in Chapter 8, by obtaining more height values for this group.

The ANCOVA analysis for MI indicated that the common slope was not significantly different from zero and the regression lines for both males and females were neither significantly different from flat, nor significantly different from each other. This is to be expected as it has already been confirmed that the MI successfully eliminates the issue of bone size. This result agrees with the MI ANCOVAs for all other groups. Because the F-ratio  $< 1$  and the p value is not significant in the multiple linear regression with MI as the dependent variable, this model is no better than using the mean as a model. If the question was; what would the MI value be if the TW3 bone-age was  $x$ , the simplest answer would be to quote the mean MI value. However, using the mean as a model would give the same answer no matter what TW3 bone-age ( $x$ ) was being used. Therefore this is clearly not an ideal model. However there were no pQCT data available for this group to add more independent variables to the model; the use of the TW3 bone-age, height and weight in 25 baseline cases was all that was available to the author, despite them not contributing to the variation in MI values. Therefore the ability to see any significant differences both in the common slope and between males and females using an ANCOVA analysis would be statistically very unlikely. Indeed that is the result of the ANCOVA analysis, which is a similar result to the other groups. Although it is likely that in reality the common slope isn't significantly different from zero (due to the nature of the MI), even if it were, it is likely that this dataset would probably not have sufficient subject numbers, or the other variables needed, to detect a difference.

However, though the ANCOVA analyses for MW and GPW did not show a significant difference between the male and female regression lines, the common slopes of both showed a significant difference from zero (a flat line). This could indicate that even



after adjusting for the covariates, there is still a significant rise in MW and GPW over time or it could mean that there are variables that have not been accounted for that are causing the slope of the model to rise. Since the main predictor in each model is TW3 bone-age, it is more likely that even after adjusting the model using the covariates, there is still a significant relationship between MW and TW3 bone-age, and GPW and TW3 bone-age.

Due to an insufficient number of subjects, it was not possible to calculate separate male and female Z scores, but overall the histogram illustrating the Z scores of males and females combined (Fig 8.4I) showed a normal distribution centred around the zero mean, which was expected and agreed with all other groups.

#### **9.6.1 Longitudinal Analysis**

Two plots were constructed plotting the first visit of a subject against their second visit approximately 18 months apart (Fig 8.6.1A, B), the latter separating males and females. These plots confirm that those with a low/high first visit score were likely to have a low/high second visit score, respectively, and there was no statistically significant difference between males and females. However, 7 of the 15 subjects showed a lower MI value at the second visit than at the first visit, which is a very similar proportion to the results seen in the Gymnast group. Although it is possible that this is due to measurement error or a difference in hand positioning in each radiograph, it is also possible that the growth process in certain individuals causes the GPW to expand more relative to the expansion rate of the MW at near the end of the pubertal growth spurt, particularly given the extensive list of other diseases present in this group. The process may then reverse itself to a certain degree by Tanner stage 5, but none of the subjects had Tanner stages available to the author, so this hypothesis could not be tested.

## 9.7 Comparison of All Groups

Table 8.7A showed the means of the MI, MW and GPW of all groups. Although the Normal group showed the highest mean MI and the Gymnast group showed the lowest mean MI, we must consider whether the difference was significant. The Gymnast group showed the highest mean MW and GPW, while the NF1 group showed the lowest mean MW and GPW, but again were these differences significant? This study is not as concerned with the differences between all the groups as it is with the differences of each case group compared to Normal. Therefore the means were compared to the Normal group adjusted for chronological age (TW3 bone-age for the CDGP group). This required three Dunnett's t-tests, one for MI, one for MW and one for GPW. Although not mentioned in Chapter 7, there were three other tests used to compare the groups: Bonferroni's test, Gabriel's procedure and Hochberg's GT2 test. All three tests are used for multiple comparisons of groups, but under different circumstances. When the number of comparisons is small, Bonferroni's test has more power and also controls well for type I errors, but it lacks overall statistical power, and while Gabriels's procedure has greater power when sample sizes are slightly different, Hochberg's GT2 test is advised if sample sizes are very different (Field, 2005). The results of each of these tests were very similar to the Dunnett's t tests, but because Dunnett's t is the only test that compares each group to a chosen control group, this test was the most appropriate for the current study and the results of the other tests were not reported. It is interesting to note that despite the fact that each test was designed to be used under different circumstances, each result in this case was similar with the Dunnett's t test for that variable.

There was only one significant MI difference between the groups, and that was between the Gymnast and Normal groups. However, Table 8.7A also illustrates a very important consideration; the mean heights of each group are all statistically different (shorter) when compared to the Normal group. Therefore each baseline Gymnast subject was matched for height and a paired t-test confirmed there was no statistically significant difference between the mean heights of these groups. However another paired t-test confirmed there was still a significant difference between the mean MIs of these groups. It was not possible to match the groups for chronological age and height. The main

predictor for the MI models was toBMD (4%). Therefore it is possible there would still be a significant difference in MI between these groups even if they could be matched for both chronological age and height. However there were an insufficient number of subjects that could be matched for both chronological age and height for this hypothesis to be tested. This confirmed that the MI is not dependent on height when comparing differences between groups. The grouped linear regression for MI (Fig 8.7D) showed that the Gymnast group had the slope with the highest gradient compared to the other groups, but the rise was neither significantly different from flat, nor significantly different from any of the other groups. This indicates that although the mean MI of Gymnasts was significantly different from Normal, this difference was not significant over the age range of 5.9 to 9.9 years.

The Dunnett's t-test for MW showed no significant differences between the groups, indicating that MW is a tightly controlled area during growth under normal conditions, under the abnormal loading conditions of gymnasts and under the disease conditions of NF1 and CDGP. The grouped linear regression (Fig 8.7E) was in agreement as the regression showed no significant differences between the groups.

The Dunnett's t-test for GPW showed one significant difference; between the Gymnast group and the Normal group (Gymnasts with a larger mean GPW). As with the MI comparisons, the same Normal controls and Gymnast cases were used to determine whether there would still be a significant difference if the groups were matched for height and there was still a significant difference. This result is expected because as stated previously, there was no significant difference in the MW between the Gymnast group and the Normal group, therefore the GPW would have to be significantly different to produce the significantly different results in the MI between these groups. The grouped linear regression for GPW (Fig 8.7F) showed that the Gymnast group had the slope with the highest gradient compared to the other groups, but although the rise was significantly different from flat, it was not significantly different from any of the other groups. This indicates that although the mean GPW of Gymnasts was significantly different from Normal, this difference was not significant over the adjusted age range.

## 9.8 DXA Bone-Age Study

The study confirmed good agreement between GP bone-ageing using DXA images and radiographs, indicating the two methods are close to being interchangeable in the age group of children included in this study. The  $r^2$  value of 0.986 ( $p < 0.001$ ) is very close to the perfect fit value of 1.0, implying that there is very little (<2%) unexplained variation in this linear model, which compares the two methods. There were two subjects outside the 95% prediction interval, one showing a +2 year difference in age (radiograph bone-age – DXA bone-age) and one showing a -2 year difference. There was no technical or clinical reason for these outliers to be excluded. On review, the explanation for the discrepancies were as follows: in one subject there was partial fusion of the epiphyses of the distal phalanges on the radiograph, which was not apparent on the DXA image, in which the epiphyses of the phalanges appeared unfused, leading to a two year underestimation of bone-age. In the second case, part of the distal radius epiphysis appeared unfused on the radiograph, but completely fused on the DXA image, leading to a two year overestimate of bone-age. Clinically, if there is less than a two year difference between chronological age and bone-age, it is still considered within normal range because of different rates of maturation. If the difference is beyond two years then further clinical investigation is required. In both outliers, the bone-age made from the DXA image was closer to the chronological age than that made from the radiograph. A limitation of the study is that there is no way of predicting in which DXA images the bone-age assessment will fail, however this was only 2% of the total in this study. A pragmatic solution would be that if there was a discrepancy of more than 2 years between DXA bone-age and chronological age, then a hand radiograph would be indicated to confirm bone-age. With regard to the 2 subjects that had a DXA bone-age within 2 years of their chronological age, but a radiograph bone-age >2 years apart from their chronological age, further bone-age assessments by another assessor and perhaps further clinical investigation are indicated.

An earlier study, also using DXA images obtained on an Hologic QDR 4500 DXA scanner, but with a different software version, found that bone-age assessment using the GP method was not reliable in children under 12 years (Ashby et al., 2002b). This was attributed to limited DXA spatial resolution causing partial volume averaging errors in

the smaller bones (Ashby et al., 2002b), resulting in the image being of insufficient quality for determining bone-age in younger subjects. In the current study, using updated DXA software, the CV of bone-ageing from DXA images was not significantly different from radiographs, which is most likely related to improved DXA image quality. The current study encountered no difficulties related to performing bone-age assessments on children less than 12 years of age. There may also be a difference in the findings between the current and previous study (Ashby et al., 2002b), due to different bone-age assessors performing the measurements. Another limitation of the current study is that there were fewer subjects aged 6-7 years (8 in total) than in the other age groups; statistically it would have been preferable if more subjects aged 6-7 years could have been recruited. Although the previous study (Ashby et al., 2002b) and the current study were both performed at the same institution, the subject groups were different.

The current results are in agreement with a previous study of 50 normal children (aged 5-18 years) and 10 with previous pituitary deficiencies (aged 8-20 years) (Pludowski et al., 2004). The precision errors for duplicate assessment were low; for radiographs <1.0% and DXA <0.9%. There was also good concordance in bone-ages assessed by both techniques with the same age being determined in 73.3% and in the remainder the discrepancies were no greater than 6 months. There was a strong correlation between bone-age results ( $r = 0.998$ ;  $r^2 = 0.996$ ;  $p < 0.001$ ). However, that study used a GE Lunar Expert (Milwaukee, WI, USA) DXA scanner with a spatial resolution of 0.83mm (Thorpe and Steel, 1999) and a significantly higher dose of ionising radiation (x10 or more) than the current fan beam DXA scanners in common use, such as that used in our study, and is no longer manufactured (Steel et al., 1998). As the resolution of DXA scanners improves in the future, it would be informative to conduct more studies of this type with the aim of acquiring complete interchangeability between radiographs and DXA images for the purposes of bone-ageing.

In general, the assessor found that determining bone-age using DXA took more time on average than when using radiographs due to the reduced spatial resolution of the DXA images. Determining bone-age from the DXA images often required zooming in and out to obtain the optimum magnification to view the different maturity markers, whereas the maturity markers on the radiographs were for the most part easier to assess due to the

higher resolution. However, there was no one bone or maturity marker that was constantly more difficult to assess. The bones of the younger subjects, including the ossification centres, were no more difficult to assess than those of the older subjects.

## **9.9 Challenges**

The main challenge faced in this thesis was the retrospective nature of the study. Study group sizes and variables were limited to what was available at the time. In the case of the Gymnast group, although there were enough subjects to ensure an overall normal distribution, once the groups were subdivided into male and female, this ceased to be true. In the case of the NF1 group, the group as a whole did not have enough subjects to ensure an overall normal distribution, which continued to be the case when the group was broken down into male and female categories. Although the CDGP had more than a sufficient number of subjects to ensure an overall normal distribution, there was a significant majority of male subjects to female subjects (89:19), meaning that the female category did not have a sufficient number of subjects to ensure a normal distribution outright. This was a particular challenge when calculating the Z scores. Z scores rely on means and SDs, which by definition requires the variable in question to be normally distributed. Therefore the significance of some of the relationships found in this study is in question due to the lack of subjects.

Another challenge was the method of digitising the films, with a calibration marker, so that a computerised MI measurement technique could be used. This will not be the case in future studies using digitally captured images stored using PACS. Any future study using films would benefit by using a flatbed radiograph scanner, which was not available for the current study. Also, the calibration markers used in this thesis are not strictly necessary if MI is the only assessment being performed, due to the MI being a ratio. This would allow the MI assessment to be performed directly from a digital image with no other equipment needed. However if the values of the GPWs and MWs are also of interest, this would either require the X-ray to be performed with a calibration marker, or at a specific focal length and settings of which the calibration had already been set and was determined to be repeatable.

The third challenge was the use of the computer-assisted measurement technique. It required the images to be at a certain orientation to be analysed. This eliminated the use of the VIDAR radiograph digitiser. In future studies using digital images, this could be overcome in 2 ways: either the computer-assisted measurement technique could be adapted to perform the measurements in any orientation, or the orientation of the limb being imaged could be taken into account by the radiographer before being taken. In future studies that are retrospective in nature, and are required to use hard-copy films, a flatbed scanner, which is a relatively inexpensive piece of equipment, could be used to overcome the orientation issue, as films can be placed in scanner at any orientation needed.

In retrospect (discussed briefly in section 6.8.2), one possible explanation for the phenomenon of increased file sizes experienced in Adobe Photoshop during image rotation, was that Photoshop was creating a background layer around the edges of the original image to avoid deleting part of the original image or altering the scale of the original image during the rotation process. Though it was suggested during the image analysis phase of the current study that this process could have had undetermined effects on the image, that does not appear to be the case. However, if the image were to be distorted in any way, then it is probable that the entire image would be distorted to the same degree, meaning the calibration marker in every image would also be distorted to the same degree. Therefore neither the absolute values of the GPW and MW, nor the MI (as a ratio), would have been affected.

The main challenge for the DXA bone-age study was placement of the hand on the bed of a full-body DXA scanner. Scanning of the hand and forearm on a body scanner for bone-age assessment is not standard practice. Some images were unusable and therefore excluded from the study due to incorrect placement resulting in the distal phalanges being excluded from the resulting image or the radius and ulna being excluded. Making radiographers aware of the requirements for bone-age assessment or having an appropriate researcher present while DXA scans are being performed is recommended.

## **9.10 Limitations**

There are two main limitations in this study: its retrospective nature and the subsequent restrictions of the statistical analysis, which have been discussed in section 9.9.

The retrospective nature of this study meant that the author had no control over the number of subjects that were recruited for any of the original study groups or the methods that were used. Although the Normal group consisted of hundreds of subjects, the Gymnast group only consisted of 36 subjects. Both the CDGP and NF1 subjects were ongoing and although there were over 100 CDGP subjects that had hand radiographs at the time of this examination, fewer than 5 subjects had had pQCT scans. This meant that during the statistical analysis comparing the Normal and CDGP groups, no pQCT measures could be used as covariates. Also, due to NHS procedures, many of the case notes of the CDGP group were held offsite and inaccessible to the author. Therefore although height was used as a covariate when comparing the Normal and CDGP groups, only 25 of the 108 subjects were used for that analysis because information on height, weight and other chronic conditions of the CDGP group were held offsite and not accessible to the author. Of those 25 subjects, some of the chronic conditions they were suffering from included several types of cancer, diabetes and asthma. This will no doubt have affected the statistical analysis of this group. The NF1 study had 29 subjects recruited at the time of this examination, however only 17 subjects were suitable for the MI examination, which is a low number for statistical analysis.

Some of the statistical analysis techniques used in this study, such as multiple linear regressions and ANCOVA, have limitations due to their linear nature. This limitation has been discussed at length in previous sections of this chapter. There is also no doubt, as in most experiments, a high amount of variation in the statistical models is due to unknown variables and variables that were not measured or able to be taken into account.



### **9.11 Comparisons with the Literature**

It has already been shown that stress in the wrist area as a result of athletic activity, such as that seen in gymnasts, will result in growth plate widening (Carter et al., 1988, Fliegel, 1986, Shih et al., 1995), which confirm the results found in this thesis. In an experiment using rabbits, one study noted an increase in the thickness of the zone of cartilage transformation (see Fig 2.5), where chondrocytes hypertrophy, using histological and microscopy techniques (Trueta and Amato, 1960), which showed similarities to patterns seen in metaphyseal fracture (Laor and Jaramillo, 1993). Horizontal metaphyseal fractures and bruises in radial metaphyseal bone also indicated that these rapidly growing areas are susceptible to trauma (Alexander, 1976, Leveau and Bernhardt, 1984). It has been suggested that metaphyseal injuries may be more important with regard to the pathophysiology of a widening growth plate, than any other factor (Shih et al., 1995). The increase in the GPW appears to be the bone's attempt to compensate for the large amount of stress and loading being experienced in gymnastics. A lower MI in the distal radius can be found in both certain disease states, as discussed in Chapter 4, but also under stress and loading conditions such as gymnastics. The results of this thesis confirm that the resulting lower MI in the Gymnast group is due to a widening of GPW and not the reduction of the MW. However, certain conditions, such as many of those discussed in Chapter 4, appear to exhibit both a widening of the GPW and a reduction of the MW.

Therefore in addition to being a tool for monitoring inwaisting, the conclusion that a higher MI in long bones is advantageous to a certain degree, seems appropriate. Where MW has been reduced in addition to a widening of the GPW, a higher MI could be advantageous in terms of resisting fracture at the metaphysis/diaphysis junction (thinner bones are more likely to fracture), as long as it does not become too high as seen in the subject with bisphosphonate induced osteopetrosis (Whyte et al., 2003, Ward et al., 2005a). A follow-up case study on the patient from the 2003 Whyte paper (Whyte et al., 2008) showed that even several years after the intravenous pamidronate therapy was halted, the abnormal metaphyses remained. Figures 9.12A and B show the abnormal sclerotic metaphyses of the distal radius and ulna. Although the author could not measure the absolute MW or GPW values for this radiograph due to the lack of a

calibration marker, the MI is a proportion and will stay the same despite magnification or reduction in size of the image. The MI for Figure 9.12A is abnormally high (0.433), however when pamidronate therapy ceased and normal modelling was allowed to resume, the MI for Figure 9.12B reduced to 0.306.

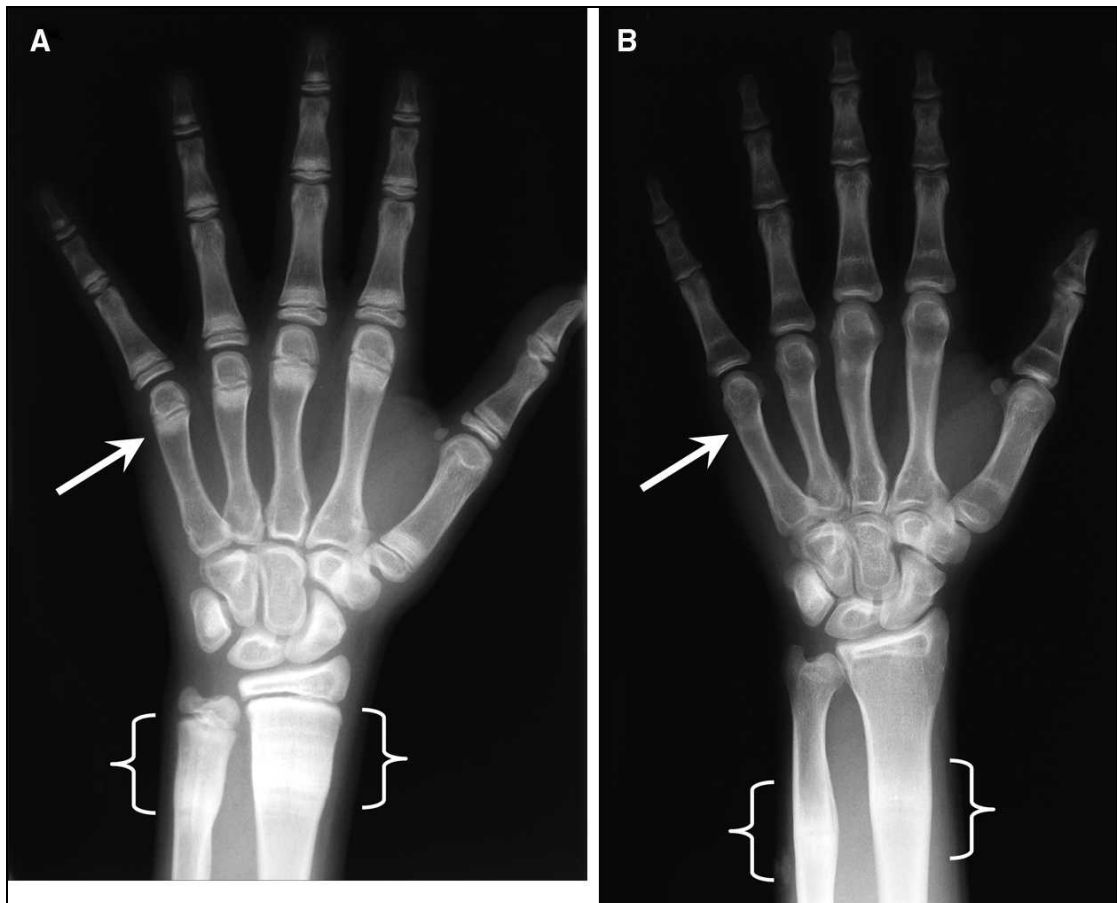


**Figure 9.12A and B: Progression of abnormal modelling in distal radius and ulna in bisphosphonate induced osteopetrosis. A: Abnormal distal radius and ulna (age 12 years – approximately 6 months after pamidronate therapy had ceased); B: longitudinal growth of the distal radius and ulna metaphyses showing normal modelling occurring after the cessation of pamidronate, but the abnormal sclerotic bone has ‘migrated’ to the diaphyses (age 17 years). Reproduced with permission and copyright © of the JBMR (Whyte et al., 2008).**

Both of these MI values are outside the  $\pm 2$  SD range, but it should be noted that the skeletal pain and idiopathic thrombocytopenia and hyperphosphatasemia were still continuing underlying conditions (Whyte et al., 2008).

Oral bisphosphonates are regularly, though not exclusively used to treat children now and instead of the discrete bands of hypermineralised bone seen at the growth plate, oral

bisphosphonates show much a broader and more uniform hypermineralised area (DiMeglio and Peacock, 2006). The MI assessment may be useful in monitoring more subtle metaphyseal changes during treatment with bisphosphonates or provide a useful monitoring tool for other diseases such as those mentioned in Chapter 4.

The highest distal radius MI result within the Normal group, including all longitudinal results, is 0.406 and the lowest is 0.292 with a mean of 0.351. This indicates that even with increasing age, the MI for normal children at the distal radius does not go beyond a range of 0.111, and that the growth and development of the distal radial metaphysis and growth plate are highly regulated physiological processes, therefore making any abnormalities and/or changes much easier to discover and monitor.

The distal radius is the most common site of fracture in children (Goulding et al., 1998). In their population-based study conducted in the U.S.A., Khosla and colleagues observed a peak incidence of distal radius fractures between the ages of 8 and 11 years in girls and 11 and 14 years in boys (Khosla et al., 2003). The graphical representations of the TW3 bone-age scores, chronological age and MI calculations seem to indicate that at the age when children experience the most fractures of the distal radius, the radius has not reached the ultimate shape for resisting fractures, i.e. has not reached the optimum MI ratio. The radius is experiencing a state of active growth and the metaphysis has not reached its peak width; the endocortical apposition rate is already very high and it appears that it cannot be further increased to the necessary levels in order to keep bone strength adapted to mechanical requirements (Rauch et al., 2001a). This is because mineralisation does not occur at the same rate as bone growth in length, therefore the increase in mechanical challenges to the distal radius caused by a fall outweighs its increase in strength during these age ranges (Rauch et al., 2001a).

## **9.12 Future Work**

The addition of more subjects to the Normal group database and the examination of other groups such as tennis players and other disease groups would improve the power of future studies and understanding of the utility of the measure. Although MI examinations lend themselves well to retrospective work, it would be beneficial to conduct a prospective study with MI as the main purpose of investigation. For example,

tennis players, particularly those who use one dominant hand to hold the racquet as opposed to both hands, would be an ideal cohort to look at how the MI differs under stress within an individual. Both hands could be radiographed and subjects could be monitored longitudinally. Another interesting group for future examination would be an OI cohort. One of the two previous studies to use the MI looked at the distal femora of OI subjects (Land et al., 2006). It would be interesting to compare the results of the MI in the distal radius (non-weight-bearing bone) to those in the distal femur (weight-bearing bone) in an OI cohort. An attempt to obtain ethics permission to examine (retrospectively) the data from two OI cohorts was made in the mid stages of this study. This attempt was abandoned however due to both time restrictions and the fact that the cohorts would have totalled no more than 20 subjects, which has already been discussed as being too few subjects for a normal distribution, making statistical analyses more difficult. A further group worth examining would be subjects with hypophosphatemic rickets as the mineral to collagen ratio in these subjects is altered (Glorieux et al., 1980), which could cause metaphyseal flaring, and therefore an abnormal MI. The current study examined the MI in a normal group, one athlete group and two disease groups, but a comparison of this study's Normal group (containing only those of white Caucasian ancestry) to groups of differing ethnicities may reveal interesting findings. Bone density reference data for non-white Caucasian ethnicities is scarce (Shepherd et al., 2005), but future work studying the MI in other ethnicities could reveal novel results and aid in creating normal reference data for non-white Caucasian groups.

The amount of data collected, the amount of patients recruited, and the fact that there are both longitudinal and cross-sectional information, will allow the original database, and the MI and bone-age information gathered in the current study to be used for a variety of other research topics in the future. Future papers using the information collected in this study could benefit from the expertise of a professional statistician to perform more in-depth analyses than have been presented here.

## **10. Conclusion**

This thesis has examined the MI at the distal radius of several groups in a retrospective study. The most commonly performed radiograph in children is that of the hand/forearm therefore an examination of the MI at the distal radius lent itself well to retrospective study. Although general studies examining metaphyseal shape have been conducted previously, this is the first study to quantify this measure in the distal radius and create a range of normal reference values, which could be useful for future work in this area. A review of the aims, objectives and hypotheses is listed below to review key findings and results.

The aims and objectives of this PhD were as follows:

1. To describe normal bone growth and development, and how diseases, deficiencies, and lifestyle choices may disturb these, with an emphasis on the metaphysis of long bones – specifically the distal radius.

An overview of normal growth conditions and various disease, nutrition, exercise and medication conditions that affect the metaphysis is located in Chapter 4. Although the two disease groups in this study showed a lower MI than in the Normal group, this was not a significant difference. However an anecdotal examination of hand/forearm radiographs of children with OI and rickets would most likely show a significantly lower MI compared to normal.

2. To measure the MI, MW and GPW of the distal radius in Normal children, young Gymnasts, children with NF1, and children CDGP.

The methods regarding how these measurements were made and subject groups are located in Chapters 5 and 6. Sections 8.7 and 9.7 show the results and discussion respectively of all groups compared. The computer-assisted method allowed the user to zoom into the distal radius without losing resolution, meaning more precise and repeatable measurements were performed.

3. To analyse and compare MI, MW and GPW measurements in the various groups of children to determine a normal range of MI, and investigate how the MI in disease groups may differ from normal.

The statistical methods, results and discussion of the above measurements are located in Chapters 7 through 9. Although linear analyses were used (e.g. simple and multiple linear regressions), they were the most pragmatic alternative to more complex non-linear analyses that would have required collaboration with a qualified statistician. Statistical analyses showed that Dunnett's t test is the most appropriate test to use for a comparison of groups such as was performed in this thesis.

4. To perform bone-age assessments in the normal children and CDGP children using the TW3 method. (Chronological age is an inappropriate method by which to compare CDGP to normal children due to the nature of CDGP).

TW3 bone-age assessments were conducted for all Normal group subjects and CDGP subjects. In section 8.7, TW3 bone-age was used in place of chronological age when all groups were compared. A comparison of MI to TW3 bone-age using a polynomial regression showed similar growth curves to chronological age in both the Normal and CDGP groups. The main difference being that in the CDGP group, the TW3 bone-age curve began earlier and started to plateau earlier due to the significant difference in chronological age and TW3 bone-age values for this group. Results of TW3 bone-age assessments are located in sections 8.3.1, 8.6, 8.6.1, 9.3.1, 9.6 and 9.6.1.

5. To investigate whether there is any correlation between pQCT measurements of the radius (toBMD, CSMA, pSSI, radius cortical area (50%) and cortical bone density (50%)), with the MI, MW and GPW values using both parametric and non-parametric statistical methods.

There were many significant correlations using Spearman's ranks and Pearson's ranks. However a clearer picture of the MI/MW/GPW variation was obtained using the multiple linear regressions. Although multiple linear regressions have their limits in growth studies (growth is not linear), the models allow the most significant predictor

variables to be seen. The results and discussions of the resulting  $r$  values and ANOVAs for the MI, MW and GPW values are located in Chapters 8 and 9.

6. To assess the MI by altering the original ratio (0.5MW/GPW) to determine whether 40% of the MW or 60% of the MW would result in a statistically more useful MW site being measured.

The results of the 40% and 60% MW/MI indicated that the 60% MW and therefore the 60% MI may be too far in the proximal direction to be a suitable place to measure. The MW and 40% MW were similar to each other indicating that both would be suitable places to measure. A more in depth study may indicate whether smaller changes become easier to detect using the 40% MW/MI. The methods, results and discussion of the 40% MI and MW and the 60% MI and MW are located in sections 7.3.2, 8.3.2 and 9.3.2.

7. To compare GP bone-age assessments performed on DXA images of the hand (Hologic DXA scanner software version 12.4) to that performed conventionally from hand radiographs.

All Normal group subjects with DXA hand images and radiographs of the hand performed at the same visit were assessed using GP bone-age. Results indicate that DXA images of the hand are very close to being interchangeable with conventional radiographs for the purposes of GP bone-age assessment. With further improvements in spatial resolution, the CV should improve further. The methods, results and discussion are located in sections 3.4, 7.8, 8.8 and 9.8.

In summary, all aims and objectives for this study were met, with some limitations in statistical analyses and subject numbers.

Next we consider the hypotheses set out at the beginning of the thesis and look at key findings related to these. The hypotheses investigated were:

10. MI should not be influenced by weight because the distal radius is not a weight bearing bone. The possible exception to this is in the gymnasts, in whom loading of the distal radius may present.

Weight was not a significant predictor for MI, MW or GPW in any group, including the Gymnast group.

11. MI should be dependent on age: MI is lower in the younger age range (5-6 years), until it comes to a plateau in mid and late teenage years.
  - i) The children with pubertal delay should have a very similar MI development pattern to normal children, except that the increase and plateau will occur later.

Chronological age is a significant predictor for MI in the Normal group only. The author believes that TW3 bone-age would have been a significant predictor for the CDGP group MI model had more subject values been used, because TW3 bone-age was a significant predictor when used in a simple linear regression. Although chronological age was not a significant predictor in the Gymnast and NF1 MI models, it is likely this was more a result of insufficient subject values and smaller age ranges of the recruited subjects. The growth curve of MI values appeared in the groups with chronological or TW3 bone-age ranges extensive enough to support this type of plot (Normal and CDGP groups).

- i) As stated previously, the beginning, rise and plateau (the latter of which is only just beginning to occur in Figure 8.6K) differences are evident and between the Normal and CDGP groups, as all three occur slightly later in the CDGP group.

12. MI should not be dependent on sex for similar reasons to 3; although the GPW and MW of males may be larger than in females, they should be in proportion, giving a similar ratio.

Comparisons of both the mean MI values and regression lines of males and females reported no statistically significant differences between the sexes. Although there was a significant difference between the mean GPW of males and females in the Normal group (this can be explained by the large age range of the Normal group), the mean MI values



and regression lines of males and females were not significantly different. Therefore it can be concluded that MI is not dependent on sex.

13. MI should not be dependent on height: bones of different lengths should still be in proportion.

Height was a statistically significant predictor in the MW and GPW regression plots, but not in the MI regression plots. Although the plots of MI against height showed typical growth curves, the relationship was never significant. However, extreme outliers (those above +2 SD or those below -2SD) in the plots tended to be those who were either very short or very tall for their age. Therefore the usefulness of the MI assessment may break down in these cases. In summary, it is concluded that an MI result be treated with scepticism if the subject measures above the 97<sup>th</sup> centile or below the 3<sup>rd</sup> centile for height with relation to the subject's age.

14. MI should always be dependent on toBA (4%) because the metaphyseal width is part of the MI ratio.

MI, along with MW and GPW values were always highly significantly correlated with toBA(4%) (results not shown). The results were not presented in the current study because of their obvious direct relationship and because of this were never used as variables in multiple regression analyses or predictors in ANCOVA analyses.

15. Increases in BMD and pSSI should not alter the MI because BMD and pSSI are not geometric measurements (i.e. will not influence the shape of the bone).

ToBMD (4%) was a significant predictor for MI in the Normal, Gymnast and NF1 groups (pQCT scans unavailable for the CDGP group). pSSI tended to be a more significant predictor in the MW and GPW regressions. This was most likely because pSSI is a volumetric measurement, which is related to bone area at the 50% radial midshaft. The hypothesis that toBMD (4%) and pSSI alterations would not change the MI could not be assessed directly as both variables tend to increase with age and height. To test the hypothesis directly would be difficult as age and height would constantly be

increasing. However, bones can be of different densities, sizes and strengths and still maintain the same proportions. This can be proved by looking at the plots of MI against chronological age. For one chronological age there are many MI values, just as for one MI value, there are many densities and many strength-strain indices (results not shown but similar curves seen). Further work would be needed to test this hypothesis over time using longitudinal measurements, perhaps in children of the same age being treated for conditions exhibiting altered mineral to collagen ratios such as rickets/osteomalacia, where the goal is to increase bone density and strength with treatment. However, it is important to note that a correlation does not necessarily imply a causal relationship.

16. MI should be altered in the case of NF1 due to metaphyseal dysplasia being one of the possible features of this disease in relation to the distal radius. However the literature concentrates on this dysplasia presenting in the femur and tibia, which are weight-bearing bones. Therefore although a change in the MI is possible due to the distal radius not being a weight bearing bone, the change may be small.

Although the mean MI was lower in the NF1 subjects, the result was not significantly different from the mean MI of the Normal group. This result may have become significantly lower if the NF1 group had had the age range and number of subjects that the Normal group had. Therefore the hypothesis that the change would be small is correct, though it most likely is unrelated to the non-weight-bearing status of the distal radius.

17. MI should be related to cross-sectional muscle area (CSMA) as muscle causes the most stress placed on bone.

MI is significantly correlated to CSMA in the Normal group, but is not significantly correlated in any other group (pQCT scans not available for CDGP group). This may have to do with the age range of the Normal group extending 11 years beyond the NF1 group and 8 years beyond the Gymnast group. CSMA was not a significant predictor for MI in any of the multiple linear regressions for the Normal, Gymnast or NF1 groups, meaning that once other more significant predictors were taken into account, CSMA was

not as important in the model. Therefore although CSMA can explain some of the variation in MI values, it's contribution is not significant.

18. MI should not be altered in the case of CDGP as the main feature of this condition is a delay in growth (smaller bones) rather than a change in the morphology, which should not affect a measurement.

This hypothesis was correct as the MI, MW and GPW in the CDGP group were not significantly different from the Normal group.

### **10.1 Summary**

The main hypothesis for the current study was that metaphyseal inwaisting, and therefore the dimensions and resulting index, would be altered at the distal radius as a result of various disease states, trauma, drugs or treatments. In addition, it was proposed that metaphyseal inwaisting could be quantified at the distal radius using a technique previously used only in the distal femur (the MI). The MI was indeed altered in the case of the Gymnast group exhibiting a significantly lower MI than the Normal group due to a widening of GPW values, not a reduction in MW values. The proportions of MW compared to GPW (MI) were maintained throughout growth under Normal, NF1 and CDGP conditions, but can be altered in cases of extreme height (short or tall) for chronological age. Significant differences from the Normal group may have appeared in the NF1 and CDGP if the age ranges of those groups had extended as far as that of the Normal group.

Furthermore, information such as that gained in the current study could be important in understanding how certain diseases/conditions affect skeletal modelling, remodelling and specifically metaphyseal inwaisting, as well as how they may increase the propensity to fracture. This information could be of use in terms of a clinical setting, e.g. being part of a diagnosis and/or whether drugs or treatments, if any, are needed in those children who fall outside the normal values, and provide a mechanism to see whether treatments are making an improvement to the skeleton. Distal radial morphology has never been quantified in this way, therefore normal reference data and ranges for the distal radius MI are the most important novel outcomes of this thesis.

## 11. References

- Aarden, E. M., Burger, E. H. & Nijweide, P. J. (1994) Function of Osteocytes in Bone. *Journal of Cellular Biochemistry*, 55, 287-299.
- Abu-Amer, Y. (2005) Advances in osteoclast differentiation and function. *Current Drug Targets: Immune, Endocrine and Metabolic Disorders*, 5, 347-355.
- Adams, J. E. (2010) Radiogrammetry and Radiographic Absorptiometry. *Radiologic Clinics of North America*, 48, 531-540.
- Adams, J. E. & Shaw, N. (Eds.) (2004) *A Practical Guide to Bone Densitometry in Children*, Bath, National Osteoporosis Society UK.
- Adams, J. S., Kantorovich, V., Wu, C., Javanbakht, M. & Hollis, B. W. (1999) Resolution of vitamin D insufficiency in osteopenic patients results in rapid recovery of bone mineral density. *Journal of Clinical Endocrinology and Metabolism*, 84, 2729-2730.
- Adams, P., Davies, G. T. & Sweetnam, P. M. (1969) Observer Error and Measurements of Metacarpal. *British Journal of Radiology*, 42, 192-197.
- Aguila, H. L. & Rowe, D. W. (2005) Skeletal development, bone remodeling, and hematopoiesis. *Immunological Reviews*, 208, 7-18.
- Aitken, J. M. (1976) Factors affecting the distribution of zinc in the human skeleton. *Calcified Tissue Research*, 20, 23-30.
- Alexander, C. J. (1976) Effect of Growth-Rate on Strength of Growth Plate-Shaft Junction. *Skeletal Radiology*, 1, 67-76.
- Alwan, S., Armstrong, L., Joe, H., Birch, P. H., Szudek, J. & Friedman, J. M. (2007) Associations of osseous abnormalities in neurofibromatosis 1. *American Journal of Medical Genetics Part A*, 143A, 1326-1333.
- Armas, L. A. G., Hollis, B. W. & Heaney, R. P. (2004) Vitamin D-2 is much less effective than vitamin D-3 in humans. *Journal of Clinical Endocrinology and Metabolism*, 89, 5387-5391.
- Ashby, R. L. (2007) Growth and Development of the Skeleton in Normal Children. *Clinical Radiology, Imaging Science and Biomedical Engineering*. Manchester, University of Manchester.
- Ashby, R. L., Hodgkinson, I. M., Harrison, E. J., Ward, K. A., Mughal, Z. & Adams, J. E. (2002a) Bone age assessment by DXA and standard radiographs; Comparison with chronological age. *Journal of Bone and Mineral Research*, 17, S298-S298.
- Ashby, R. L., Hodgkinson, I. M., Harrison, E. J., Ward, K. A., Mughal, Z. & Adams, J. E. (2002b) The reliability of bone age estimated from digital images of the hand and wrist generated by dual energy x-ray absorptiometry and standard radiograph. *Calcified Tissue International*, 70, 372.
- Ashby, R. L., Ward, K. A., Roberts, S. A., Edwards, L., Mughal, M. Z. & Adams, J. E. (2008) A reference database for the Stratec XCT-2000 peripheral quantitative computed tomography (pQCT) scanner in healthy children and young adults aged 6-19 years. *Osteoporosis International*, 20, 1337-1346.
- Bach, A. U., Anderson, S. A., Foley, A. L., Williams, E. C., Suttie, J. W. & Suttie, J. W. (1996) Assessment of vitamin K status in human subjects administered "minidose" warfarin. *American Journal of Clinical Nutrition*, 64, 894-902.

- Bachrach, L. K. & Ward, L. M. (2009) Clinical review 1: Bisphosphonate use in childhood osteoporosis. *Journal of Clinical Endocrinology and Metabolism*, 94, 400-409.
- Bailey, D. A., Faulkner, R. A. & McKay, H. A. (1996) Growth, physical activity, and bone mineral acquisition. *Exercise and Sport Sciences Reviews*, 24, 233-266.
- Ballock, R. T. & O'Keefe, R. J. (2003) Physiology and pathophysiology of the growth plate. *Birth Defects Research (Part C) Embryo Today*, 69, 123-143.
- Barceloux, D. G. (1999) Copper. *Clinical Toxicology*, 37, 217-230.
- Bardeen, C. R. & Lewis, W. H. (1901) Development of the limbs, body-wall and back in man. *American Journal of Anatomy*, 1, 1-53.
- Barnett, E. & Nordin, B. E. (1960) The radiological diagnosis of osteoporosis: a new approach. *Clinical Radiology*, 11, 166-174.
- Baron, R. (1999) Anatomy and Ultrastructure of Bone. IN Lian, J. B. & Goldring, S. R. (Eds.) *Primer on the Metabolic Bone Diseases and Disorder of Mineral Metabolism*. 4th ed. Philadelphia, Lippincott Williams & Wilkins.
- Bass, W. (1995) *Human Osteology: A Laboratory and Field Manual (4th Ed.)*, Missouri, Missouri Archaeological Society.
- Beard, J. L. (2001) Iron biology in immune function, muscle metabolism and neuronal functioning. *Journal of Nutrition*, 131, 568S-580S.
- Beck, T. (2003) Measuring the structural strength of bones with dual-energy X-ray absorptiometry: principles, technical limitations, and future possibilities. *Osteoporosis International*, 14 Suppl 5, S81-S88.
- Bell, K. L., Loveridge, N., Power, J., Garrahan, N., Meggitt, B. F. & Reeve, J. (1999) Regional differences in cortical porosity in the fractured femoral neck. *Bone*, 24, 57-64.
- Bellus, G. A., Mcintosh, I., Smith, E. A., Aylsworth, A. S., Kaitila, I., Horton, W. A., Greenhaw, G. A., Hecht, J. T. & Francomano, C. A. (1995) A Recurrent Mutation in the Tyrosine Kinase Domain of Fibroblast Growth-Factor Receptor-3 Causes Hypochondroplasia. *Nature Genetics*, 10, 357-359.
- Bertelloni, S., Baroncelli, G. I., Ferdeghini, M., Perri, G. & Saggese, G. (1998) Normal volumetric bone mineral density and bone turnover in young men with histories of constitutional delay of puberty. *Journal of Clinical Endocrinology & Metabolism*, 83, 4280-4283.
- Bertelloni, S., Baroncelli, G. I. & Saggese, G. (1999) Normal volumetric bone mineral density in young men with histories of constitutional delay of puberty - Authors' response. *Journal of Clinical Endocrinology & Metabolism*, 84, 3403-3404.
- Bierich, J. R. & Potthoff, K. (1979) Spontaneous Secretion of Growth-Hormone in Children with Constitutional Delay of Growth and Adolescence and with Early Normal Puberty. *Monatsschrift Kinderheilkunde*, 127, 561-565.
- Black, D. M., Palermo, L., Sorensen, T., Jorgensen, J. T., Lewis, C., Tylavsky, F., Wallace, R., Harris, E. & Cummings, S. R. (2001) A normative reference database study for Pronosco X-posure System (TM). *Journal of Clinical Densitometry*, 4, 5-12.
- Black, R. E., Williams, S. M., Jones, I. E. & Goulding, A. (2002) Children who avoid drinking cow milk have low dietary calcium intakes and poor bone health. *American Journal of Clinical Nutrition*, 76, 675-680.

- Blair, H. C., Kahn, A. J., Crouch, E. C., Jeffrey, J. J. & Teitelbaum, S. L. (1986) Isolated osteoclasts resorb the organic and inorganic components of bone. *Journal of Cell Biology*, 102, 1164-72.
- Bland, J. & Altman, D. (1986) Statistical methods for assessing agreement between two methods of clinical measurement. *Lancet*, 1, 307-310.
- Bonen, D. K. & Schmid, T. M. (1991) Elevated Extracellular Calcium Concentrations Induce Type-X Collagen-Synthesis in Chondrocyte Cultures. *Journal of Cell Biology*, 115, 1171-1178.
- Booth, S. L. (2003) Dietary Vitamin K and Skeletal Health. IN Bonjour, J. P. & New, S. A. (Eds.) *Nutritional Aspects of Bone Health*. Cambridge, UK, The Royal Society of Chemistry.
- Booth, S. L., Broe, K. E., Gagnon, D. R., Tucker, K. L., Hannan, M. T., McLean, R. R., Dawson-Hughes, B., Wilson, P. W., Cupples, L. A. & Kiel, D. P. (2003) Vitamin K intake and bone mineral density in women and men. *American Journal of Clinical Nutrition*, 77, 512-516.
- Bourrin, S., Genty, C., Palle, S., Gharib, C. & Alexandre, C. (1994) Adverse-Effects of Strenuous Exercise - a Densitometric and Histomorphometric Study in the Rat. *Journal of Applied Physiology*, 76, 1999-2005.
- Bowen, R. (2007) Vitamin D (Calcitriol). Colorado, Colorado State University.
- Braun, H. S., Nurnberg, P. & Tinschert, S. (2001) Metaphyseal dysplasia: A new autosomal dominant type in a large German kindred. *American Journal of Medical Genetics*, 101, 74-77.
- Breen, S. A., Millest, A. J., Loveday, B. E., Johnstone, D. & Waterton, J. C. (1996) Regional analysis of bone mineral density in the distal femur and proximal tibia using peripheral quantitative computed tomography in the rat in vivo. *Calcified Tissue International*, 58, 449-453.
- Brianza, S. Z. M., Delise, M., Maddalena Ferraris, M., D'Amelio, P. & Botti, P. (2006) Cross-sectional geometrical properties of distal radius and ulna in large, medium and toy breed dogs. *Journal of Biomechanics*, 39, 302-311.
- Bridgewater, L. C., Lefebvre, V. & de Crombrughe, B. (1998) Chondrocyte-specific enhancer elements in the Col11a2 gene resemble the Col2a1 tissue-specific enhancer. *Journal of Biological Chemistry*, 273, 14998-15006.
- Brooks, M. H., Bell, N. H., Love, L., Stern, P. H., Orfei, E., Queener, S. F., Hamstra, A. J. & Deluca, H. F. (1978) Vitamin-D-Dependent Rickets Type-II - Resistance of Target Organs to 1,25-Dihydroxyvitamin-D. *New England Journal of Medicine*, 298, 996-999.
- Brown, J. J. & Zacharin, M. R. (2009) Safety and Efficacy of Intravenous Zoledronic Acid in Paediatric Osteoporosis. *Journal of Pediatric Endocrinology & Metabolism*, 22, 55-63.
- Brumsen, C., Hamdy, N. A. & Papapoulos, S. E. (1997) Long-term effects of bisphosphonates on the growing skeleton: Studies of young patients with severe osteoporosis. *Medicine (Baltimore)*, 76, 266-83.
- Burger, E. H. & Klein-Nulend, J. (1999) Mechanotransduction in bone--role of the lacuno-canalicular network. *Federation of American Societies for Experimental Biology Journal*, 13 Suppl, S101-S112.

- Burton, D. W., Foster, M., Johnson, K. A., Hiramoto, M., Defetos, L. J. & Terkeltaub, R. (2005) Chondrocyte calcium-sensing receptor expression is up-regulated in early guinea pig knee osteoarthritis and modulates PTHrP, MMP-13, and TIMP-3 expression. *Osteoarthritis and Cartilage*, 13, 395-404.
- Cancela, L., Hsieh, C. L., Francke, U. & Price, P. A. (1990) Molecular-Structure, Chromosome Assignment, and Promoter Organization of the Human Matrix Gla Protein Gene. *Journal of Biological Chemistry*, 265, 15040-15048.
- Carmel, R., Lau, K. H., Baylink, D. J., Saxena, S. & Singer, F. R. (1988) Cobalamin and osteoblast-specific proteins. *New England Journal of Medicine*, 319, 70-75.
- Carter, D. R., Bouxsein, M. L. & Marcus, R. (1992) New approaches for interpreting projected bone densitometry data. *Journal of Bone and Mineral Research*, 7, 137-145.
- Carter, S. R., Aldridge, M. J., Fitzgerald, R. & Davies, A. M. (1988) Stress changes of the wrist in adolescent gymnasts. *Br J Radiol*, 61, 109-112.
- Cashman, K. D. (2005) Vitamin K status may be an important determinant of childhood bone health. *Nutrition Reviews*, 63, 284-289.
- Chevrel, G., Schott, A. M., Fontanges, E., Charrin, J. E., Lina-Granade, G., Duboeuf, F., Garnero, P., Arlot, M., Raynal, C. & Meunier, P. J. (2006) Effects of oral alendronate on BMD in adult patients with osteogenesis imperfecta: a 3-year randomized placebo-controlled trial. *Journal of Bone and Mineral Research*, 21, 300-306.
- Christoffersen, J. & Landis, W. (1991) A Contribution With Review to the Description of Mineralization of Bone and Other Calcified Tissues In Vivo. *The Anatomical Record*, 230, 435-450.
- Clark, E. M., Ness, A. R. & Tobias, J. H. (2006) Gender differences in the ratio between humerus width and length are established prior to puberty. *Osteoporosis International*, e-publication.
- Clayton, P. E., Shalet, S. M., Price, D. A. & Addison, G. M. (1988) Growth and Growth-Hormone Responses to Oxandrolone in Boys with Constitutional Delay of Growth and Puberty (Cdgp). *Clinical Endocrinology*, 29, 123-130.
- Cooper, C., Dennison, E. M., Leufkens, H. G., Bishop, N. & van Staa, T. P. (2004) Epidemiology of childhood fractures in Britain: a study using the general practice research database. *Journal of Bone and Mineral Research*, 19, 1976-1981.
- Corathers, S. D. (2006) Focus on Diagnosis: The Alkaline Phosphatase Level: Nuances of a Familiar Test. *Pediatrics in Review*, 27, 382-384.
- Cowin, S. C. (2002) Mechanosensation and fluid transport in living bone. *Journal of Musculoskeletal and Neuronal Interactions*, 2, 256-260.
- Cowin, S. C., Moss-Salentijn, L. & Moss, M. L. (1991) Candidates for the mechanosensory system in bone. *Journal of Biomechanical Engineering*, 113, 191-197.
- Crabtree, N. J., Kent, K. & Zemel, B. S. (2007a) Acquisition of DXA in Children and Adolescents. IN Sawyer, A. J., Bachrach, L. K. & Fung, E. B. (Eds.) *Bone Densitometry in Growing Patients: Guides for Clinical Practice*. New Jersey, Humana Press.

- Crabtree, N. J., Leonard, M. B. & Zemel, B. S. (2007b) Dual-Energy X-Ray Absorptiometry. IN Sawyer, A. J., Bachrach, L. K. & Fung, E. B. (Eds.) *Bone Densitometry in Growing Patients: Guides for Clinical Practice*. New Jersey, Humana Press.
- Cundy, T., Hegde, M., Naot, D., Chong, B., King, A., Wallace, R., Mulley, J., Love, D. R., Seidel, J., Fawcner, M., Banovic, T., Callon, K. E., Grey, A. B., Reid, I. R., Middleton-Hardie, C. A. & Cornish, J. (2002) A mutation in the gene TNFRSF11B encoding osteoprotegerin causes an idiopathic hyperphosphatasia phenotype. *Human Molecular Genetics*, 11, 2119-2127.
- Cundy, T., Wheadon, L. & King, A. (2004) Treatment of idiopathic hyperphosphatasia with intensive bisphosphonate therapy. *Journal of Bone and Mineral Research*, 19, 703-711.
- Curry, J. D. (2002) *Bones: Structure and Mechanics*, Woodstock, UK, Princeton University Press.
- Danks, D. (1995) Disorders of Copper Transport. IN Scriver, C., Beaudet, A., Sly, W. & Valle, D. (Eds.) *The Metabolic and Molecular Bases of Inherited Disease*. 7th ed. New York, McGraw-Hill.
- Davidson, P. L., Goulding, A. & Chalmers, D. J. (2003) Biomechanical analysis of arm fracture in obese boys. *Journal of Paediatrics and Child Health*, 39, 657-664.
- Davison, K. K., Susman, E. J. & Birch, L. L. (2003) Percent Body Fat at Age 5 Predicts Earlier Pubertal Development Among Girls at Age 9. *Pediatrics*, 111, 815-821.
- de Crombrughe, B., Lefebvre, V., Behringer, R. R., Bi, W. M., Murakami, S. & Huang, W. D. (2000) Transcriptional mechanisms of chondrocyte differentiation. *Matrix Biology*, 19, 389-394.
- De Luca, F., Uyeda, J. A., Mericq, V., Mancilla, E. E., Yanovski, J. A., Barnes, K. M., Zile, M. H. & Baron, J. (2000) Retinoic acid is a potent regulator of growth plate chondrogenesis. *Endocrinology*, 141, 346-353.
- Declue, J. E., Papageorge, A. G., Fletcher, J. A., Diehl, S. R., Ratner, N., Vass, W. C. & Lowy, D. R. (1992) Abnormal Regulation of Mammalian P21(Ras) Contributes to Malignant-Tumor Growth in Vonrecklinghausen (Type-1) Neurofibromatosis. *Cell*, 69, 265-273.
- DeLuca, H. (1979) Vitamin D. Metabolism and function. IN DeLuca, H. (Ed.) *Monographs on Endocrinology*. Berlin, Springer-Verlag.
- Dhar, S., Dangerfield, P. H., Dorgan, J. C. & Klenerman, L. (1993) Correlation Between Bone Age and Risser's Sign in Adolescent Idiopathic Scoliosis. *Spine*, 18, 14-19.
- Dhonukshe-Rutten, R. A., van Dusseldorp, M., Schneede, J., de Groot, L. C. & van Staveren, W. A. (2005) Low bone mineral density and bone mineral content are associated with low cobalamin status in adolescents. *European Journal of Nutrition*, 44, 341-347.
- DiMeglio, L. A., Ford, L., McClintock, C. & Peacock, M. (2005) A comparison of oral and intravenous bisphosphonate therapy for children with osteogenesis imperfecta. *Journal of Pediatric Endocrinology and Metabolism*, 18, 43-53.
- DiMeglio, L. A. & Peacock, M. (2006) Two-year clinical trial of oral alendronate versus intravenous pamidronate in children with osteogenesis imperfecta. *Journal of Bone and Mineral Research*, 21, 132-140.



- Dodds, R. A., Catterall, A., Bitensky, L. & Chayen, J. (1986) Abnormalities in fracture healing induced by vitamin B6-deficiency in rats. *Bone*, 7, 489-495.
- Doneray, H. & Orbak, Z. (2008) Association between bone turnover markers and bone mineral density in puberty and constitutional delay of growth and puberty. *West Indian Medical Journal*, 57, 33-39.
- Ducher, G., Tournaire, N., Meddahi-Pelle, A., Benhamou, C. L. & Courteix, D. (2006) Short-term and long-term site-specific effects of tennis playing on trabecular and cortical bone at the distal radius. *Journal of Bone and Mineral Metabolism*, 24, 484-490.
- Duke, P. M., Litt, I. F. & Gross, R. T. (1980) Adolescents' Self-Assessment of Sexual Maturation. *Pediatrics*, 66, 918-920.
- Duprez, L., Parma, J., Van Sande, J., Allgeier, A., Leclère, J., Schwartz, C., Delisle, M., Decoulx, M., Orgiazzi, J., Dumont, J. & Vassart, G. (1994) Germline mutations in the thyrotropin receptor gene cause non-autoimmune autosomal dominant hyperthyroidism. *Nature Genetics*, 7, 396-401.
- Dyson, K., Blimkie, C. J. R., Davison, K. S., Webber, C. E. & Adachi, J. D. (1997) Gymnastic training and bone density in pre adolescent females. *Medicine and Science in Sports and Exercise*, 29, 443-450.
- Einhorn, T. A. (1996) The Bone Organ System: Form and Function. IN Marcus, R., Feldman, D. & Kelsey, J. (Eds.) *Osteoporosis*. London, Academic Press Limited.
- Everts, V., Delaisse, J. M., Korper, W., Jansen, D. C., Tigchelaar-Gutter, W., Saftig, P. & Beertsen, W. (2002) The bone lining cell: Its role in cleaning Howship's lacunae and initiating bone formation. *Journal of Bone and Mineral Research*, 17, 77-90.
- Faerk, J., Peitersen, B., Petersen, S. & Michaelsen, K. F. (2002) Bone mineralisation in premature infants cannot be predicted from serum alkaline phosphatase or serum phosphate. *Archives of Disease in Childhood: Fetal Neonatal Edition*, 87, F133-136.
- Fan, J. & Zhu, Q. (1999) [Effects of vitamin A deficiency on the development and growth of rat embryos]. *Wei Sheng Yan Jiu*, 28, 235-236.
- Favus, M., Bushinsky, D. & Lemann Jr., J. (2006) Regulation of Calcium, Magnesium and Phosphate Metabolism. IN Favus, M. (Ed.) *Primer on the Metabolic Bone Diseases and Disorders of Mineral Metabolism*. 6th ed. Washington DC, ASBMR.
- Ferrari, S. L., Chevalley, T., Bonjour, J. P. & Rizzoli, R. (2006) Childhood fractures are associated with decreased bone mass gain during puberty: An early marker of persistent bone fragility? *Journal of Bone and Mineral Research*, 21, 501-507.
- Ferretti, J. L. (1995) Perspectives of pQCT Technology Associated to Biomechanical Studies in Skeletal Research Employing Rat Models. *Bone*, 17, S353-S364.
- Ferretti, J. L., Gaffuri, O., Capozza, R., Cointy, G., Bozzini, C., Olivera, M., Zanchetta, J. R. & Bozzini, C. E. (1995) Dexamethasone effects on mechanical, geometric and densitometric properties of rat femur diaphyses as described by peripheral quantitative computerized tomography and bending tests. *Bone*, 16, 119-124.
- Fewtrell, M. S., Gordon, I., Biassoni, L. & Cole, T. J. (2005) Dual X-ray absorptiometry (DXA) of the lumbar spine in a clinical paediatric setting: Does the method of size-adjustment matter? *Bone*, 37, 413-419.

- Field, A. (2005) *Discovering Statistics Using SPSS: Sex, Drugs and Rock'n'roll*, London, Sage Publications Ltd.
- Field, R. E., Buchanan, J. A., Copplemans, M. G. & Aichroth, P. M. (1994) Bone-marrow transplantation in Hurler's syndrome. Effect on skeletal development. *Journal of Bone and Joint Surgery - British*, 76, 975-981.
- Finkelstein, J. S., Klibanski, A. & Neer, R. M. (1996) A longitudinal evaluation of bone mineral density in adult men with histories of delayed puberty. *Journal of Clinical Endocrinology & Metabolism*, 81, 1152-1155.
- Finkelstein, J. S., Klibanski, A. & Neer, R. M. (1999) Comment on Normal Volumetric Bone Mineral Density and Bone Turnover in Young Men with Histories of Constitutional Delay of Puberty. *Journal of Clinical Endocrinology & Metabolism*, 84, 3400a-3402.
- Finkelstein, J. S., Neer, R. M., Biller, B. M. K., Crawford, J. D. & Klibanski, A. (1992) Osteopenia in Men with a History of Delayed Puberty. *New England Journal of Medicine*, 326, 600-604.
- Fliegel, C. P. (1986) *Stress related widening of the radial growth plate in adolescents*, Paris, Expansion scientifique publications.
- Foresta, C., Ruzza, G., Mioni, R., Guarneri, G., Gribaldo, R., Meneghello, A. & Mastrogiacomo, I. (1984) Osteoporosis and Decline of Gonadal-Function in the Elderly Male. *Hormone Research*, 19, 18-22.
- Frank, G. R. (2003) Constitutional delay of growth and puberty. *Endocrinologist*, 13, 341-346.
- Frankel, V. H. & Nordin, M. (2001) Biomechanics of Bone. IN Nordin, M. & Frankel, V. H. (Eds.) *Basic Biomechanics of the Musculoskeletal System*. Philadelphia, Lippincott, Williams and Wilkins.
- Freeman, J. V., Cole, T. J., Chinn, S., Jones, P. R., White, E. M. & Preece, M. A. (1995a) Cross sectional stature and weight reference curves for the UK, 1990. *Archives of Disease in Childhood*, 73, 17-24.
- Freeman, J. V., Cole, T. J., Chinn, S., Jones, P. R. M., White, E. M. & Preece, M. A. (1995b) Cross-Sectional Stature and Weight Reference Curves for the UK 1990. *Archives of Disease in Childhood*, 73, 17-24.
- Fricke, O. & Schoenau, E. (2007) The 'Functional Muscle-Bone Unit': Probing the relevance of mechanical signals for bone development in children and adolescents. *Growth Hormone & IGF Research*, 17, 1-9.
- Frost, H. M. (1960) Presence of microscopic cracks in vivo in bone. *Henry Ford Hospital Medical Bulletin*, 8, 25-35.
- Frost, H. M. (1966a) Bone Dynamics and Metabolic Bone Disease. *Journal of Bone and Joint Surgery*, 48A, 1192-1203.
- Frost, H. M. (1966b) *Bone Dynamics in Osteoporosis and Osteomalacia*, Springfield, Charles C. Thomas.
- Frost, H. M. (1987) The Mechanostat - a Proposed Pathogenic Mechanism of Osteoporoses and the Bone Mass Effects of Mechanical and Nonmechanical Agents. *Bone and Mineral*, 2, 73-85.
- Frost, H. M. (1996) Perspectives: a proposed general model of the "mechanostat" (suggestions from a new skeletal-biologic paradigm). *Anatomical Record*, 244, 139-147.

- Frost, H. M. (1997) Changing concepts in skeletal physiology: Wolff's Law, the Mechanostat, and the "Utah Paradigm". *American Journal of Human Biology*, 10, 599-605.
- Frost, H. M. (1998) Changing concepts in skeletal physiology: Wolff's Law, the Mechanostat, and the "Utah Paradigm". *American Journal of Human Biology*, 10, 599-605.
- Frost, H. M. (2000a) Muscle, bone, and the Utah paradigm: a 1999 overview. *Medicine and Science in Sports and Exercise*, 32, 911-917.
- Frost, H. M. (2000b) The Utah paradigm of skeletal physiology: an overview of its insights for bone, cartilage and collagenous tissue organs. *Journal of Bone and Mineral Metabolism*, 18, 305-316.
- Frost, H. M. (2001a) From Wolff's law to the Utah paradigm: Insights about bone physiology and its clinical applications. *The Anatomical Record*, 262, 398-419.
- Frost, H. M. (2001b) The Utah paradigm of skeletal physiology: what is it? *Veterinary and Comparative Orthopaedics and Traumatology*, 14, 179-184.
- Frost, H. M. (2004a) A 2003 update of bone physiology and Wolff's Law for clinicians. *Angle Orthodontist*, 74, 3-15.
- Frost, H. M. (2004b) *The Utah Paradigm of Skeletal Physiology: Volume 1 - Bone and Bones and Associated Problems*, Athens, International Society of Musculoskeletal and Neuronal Interactions.
- Frost, H. M. (2004c) *The Utah Paradigm of Skeletal Physiology: Volume 2 - Fibrous (Collagenous) Tissues, Cartilage, Synovial Joints and Associated Problems*, Athens, International Society of Musculoskeletal and Neuronal Interactions.
- Fu, X. Y., Wang, X. D., Mernitz, H., Wallin, R., Shea, M. K. & Booth, S. L. (2008) 9-Cis Retinoic Acid Reduces 1 alpha,25-Dihydroxycholecalciferol-Induced Renal Calcification by Altering Vitamin K-Dependent gamma-Carboxylation of Matrix gamma-Carboxyglutamic Acid Protein in AM Male Mice. *Journal of Nutrition*, 138, 2337-2341.
- Garabedian, M., Tanaka, Y., Holick, M. F. & Deluca, H. F. (1974) Response of Intestinal Calcium-Transport and Bone Calcium Mobilization to 1,25-Dihydroxyvitamin D3 in Thyroparathyroidectomized Rats. *Endocrinology*, 94, 1022-1027.
- Gerrior, S., Putnam, J. & L, B. (1998) Milk and milk products: their importance in the American diet. *Food Review*, 2, 29-37.
- Gilsanz, V. (1998) Bone density in children: a review of the available techniques and indications. *European Journal of Radiology*, 26, 177-182.
- Gilsanz, V. & Ratib, O. (2005) *Hand Bone Age: A Digital Atlas of Skeletal Maturity*, New York, Springer-Verlag Berlin Heidelberg.
- Glorieux, F. H., Marie, P. J., Pettifor, J. M. & Delvin, E. E. (1980) Bone Response to Phosphate Salts, Ergocalciferol, and Calcitriol in Hypophosphatemic Vitamin-D-Resistant Rickets. *New England Journal of Medicine*, 303, 1023-1031.
- Gluer, C. C., Blake, G., Lu, Y., Blunt, B. A., Jergas, M. & Genant, H. K. (1995) Accurate Assessment of Precision Errors - How to Measure the Reproducibility of Bone Densitometry Techniques. *Osteoporosis International*, 5, 262-270.

- Gordon, C. C. (2004) Peripheral quantitative computed tomography and micro-computed tomography. IN Langton, C. M. & Njeh, C. F. (Eds.) *The Physical Measurement of Bone*. London, Institute of Physics Publishing Ltd.
- Goulding, A. (2007) Childhood fractures: Time to implement strategies to reduce these events. *International Congress Series*, 1297, 3-14.
- Goulding, A., Cannan, R., Williams, S. M., Gold, E. J., Taylor, R. W. & Lewis-Barned, N. J. (1998) Bone mineral density in girls with forearm fractures. *Journal of Bone and Mineral Research*, 13, 143-148.
- Goulding, A., Grant, A. M. & Williams, S. M. (2005) Bone and body composition of children and adolescents with repeated forearm fractures. *Journal of Bone and Mineral Research*, 20, 2090-2096.
- Goulding, A., Jones, I. E., Taylor, R. W., Manning, P. J. & Williams, S. M. (2000) More broken bones: a 4-year double cohort study of young girls with and without distal forearm fractures. *Journal of Bone and Mineral Research*, 15, 2011-2018.
- Goulding, A., Jones, I. E., Taylor, R. W., Piggot, J. M. & Taylor, D. (2003) Dynamic and static tests of balance and postural sway in boys: effects of previous wrist bone fractures and high adiposity. *Gait & Posture*, 17, 136-141.
- Goulding, A., Jones, I. E., Taylor, R. W., Williams, S. M. & Manning, P. J. (2001) Bone mineral density and body composition in boys with distal forearm fractures: a dual-energy x-ray absorptiometry study. *Journal of Pediatrics*, 139, 509-15.
- Goulding, A., Rockell, J. E. P., Black, R. E., Grant, A. M., Jones, I. E. & Williams, S. M. (2004) Children who avoid drinking cow's milk are at increased risk for prepubertal bone fractures. *Journal of the American Dietetic Association*, 104, 250-253.
- Grampp, S., Lang, P., Jergas, M., Gluer, C. C., Mathur, A., Engelke, K. & Genant, H. K. (1995) Assessment of the skeletal status by peripheral quantitative computed tomography of the forearm: short-term precision in vivo and comparison to dual X-ray absorptiometry. *Journal of Bone and Mineral Research*, 10, 1566-1576.
- Greulich, W. & Pyle, S. (1950) *Radiographic Atlas of Skeletal Development of the Hand and Wrist*, Stanford, Stanford University Press.
- Greulich, W. & Pyle, S. (1959) *Radiographic Atlas of Skeletal Development of the Hand and Wrist, Second Edition*, Stanford, Stanford University Press.
- Guglielmi, G., De Serio, A., Fusilli, S., Scillitani, A., Chiodini, I., Torlontano, M. & Cammisa, M. (2000) Age-related changes assessed by peripheral QCT in healthy Italian women. *European Radiology*, 10, 609-614.
- Gunter, K., Baxter-Jones, A. D. G., Mirwald, R. L., Almstedt, H., Fuller, A., Durski, S. & Snow, C. (2008) Jump starting skeletal health: A 4-year longitudinal study assessing the effects of jumping on skeletal development in pre and circum pubertal children. *Bone*, 42, 710-718.
- Gupta, S. K., Tuli, S. M., Srivastava, T. P., Khanna, S., Rao, T. V. & Sahai, R. P. (1985) Skeletal overgrowth with modelling error in neurofibromatosis. *Clinical Radiology*, 36, 643-645.
- Haapasalo, H., Kontulainen, S., Sievanen, H., Kannus, P., Jarvinen, M. & Vuori, I. (2000) Exercise-induced bone gain is due to enlargement in bone size without a change in volumetric bone density: a peripheral quantitative computed tomography study of the upper arms of male tennis players. *Bone*, 27, 351-7.

- Hagler, W., Briody, J., Woodhead, H. J., Chan, A. & Cowell, C. T. (2003) Importance of lean mass in the interpretation of total body densitometry in children and adolescents. *The Journal of Pediatrics*, 143, 81-88.
- Haines, R. W. (1975) Histology of Epiphyseal Union in Mammals. *Journal of Anatomy*, 120, 1-25.
- Hangartner, T. N. & Johnston, C. C. (1990) Influence of fat on bone measurements with dual-energy absorptiometry. *Bone and Mineral*, 9, 71-81.
- Harris, S. S., Hunt, C. E., Alvarez, C. J. & Navia, J. M. (1978) Vitamin A deficiency and new bone growth: histologic changes. *Journal of Oral Pathology*, 7, 85-90.
- Henderson, R. C., Lark, R. K., Kecskemethy, H. H., Miller, F., Harcke, H. T. & Bachrach, S. J. (2002) Bisphosphonates to treat osteopenia in children with quadriplegic cerebral palsy: A randomized, placebo-controlled clinical trial. *Journal of Pediatrics*, 141, 644-651.
- Hill, P. & Orth, M. (1998) Bone Remodelling. *British Journal of Orthodontics*, 25, 101-107.
- Hill, T. & Lewicki, P. (2005) *Statistics: Methods and Applications*, Tulsa, USA, StatSoft Inc.
- Ho, M. S. P., Tsang, K. Y., Lo, R. L. K., Susic, M., Makitie, O., Chan, T. W. Y., Ng, V. C. W., Sillence, D. O., Boot-Handford, R. P., Gibson, G., Cheung, K. M. C., Cole, W. G., Cheah, K. S. E. & Chan, D. (2007) COL10A1 nonsense and frame-shift mutations have a gain-of-function effect on the growth plate in human and mouse metaphyseal chondrodysplasia type Schmid. *Human Molecular Genetics*, 16, 1201-1215.
- Holick, M. F. (2006) High Prevalence of Vitamin D Inadequacy and Implications for Health. *Mayo Clinic Proceedings*, 81, 353-373.
- Holick, M. F., Biancuzzo, R. M., Chen, T. C., Klein, E. K., Young, A., Bibuld, D., Reitz, R., Salameh, W., Ameri, A. & Tannenbaum, A. D. (2008) Vitamin D-2 is as effective as vitamin D-3 in maintaining circulating concentrations of 25-hydroxyvitamin D. *Journal of Clinical Endocrinology & Metabolism*, 93, 677-681.
- Horlick, M., Wang, J., Pierson, R. N. & Thornton, J. C. (2004) Prediction models for evaluation of total-body bone mass with dual-energy X-ray absorptiometry among children and adolescents. *Pediatrics*, 114, E337-E345.
- Hruska, K. (2006) Hyperphosphatemia and Hypophosphatemia. IN Favus, M. (Ed.) *Primer on the Metabolic Bone Diseases and Disorders of Mineral Metabolism*. 6th ed. Washington DC, ASBMR.
- Huda, W. & Gkanatsios, N. A. (1998) Radiation Dosimetry for Extremity Radiographs. *Health Physics*, 75, 492-499.
- Hurley, L. S., Everson, G. J., Wooten, E. & Asling, C. W. (1961) Disproportionate Growth in Offspring of Manganese-Deficient Rats: I. The Long Bones. *J. Nutr.*, 74, 274-281.
- Ilich-Ernst, J. Z., McKenna, A. A., Badenhop, N. E., Clairmont, A. C., Andon, M. B., Nahhas, R. W., Goel, P. & Matkovic, V. (1998) Iron status, menarche, and calcium supplementation in adolescent girls. *American Journal of Clinical Nutrition*, 68, 880-887.

- Inada, M., Yasui, T., Nomura, S., Miyake, S., Deguchi, K., Himeno, M., Sato, M., Yamagiwa, H., Kimura, T., Yasui, N., Ochi, T., Endo, N., Kitamura, Y., Kishimoto, T. & Komori, T. (1999) Maturational disturbance of chondrocytes in *Cbfa1*-deficient mice. *Developmental Dynamics*, 214, 279-290.
- IRCP (1975) Report of the Task Group on Reference Man: ICRP publication 23. Pergamon Press, Oxford, UK, International Commission on Radiological Protection.
- Isaksson, H., Tolvanen, V., Finnila, M. A. J., Iivarinen, J., Tuukkanen, J., Seppanen, K., Arokoski, J. P. A., Brama, P. A., Jurvelin, J. S. & Helminen, H. J. (2009) Physical Exercise Improves Properties of Bone and Its Collagen Network in Growing and Maturing Mice. *Calcified Tissue International*, 85, 247-256.
- Jaffe, N. R. & Johnson, E. M. (1973) Alterations in Ontogeny and Specific Activity of Phosphomonoesterases Associated with Abnormal Chondrogenesis and Osteogenesis in Limbs of Fetuses from Folic Acid-Deficient Pregnant Rats. *Teratology*, 8, 33-49.
- Jamsa, T., Jalovaara, P., Peng, Z., Vaananen, H. K. & Tuukkanen, J. (1998) Comparison of three-point bending test and peripheral quantitative computed tomography analysis in the evaluation of the strength of mouse femur and tibia. *Bone*, 23, 155-161.
- Jee, W. S. S. (1983) The Skeletal Tissues. IN Weiss, L. (Ed.) *Histology, Cell and Tissue Biology*. 5th ed. New York, Elsevier Biomedical.
- Jee, W. S. S. (2006) H.M.Frost's Legacy : The Utah Paradigm of Skeletal Physiology. *Niigata Journal of Health and Welfare*, 6, 1-9.
- Johannsson, G., Rosen, T., Bosaeus, I., Sjostrom, L. & Bengtsson, B. A. (1996) Two years of growth hormone (GH) treatment increases bone mineral content and density in hypopituitary patients with adult-onset GH deficiency. *Journal of Clinical Endocrinology & Metabolism*, 81, 2865-2873.
- Johnson, R. K. & Frary, C. (2001) Choose beverages and foods to moderate your intake of sugars: The 2000 Dietary Guidelines for Americans - What's all the fuss about? *Journal of Nutrition*, 131, 2766S-2771S.
- Jones, I. E., Taylor, R. W., Williams, S. M., Manning, P. J. & Goulding, A. (2002) Four-year gain in bone mineral in girls with and without past forearm fractures: a DXA study. Dual energy X-ray absorptiometry. *Journal of Bone and Mineral Research*, 17, 1065-1072.
- Jordan, G. R., Loveridge, N., Bell, K. L., Power, J., Rushton, N. & Reeve, J. (2000) Spatial clustering of remodeling osteons in the femoral neck cortex: a cause of weakness in hip fracture? *Bone*, 26, 305-313.
- Judex, S. & Zernicke, R. F. (2000a) Does the mechanical milieu associated with high-speed running lead to adaptive changes in diaphyseal growing bone? *Bone*, 26, 153-159.
- Judex, S. & Zernicke, R. F. (2000b) High-impact exercise and growing bone: relation between high strain rates and enhanced bone formation. *Journal of Applied Physiology*, 88, 2183-2191.
- Kane, S. A. (2005) *Introduction to Physics in Modern Medicine*, New York, Taylor & Francis.

- Kanumakala, S., Boneh, A. & Zacharin, M. (2002) Pamidronate treatment improves bone mineral density in children with Menkes disease. *Journal of Inherited Metabolic Disease*, 25, 391-398.
- Katsumata, S. I., Katsumata-Tsuboi, R., Uehara, M. & Suzuki, K. (2009) Severe Iron Deficiency Decreases Both Bone Formation and Bone Resorption in Rats. *Journal of Nutrition*, 139, 238-243.
- Kelly, T. L., Slovik, D. M., Schoenfeld, D. A. & Neer, R. M. (1988) Quantitative digital radiography versus dual photon absorptiometry of the lumbar spine. *Journal of Clinical Endocrinology and Metabolism*, 67, 839-844.
- Kennedy, E. & Goldberg, J. (1995) What are American children eating? Implications for public policy. *Nutrition Reviews*, 53, 111-126.
- Khan, A. J. & Partridge, N. C. (1991) Bone Resorption in Vivo. IN Hall, B. K. (Ed.) *Bone: The Osteoclast*. Boca Raton, CRC Press.
- Khosla, S., Melton, L. J., 3rd, Dekutoski, M. B., Achenbach, S. J., Oberg, A. L. & Riggs, B. L. (2003) Incidence of childhood distal forearm fractures over 30 years: a population-based study. *Journal of the American Medical Association*, 290, 1479-1485.
- Kirsch, T., Harrison, G., Worch, K. P. & Golub, E. E. (2000) Regulatory roles of zinc in matrix vesicle-mediated mineralization of growth plate cartilage. *Journal of Bone and Mineral Research*, 15, 261-270.
- Kitagawa, Y., Tamai, K. & Ito, H. (2004) Oral alendronate treatment for polyostotic fibrous dysplasia: a case report. *Journal of Orthopaedic Science*, 9, 521-525.
- Klein-Nulend, J., Nijweide, P. J. & Burger, E. H. (2003) Osteocyte and bone structure. *Current Osteoporosis Reports*, 1, 5-10.
- Knapen, M. H. J., Schurgers, L. J. & Vermeer, C. (2007) Vitamin K-2 supplementation improves hip bone geometry and bone strength indices in postmenopausal women. *Osteoporosis International*, 18, 963-972.
- Kobayashi, T. & Kronenberg, H. (2005) Minireview: Transcriptional regulation in development of bone. *Endocrinology*, 146, 1012-1017.
- Kohler, R., Solla, F., Pinson, S., Romana, C., Chau, E. & Dohin, B. (2005) [Congenital pseudarthrosis of the forearm in a neurofibromatosis patient: case report and review of the literature]. *Revue de Chirurgie Orthopédique et Réparatrice de l'Appareil Moteur*, 91, 773-781.
- Kölliker, A. (1889) *Handbuch der Gewebelehre des Menschen*, Leipzig, W. Engelmann.
- Kontulainen, S., Sievanen, H., Kannus, P., Pasanen, M. & Vuori, I. (2003) Effect of long-term impact-loading on mass, size, and estimated strength of humerus and radius of female racquet-sports players: a peripheral quantitative computed tomography study between young and old starters and controls. *Journal of Bone and Mineral Research*, 18, 352-359.
- Kroger, H., Kotaniemi, A., Vainio, P. & Alhava, E. (1992) Bone densitometry of the spine and femur in children by dual-energy x-ray absorptiometry. *Bone and Mineral*, 17, 75-85.
- Land, C., Rauch, F. & Glorieux, F. H. (2006) Cyclical intravenous pamidronate treatment affects metaphyseal modeling in growing patients with osteogenesis imperfecta. *Journal of Bone and Mineral Research*, 21, 374-379.

- Landin, L. A. (1983) Fracture patterns in children. Analysis of 8,682 fractures with special reference to incidence, etiology and secular changes in a Swedish urban population 1950-1979. *Acta Orthopaedica Scandinavica Supplementum*, 202, 1-109.
- Langlois, J. A., Rosen, C. J., Visser, M., Hannan, M. T., Harris, T., Wilson, P. W. F. & Kiel, D. P. (1998) Association between insulin-like growth factor I and bone mineral density in older women and men: The Framingham Heart Study. *Journal of Clinical Endocrinology and Metabolism*, 83, 4257-4262.
- Laor, T. & Jaramillo, D. (1993) Metaphyseal abnormalities in children: pathophysiology and radiologic appearance. *American Journal of Roentgenology*, 161, 1029-1036.
- Latchman, D. S. (1997) Transcription factors: An overview. *International Journal of Biochemistry & Cell Biology*, 29, 1305-1312.
- Lefebvre, V., Huang, W. D., Harley, V. R., Goodfellow, P. N. & deCrombrugge, B. (1997) SOX9 is a potent activator of the chondrocyte-specific enhancer of the pro alpha 1(II) collagen gene. *Molecular and Cellular Biology*, 17, 2336-2346.
- Leonard, M. B., Shults, J., Elliott, D. M., Stallings, V. A. & Zemel, B. S. (2004) Interpretation of whole body dual energy X-ray absorptiometry measures in children: comparison with peripheral quantitative computed tomography. *Bone*, 34, 1044-52.
- Leveau, B. F. & Bernhardt, D. B. (1984) Developmental Biomechanics - Effect of Forces on the Growth, Development, and Maintenance of the Human-Body. *Physical Therapy*, 64, 1874-1882.
- Lewis, D., Carpenter, C., Evans, A. & Thomas, P. (2007) Rickets and Scurvy presenting in a Child as apparent Non Accidental Injury. *The Internet Journal of Orthopedic Surgery*, 4.
- Li, K. C., Zernicke, R. F., Barnard, R. J. & Li, A. F. Y. (1991) Differential Response of Rat Limb Bones to Strenuous Exercise. *Journal of Applied Physiology*, 70, 554-560.
- Lian, J. B., Stein, G. S., Canalis, E., Robey, P. G. & Boskey, A. L. (1999) Bone Formation: Osteoblast Lineage Cells, Growth Factors, Matrix Proteins, and the Mineralization Process. IN Lian, J. B. & Goldring, S. R. (Eds.) *Primer on the Metabolic Bone Diseases and Disorders of Mineral Metabolism*. 4th ed. Philadelphia, Lippincott, Williams & Wilkins.
- Litchfield, T. M., Ishikawa, Y., Wu, L. N., Wuthier, R. E. & Sauer, G. R. (1998) Effect of metal ions on calcifying growth plate cartilage chondrocytes. *Calcified Tissue International*, 62, 341-349.
- Longas, A. F., Mayayo, E., Valle, A., Soria, J. & Labarta, J. I. (1996) Constitutional delay in growth and puberty: A comparison of final height achieved between treated and untreated children. *Journal of Pediatric Endocrinology & Metabolism*, 9, 345-357.
- Luckman, S. P., Hughes, D. E., Coxon, F. P., Russell, R. G. G. & Rogers, M. J. (1998) Nitrogen-containing bisphosphonates inhibit the mevalonate pathway and prevent post-translational prenylation of GTP-binding proteins, including Ras. *Journal of Bone and Mineral Research*, 13, 581-589.



- Luo, G. B., Ducey, P., McKee, M. D., Pinero, G. J., Loyer, E., Behringer, R. R. & Karsenty, G. (1997) Spontaneous calcification of arteries and cartilage in mice lacking matrix GLA protein. *Nature*, 386, 78-81.
- MacDonald, H., Kontulainen, S., Petit, M., Janssen, P. & McKay, H. (2006) Bone strength and its determinants in pre- and early pubertal boys and girls. *Bone*, 39, 598-608.
- Madenci, E., Yilmaz, K., Yilmaz, M. & Coskun, Y. (2006) Alendronate treatment in osteogenesis imperfecta. *Journal of Clinical Rheumatology*, 12, 53-56.
- Malabanan, A., Veronikis, I. E. & Holick, M. F. (1998) Redefining vitamin D insufficiency. *Lancet*, 351, 805-806.
- Mandalunis, P., Gibaja, F. & Ubios, A. M. (2002) Experimental renal failure and iron overload: a histomorphometric study in the alveolar bone of rats. *Experimental and Toxicologic Pathology*, 54, 85-90.
- Mandalunis, P. & Ubios, A. (2005) Experimental renal failure and iron overload: a histomorphometric study in rat tibia. *Toxicologic Pathology*, 33, 398-403.
- Mansfield, K., Pucci, B., Adams, C. S. & Shapiro, I. M. (2003) Induction of apoptosis in skeletal tissues: Phosphate-mediated chick chondrocyte apoptosis is calcium dependent. *Calcified Tissue International*, 73, 161-172.
- Marini, J. C. (2003) Do Bisphosphonates Make Children's Bones Better or Brittle? *N Engl J Med*, 349, 423-426.
- Marotti, G., Palazzini, S., Palumbo, C. & Ferretti, M. (1996) Ultrastructural evidence of the existence of a dendritic network throughout the cells of the osteogenic lineage: The novel concept of wiring- and volume-transmission in bone. *Bone*, 19, (Iss 3, Suppl 1), 151.
- Martin, R. B. (2003) Fatigue microdamage as an essential element of bone mechanics and biology. *Calcified Tissue International*, 73, 101-107.
- Masterjohn, C. (2007) Vitamin D toxicity redefined: Vitamin K and the molecular mechanism. *Medical Hypotheses*, 68, 1026-1034.
- Mature Long Bone - Femur. (2002) *Index of MedTech Anatomy01* - [www.sweethaven02.com/MedTech/Anatomy01/fig0401.jpg](http://www.sweethaven02.com/MedTech/Anatomy01/fig0401.jpg).
- McLean, F. & Urist, M. (1961) *Bone*, Chicago, University of Chicago Press.
- Medeiros, D. M., Ilich, J., Ireton, J., Matkovic, V., Shiry, L. & Wildman, R. (1997) Femurs from rats fed diets deficient in copper or iron have decreased mechanical strength and altered mineral composition. *Journal of Trace Elements in Experimental Medicine*, 10, 197-203.
- Meikle, M. C., Bord, S., Hembry, R. M., Compston, J., Croucher, P. I. & Reynolds, J. J. (1992) Human osteoblasts in culture synthesize collagenase and other matrix metalloproteinases in response to osteotropic hormones and cytokines. *Journal of Cell Science*, 103 ( Pt 4), 1093-1099.
- Molgaard, C., Thomsen, B. L., Prentice, A., Cole, T. J. & Michaelsen, K. F. (1997) Whole body bone mineral content in healthy children and adolescents. *Archives of Disease in Childhood*, 76, 9-15.
- Moreira-Andres, M. N., Canizo, F. J., de la Cruz, F. J., Gomez-de la Camara, A. & Hawkins, F. G. (1998) Bone mineral status in prepubertal children with constitutional delay of growth and puberty. *European Journal of Endocrinology*, 139, 271-275.

- Morton, J. F. & Guthrie, J. F. (1998) Changes in Children's Total Fat Intakes and Their Food Group Sources of Fat, 1989-91 Versus 1994-95: Implications for Diet Quality. *Family Economics and Nutrition Review*, 11, 44-57.
- Moyer-Mileur, L., Xie, B., Ball, S., Bainbridge, C., Stadler, D. & Jee, W. S. (2001) Predictors of bone mass by peripheral quantitative computed tomography in early adolescent girls. *Journal of Clinical Densitometry*, 4, 313-323.
- Mughal, Z. (2002) Rickets in childhood. *Semin Musculoskelet Radiol*, 6, 183-90.
- Muller, A., Ruegsegger, E. & Ruegsegger, P. (1989) Peripheral QCT: a low-risk procedure to identify women predisposed to osteoporosis. *Physics in Medicine and Biology*, 34, 741-749.
- Müller, F. & O'Rahilly, R. (1986) Somitic-vertebral correlation and vertebral levels in the human embryo. *American Journal of Anatomy*, 177, 3-19.
- Müller, F. & O'Rahilly, R. (2003) Segmentation in staged human embryos: the occipitocervical region revisited. *Journal of Anatomy*, 203, 297-315.
- Mundy, G. R. (1999) *Bone Remodeling and its Disorders*, London, Martin Dunitz Ltd.
- Munroe, P. B., Olgunturk, R. O., Fryns, J. P., Van Maldergem, L., Ziereisen, F., Yuksel, B., Gardiner, R. M. & Chung, E. (1999) Mutations in the gene encoding the human matrix Gla protein cause Keutel syndrome. *Nature Genetics*, 21, 142-144.
- Murray, R. D., Adams, J. E. & Shalet, S. M. (2006) A densitometric and morphometric analysis of the skeleton in adults with varying degrees of growth hormone deficiency. *Journal of Clinical Endocrinology and Metabolism*, 91, 432-438.
- Nara-Ashizawa, N., Liu, L. J., Higuchi, T., Tokuyama, K., Hayashi, K., Shirasaki, Y., Amagai, H. & Saitoh, S. (2002) Paradoxical adaptation of mature radius to unilateral use in tennis playing. *Bone*, 30, 619-623.
- Narisawa, S., Wennberg, C. & Millan, J. L. (2001) Abnormal vitamin B6 metabolism in alkaline phosphatase knock-out mice causes multiple abnormalities, but not the impaired bone mineralization. *Journal of Pathology*, 193, 125-133.
- Nettle, D. (2002) Women's height, reproductive success and the evolution of sexual dimorphism in modern humans. *Proceedings of the Royal Society of London Series B-Biological Sciences*, 269, 1919-1923.
- Neu, C. M., Manz, F., Rauch, F., Merkel, A. & Schoenau, E. (2001a) Bone densities and bone size at the distal radius in healthy children and adolescents: a study using peripheral quantitative computed tomography. *Bone*, 28, 227-232.
- Neu, C. M., Rauch, F., Manz, F. & Schoenau, E. (2001b) Modeling of cross-sectional bone size, mass and geometry at the proximal radius: a study of normal bone development using peripheral quantitative computed tomography. *Osteoporosis International*, 12, 538-47.
- New, S. A., Robins, S. P., Campbell, M. K., Martin, J. C., Garton, M. J., Bolton-Smith, C., Grubb, D. A., Lee, S. J. & Reid, D. M. (2000) Dietary influences on bone mass and bone metabolism: further evidence of a positive link between fruit and vegetable consumption and bone health? *American Journal of Clinical Nutrition*, 71, 142-151.
- Nichols, D. L., Sanborn, C. F., Bonnick, S. L., Ben-Ezra, V. I. C., Gench, B. & DiMarco, N. M. (1994) The effects of gymnastics training on bone mineral density. *Medicine & Science in Sports & Exercise*, 26, 1220-1225.

- Nickols-Richardson, S. M., O'Connor, P. J., Shapses, S. A. & Lewis, R. D. (1999) Longitudinal Bone Mineral Density Changes in Female Child Artistic Gymnasts. *Journal of Bone and Mineral Research*, 14, 994-1002.
- Nielsen, S. P. (2001) The Metacarpal Index Revisited: a brief overview. *Journal of Clinical Densitometry*, 4, 199-207.
- Nieves, J. W., Formica, C., Ruffing, J., Zion, M., Garrett, P., Lindsay, R. & Cosman, F. (2005) Males Have Larger Skeletal Size and Bone Mass Than Females, Despite Comparable Body Size. *Journal of Bone and Mineral Research*, 20, 529-535.
- NIH (1988) Neurofibromatosis Conference Statement National-Institutes-of-Health Consensus Development Conference. *Archives of Neurology*, 45, 575-578.
- Nilsson, O., Marino, R., De Luca, F., Phillip, M. & Baron, J. (2005) Endocrine regulation of the growth plate. *Hormone Research*, 64, 157-165.
- Njeh, C. F. (2004) Radiation Safety Considerations. IN Langman, C. B. & Njeh, C. F. (Eds.) *The Physical Measurement of Bone*. Philadelphia, Institute of Physics Publishing.
- Njeh, C. F. & Shepherd, J. A. (2004) Absorptiometric Measurement. IN Langman, C. B. & Njeh, C. F. (Eds.) *The Physical Measurement of Bone*. Philadelphia, Institute of Physics Publishing.
- O'Rahilly, R. & Gardner, E. (1975) The timing and sequence of events in the development of the limbs in the human embryo. *Anatomy and Embryology*, 148, 1-23.
- Ogawa, T., Yamagiwa, H., Hayami, T., Liu, Z., Huang, K. Y., Tokunaga, K., Murai, T. & Endo, N. (2002) Human PTH (1-34) induces longitudinal bone growth in rats. *Journal of Bone and Mineral Metabolism*, 20, 83-90.
- Osman, M. Z. & Girdany, B. R. (1973) Osteoectasia with Hyperphosphatasia. *Seminars in Roentgenology*, 8, 230.
- Palacios, C. (2006) The role of nutrients in bone health, from A to Z. *Critical Reviews in Food Science and Nutrition*, 46, 621-628.
- Parfitt, A. M. (1994) Osteonal and hemi-osteonal remodeling: the spatial and temporal framework for signal traffic in adult human bone. *Journal of Cellular Biochemistry*, 55, 273-86.
- Parry, N. M. A., Phillipppo, M., Reid, M. D., McGaw, B. A., Flint, D. J. & Loveridge, N. (1993) Molybdenum-Induced Changes in the Epiphyseal Growth-Plate. *Calcified Tissue International*, 53, 180-186.
- Pease, C. N. (1962) Focal Retardation and Arrestment of Growth of Bones Due to Vitamin a Intoxication. *Journal of the American Medical Association*, 182, 980-985.
- Perry, R. J., Farquharson, C. & Ahmed, S. F. (2008) The role of sex steroids in controlling pubertal growth. *Clinical Endocrinology (Oxf)*, 68, 4-15.
- Petit, M. A., Beck, T. J. & Kontulainen, S. A. (2005) Examining the developing bone: What do we measure and how do we do it? *Journal of Musculoskeletal and Neuronal Interactions*, 5, 213-24.
- Petridou, E., Karpathios, T., Dessypris, N., Simou, E. & Trichopoulos, D. (1997) The role of dairy products and non alcoholic beverages in bone fractures among schoolage children. *Scandinavian Journal of Social Medicine*, 25, 119-125.

- Pettersson, U., Nordstrom, P., Alfredson, H., Henriksson-Larsen, K. & Lorentzon, R. (2000) Effect of high impact activity on bone mass and size in adolescent females: A comparative study between two different types of sports. *Calcified Tissue International*, 67, 207-14.
- Pizones, J., Plotkin, H., Parra-Garcia, J. I., Alvarez, P., Gutierrez, P., Bueno, A. & Fernandez-Arroyo, A. (2005) Bone healing in children with osteogenesis imperfecta treated with bisphosphonates. *Journal of Pediatric Orthopaedics*, 25, 332-335.
- Plotkin, H., Rauch, F., Zeitlin, L., Munns, C., Travers, R. & Glorieux, F. H. (2003) Effect of pamidronate treatment in children with polyostotic fibrous dysplasia of bone. *Journal of Clinical Endocrinology & Metabolism*, 88, 4569-4575.
- Pludowski, P., Lebedowski, M. & Lorenc, R. S. (2004) Evaluation of the possibility to assess bone age on the basis of DXA derived hand scans - preliminary results. *Osteoporosis International*, 15, 317-322.
- Prentice, A., Parsons, T. J. & Cole, T. J. (1994) Uncritical use of bone mineral density in absorptiometry may lead to size-related artifacts in the identification of bone mineral determinants. *American Journal of Clinical Nutrition*, 60, 837-842.
- Prentice, A., Schoenmakers, I., Laskey, M. A., de Bono, S., Ginty, F. & Goldberg, G. R. (2006) Nutrition and bone growth and development. *The Proceedings of the Nutrition Society*, 65, 348-360.
- Proudfoot, D. & Shanahan, C. M. (2006) Molecular mechanisms mediating vascular calcification: Role of matrix Gla protein. *Nephrology*, 11, 455-461.
- Quick, J. L., Ward, K. A., Adams, J. E. & Mughal, M. Z. (2006) Cortical bone geometry in asthmatic children. *Archives of Disease in Childhood*, 91, 346-348.
- Rajakumar, K. (2006) Scurvy. IN Schwarz, S., Windle, M., Poth, M. & Bhatia, J. (Eds.) *Nutrition*.
- Ramelli, G. P., Slongo, T., Tschappeler, H. & Weis, J. (2001) Congenital pseudarthrosis of the ulna and radius in two cases of neurofibromatosis type 1. *Paediatric Surgery International*, 17, 239-241.
- Rauch, F. (2006) Material matters: a mechanostat-based perspective on bone development in osteogenesis imperfecta and hypophosphatemic rickets. *Journal of Musculoskeletal and Neuronal Interactions*, 6, 142-146.
- Rauch, F., Cornibert, S., Cheung, M. & Glorieux, F. H. (2007) Long-bone changes after pamidronate discontinuation in children and adolescents with osteogenesis imperfecta. *Bone*, 40, 821-827.
- Rauch, F., Neu, C., Manz, F. & Schoenau, E. (2001a) The development of metaphyseal cortex--implications for distal radius fractures during growth. *Journal of Bone and Mineral Research*, 16, 1547-1555.
- Rauch, F. & Schoenau, E. (2005) Peripheral quantitative computed tomography of the distal radius in young subjects - new reference data and interpretation of results. *Journal of Musculoskeletal and Neuronal Interactions*, 5, 119-26.
- Rauch, F., Tuttlewski, B., Fricke, O., Rieger-Wettengl, G., Schauseil-Zipf, U., Herkenrath, P., Neu, C. M. & Schoenau, E. (2001b) Analysis of cancellous bone turnover by multiple slice analysis at distal radius: a study using peripheral quantitative computed tomography. *Journal of Clinical Densitometry*, 4, 257-262.

- Rauch, F., Tuttlewski, B. & Schoenau, E. (2001c) Peripheral quantitative computed tomography at the distal radius: cross-calibration between two scanners. *Journal of Musculoskeletal and Neuronal Interactions*, 2, 153-155.
- Reynolds, N., Blumsohn, A., Baxter, J. P., Houston, G. & Pennington, C. R. (1998) Manganese requirement and toxicity in patients on home parenteral nutrition. *Clinical Nutrition*, 17, 227-230.
- Ridanpaa, M., Jain, P., McKusick, V. A., Francomano, C. A. & Kaitila, I. (2003) The major mutation in the RMRP gene causing CHH among the Amish is the same as that found in most Finnish cases. *American Journal of Medical Genetics Part C-Seminars in Medical Genetics*, 121C, 81-83.
- Ridanpaa, M., van Eenennaam, H., Pelin, K., Chadwick, R., Johnson, C., Yuan, B., vanVenrooij, W., Pruijn, G., Salmela, R., Rockas, S., Makitie, O., Kaitila, I. & de la Chapelle, A. (2001) Mutations in the RNA component of RNase MRP cause a pleiotropic human disease, cartilage-hair hypoplasia. *Cell*, 104, 195-203.
- Roche, A., Chumlea, W. & Thissen, D. (1988) *Assessing the skeletal maturity of the hand-wrist: FELS method*, Springfield, IL, Charles C. Thomas.
- Rockell, J. E. P., Williams, S. M., Taylor, R. W., Grant, A. M., Jones, I. E. & Goulding, A. (2005) Two-year changes in bone and body composition in young children with a history of prolonged milk avoidance. *Osteoporosis International*, 16, 1016-1023.
- Rodda, R. A. (1975) Bone growth changes in pyridoxine-deficient rats. *Journal of Pathology*, 117, 131-137.
- Rodriguez, J. P., Rios, S. & Gonzalez, M. (2002) Modulation of the proliferation and differentiation of human mesenchymal stem cells by copper. *Journal of Cellular Biochemistry*, 85, 92-100.
- Roldan, E. J., Capigliani, R., Cointry, C. R., Capozza, R. F. & Ferretti, J. L. (2001) Postmenopausal changes in the distribution of the volumetric BMD of cortical bone. A pQCT study of the human leg. *Journal of Musculoskeletal and Neuronal Interactions*, 2, 157-162.
- Rosen, C. J. (2004) Anatomy, Physiology and Disease. IN Langton, C. M. & Njeh, C. F. (Eds.) *The Physical Measurement of Bone*. London, Institute of Physics Publishing Ltd.
- Rossi, L., Migliaccio, S., Corsi, A., Marzia, M., Bianco, P., Teti, A., Gambelli, L., Cianfarani, S., Paoletti, F. & Branca, F. (2001) Reduced growth and skeletal changes in zinc-deficient growing rats are due to impaired growth plate activity and inanition. *Journal of Nutrition*, 131, 1142-1146.
- Rubin, C. T. & Lanyon, L. E. (1984) Regulation of Bone-Formation by Applied Dynamic Loads. *Journal of Bone and Joint Surgery-American Volume*, 66A, 397-402.
- Rude, R. K., Gruber, H. E., Wei, L. Y., Frausto, A. & Mills, B. G. (2003) Magnesium deficiency: effect on bone and mineral metabolism in the mouse. *Calcified Tissue International*, 72, 32-41.
- Sabin, A. (1939) Vitamin C in Relation to experimental Poliomyelitis: With Incidental Observations on Certain Manifestations in Macacus Rhesus Monkeys on a Scorbutic Diet. *Journal of Experimental Medicine*, 69, 507-515.

- Saggese, G., Baroncelli, G. I. & Bertelloni, S. (2001) Osteoporosis in children and adolescents: Diagnosis, risk factors, and prevention. *Journal of Pediatric Endocrinology & Metabolism*, 14, 833-859.
- Schiessl, H., Ferretti, J. L., Tysarczyk-Niemeyer, G. & Willnecker, J. (1996) Noninvasive bone strength index as analysed by peripheral quantitative computed tomography (pQCT). IN Schoenau, E. (Ed.) *Paediatric Osteology: New Developments in Diagnostics and Therapy*. 1st ed. Cologne, Germany, Elsevier Science.
- Schiessl, H., Frost, H. M. & Jee, W. S. (1998) Estrogen and bone-muscle strength and mass relationships. *Bone*, 22, 1-6.
- Schoenau, E. (2005) From mechanostat theory to development of the "Functional Muscle-Bone-Unit". *Journal of Musculoskeletal and Neuronal Interactions*, 5, 232-8.
- Schoenau, E. & Frost, H. M. (2002) The "muscle-bone unit" in children and adolescents. *Calcified Tissue International*, 70, 405-407.
- Schoenau, E., Neu, C. M., Beck, B., Manz, F. & Rauch, F. (2002a) Bone mineral content per muscle cross-sectional area as an index of the functional muscle-bone unit. *Journal of Bone and Mineral Research*, 17, 1095-101.
- Schoenau, E., Neu, C. M., Rauch, F. & Manz, F. (2002b) Gender-specific pubertal changes in volumetric cortical bone mineral density at the proximal radius. *Bone*, 31, 110-113.
- Sekiya, I., Tsuji, K., Koopman, P., Watanabe, H., Yamada, Y., Shinomiya, K., Nifuji, A. & Noda, M. (2000) SOX9 enhances aggrecan gene promoter/enhancer activity and is up-regulated by retinoic acid in a cartilage-derived cell line, TC6. *Journal of Biological Chemistry*, 275, 10738-10744.
- Senthilnathan, S., Walker, E. & Bishop, N. J. (2008) Two doses of pamidronate in infants with osteogenesis imperfecta. *Archives of Disease in Childhood*, 93, 398-400.
- Shaw, N. J. & Bishop, N. J. (2005) Bisphosphonate treatment of bone disease. *Archives of Disease in Childhood*, 90, 494-499.
- Shearer, M. J. (1995) Vitamin K. *Lancet*, 345, 229-234.
- Shepherd, J., Meta, M., Landau, J., Sherrer, Y., Goddard, D., Ovalle, M., Rosholm, A. & Genant, H. (2005) Metacarpal index and bone mineral density in healthy African-American women. *Osteoporosis International*, 16, 1621-1626.
- Shiang, R., Thompson, L. M., Zhu, Y. Z., Church, D. M., Fielder, T. J., Bocian, M., Winokur, S. T. & Wasmuth, J. J. (1994) Mutations in the Transmembrane Domain of Fgfr3 Cause the Most Common Genetic Form of Dwarfism, Achondroplasia. *Cell*, 78, 335-342.
- Shih, C., Chang, C. Y., Penn, I. W., Tiu, C. M., Chang, T. & Wu, J. J. (1995) Chronically stressed wrists in adolescent gymnasts: MR imaging appearance. *Radiology*, 195, 855-859.
- Shore, R. M. & Poznanski, A. K. (1999) Radiologic Evaluation of Bone Mineral in Children. IN Langman, C. B. & Shoback, D. M. (Eds.) *Primer on the Metabolic Bone Diseases and Disorder of Mineral Metabolism*. 4th ed. Philadelphia, Lippincott Williams & Wilkins.

- Siu, W. S., Qin, L. & Leung, K. S. (2003) pQCT bone strength index may serve as a better predictor than bone mineral density for long bone breaking strength. *Journal of Bone and Mineral Metabolism*, 21, 316-322.
- Sjogren, K., Sheng, M., Moverare, S., Liu, J. L., Wallenius, K., Tornell, O., Isaksson, O., Jansson, J. O., Mohan, S. & Ohlsson, C. (2002) Effects of liver-derived insulin-like growth factor I on bone metabolism in mice. *Journal of Bone and Mineral Research*, 17, 1977-1987.
- Skerry, T. M., Bitensky, L., Chayen, J. & Lanyon, L. E. (1989) Early strain-related changes in enzyme activity in osteocytes following bone loading in vivo. *Journal of Bone and Mineral Research*, 4, 783-788.
- Skerry, T. M. & Peet, N. M. (1997) "Unloading" exercise increases bone formation in rats. *Journal of Bone and Mineral Research*, 12, O6-O6.
- Slatopolsky, E., Brown, A. & Dusso, A. (1999) Pathogenesis of Secondary Hyperparathyroidism. *Kidney International*, 56, S14-S19.
- Slomianka, L. (2006) Blue Histology - Skeletal Tissues - Bone. *School of Anatomy and Human Biology - The University of Western Australia*.
- Smith, B. J., King, J. B., Lucas, E. A., Akhter, M. P., Arjmandi, B. H. & Stoecker, B. J. (2002) Skeletal Unloading and Dietary Copper Depletion Are Detrimental to Bone Quality of Mature Rats. *Journal of Nutrition*, 132, 190-196.
- Smith, E. P., Boyd, J., Frank, G. R., Takahashi, H., Cohen, R. M., Specker, B., Williams, T. C., Lubahn, D. B. & Korach, K. S. (1994) Estrogen Resistance Caused by a Mutation in the Estrogen-Receptor Gene in a Man. *New England Journal of Medicine*, 331, 1056-1061.
- Smith, J. W. (1960) The Arrangement of Collagen Fibres in Human Secondary Osteones. *Journal of Bone and Joint Surgery*, 42-B, 588-605.
- Snapper, I. (1957) *Bone Disease in Medical Practice*, New York, Grune and Stratton.
- Sommerfeldt, D. W. & Rubin, C. T. (2001) Biology of bone and how it orchestrates the form and function of the skeleton. *European Spine Journal*, 10, S86-S95.
- Spector, R. (1978) Vitamin B6 transport in the central nervous system: in vivo studies. *Journal of Neurochemistry*, 30, 881-887.
- Sprague, B. L. & Brown, G. A. (1974) Congenital pseudarthrosis of the radius. *The Journal of Bone and Joint Surgery: American Volume*, 56, 191-194.
- Standeven, A. M., Davies, P. J., Chandraratna, R. A., Mader, D. R., Johnson, A. T. & Thomazy, V. A. (1996) Retinoid-induced epiphyseal plate closure in guinea pigs. *Fundamental and Applied Toxicology*, 34, 91-98.
- Stark, Z. & Savarirayan, R. (2009) Osteopetrosis. *Orphanet Journal of Rare Diseases*, 4, 5.
- Steel, S. A., Baker, A. J. & Saunderson, J. R. (1998) An assessment of the radiation dose to patients and staff from a Lunar Expert-XL fan beam densitometer. *Physiological Measurement*, 19, 17-26.
- Stengel, S. V., Kemmler, W., Pintag, R., Beeskow, C., Weineck, J., Lauber, D., Kalender, W. A. & Engelke, K. (2005) Power training is more effective than strength training for maintaining bone mineral density in postmenopausal women. *Journal of Applied Physiology*, 99, 181-188.
- Stevenson, D. A., Birch, P. H., Friedman, J. M., Viskochil, D. H., Balestrazzi, P., Boni, S., Buske, A., Korf, B. R., Niimura, M., Pivnick, E. K., Schorry, E. K., Short, M.

- P., Tenconi, R., Tonggard, J. H. & Carey, J. C. (1999) Descriptive analysis of tibial pseudarthrosis in patients with neurofibromatosis 1. *American Journal of Medical Genetics*, 84, 413-419.
- Strause, L. G., Hegenauer, J., Saltman, P., Cone, R. & Resnick, D. (1986) Effects of Long-Term Dietary Manganese and Copper Deficiency on Rat Skeleton. *Journal of Nutrition*, 116, 135-141.
- Superti-Furga, A., Unger, S. & Society, N. G. o. t. I. S. D. (2007) Nosology and classification of genetic skeletal disorders: 2006 revision. *American Journal of Medical Genetics Part A*, 143A, 1-18.
- Takata, S., Nishimura, G., Ikegawa, S., Kuroda, Y., Nishino, M., Matsui, Y. & Yasui, N. (2006) Metaphyseal dysplasia of Braun-Tinschert type: Report of a Japanese girl. *American Journal of Medical Genetics Part A*, 140A, 1234-1237.
- Tanner, J. (1962) *Growth at Adolescence: with a general consideration of the effects of hereditary and environmental factors upon growth and maturation from birth to maturity* Oxford, Blackwell Scientific Publications Ltd.
- Tanner, J., Healy, M., Goldstein, H. & Cameron, N. (2001) *Assessment of Skeletal Maturity and Prediction of Adult Height (TW3 Method)*, London, Saunders.
- Tanner, J., Whitehouse, R., Cameron, N., Marshall, W., Healy, M. & Goldstein, H. (1983) *Assessment of Skeletal Maturity and Prediction of Adult Height (TW2 Method)*, London, Academic Press, Harcourt Brace Jovanovich.
- Tanner, J., Whitehouse, R. & Healy, M. (1962) *A New System for Estimating Skeletal Maturity from the Hand and Wrist, with Standards Derived from a Study of 2,600 Healthy British Children. Part II: The Scoring System*, Paris, International Children's Centre.
- Tavormina, P. L., Bellus, G. A., Webster, M. K., Bamshad, M. J., Fraley, A. E., McIntosh, I., Szabo, J., Jiang, W., Jabs, E. W., Wilcox, W. R., Wasmuth, J. J., Donoghue, D. J., Thompson, L. M. & Francomano, C. A. (1999) A novel skeletal dysplasia with developmental delay and acanthosis nigricans is caused by a Lys650Met mutation in the fibroblast growth factor receptor 3 gene. *American Journal of Human Genetics*, 64, 722-731.
- Tavormina, P. L., Shiang, R., Thompson, L. M., Zhu, Y. Z., Wilkin, D. J., Lachman, R. S., Wilcox, W. R., Rimoin, D. L., Cohn, D. H. & Wasmuth, J. J. (1995) Thanatophoric Dysplasia (Type-I and Type-II) Caused by Distinct Mutations in Fibroblast Growth-Factor Receptor-3. *Nature Genetics*, 9, 321-328.
- Thorpe, J. A. & Steel, S. A. (1999) Image resolution of the Lunar Expert-XL. *Osteoporosis International*, 10, 95-101.
- Todd, T. (1930) The anatomical features of epiphyseal union. *Child Development*, 1, 186-194.
- Tothill, P. (1989) Methods of bone mineral measurement. *Physics in Medicine and Biology*, 34, 543-572.
- Trang, H. M., Cole, D. E. C., Rubin, L. A., Pierratos, A., Siu, S. & Vieth, R. (1998) Evidence that vitamin D-3 increases serum 25-hydroxyvitamin D more efficiently than does vitamin D-2. *American Journal of Clinical Nutrition*, 68, 854-858.
- Trueta, J. & Amato, V. P. (1960) THE VASCULAR CONTRIBUTION TO OSTEOGENESIS: III. Changes in the Growth Cartilage Caused by



- Experimentally Induced Ischaemia. *Journal of Bone Joint Surgery*, 42-B, 571-587.
- Umemura, Y., Ishiko, T., Tsujimoto, H., Miura, H., Mokushi, N. & Suzuki, H. (1995) Effects of Jump Training on Bone Hypertrophy in Young and Old Rats. *International Journal of Sports Medicine*, 16, 364-367.
- Vaananen, H. K., Zhao, H., Mulari, M. & Halleen, J. M. (2000) The cell biology of osteoclast function. *Journal of Cell Science*, 113, 377-381.
- Vajo, Z., Francomano, C. A. & Wilkin, D. J. (2000) The molecular and genetic basis of fibroblast growth factor receptor 3 disorders: The achondroplasia family of skeletal dysplasias, Muenke craniosynostosis, and Crouzon syndrome with acanthosis nigricans. *Endocrine Reviews*, 21, 23-39.
- van Donkelaar, C. C. & Huisjes, R. (2007) The PTHrP-Ihh feedback loop in the embryonic growth plate allows PTHrP to control hypertrophy and Ihh to regulate proliferation. *Biomechanics and Modeling in Mechanobiology*, 6, 55-62.
- van Donkelaar, C. C., Janssen, X. J. A. & de Jong, A. M. (2007) Distinct developmental changes in the distribution of calcium, phosphorus and sulphur during fetal growth-plate development. *Journal of Anatomy*, 210, 186-194.
- van Summeren, M. J., van Coeverden, S. C., Schurgers, L. J., Braam, L. A., Noirt, F., Uiterwaal, C. S., Kuis, W. & Vermeer, C. (2008) Vitamin K status is associated with childhood bone mineral content. *British Journal of Nutrition*, 1-7.
- Vanderschueren, D., Vandenput, L., Boonen, S., Lindberg, M. K., Bouillon, R. & Ohlsson, C. (2004) Androgens and bone. *Endocrine Reviews*, 25, 389-425.
- Venken, K., Schuit, F., Van Lommel, L., Tsukamoto, K., Kopchick, J. J., Coschigano, K., Ohlsson, C., Moverare, S., Boonen, S., Bouillon, R. & Vanderschueren, D. (2005) Growth without growth hormone receptor: Estradiol is a major growth hormone-independent regulator of hepatic IGF-I synthesis. *Journal of Bone and Mineral Research*, 20, 2138-2149.
- Virtama, P. & Mahonen, H. (1960) Thickness of the cortical layer as an estimate of mineral content of human finger bones. *British Journal of Radiology*, 33, 60-62.
- Wagner, C. L. & Greer, F. R. (2008) Prevention of Rickets and Vitamin D Deficiency in Infants, Children, and Adolescents. *Pediatrics*, 122, 1142-1152.
- Wallwork, J. C. & Sandstead, H. H. (1990) Zinc. IN Simmons, D. J. (Ed.) *Nutrition and Bone Development* New York, Oxford University Press.
- Wang, J., Zhou, J. & Bondy, C. A. (1999) Igf1 promotes longitudinal bone growth by insulin-like actions augmenting chondrocyte hypertrophy. *Faseb Journal*, 13, 1985-1990.
- Wang, Q. J., Alen, M., Nicholson, P., Lyytikainen, A., Suuriniemi, M., Helkala, E., Suominen, H. & Cheng, S. L. (2005) Growth patterns at distal radius and tibial shaft in pubertal girls: a 2-year longitudinal study. *Journal of Bone and Mineral Research*, 20, 954-961.
- Wang, W. & Kirsch, T. (2002) Retinoic acid stimulates annexin-mediated growth plate chondrocyte mineralization. *Journal of Cell Biology*, 157, 1061-1069.
- Ward, K., Cowell, C. T. & Little, D. G. (2005a) Quantification of metaphyseal modeling in children treated with bisphosphonates. *Bone*, 36, 999-1002.
- Ward, K., Mughal, M. Z. & Adams, J. E. (2007a) Tools for Measuring Bone in Children and Adolescents. IN Sawyer, A. J., Bachrach, L. K. & Fung, E. B. (Eds.) *Bone*

- Densitometry in Growing Patients: Guides for Clinical Practice*. New Jersey, Humana Press.
- Ward, K. A., Ashby, R. L., Roberts, S. A., Adams, J. E. & Zulf Mughal, M. (2007b) UK reference data for the Hologic QDR Discovery dual-energy x ray absorptiometry scanner in healthy children and young adults aged 6-17 years. *Archives of Disease in Childhood*, 92, 53-59.
- Ward, K. A., Caulton, J. M., Adams, J. E. & Mughal, M. Z. (2006) Perspective: cerebral palsy as a model of bone development in the absence of postnatal mechanical factors. *Journal of Musculoskeletal and Neuronal Interactions*, 6, 154-159.
- Ward, K. A., Roberts, S. A., Adams, J. E. & Mughal, M. Z. (2005b) Bone geometry and density in the skeleton of pre-pubertal gymnasts and school children. *Bone*, 36, 1012-1018.
- Weinmann, J. & Sicher, H. (1955) *Bone and Bones*, St Louis, CV Mosby.
- Wenzel, A., Droschl, H. & Melsen, B. (1984) Skeletal Maturity in Austrian Children Assessed by the GP and TW-2 Methods. *Annals of Human Biology*, 11, 173-177.
- Whitehouse, R. W. (2002) Paget's disease of bone. *Seminars in Musculoskeletal Radiology*, 6, 313-322.
- Whyte, M. P., McAlister, W. H., Novack, D. V., Clements, K. L., Schoenecker, P. L. & Wenkert, D. (2008) Bisphosphonate-Induced Osteopetrosis: Novel Bone Modeling Defects, Metaphyseal Osteopenia, and Osteosclerosis Fractures After Drug Exposure Ceases. *Journal of Bone and Mineral Research*, 23, 1698-1707.
- Whyte, M. P., Singhellakis, P. N., Petersen, M. B., Davies, M., Totty, W. G. & Mumm, S. (2007) Juvenile Paget's disease: The second reported, oldest patient is homozygous for the TNFRSF11B "Balkan" mutation (966\_969delTGACinsCTT), which elevates circulating immunoreactive osteoprotegerin levels. *Journal of Bone and Mineral Research*, 22, 938-946.
- Whyte, M. P., Wenkert, D., Clements, K. L., McAlister, W. H. & Mumm, S. (2003) Brief report: Bisphosphonate-induced osteopetrosis. *New England Journal of Medicine*, 349, 457-463.
- Wiley, G. (2005) The Prophet Motive: How PACS was Developed and Sold. *Imaging Economics*.
- Williams, G. R., Robson, H. & Shalet, S. M. (1998) Thyroid hormone actions on cartilage and bone: interactions with other hormones at the epiphyseal plate and effects on linear growth. *Journal of Endocrinology*, 157, 391-403.
- Williams, V. C., Lucas, J., Babcock, M. A., Gutmann, D. H., Korf, B. & Maria, B. L. (2009) Neurofibromatosis Type 1 Revisited. *Pediatrics*, 123, 124-133.
- Wolbach, S. B. (1947) Vitamin-a Deficiency and Excess in Relation to Skeletal Growth. *Journal of Bone and Joint Surgery*, 29, 171-192.
- Wolff, J. (1892) *Das Gesetz der Transformation der Knochen (The Law of Bone Remodelling)*, Berlin, Hirschwald (Springer-Verlag, 1986).
- Wolpert, L. (1999) Vertebrate Limb Development and Malformations. *Pediatric Research*, 46, 247-254.
- Wu, S. F., Palese, T., Mishra, O. P., Delivoria-Papadopoulos, M. & De Luca, F. (2003) Effects of Ca<sup>2+</sup>-sensing receptor activation in the growth plate. *Faseb Journal*, 17, 143-145.

- Xie, W. F., Zhang, X., Sakano, S., Lefebvre, V. & Sandell, L. J. (1999) Trans-activation of the mouse cartilage-derived retinoic acid-sensitive protein gene by Sox9. *Journal of Bone and Mineral Research*, 14, 757-763.
- Yakar, S., Rosen, C. J., Beamer, W. G., Ackert-Bicknell, C. L., Wu, Y., Liu, J.-L., Ooi, G. T., Setser, J., Frystyk, J., Boisclair, Y. R. & LeRoith, D. (2002) Circulating levels of IGF-1 directly regulate bone growth and density. *The Journal of Clinical Investigation*, 110, 771-781.
- Yoshida, C. A., Yamamoto, H., Fujita, T., Furuichi, T., Ito, K., Inoue, K. I., Yamana, K., Zanma, A., Takada, K., Ito, Y. & Komori, T. (2004) Runx2 and Runx3 are essential for chondrocyte maturation, and Runx2 regulates limb growth through induction of Indian hedgehog. *Genes & Development*, 18, 952-963.
- You, L., Cowin, S. C., Schaffler, M. B. & Weinbaum, S. (2001) A model for strain amplification in the actin cytoskeleton of osteocytes due to fluid drag on pericellular matrix. *Journal of Biomechanics*, 34, 1375-1386.
- Young, M. F., Kerr, J. M., Ibaraki, K., Heegaard, A. M. & Robey, P. G. (1992) Structure, expression, and regulation of the major noncollagenous matrix proteins of bone. *Clinical Orthopaedics and Related Research*, 275-94.
- Yu, X., Chen, S., Potter, O. L., Murthy, S. M., Li, J., Pulcini, J. M., Ohashi, N., Winata, T., Everett, E. T., Ingram, D., Clapp, W. D. & Hock, J. M. (2005) Neurofibromin and its inactivation of Ras are prerequisites for osteoblast functioning. *Bone*, 36, 793-802.
- Zelzer, E. & Olsen, B. R. (2003) The genetic basis for skeletal diseases. *Nature*, 423, 343-348.
- Zemel, B., Bass, S., Binkley, T., Ducher, G., Macdonald, H., McKay, H., Moyer-Mileur, L., Shepherd, J., Specker, B., Ward, K. & Hans, D. (2008) Peripheral Quantitative Computed Tomography in Children and Adolescents: The 2007 ISCD Pediatric Official Positions. *Journal of clinical densitometry: the official journal of the International Society for Clinical Densitometry*, 11, 59-74.
- Zemel, B. S. & Petit, M. (2007) Evaluation. IN Sawyer, A. J., Bachrach, L. K. & Fung, E. B. (Eds.) *Bone Densitometry in Growing Patients: Guides for Clinical Practice*. New Jersey, Humana Press.
- Zuscik, M. J., D'Souza, M., Gunter, K. K., Gunter, T. E., O'Keefe, R. J., Schwarz, E. M., Puzas, J. E. & Rosier, R. N. (2002) Growth plate chondrocyte maturation is regulated by basal intracellular calcium. *Experimental Cell Research*, 276, 310-319.

## 12. Appendices

### 12.1 Appendix 1 – Abstracts and Posters

#### **ASSESSMENT OF THE METAPHYSEAL INDEX TO STUDY BONE DEVELOPMENT OF THE DISTAL RADIUS IN HEALTHY CHILDREN**

*LC Reddie<sup>1</sup>, JE Adams<sup>1</sup>, KA Ward<sup>1</sup>*

<sup>1</sup> Clinical Radiology, Imaging Science and Biomedical Engineering, School of Cancer and Imaging Science, University of Manchester, Stopford Building, Oxford Road, Manchester, M13 9PT, UK

The Metaphyseal Index (MI) has been proposed as an outcome to study bone development during childhood and studies metaphyseal width in comparison to growth plate width. During longitudinal bone growth a rapid reshaping and remodelling process occurs known as metaphyseal inwaisting. In a healthy child, metaphyseal inwaisting results in proportional decreases in metaphyseal width and increases in growth plate width, thus the MI remains constant. In situations where normal bone growth is impaired, the MI will be altered. To date, reference values for the MI have been calculated and applied to the femur in only one study. However, the most commonly taken radiograph in children is that of the hand and forearm.


The aim of this study was to investigate the development of the distal radius MI and to compare two methods of measuring MI.

Postero-Anterior hand radiographs of 67 healthy white Caucasian children (34 male) aged 5-18 years were taken and digitised using a Vidar radiograph scanner. Two methods were used to measure MI: 1) Semi automated computerised method: After orientation and magnification of each radiograph, a region of interest was defined from the growth plate to the metaphysis (at 0.5 distal radius growth plate width (GPW)); a computer program (Leica QWin©) provides automated measurements of GPW and 0.5GPW. 2) Manual method: manual calliper measurements (Lineartools Electronic Digital Calliper) of the GPW and 0.5GPW were made. 20 repeat MI's were measured for each method. One-way ANOVA was used to calculate precision (co-efficient of variation, CV%).

The CV's for the semi-automated method = 0.98% (0.5W), 0.94% (GPW) and 0.97% (MI). The CV's for the manual method = 1.24% (0.5W), 2.73% (GPW) and 2.90% (MI). Precision is better using the semi automated method.

Using a semi-automated computerised method to measure MI in the distal radius in children is a quick and precise way to assess bone growth and development. With the creation of a larger reference database, it has the potential to be used in assessing metaphyseal inwaisting of children with clinical conditions, or undergoing treatments that may affect bone development.


**Abstract 12.1A: Abstract submitted and accepted to the National Osteoporosis Society Conference, Edinburgh 2007.**



MANCHESTER  
UNIVERSITY

# Assessment of the Metaphyseal Index to Study Bone Development of the Distal Radius in Healthy Children.

\*Reddie LCR, \*Adams JE, \*Ward KA  
\*Clinical Radiology, Imaging Sciences & Biomedical Engineering, University of Manchester, Manchester UK



ISBE  
Imaging Science and  
Biomedical Engineering

---

## Introduction

>During longitudinal bone growth, a rapid reshaping and remodelling process occurs known as metaphyseal inwaisting. In a healthy child, metaphyseal inwaisting results in proportional decreases in metaphyseal width and increases in growth plate width.  
 >The Metaphyseal Index (MI) compares metaphyseal width to growth plate width. During normal growth, changes in metaphyseal width and growth plate width are proportional. When normal bone growth is impaired, the MI may be altered, increasing skeletal fragility.  
 >Reference values for children have been calculated for the distal femur MI<sup>(1)</sup>. However, the most commonly performed radiograph in children is that of the hand and forearm for bone-ageing purposes.

**Primary Aim:**

>To compare two methods of measuring the distal radius MI; manual and computer assisted.

## Table 1: Example of Computer Measurement Output

Features	2		
Number	X FCP	Y FCP	Width (mm)
1	1062	469	29.289
2	992	779	21.611

Table 1: Feature 1 = GPW, Feature 2 = MW, X and Y FCP = feature count point (pixel co-ordinates).  
 MI = 0.5MW / GPW

---

## Methods

Postero-anterior hand radiographs of 205 healthy white Caucasian children (79 male), aged 5-18 years were obtained and digitised using a Canon EOS 20D (with Canon Macro lens EF 100mm auto focus) digital camera. Two methods were used to measure MI:  
 >Semi automated computerised method: the computer program QWin by Leica Microsystems (Milton Keynes, UK), provided automated measurements of the distal radius growth plate width (GPW) and the metaphyseal width (MW). After setting the correct calibration, the GPW was measured. Half of the GPW was used to calculate the metaphysis measurement point and then the MW was measured. MI = 0.5MW / GPW  
 >Manual method: manual calliper measurements of the GPW and MW were made using the Lineartools Electronic Digital Calliper (Middlesex, UK).  
 >30 repeat MI's were measured for each method. One-way ANOVA was used to calculate precision (co-efficient of variation, CV%).

## Results

### Table 2: Precision Results – Manual vs. Computer

Measurements	CV %
Manual 0.5MW	1.81%
Manual GPW	2.35%
Manual MI	2.91%
Computer Assisted 0.5MW	0.92%
Computer Assisted GPW	1.28%
Computer Assisted MI	1.05%

CV% = (within subject standard deviation / mean) x 100

---

## Conclusion

Using a semi-automated computerised method to measure MI in the distal radius in children is a quick and precise way to assess bone growth and development. With the creation of a larger reference database, computer assisted measurement of the MI has the potential to be used in assessing metaphyseal inwaisting of children with clinical conditions<sup>(2)</sup>, or undergoing treatments, that may affect bone development.

## References

- 1) Ward, K., Cowell, C. T. & Little, D. G. (2005) Quantification of metaphyseal modeling in children treated with bisphosphonates. *Bone*, 36, 999-1002.
- 2) Land, C., Rauch, F. & Glorieux, F. H. (2006) Cyclical intravenous pamidronate treatment affects metaphyseal modeling in growing patients with osteogenesis imperfecta. *Journal of Bone and Mineral Research*, 21, 374-379.

Primary Author Contact: [lianne.reddie@student.manchester.ac.uk](mailto:lianne.reddie@student.manchester.ac.uk)

---

## Figure 1: Computer Assisted Measurement of MI

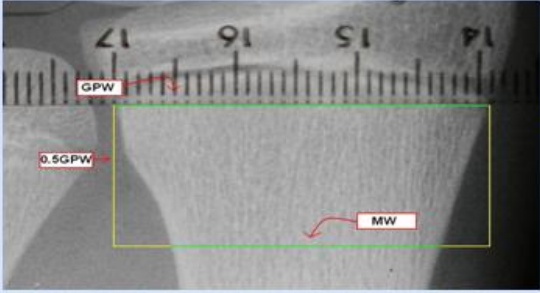


Fig 1: Bone edge detection is performed by the operator. The computer measures the green lines and discards the yellow lines.

## References

- 1) Ward, K., Cowell, C. T. & Little, D. G. (2005) Quantification of metaphyseal modeling in children treated with bisphosphonates. *Bone*, 36, 999-1002.
- 2) Land, C., Rauch, F. & Glorieux, F. H. (2006) Cyclical intravenous pamidronate treatment affects metaphyseal modeling in growing patients with osteogenesis imperfecta. *Journal of Bone and Mineral Research*, 21, 374-379.

Primary Author Contact: [lianne.reddie@student.manchester.ac.uk](mailto:lianne.reddie@student.manchester.ac.uk)

Figure 12.1A: Poster displayed at the National Osteoporosis Society Conference, Edinburgh 2007.

## The Metaphyseal Index for Assessing Development of the Distal Radius

*LC Reddie<sup>1</sup>, KA Ward<sup>1</sup>, MZ Mughal<sup>2</sup>, SM Astley<sup>1</sup>, JE Adams<sup>1</sup>*

<sup>1</sup> Clinical Radiology, Imaging Science and Biomedical Engineering, School of Cancer and Imaging Science, University of Manchester, Stopford Building, Oxford Road, Manchester, M13 9PT, United Kingdom

<sup>2</sup> St Mary's Hospital for Women & Children, Department of Paediatric Medicine, Hathersage Road, Manchester, M13 0JH, United Kingdom

### Introduction

During skeletal growth and maturation remodelling of the ends of long bones, a process occurs known as metaphyseal inwaisting. In a healthy child, metaphyseal inwaisting results in proportional decreases in metaphyseal width (MW) and increases in growth plate width (GPW). The Metaphyseal Index (MI) compares MW to GPW. MI of the distal femur has been examined (Ward et al, 2005; Land et al, 2006). However, the most commonly performed radiograph in children is the hand/forearm for bone-ageing.

**Primary Aim:** To examine distal radius morphology, measure MI in healthy children and compare these reference data to examples from different disease/athlete groups, specifically Neurofibromatosis type 1 (NF1) and gymnasts.

**Hypotheses:** The gymnast group would show a similar age distribution of MI to the normal group but with higher MI values; The NF1 group would show a similar age distribution of MI to the normal group but with lower MI values.

### Materials and Methods

Posterior-anterior hand radiographs of 378 (156 male) healthy white Caucasian children, 36 (15 male) healthy gymnasts and 17 (6 male) children with NF1, aged between 5 and 19 years were digitised and semi-automated measurements of GPW and MW were obtained using QWin by Leica Microsystems (Milton Keynes, UK).  $MI = 0.5MW / GPW$ .

### Results

The MI increases with age in both sexes and all groups, then levels off in the teenage years. Mean MI results: Normal group: 0.351 ( $\pm 0.018$  SD); Gymnast group: 0.335 ( $\pm 0.015$  SD); NF1 group: 0.339 ( $\pm 0.023$  SD).

### Discussion

Unexpectedly, the mean MI of the gymnast group was similar to that of the NF1 group. This may be due to small sample size. Age and gender matching with normal controls is in progress and may shed further light on these results.

### References

- 1) Ward, K., Cowell, C.T., & Little, D.G. (2005) Quantification of metaphyseal modeling in children treated with bisphosphonates. *Bone*, 36, 999-1002.
- 2) Land, C., Rauch, F. & Glorieux, F.H. (2006) Cyclical intravenous pamidronate treatment affects metaphyseal modeling in growing patients with osteogenesis imperfecta. *J. Bone. Miner. Res.* 21, 374-379.

**Abstract 12.1B: Abstract submitted and accepted at the Joint Meeting of the Bone Research Society and the British Society of Matrix Biology, London 2009.**





MANCHESTER  
UNIVERSITY

# The Metaphyseal Index for Assessing Development of the Distal Radius

Reddie L CR<sup>1</sup>, Mughal, MZ<sup>2</sup>, Astley SM<sup>1</sup>, Ward KA<sup>1</sup>, Adams JE<sup>1</sup>  
<sup>1</sup>Imaging Sciences & Biomedical Engineering, University of Manchester, Manchester UK  
<sup>2</sup>St Mary's Hospital for Women & Children, Department of Paediatric Medicine, Manchester, UK



ISBE  
Imaging Science and  
Biomedical Engineering

---

### Introduction

>During longitudinal bone growth, a rapid reshaping and remodelling process occurs known as metaphyseal inwaisting. In a healthy child, metaphyseal inwaisting results in proportional decreases in metaphyseal width (MW) and increases in growth plate width (GPW).  
 >The Metaphyseal Index (MI) compares MW to GPW. During normal growth, changes in MW and GPW are proportional. When normal bone growth is impaired, the MI may be altered, increasing skeletal fragility.  
 >Reference values for children have been calculated for the distal femur MI<sup>(1)</sup>. However, the most commonly performed radiograph in children is that of the hand and forearm for bone-ageing purposes.

**Primary Aim:** Compare MI development of normal children to groups with a potentially altered MI; Neurofibromatosis Type I (NF1), Gymnasts and Constitutional Puberty Delay (CPD).

**Hypothesis:** MI will be lower in younger children and plateau in teens. Gymnast MI will show a similar distribution but have higher values. NF1 MI will show a similar distribution but have lower than normal values.

### Results

**MI Results to Date: (CV = 1.05%; MI near 1.0 → GPW and MW are similar; MI near 0 → GPW and MW differ)**

	Min	Max	Mean	Upper 95% CI	Lower 95% CI
<b>Norm</b>	0.295	0.406	0.351	0.353	0.349
<b>Gym</b>	0.307	0.372	0.335	0.340	0.330
<b>NF1</b>	0.292	0.375	0.339	0.352	0.327

**Graphs of MI vs Age in Normal, Gymnast & NF1**

**MI vs Chronological Age in Normal Children**



**MI vs Chronological Age in Gymnast Children**



**MI vs Chronological Age in NF1 Children**



---

### Methods

Postero-anterior hand radiographs of 376 healthy white Caucasian children (157 male), 36 healthy gymnasts (15 male) and 16 children with NF1 (6 male), aged between 5 and 19 years, were obtained and digitised using a Canon EOS 20D (with Canon Macro lens EF 100mm auto focus) digital camera. \*CPD data not presented here.  
 >Semi-automated computerised method: the computer program QWin by Leica Microsystems (Milton Keynes, UK), provided semi-automated measurements of the distal radius GPW and the MW. After setting the correct calibration, the GPW was measured. Half of the GPW was used to calculate the metaphysis measurement point and then the MW was measured.  $MI = 0.5MW / GPW$   
 >30 repeat MI's were performed on the normal group. One-way ANOVA was used to calculate precision (coefficient of variation, CV%).

### Discussion

The hypothesis that the Gymnast group would exhibit higher values and therefore a higher mean than both the normal and NF1 groups, was not correct. The healthy gymnasts are showing a similarly shaped radius to those in the NF1 group. This may be due to the fact that the normal group has post-pubertal children. Future work will involve age and sex matched controls.

---

**Figure 1: Semi-Automated Measurement of the MI**



Fig 1: Bone edge detection is performed by the operator. The computer measures the green lines and discards the yellow lines.

### Conclusion

Using the MI to assess the distal radius of children is a quick and precise way to assess bone growth and development. The reference database for the MI in normal children has the potential to be used in assessing metaphyseal inwaisting of children with other clinical conditions<sup>(2)</sup>, or undergoing treatments (such as bisphosphonates) that may affect bone development.

---

### References

- 1) Ward, K., Cowell, C. T. & Little, D. G. (2005) Quantification of metaphyseal modeling in children treated with bisphosphonates. *Bone*, 36, 999-1002.
- 2) Land, C., Rauch, F. & Glorieux, F. H. (2006) Cyclical intravenous pamidronate treatment affects metaphyseal modeling in growing patients with osteogenesis imperfecta. *Journal of Bone and Mineral Research*, 21, 374-379.

Primary Author Contact: lianne.reddie@student.manchester.ac.uk

### References

Figure 12.1B: Poster displayed at the Joint Meeting of the Bone Research Society and the British Society of Matrix Biology, London 2009.

## **THE METAPHYSEAL INDEX OF THE DISTAL RADIUS: A COMPARISON BETWEEN GYMNASTS AND NORMAL CHILDREN**

L. Reddie\*, K. Ward 1, Z. Mughal 2, S. Astley 1, J. Adams 1  
1HSBE, UNIVERSITY OF MANCHESTER, 2Paediatric Medicine, St Mary's Hospital, Manchester, United Kingdom

### **Introduction**

Metaphyseal inwaisting is a process that occurs during long bone growth & remodelling of epiphyses & results in a proportional increase in growth plate width (GPW) and a decrease in metaphyseal width (MW). The Metaphyseal Index (MI) compares GPW to MW, usually in the distal femur (Ward et al, 2005; Land et al, 2006). However, due to bone-ageing, the most commonly performed radiograph in children is the hand/forearm. Previous work showed that gymnasts have a lower mean MI of the distal radius than normal children (Reddie et al, 2009), but that study did not use age & sex-matched controls, nor did it compare correlation of MI with pQCT.

**Aims:** Examine distal radius morphology of gymnast children (cases) and normal children (controls) and investigate whether MI correlates with pQCT parameters: density [trabecular (TrD), cortical + subcortical (CSD), total (ToD)], total cross-sectional area (ToA), cross-sectional muscle area (CSMA) and polar strength-strain index (pSSI).

### **Methods**

Posterior-anterior hand radiographs and pQCT scans of the non-dominant hand were taken in 378 (156 male) normal children aged between 5 and 20 years, and 36 (15 male) gymnasts aged between 5 and 12 years (mean = 9.1). GPW and MW measurements were obtained using QWin by Leica (Milton Keynes, UK). Each case had 2 controls from the normal group and were matched based on sex and age within 1 year. Heights were within 11cm and weights within 11kg.  $MI=0.5MW/GPW$ .

### **Results**

MI of cases & controls were significantly different from each other (mean MI case=0.334167, mean MI control=0.345889,  $P=0.0004$ ). MI did not correlate with any of the aforementioned pQCT parameters (all  $r^2$  values<0.15) for either cases or controls.

### **Discussion**

The results confirm previous work that the mean distal radius MI of gymnasts is significantly lower than in normal children. Further work is needed to determine the reason(s) for this difference. The results also show that MI does not correlate with pQCT parameters. Future work will involve analysing the MI of children with neurofibromatosis & delayed puberty.

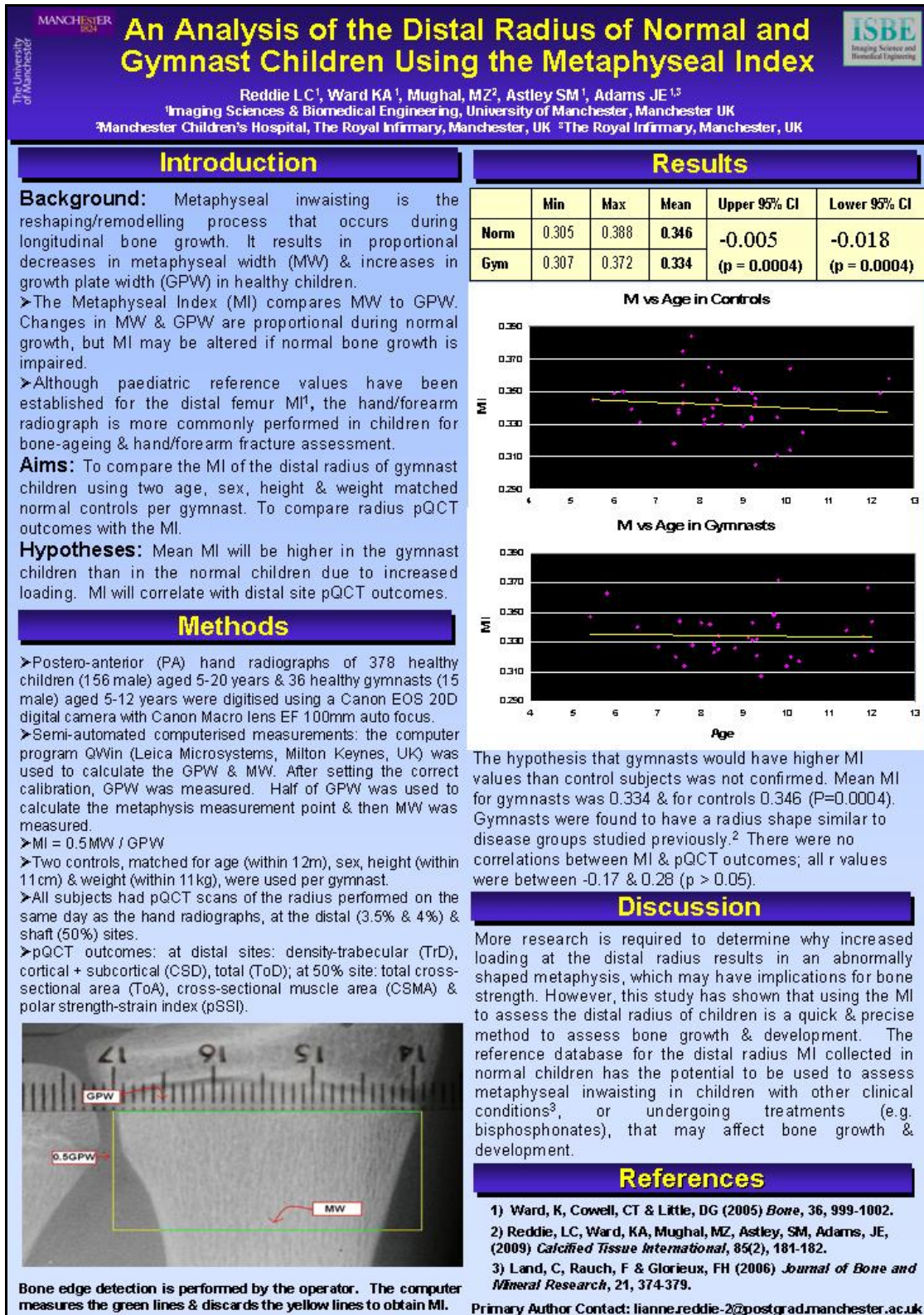
### **References**

- 1) Ward, K et al, (2005) Bone, 36, 999-1002.
- 2) Land, C et al, (2006) J. Bone. Miner. Res. 21, 374-379.
- 3) Reddie, L et al, (2009) Calcif Tissue Int. 85 (2), 181-182.

**Abstract 12.1C: Abstract submitted and accepted to the Joint Meeting of the Bone Research Society and the European Calcified Tissue Society, Glasgow 2010.**

**\*Awarded a BRS Travel Award of £250 for this abstract.**





### Discussion

More research is required to determine why increased loading at the distal radius results in an abnormally shaped metaphysis, which may have implications for bone strength. However, this study has shown that using the MI to assess the distal radius of children is a quick & precise method to assess bone growth & development. The reference database for the distal radius MI collected in normal children has the potential to be used to assess metaphyseal inwaisting in children with other clinical conditions<sup>3</sup>, or undergoing treatments (e.g. bisphosphonates), that may affect bone growth & development.

### References

- 1) Ward, K, Cowell, CT & Little, DG (2005) *Bone*, 36, 999-1002.
- 2) Reddie, LC, Ward, KA, Mughal, MZ, Astley, SM, Adams, JE, (2009) *Calcified Tissue International*, 85(2), 181-182.
- 3) Land, C, Rauch, F & Glorieux, FH (2006) *Journal of Bone and Mineral Research*, 21, 374-379.

Primary Author Contact: lianne.reddie-2@postgrad.manchester.ac.uk

**Figure 12.1C: Poster displayed at the Joint Meeting of the Bone Research Society and the European Calcified Tissue Society, Glasgow 2010.**

## 12.2 Appendix 2 – Further Information regarding X-rays

### 12.2.1 X-Rays and How They are Generated

X-rays are generated in a device called an X-ray tube. These devices have several components including a vacuum tube, a tungsten or molybdenum filament, a cathode, an anode and a rotor (Fig. 12.2A). The tungsten filament, which is similar to those used in an average light bulb, has an electrical current passing through it that causes the filament to heat up. The cathode is a metal assembly that surrounds the filament. When the filament reaches a sufficiently high temperature, some of the electrons in the filament will have enough thermal energy to escape their bonds to the filament's metal atoms and

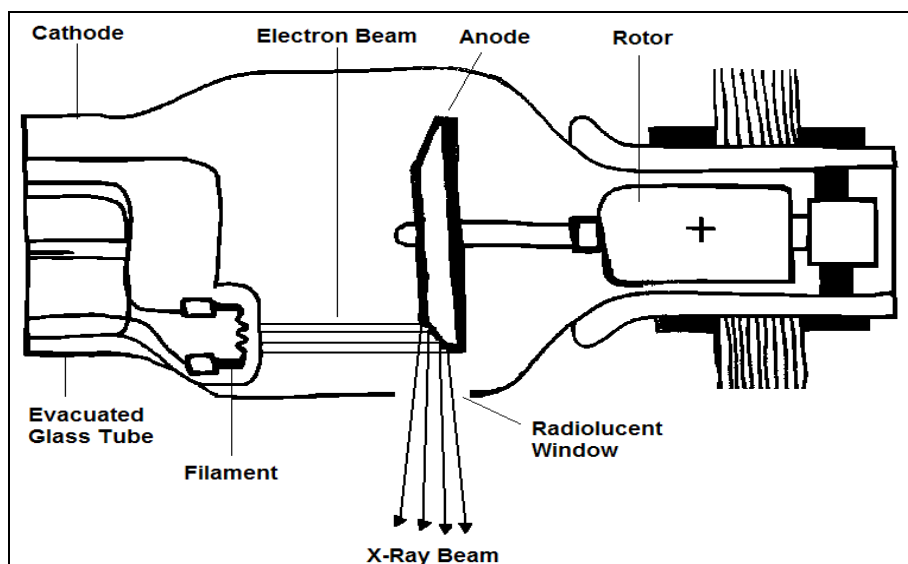


Figure 12.2A: Construction of an X-Ray tube with a rotating anode, adapted from (Kane, 2003).

will collect in the vacuum tube. The anode is a piece of metal, again often tungsten or molybdenum, located some distance away from the cathode. The anode is often on a rotor rather than being stationary, which aids in dissipating the heat that is a by-product of producing X-rays. When a high electrical voltage, the polarity of which is chosen in order to render the cathode negative and the anode positive, is passed between the cathode and anode, the positive anode attracts the electrons freed by heating the filament and accelerates them towards the anode. The shape of the cathode is designed in order to focus the beam of electrons into striking the anode in a very small area. When

electrons collide with the anode, their kinetic energy is released due to interactions with the atoms comprising the metal anode. Most of the kinetic energy released is in the form of heat; less than 1% of the energy contributes to the production of X-rays. The act of the electron changing its velocity (i.e. slowing down when it collides with the atoms in the anode), will cause it to emit radiation. Low-energy X-rays are produced by glancing collisions, while high-energy X-rays are produced when a collision results in all of the electron's original energy being converted into a photon. After traversing the gap between the anode and cathode, each electron has the equivalent energy in kilo electron-Volts (keV) to the voltage in kilovolts, (kV) being passed between the anode and the cathode. Therefore, if the peak kiloVoltage (kVp) is 100 kV, then the kinetic energy of the electrons will be equal to 100 keV just prior to striking the anode.

Both molybdenum and tungsten produce a broad spectrum of radiation, but because the X-ray sources are operated at different voltages, the maximum emitted X-ray energy differs: molybdenum has a kVp of 30 volts (equal to 30 keV), whereas tungsten has a kVp of 100 volts (equal to 100 keV). The lower atomic number of molybdenum, 42, compared to tungsten, 74, means that molybdenum is not as effective at accelerating the electron beam and therefore produces less X-rays under the same operating conditions. This is one reason molybdenum is most commonly used in mammography and tungsten is used for full chest or body imaging (Kane, 2005). Another advantage of these substances is that both tungsten and molybdenum have thermal properties which make them good at dissipating heat.

### **12.2.2 X-Rays and Their Interaction with Tissue**

The Photoelectric Effect states: An inner-orbital electron of an atom within the body becomes excited when an X-ray photon interacts with it. The X-ray photon is absorbed entirely, while the resulting photoelectron is free to travel.

The Compton Effect states: When an incoming X-ray photon collides with an outer-orbital electron, it will lead to that electron being ejected and the X-ray photon will scatter in a different direction.

The Compton Effect requires less energy to occur than the Photoelectric Effect and is therefore more likely to occur in soft tissues such as fat and skin (Kane, 2005). The

likelihood of the Photoelectric Effect occurring increases as the cube of the atomic number ( $Z^3$ ) increases. It is for this reason that calcium (i.e. present in the skeleton) and heavy metals such as lead (used to line rooms and vests in order to protect from radiation exposure), are good absorbers.

Different structures in the body have different attenuation co-efficients ( $\mu$ ), which depend on  $Z$  and electron density. The higher the value of  $\mu$ , the more readily a material will attenuate X-rays of a certain energy. Bone, with its high calcium content, is more radiodense than other tissues, meaning it is not transparent to radiation and appears white on a radiograph. Whereas the more radiolucent something is, the darker it will appear on a radiograph, i.e. air. Fat also appears radiolucent (black) and other soft tissues appear in varying shades of grey.

Table 12.2.2A shows the  $\mu$  for various tissues and substances at 60 keV (Kane, 2005). Only 37% of X-rays remain after passing through a thickness of a substance equal to  $1/\mu$ , which is the range of travel for X-rays. The keV may need to be raised when imaging thicker parts of the body or individuals with a large girth (Kane, 2005).

<b>Table 12.2.2A: Attenuation Co-Efficients at 60 keV &amp; Density for Tissues and Substances Important to Medical Imaging</b>		
Absorbing Material	Attenuation Co-Efficient at 60 keV $\mu$ ( $\text{cm}^{-1}$ )	Density $\rho$ ( $\text{g}/\text{cm}^{-3}$ )
Fat	0.1788	0.90
Soft tissues other than fat (muscle, bodily fluids)	0.2045	1.00
Water	0.2055	1.00
Air	$\sim 3 \times 10^{-4}$	0.00129
Bone	0.466 – 0.548	1.65 – 2.00

**Table 12.2.2A: Attenuation Co-Efficients at 60 keV & Density for Tissues and Substances Important to Medical Imaging, adapted from (Kane, 2005).**

### 12.3 Appendix 3 - Tanner Pubertal Stage Self-Assessment Sheets

**Pubertal Staging Self Assessment**

This is a self examination which will help us to know which stage of puberty you are in. The examination will be carried out in a private room. You can do this by yourself, or you may wish to have your Mum or Dad, or one of them, present. Before you start please make sure the door is locked.

**Pubic hair**  
First you need to look at the area between your tummy and the top of your legs. This is the pubic area. The pictures below show you how your pubic hair will grow in this area. Look at the pictures and put a tick underneath the picture that looks most like your own pubic area.

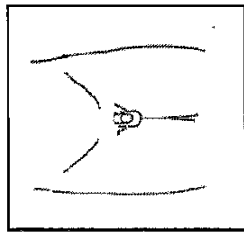
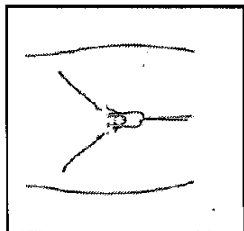
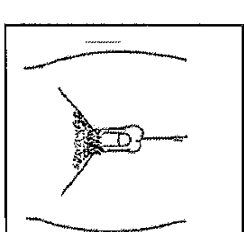
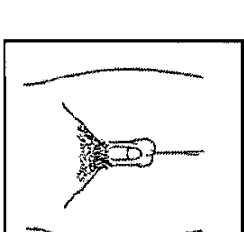
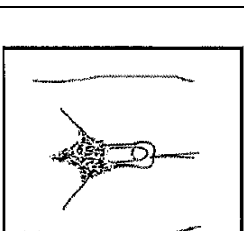
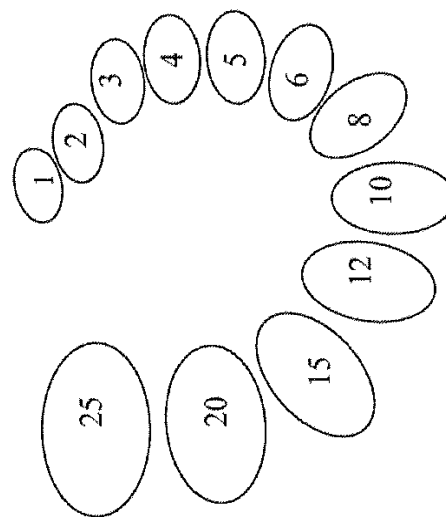
				
<input type="checkbox"/>	<input type="checkbox"/>	<input type="checkbox"/>	<input type="checkbox"/>	<input type="checkbox"/>

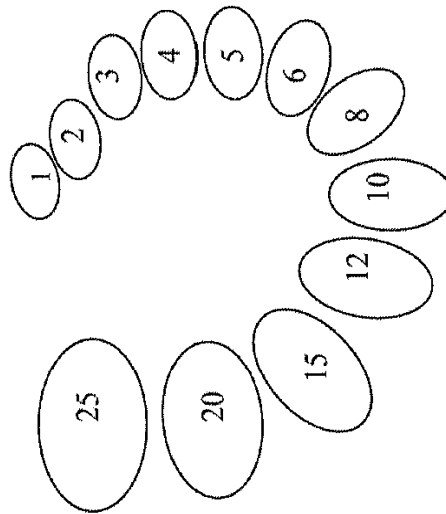
Figure 12.3A: Tanner pubertal stage self-assessment form for male pubic area.

### Testes

The pictures below represent the growth of the testes. You need to feel your own testes, on at a time, and compare the size of each testicle to the beads you have been given. Decide which bead feels most like your testicle in size. On each bead there is a number. The numbers are the same as those shown on the beads in the picture. Put a tick on the picture of the bead with the same number as the one which feels most like your own testicle. Do this first for your left testicle and then again for your right testicle. The number may or may not be the same for both sides.



The size of your *Left* testicle



The size of your *Right* testicle

Figure 12.3B: Tanner pubertal stage self-assessment form for male testicular volume.

## Pubertal Staging Self Assessment

This is a self examination which will help us to know which stage of puberty you are in. The examination will be carried out in a private room. You can do this by yourself, or you may wish to have your Mum or Dad, or one of them, present. Before you start please make sure the door is locked.

### Pubic hair

First you need to look at the area between your tummy and the top of your legs. This is the pubic area. The pictures below show you how your pubic hair will grow in this area. Look at the pictures and put a tick underneath the picture that looks most like your own pubic area.

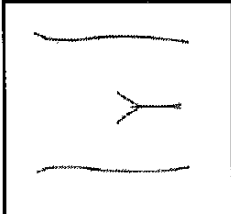
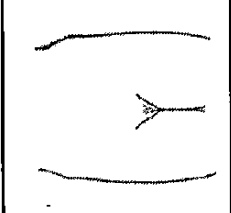
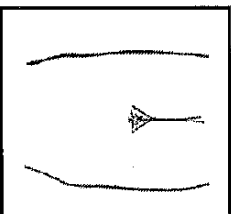
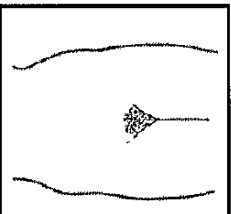
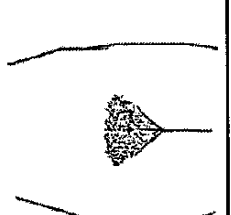
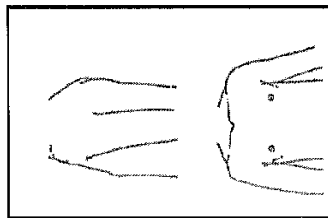
				
<input type="checkbox"/>	<input type="checkbox"/>	<input type="checkbox"/>	<input type="checkbox"/>	<input type="checkbox"/>

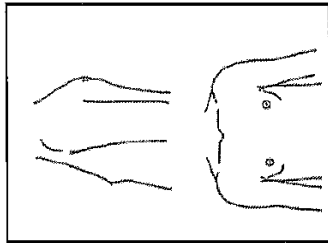
Figure 12.3C: Tanner pubertal stage self-assessment form for female pubic area.

**Breasts**

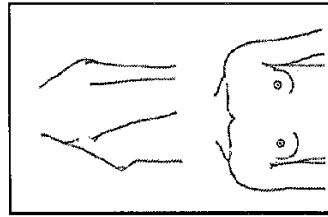
The pictures below show the growth of the breasts. Look at your own breasts and put a tick in the box under the picture which looks most like your own breasts.



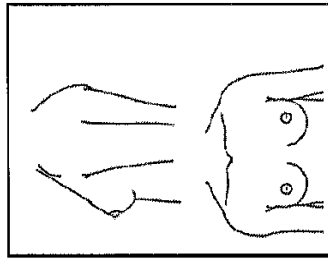
No breast development.



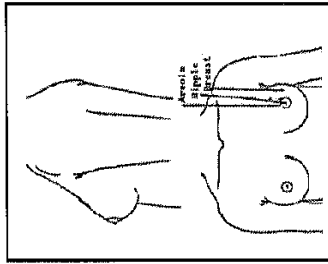
Breast development starts. The areola (the coloured area around the nipple) forms a small mound that sticks out from the rest of the breast.



Smooth contour between the breast, the areola and the nipple.



The areola and nipple stand out from the breast.



Adult breast. Smooth contour between the areola and breast. The nipple stands out from the areola.

Figure 12.3D: Tanner pubertal stage self-assessment form for female breast development.



## 12.4 Appendix 4 - Figures from Chapter 8 Results

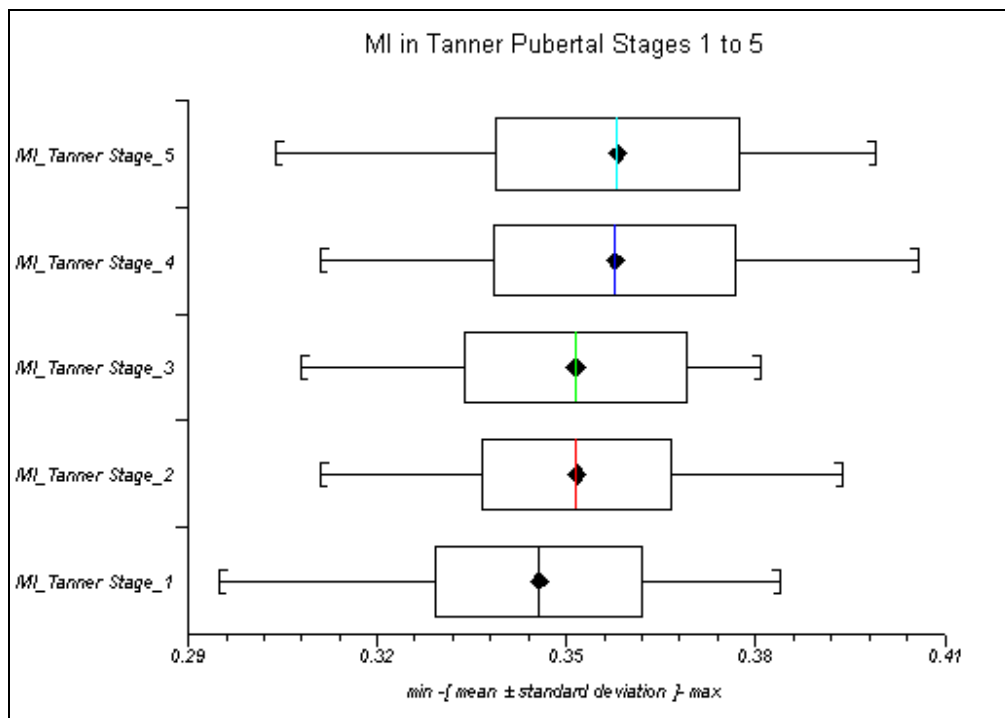


**Figure 8.3I:** MI in Tanner stages 1 through 5 in the Normal group (baseline values). This box and whisker plot illustrates that the MI increases as puberty develops.

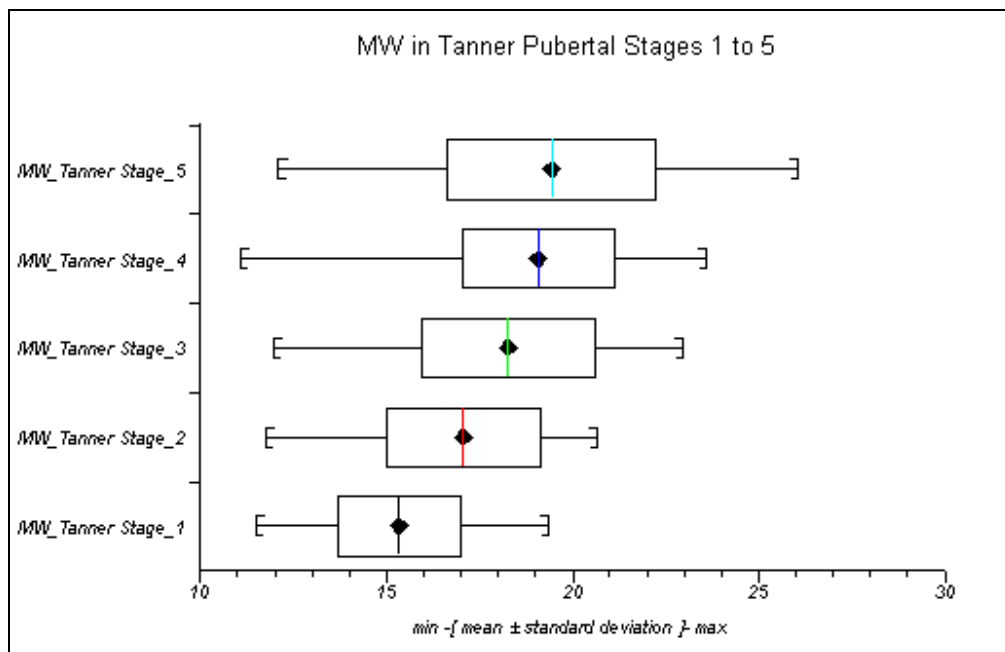


**Figure 8.3J:** MW in Tanner stages 1 through 5 in the Normal group (baseline values). This box and whisker plot illustrates that the MW increases as puberty develops.

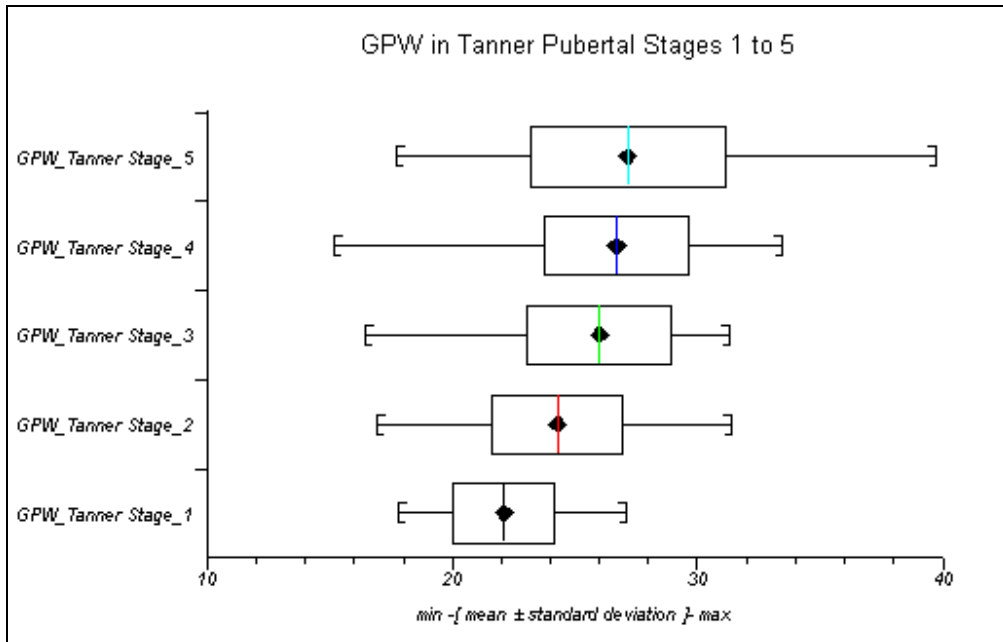


**Figure 8.3K: GPW in Tanner stages 1 through 5 in the Normal group (baseline values).** This box and whisker plot illustrates that the GPW increases as puberty develops.

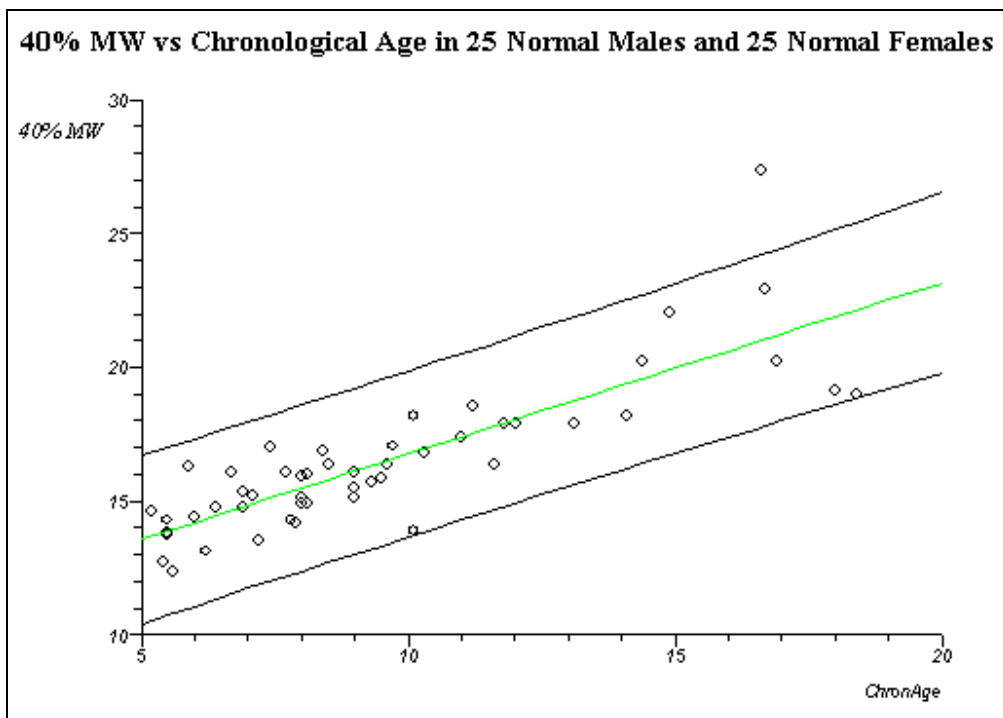


**Figure 8.3.2C: 40% MW vs chronological age (years) using 25 males and 25 females from the Normal group (baseline values).** This plot illustrates that the 40% MW increases with age.

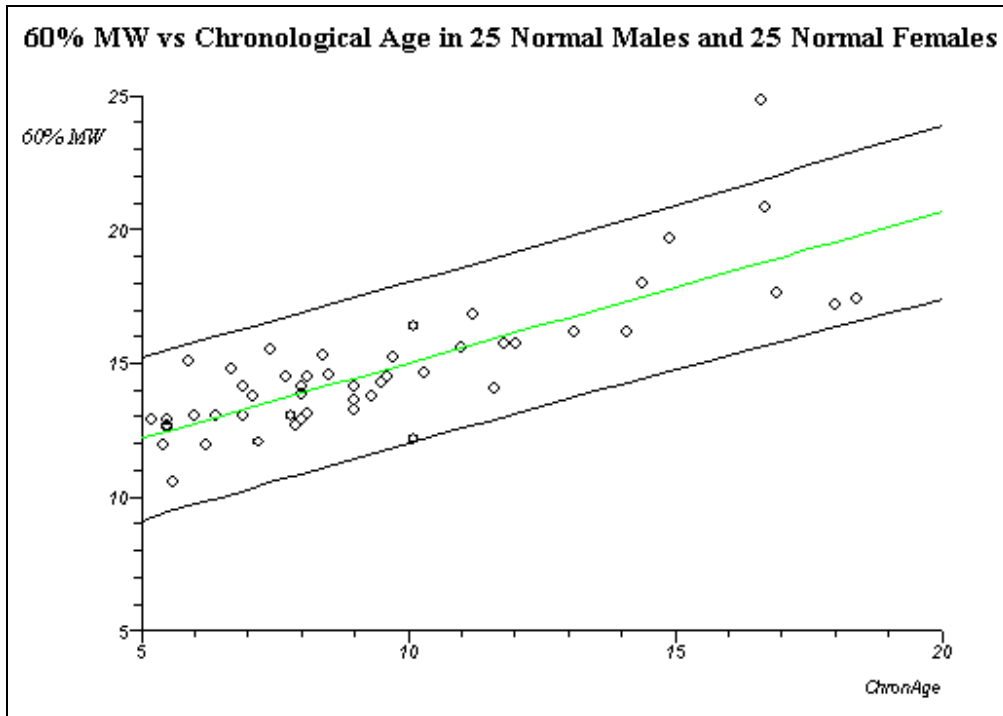


Figure 8.3.2D: 60% MW vs chronological age (years) using 25 males and 25 females from the Normal group (baseline values). This plot illustrates that the 60% MW increases with age.

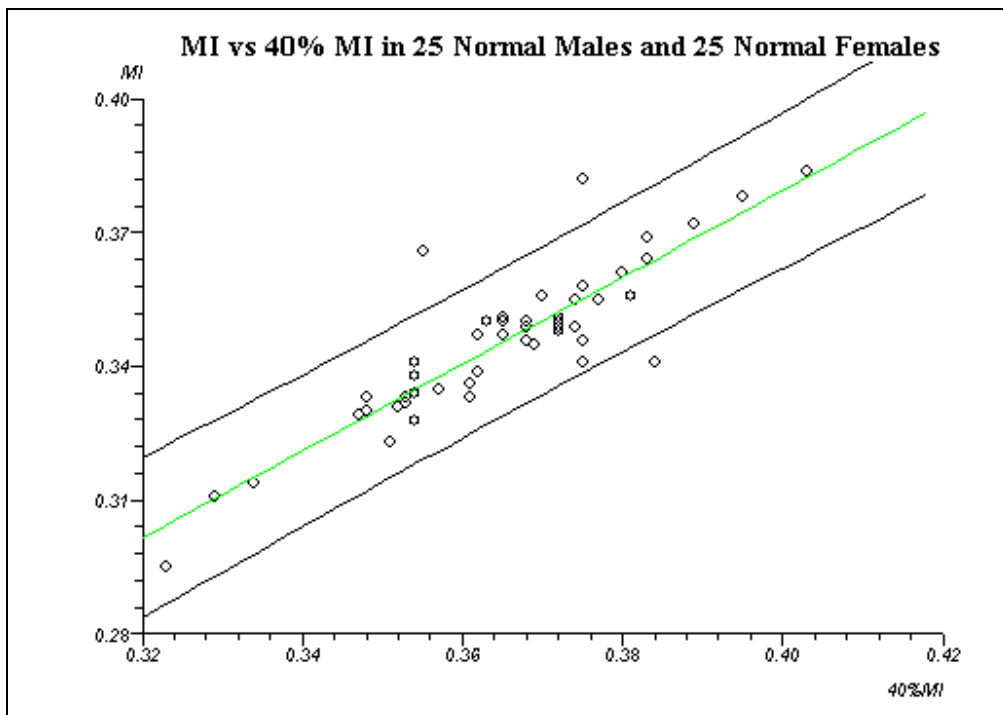


Figure 8.3.2E: MI compared to 40% MI in 25 normal males and 25 normal females. This plot illustrates a good correlation between the MI and 40% MI.

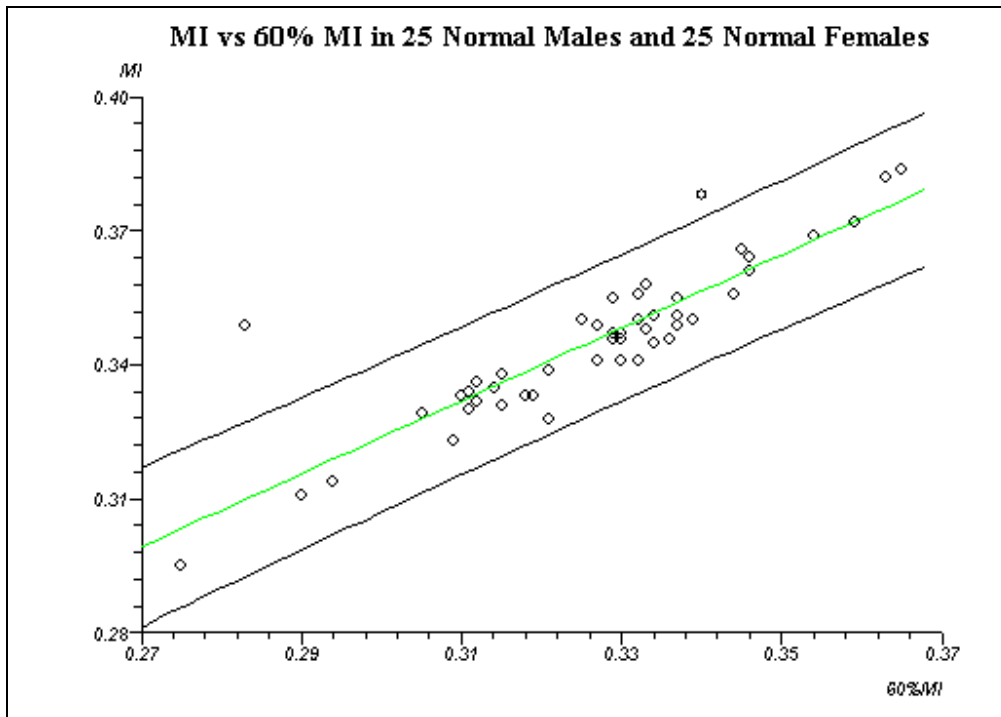


Figure 8.3.2F: MI compared to 60% MI in 25 normal males and 25 normal females. This plot illustrates a good correlation between the MI and 60% MI.

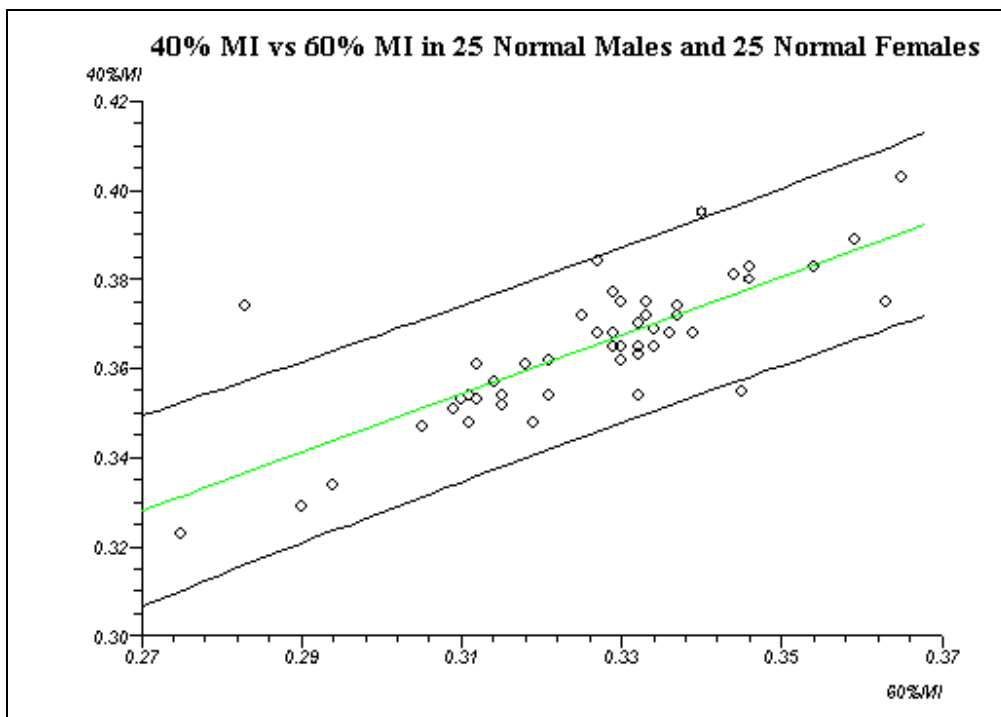


Figure 8.3.2G: 40% MI compared to 60% MI in 25 normal males and 25 normal females. This plot illustrates a good correlation between the 40% and 60% MI.

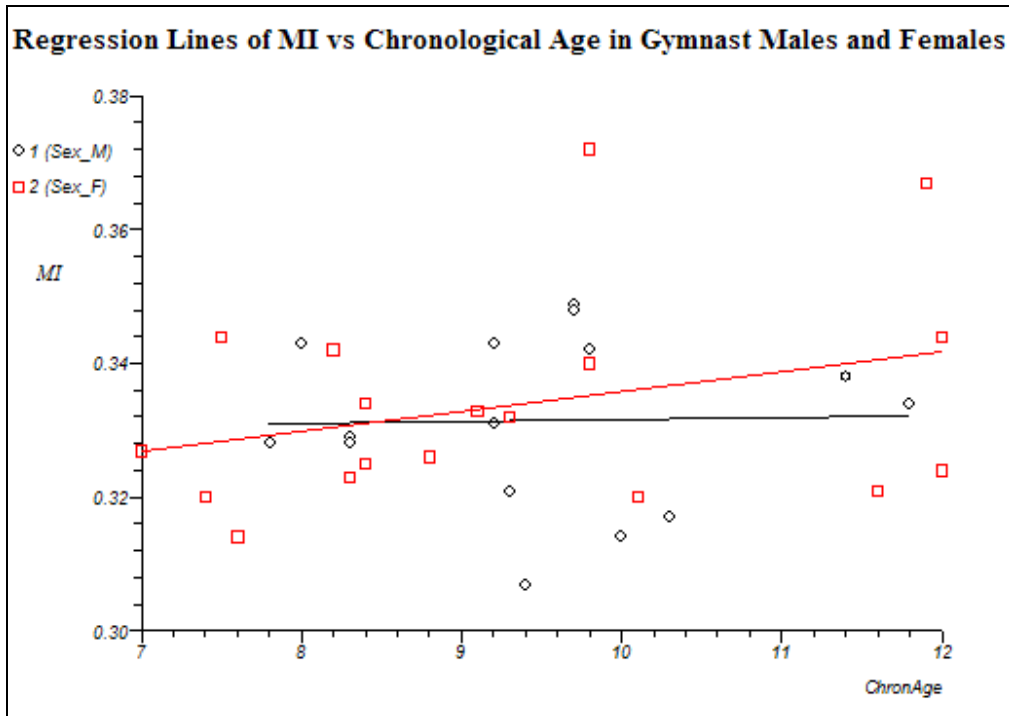


Figure 8.4C: MI compared to chronological age in Gymnast males and females. The regression lines show a slight difference in the slopes for males and females, but it is not significant ( $p = 0.502$ ).

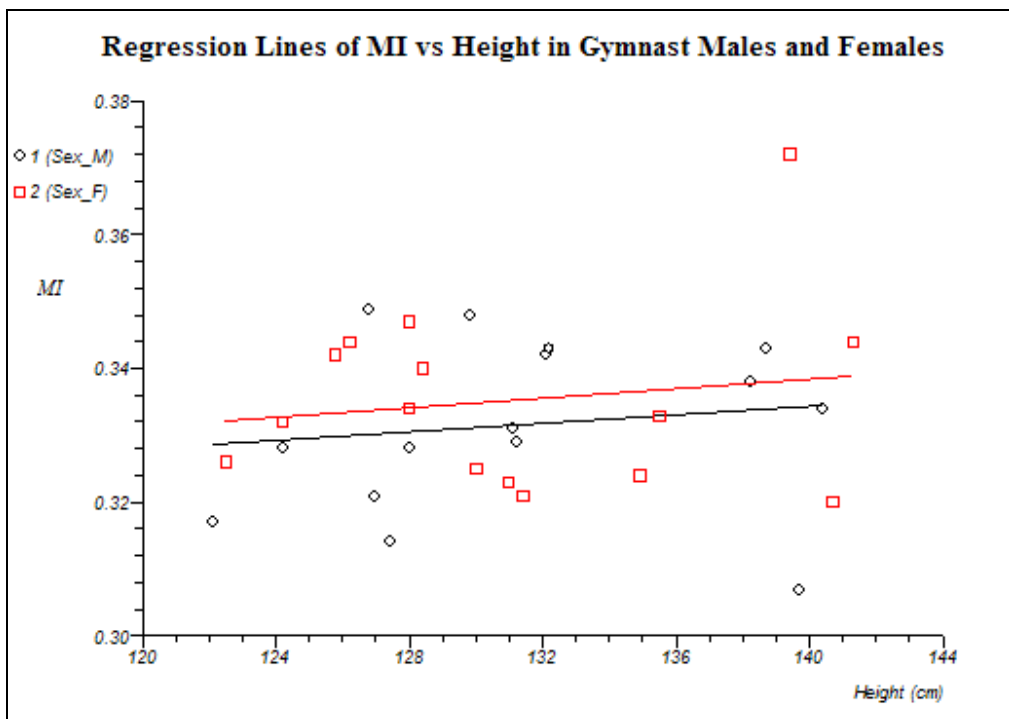


Figure 8.4D: MI compared to height (cm) in Gymnast males and females. The regression lines show the slopes for males and females are almost parallel, but the vertical distance between the lines is not significant ( $p = 0.959$ ).

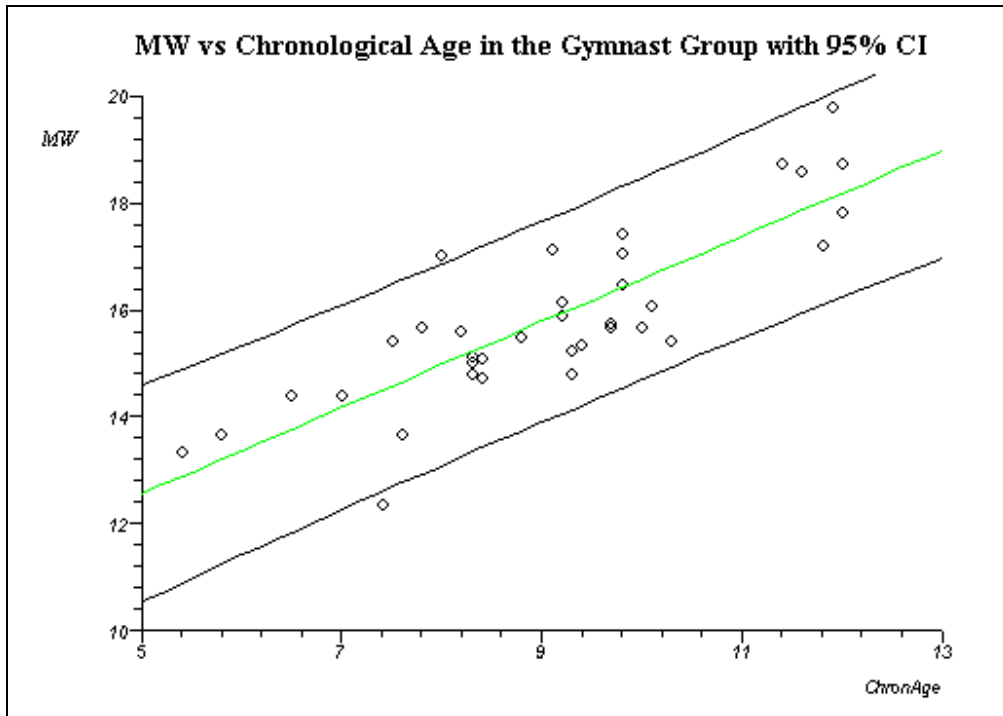


Figure 8.4E: MW (mm) vs chronological age in the Normal group (baseline values). This cross-sectional plot illustrates that the MW increases with age.

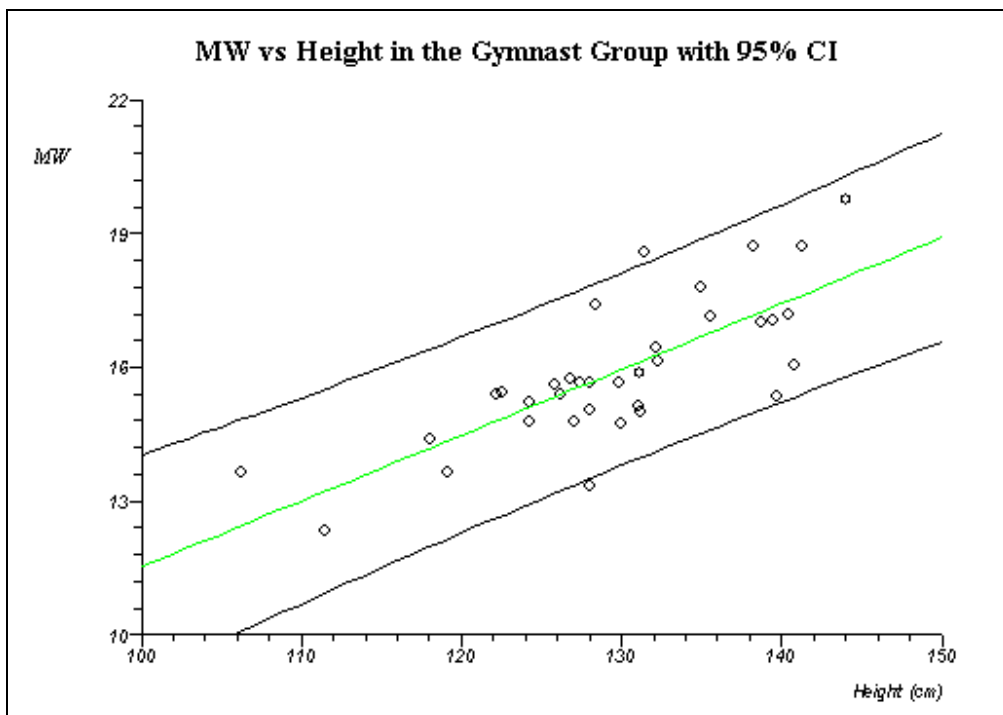


Figure 8.4F: MW (mm) vs height (cm) in the Normal group (baseline values). This cross-sectional plot illustrates that the MW increases as height increases.

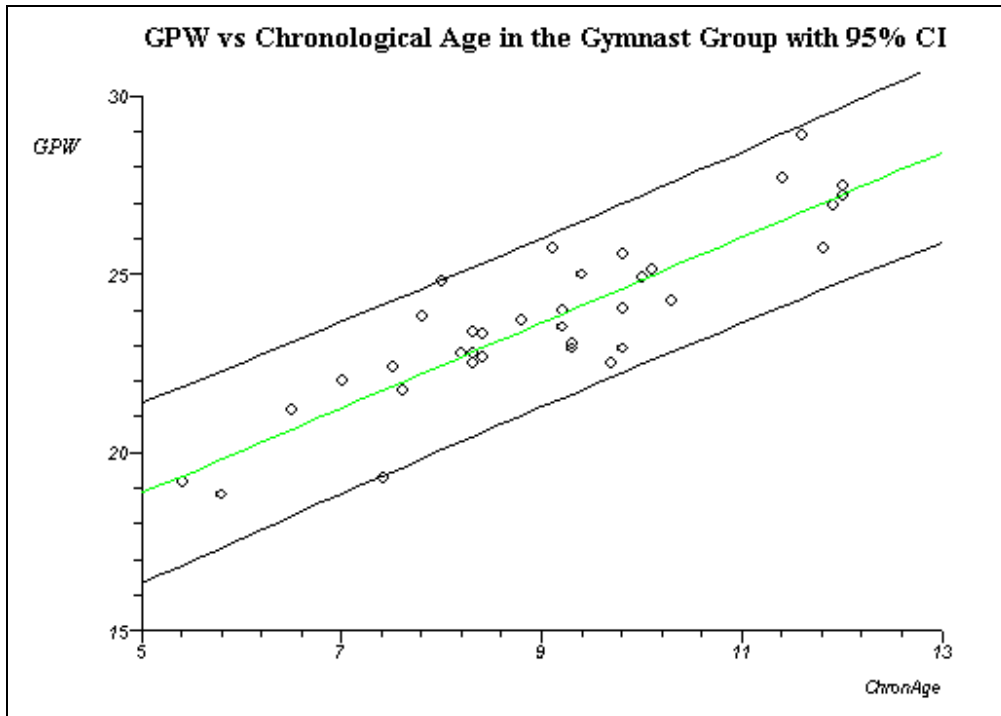


Figure 8.4G: GPW (mm) vs chronological age in the Gymnast group (baseline values). This cross-sectional plot illustrates a similar result to the MW plot - that the GPW increases with age.

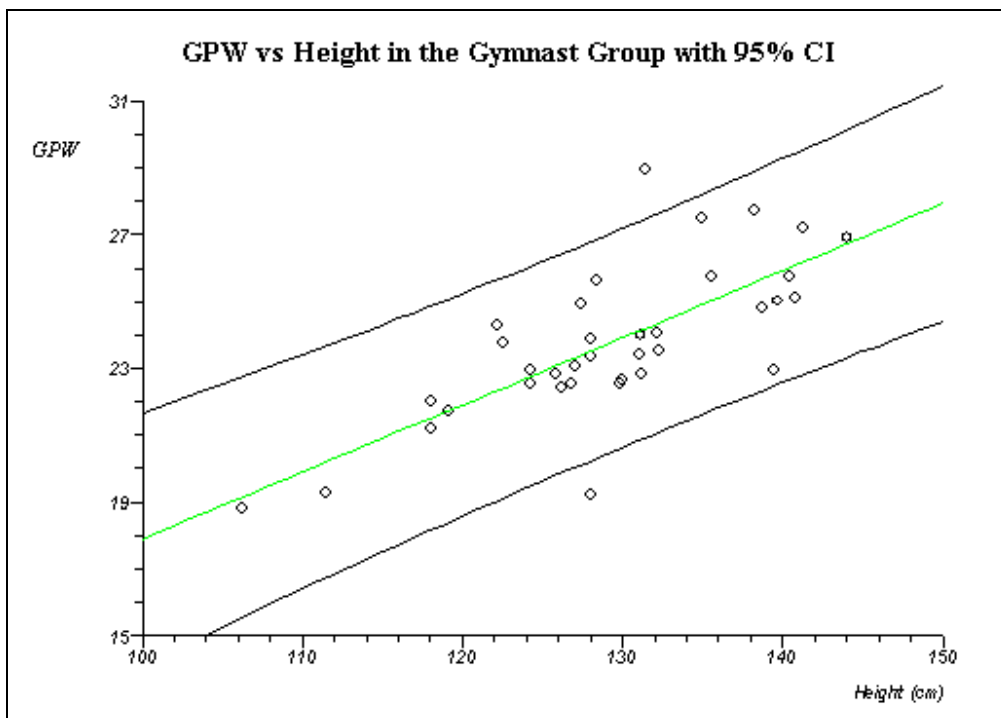


Figure 8.4H: GPW (mm) compared to height in the Gymnast group (baseline values). This plot illustrates a similar result to the MW plot - that the GPW increases as height increases.

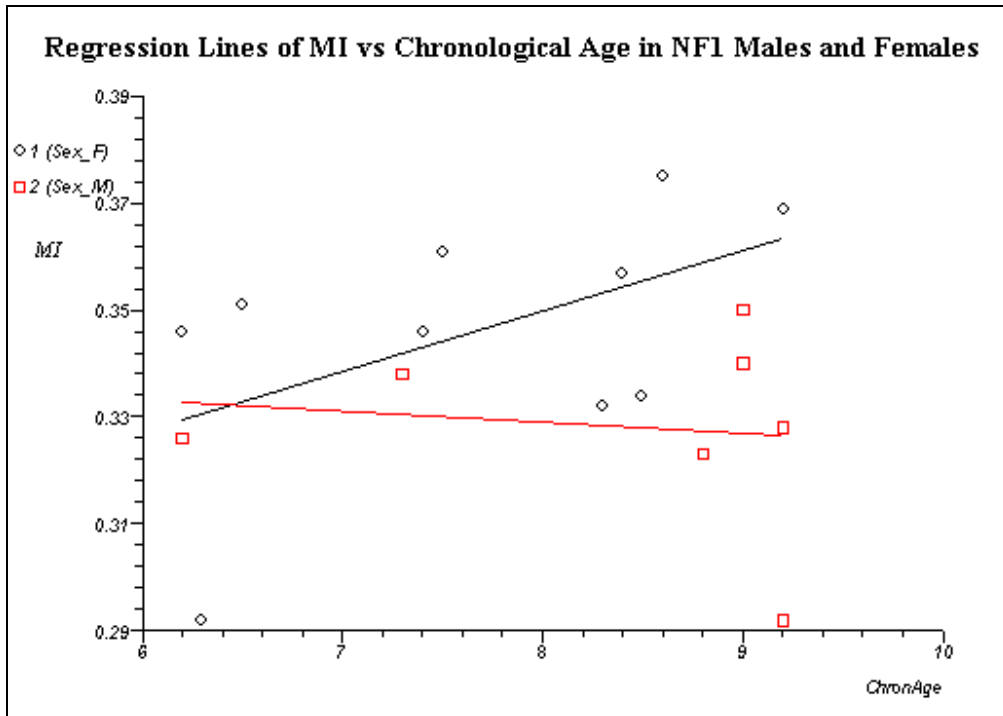


Figure 8.5C: MI compared to chronological age in NF1 males and females. The regression lines appear to show a large difference between the slopes, but it is not significant ( $p = 0.882$ ).

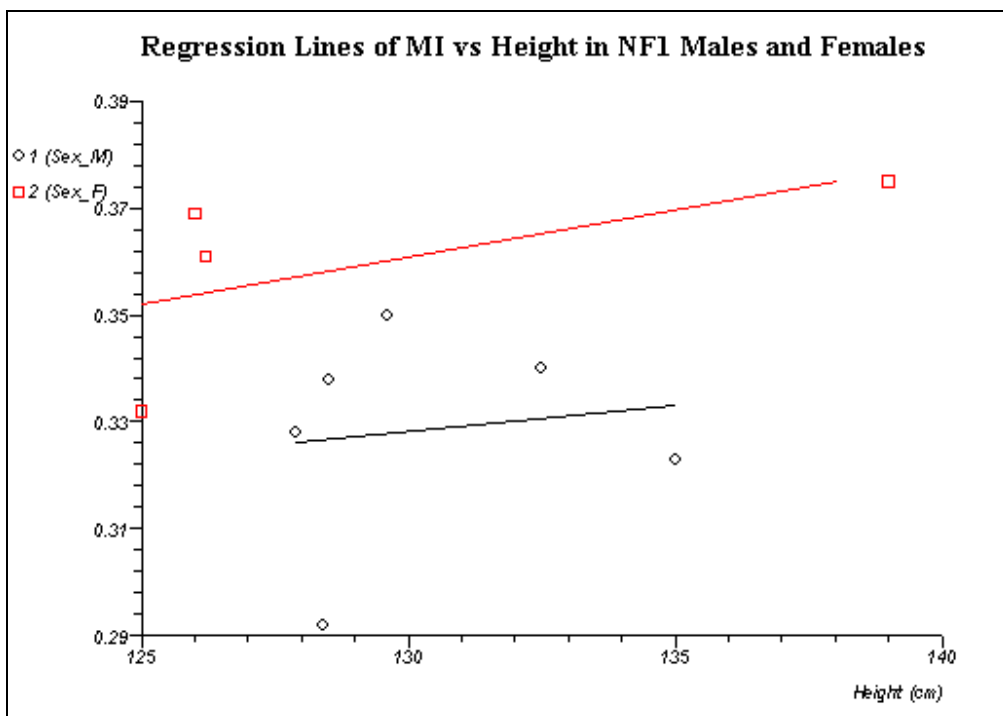


Figure 8.5D: MI compared to height in NF1 males and females. The regression lines show the two slopes are almost parallel, but the vertical distance between them is not significant ( $p = 0.840$ ).



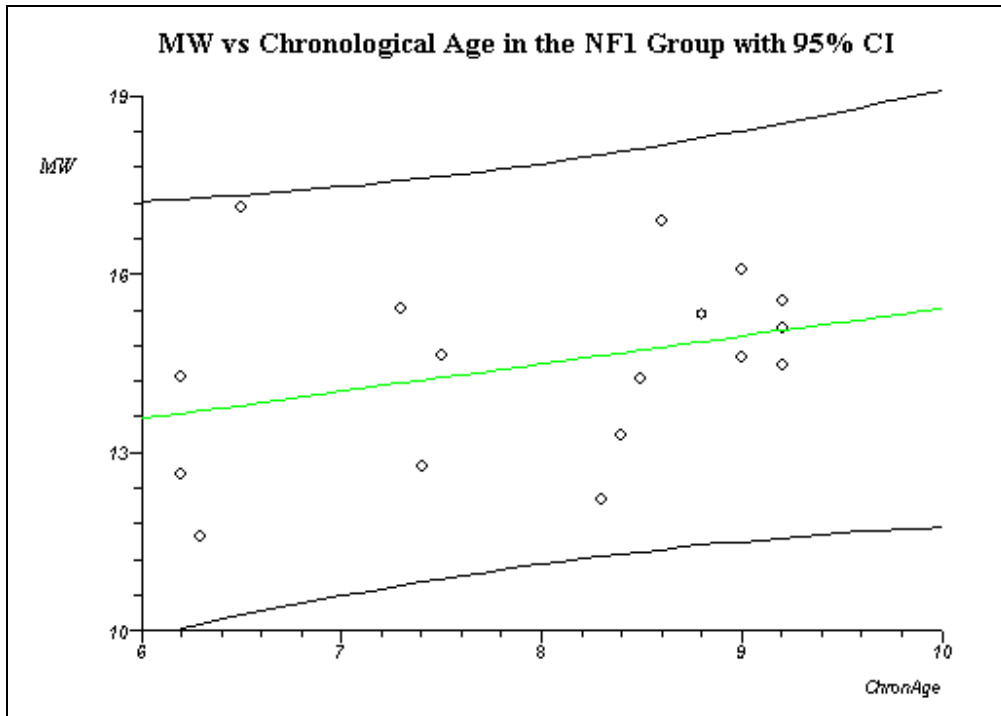


Figure 8.5E: MW (mm) vs chronological age in the NF1 group. This cross-sectional plot appears to show the MW increasing with age, but the regression is not significant ( $p = 0.159$ ).

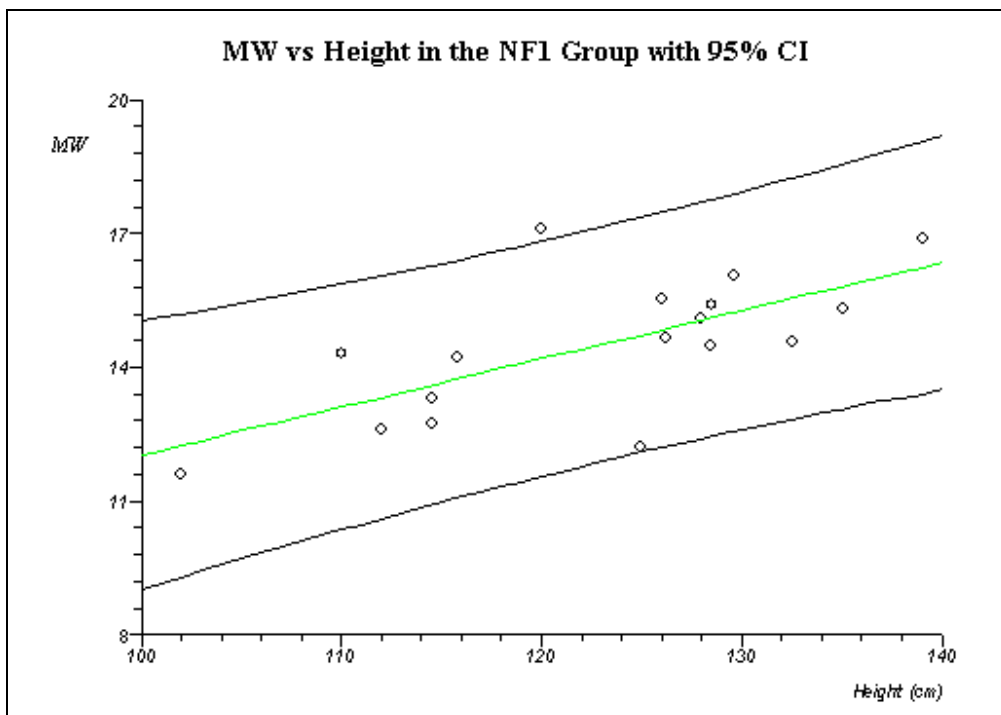


Figure 8.5F: MW (mm) vs height (cm) in the NF1 group. This cross-sectional plot illustrates that the MW increases as height increases ( $p = 0.003$ ).

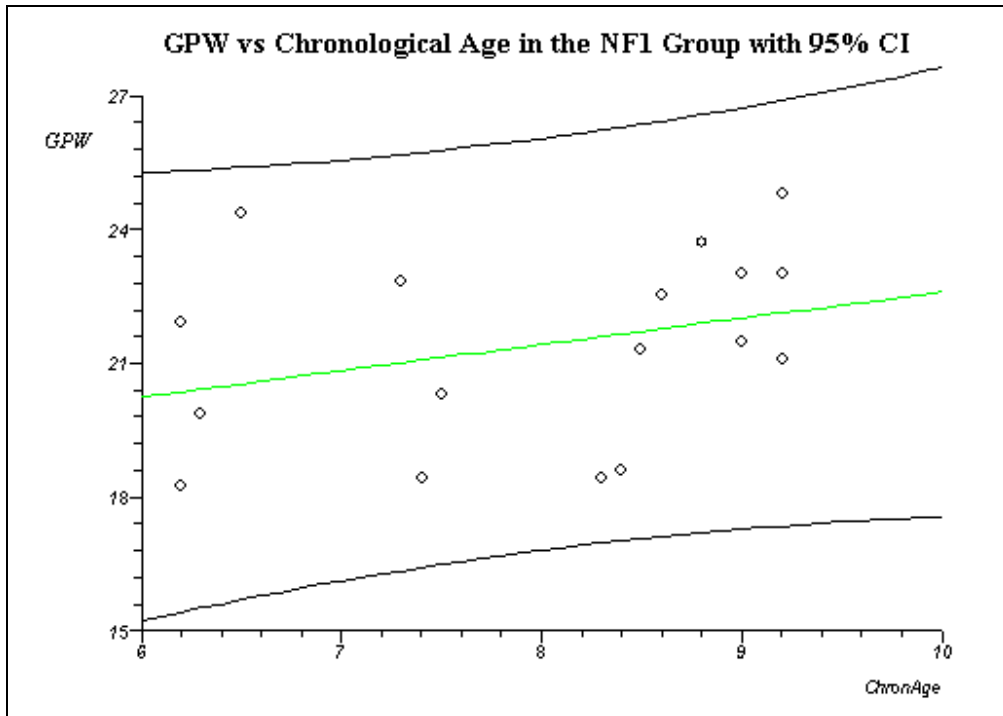


Figure 8.5G: GPW (mm) vs chronological age in the NF1 group. This cross-sectional plot appears to show an increase in GPW as subjects age, but the relationship is not significant ( $p = 0.082$ ).

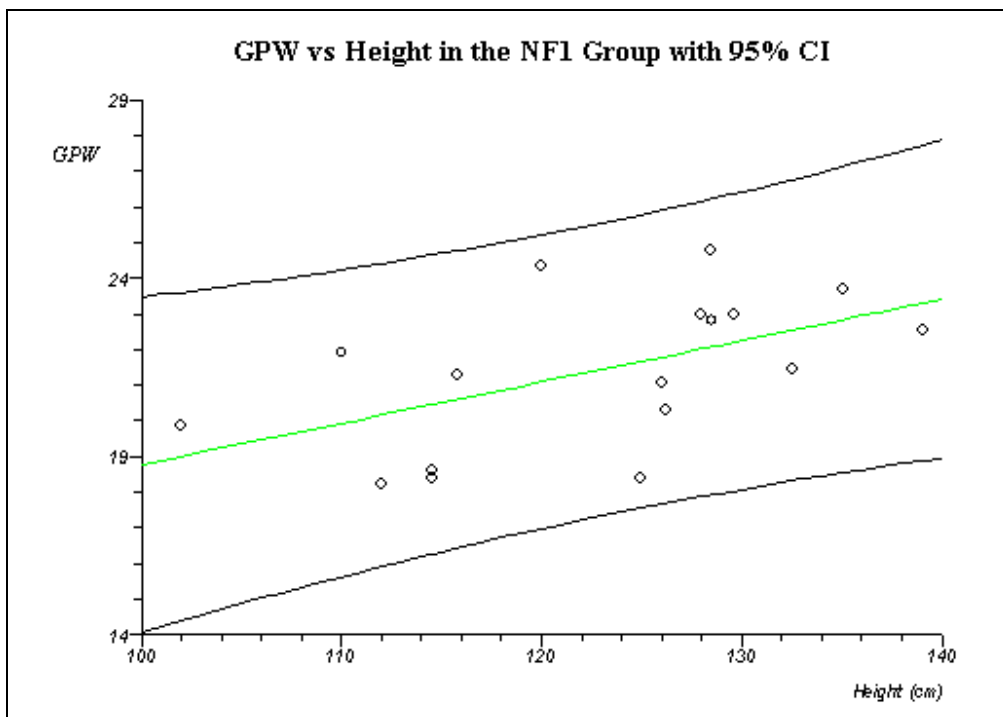


Figure 8.5H: GPW (mm) vs height in the NF1 group. This cross-sectional plot illustrates a similar result to the MW plot - that the GPW increases as height increases ( $p = 0.013$ ).

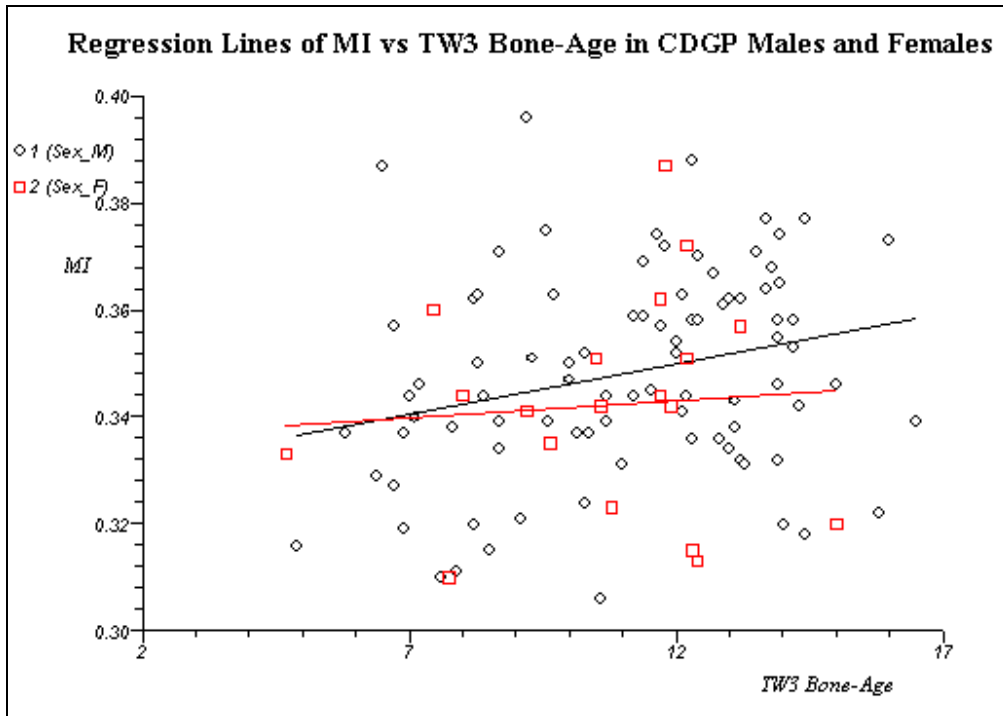


Figure 8.6C: MI compared to TW3 bone-age in CDGP males and females. The regression lines show a slight difference in the slopes for males and females, but this is not significant ( $p = 0.550$ ).

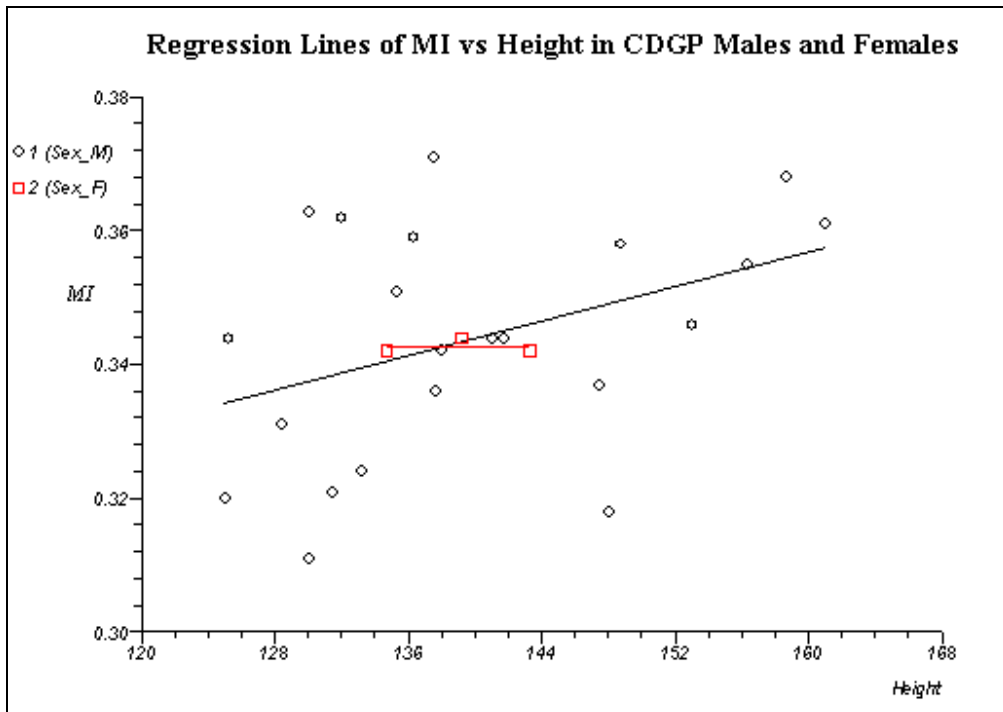


Figure 8.6D: MI compared to height (cm) in CDGP males and females. The regression lines appear to show a large difference between the slopes of males and females, but the vertical distance between the lines is not significant ( $p = 0.812$ ).

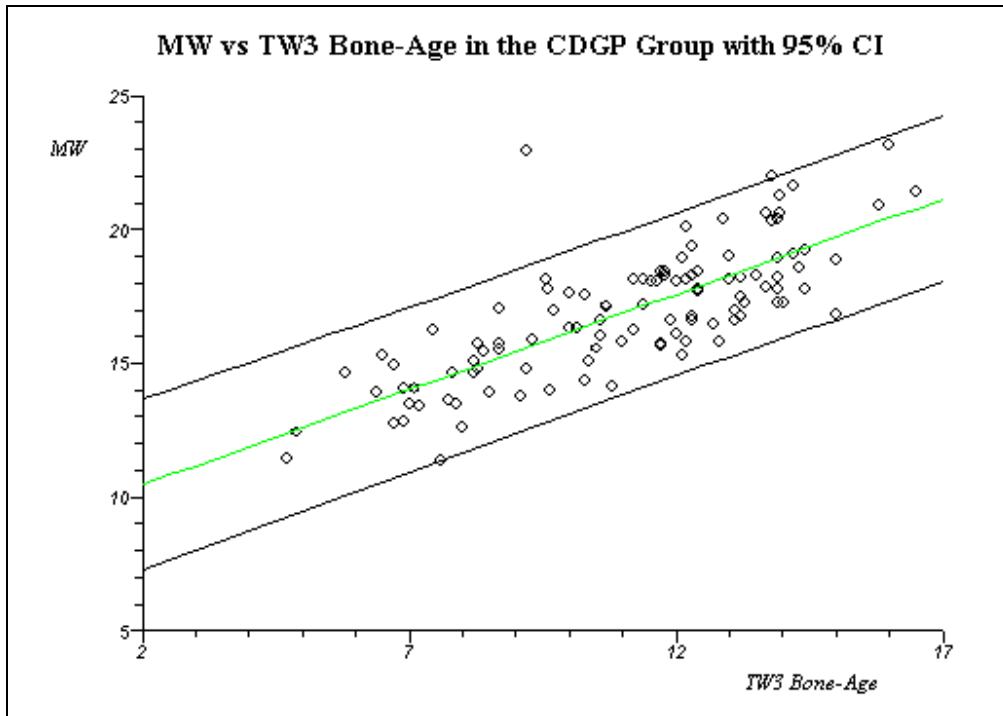


Figure 8.6E: MW (mm) vs chronological age in the CDGP group using all baseline values. This cross-sectional plot illustrates that the MW increases with age.

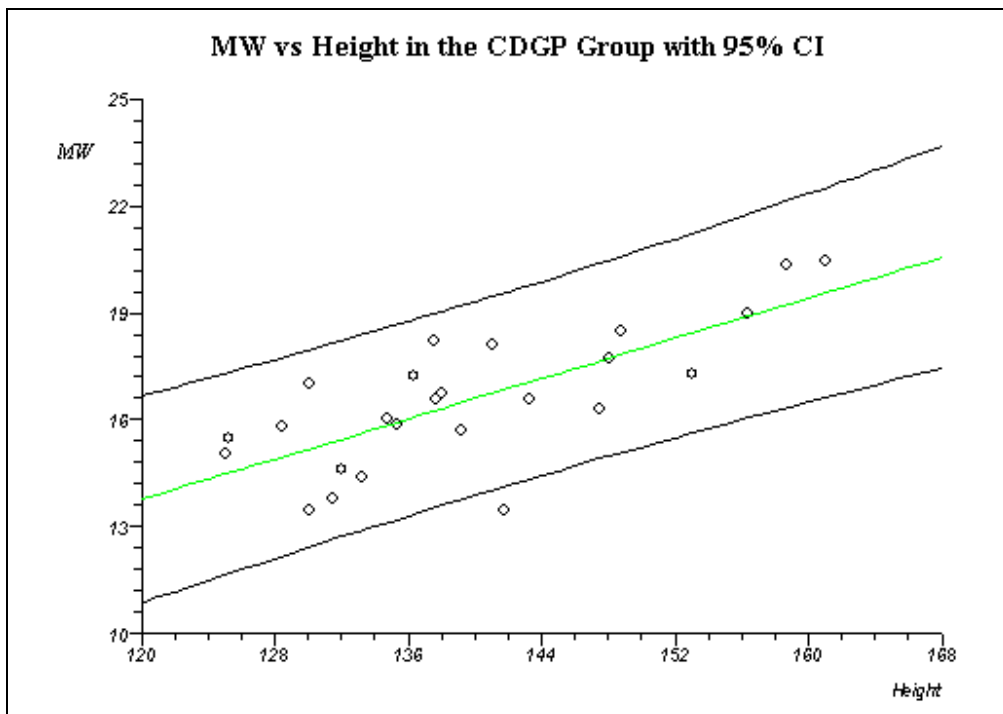


Figure 8.6F: MW (mm) vs height (cm) in the CDGP group using 25 baseline values. This cross-sectional plot illustrates that the MW increases as height increases.

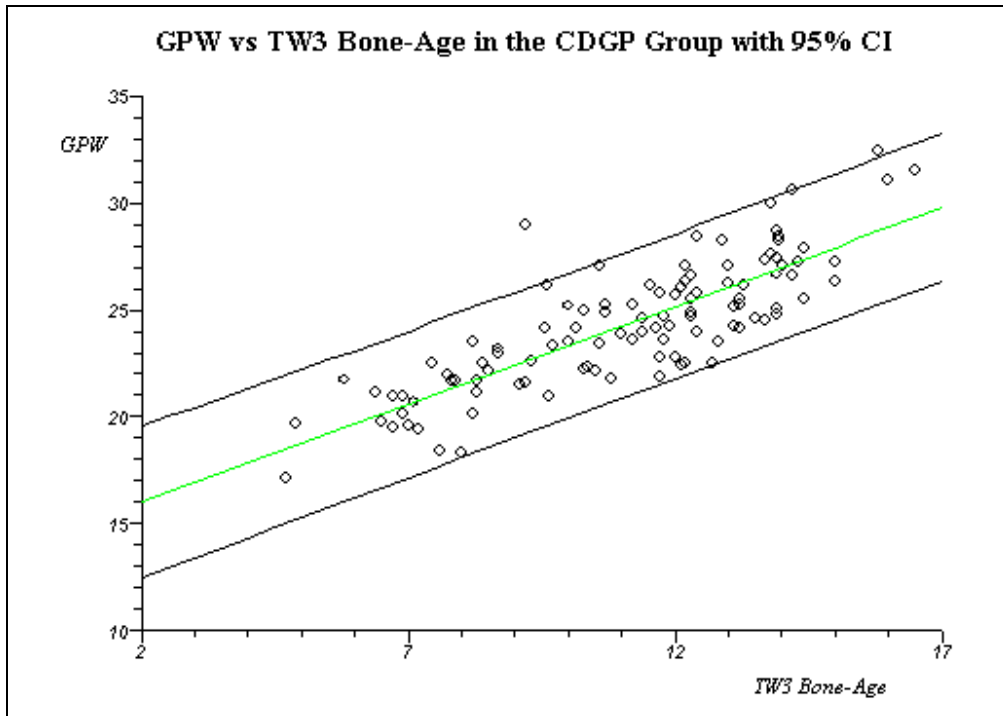


Figure 8.6G: GPW (mm) compared to TW3 bone-age in the CDGP group (all baseline values). This cross-sectional plot illustrates a similar result to the MW plot - that the GPW increases with age.

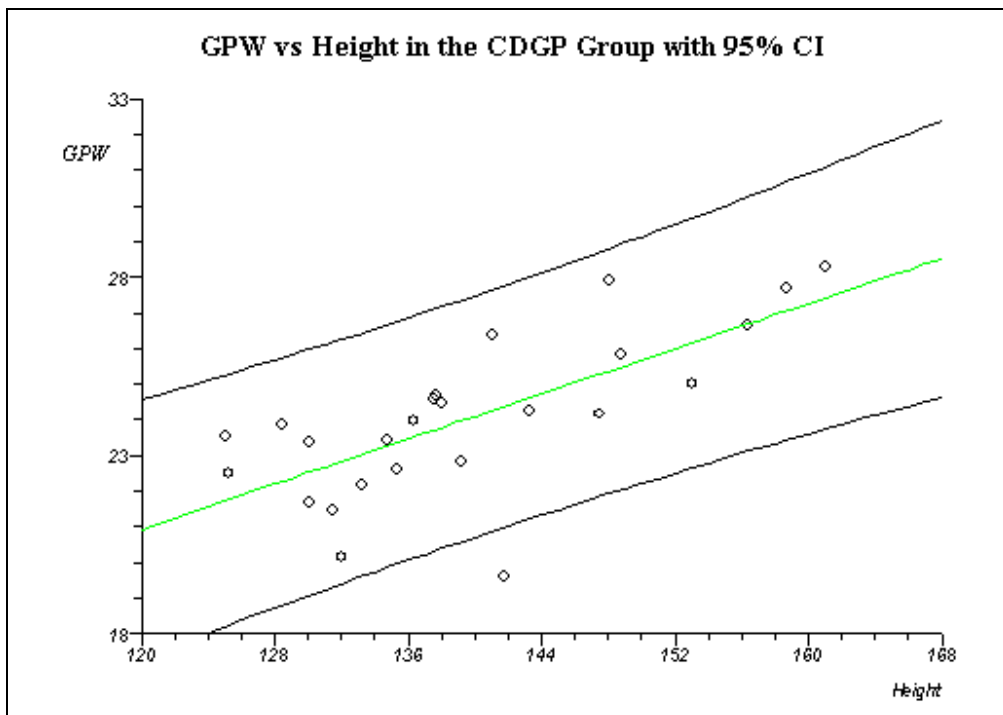


Figure 8.6H: GPW (mm) compared to height in the CDGP group (25 baseline values). This cross-sectional plot illustrates a similar result to the MW plot - that the GPW increases as height increases.

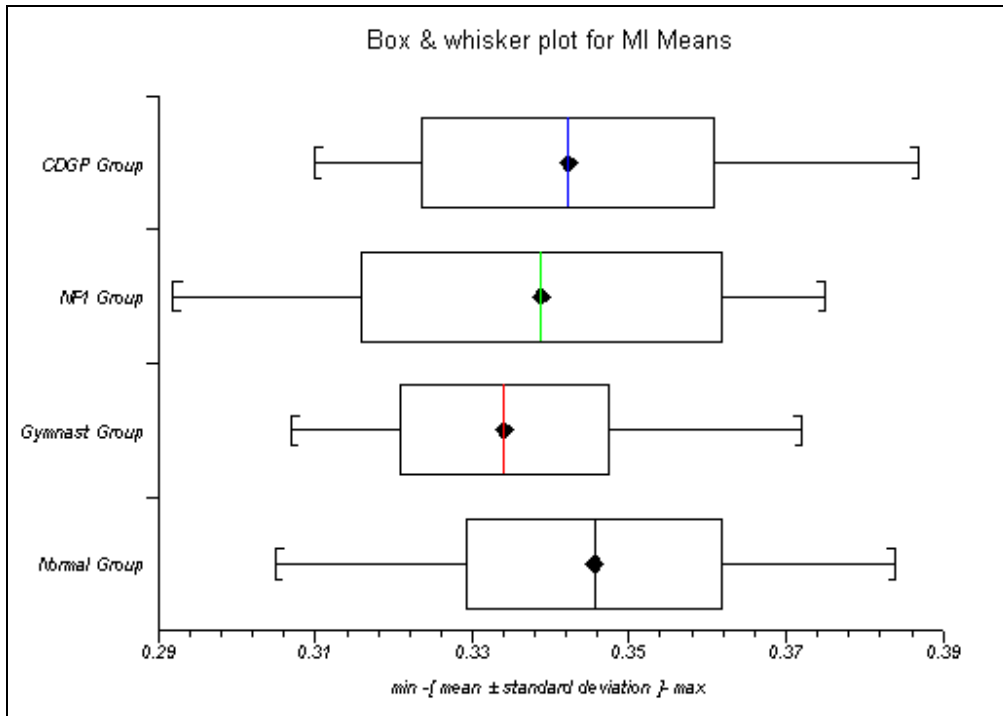


Figure 8.7A: Box and whisker plot illustrating the MI means, standard deviations and ranges of the Normal, Gymnast, NF1 and CDGP groups.

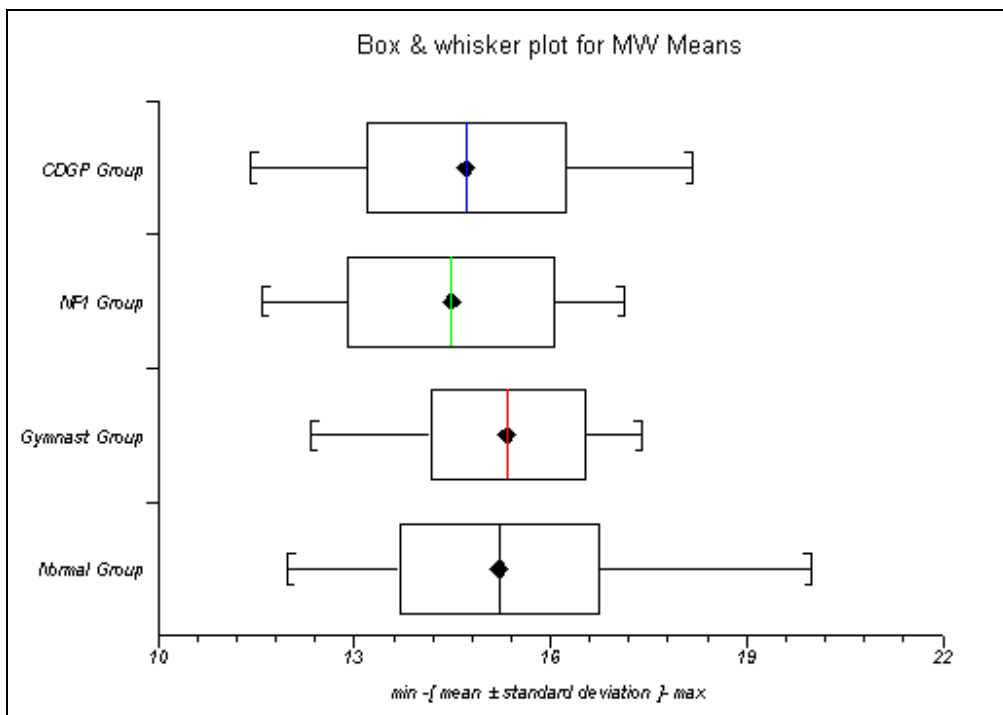
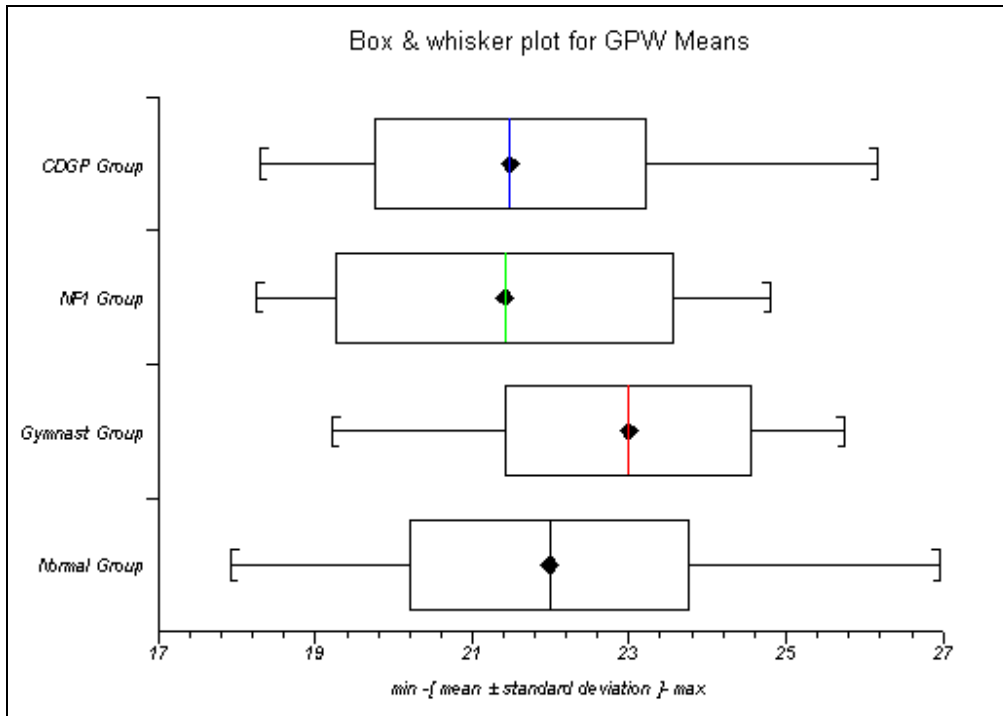


Figure 8.7B: Box and whisker plot illustrating the MW means, standard deviations and ranges of the Normal, Gymnast, NF1 and CDGP groups.



**Figure 8.7C:** Box and whisker plot illustrating the GPW means, standard deviations and ranges of the Normal, Gymnast, NF1 and CDGP groups.